UNIVERSIDAD AUTÓNOMA DE MADRID

DEPARTAMENTO DE BIOQUÍMICA

USO DE LOS PÉPTIDOS GSE24.2 Y GSE4 COMO POSIBLE TRATAMIENTO DE CÉLULAS DE PACIENTES DE ATAXIA TELANGIECTASIA

TESIS DOCTORAL

LAURA PINTADO BERNINCHES

Madrid, 2017

DEPARTAMENTO BIOQUÍMICA

FACULTAD DE MEDICINA

UNIVERSIDAD AUTÓNOMA DE MADRID

USO DE LOS PÉPTIDOS GSE24.2 Y GSE4 COMO POSIBLE TRATAMIENTO DE CÉLULAS DE PACIENTES DE ATAXIA TELANGIECTASIA

Memoria presentada por

LAURA PINTADO BERNINCHES

Licenciada en Bioquímica, para optar al grado de Doctor por la Universidad Autónoma de Madrid

Director de tesis:

Dra. Rosario Perona Abellón

Profesor de Investigación

Instituto de Investigaciones Biomédicas “Alberto Sols”

CSIC-UAM

GOBIERNO DE ESPAÑA
MINISTERIO DE ECONOMÍA, INDUSTRIA Y COMPETITIVIDAD
CSIC
CONSEJO SUPERIOR DE INVESTIGACIONES CIENTÍFICAS
UAM UNIVERSIDAD AUTONOMA DE MADRID
Instituto de Investigaciones Biomédicas "Alberto Sols"

Por la presente, **Rosario Perona Abellón**, Profesor de Investigación del CSIC y adscrito al Instituto de Investigaciones Biomédicas de Madrid "Alberto Sols", certifico que:

Dña Laura Pintado Berninches, Licenciada en Bioquímica por la Universidad Autónoma de Madrid, ha realizado bajo mi dirección su Tesis Doctoral titulada:

"**USO DE LOS PÉPTIDOS GSE24.2 Y GSE4 COMO POSIBLE TRATAMIENTO DE CÉLULAS DE PACIENTES DE ATAXIA TELANGIECTASIA**" en el Instituto de Investigaciones Biomédicas de Madrid "Alberto Sols".

Considero que la presente Tesis Doctoral reúne a mi juicio las condiciones de originalidad y rigor necesarios y, por lo tanto, se encuentra en condiciones de ser presentada y defendida públicamente para optar al grado de Doctor por la Universidad Autónoma de Madrid.

Para que conste a todos los efectos, firmo la presente autorización para la defensa de esta Tesis en Madrid a 6 de Marzo de 2017.

Dra Rosario Perona Abellón

Director de la Tesis

Profesor de Investigación

CSIC

A mis dos familias

"Cada vez que decimos "no sé" nos cerramos una puerta de nuestra propia fuente de sabiduría, que es infinita"

(Louise L. Hay)

AGRADECIMIENTOS

Durante estos años son muchas las personas que han compartido momentos conmigo y a quienes quiero expresar mi gratitud por el apoyo y la confianza que me han prestado de forma desinteresada.

Recuerdo el día que llegué al laboratorio de Rosario para hacer el proyecto de fin de carrera. En ese momento no era consciente de la suerte que tenía de haber llegado al 1.11, pero el tiempo me ha hecho darme cuenta de ello. El 1.11 es como una familia y por ello Rosario te quiero dar las gracias, por acogerme, por enseñarme todo lo que he aprendido… ¡y lo que me queda!, por tu paciencia y por tu constante seguimiento y supervisión, también por todos tus fines de semana utilizados para que pudiera depositarla a tiempo y sobre todo por ese trato tan cercano que tienes con todas nosotras.

Pero todo esto no lo hubiera conseguido sin mis compis del labo sobre todo gracias, con especial cariño a Cris, la persona que más ha sufrido conmigo la tesis y por la que siento un gran aprecio, porque además de compañera eres una amiga, y porque compartes conmigo todos los picotos y bolis. No sé cómo podré agradecerte todo tu tiempo, esfuerzo y sacrificio que has dedicado para ayudarme con la maquetación, papeleo, figuras… esta tesis lleva mucho de ti.

A ti Patri, porque lo que empezó con un cafecito se convirtió en una compañera de poyata a la que tengo mucho cariño y con la que espero poder compartir muchos momentos más, a ti Bea por preguntarme como íbamos con las correcciones y ofrecerte a ayudarme con los experimentos, eres muy buena compañera y que no te falte nunca esa perseverancia que tienes en el trabajo, a ti Elena, por hacerme huecos para mis PCRs y llenarme de dulces para afrontar mejor el trabajo, eres una compañera de la que tengo mucho que aprender, a ti María, que aunque nos conocemos poco, sé que eres una chica muy divertida y motivada con tu proyecto, y recuerda siempre logaritmo…(nunca lineal). A ti Natalia (La Paz) porque eres genial, divertida, honesta y a la vez mentirosilla… no olvidaré la encerrona del 100 montaditos junto con Patri. Gracias a todas por todo.

Al 2.13, en primer lugar agradecer a Leandro su predisposición en ayudarnos con las centrífugas, con la qPCR, con los diseños de oligos…porque siempre podemos contar contigo. A ti Blanca, porque fuiste junto con Cris mi compañera, y ahora tengo dos amigas con las que poder hacer planes de presillas y cenas (que por cierto hay que retomar), por esos cafés con barquitos y por seguir cayendo en mis bromas, eso te hace ser única, has sido mi mejor profesora de animalario, lugar en el que te he “echado una mano” siempre que lo he visto necesario, ¡quien iba a decir que ahora le tocaba a la Luni defender la tesis! Laura I gracias por ayudarme con las infecciones y por debatir todo conmigo, sabes que me encanta. A ti Javi, el chico mejor rodeado del IIB, y el que nos hace reir tanto durante las comidas, por esos momentos de estrés estos últimos meses, viendo la que se nos avecinaba, ahora te paso el relevo. A Bea porque te has ganado un hueco en el 2.13 bien merecido por tu actitud positiva y tus ganas de aprender. A ti Inma, que, siempre se te ve predispuesta, sigue así.

Además he compartido muchos otros momentos con otras personas, Inma (La Paz) porque siempre ves lo positivo y nos lo transmites con una dulzura que es caraterística tuya, y, a todo tu equipo (Julia, Olgas, Javi y Carlos) con los que he compartido muchos western y horas de cultivos; a Luci, nuestra vecina más

dicharachera, ójala todos los vecinos fueran como tú. El labo 1.9 que nos permite escuchar música en directo sin necesidad de radio, el 1.13 que me ceden el pHímetro siempre calibrado, en especial con Ali que compartimos nuestros momentos de estrés, el 2.14, en especial a Isa por resolvernos cualquier duda académica y a Natalia y Jone porque sois unas chicas fantásticas.

A mis amigas de Cerce, a ti Lau porque sé que siempre estás ahí, a ti Nata porque eres tan leal que todo el mundo te quiere cerca, a ti Virgi por organizar las quedadas para vernos, a ti Yoli, porque eres pequeña pero tienes un grandísimo corazón, Laura Niño porque no te pierdes una y a ti Bea porque siempre haces un hueco para quedar.

A mis bioquis favoritos, por todos los over-night y las horas de biblioteca, cada uno de vosotros sois especiales para mí. Ale, mi primera compy del 1.11, qué recuerdos más bonitos y qué despedida tuvimos con tu viaje a NY, inolvidable; tu dulzura acompañado de tus sonrisa hace que deprendas una positividad inmensa. Moni, mi compañera vinícola por excelencia, tu espontaneidad es única e incalculable. Pau, juntas iniciamos la carrera y juntas vamos a acabar la tesis, la capacidad que tienes para que no te saquemos de quicio es infinita, incluso cuando sólo hablo en números. Alfon, el amigo más organizado que tengo y el que se desvive por estar siempre con todos, eres muy grande. Frías, por ser como eres, tan buen amigo ayudando siempre con todo lo que está en tus manos. Lendínez, el desaparecido, porque sólo te vemos de celebración en celebración.

A mis biólogas Dory y Delia, porque valéis tanto… no se puede ser más buena gente, sois geniales.

A mi equipo Marcelinas (Nuri, Andrea, Malu, Bea y Cris) por esos terceros tiempos que nos permiten desconectar de la semana.

A mi familia, en primer lugar a mis padres, por haberme proporcionado la mejor educación y por haberme enseñado que con trabajo y constancia todo se consigue, con especial mención a mi madre, por todo el esfuerzo que ha realizado toda su vida para que yo haya podido llegar hasta aquí (¡eres la mejor madre sin duda alguna!), a mis hermanos Miri, Bea, Vero y Diego, la mejor tropa, por preocuparos tanto por la tesis, por Leyre y por mí, porque durante todos estos años habéis estado a mi lado, apoyándome para que este sueño se hiciera realidad. Gracias también a mis abuelas por estar siempre ahí.

Y, por supuesto, te lo tengo que agradecer a ti, David, porque has sido y eres mi apoyo incondicional, porque me das la fuerza que necesito y me transmites esa energía positiva que a veces me falta y por ser el mejor compañero de viaje. Por fin todo el tiempo que has dedicado conmigo a la tesis ya tiene recompensa. Ahora afrontaremos juntos un nuevo reto.

Finalmente, pero quizá el más importante, mi padre, al que no podría faltarle una dedicación como se merece, porque me acompaña en cada paso que doy. De él aprendí que las puertas del cielo están en la ilusión, la que puso en todo en la vida, la que me transmitió por el trabajo bien hecho. Esta tesis es oro molido, va por ti papá.

RESUMEN/ABSTRACT

La Ataxia Telangiectasia (A-T) es un desorden autosómico recesivo, englobado dentro de las denominadas enfemedades raras con una prevalencia 1:100.000 nacimientos, con un fenotipo altamente complejo afectando en gran medida al sistema nervioso y al inmunológico. Se caracteriza por una ataxia cerebelar progresiva, neurodegeneración, radiosensibilidad, telangiectasia de la conjuntiva, defectos en los controles del ciclo celular, inestabilidad genómica, infecciones recurrentes y cáncer, siendo los más frecuentes leucemias y linfomas.

En este trabajo nos hemos propuesto estudiar el posible papel terapeútico de los péptidos GSE24.2 y GSE4 en A-T. El péptido GSE24.2 es una parte de la proteína disquerina, la cual forma parte del complejo telomerasa. Este péptido junto con un derivado de menor tamaño GSE4 reactivan la actividad telomerasa en células de enfermos con disqueratosis congenita (DC). Ambos péptidos han sido clasificados como medicamentos huérfanos por la EMA tras evaluar su eficacia in vitro en DC. Esta enfermedad comparte con A-T muchas características como son un elevado estrés oxidativo, daño persistente al ADN y deficiencias de expresión de enzimas antioxidantes, entre otros. Estudios previos habían mostrado que la expresión del GSE24.2 y GSE4 en líneas celulares DC disminuye el daño al ADN, el estrés oxidativo, la senescencia y aumenta la capacidad proliferativa. En base a estos resultados ensayamos la actividad de estos péptidos en líneas celulares A-T.

Los resultados obtenidos en esta tesis muestran la eficiencia del uso de lentivirus que expresan estos péptidos induciendo una disminución del daño en el ADN en células de enfermos A-T acompañado de menor estrés oxidativo medido por los niveles de radicales libres, aumento en la expresión de genes con capacidad antioxidante, menor senescencia y menor expresión de citoquinas inflamatorias como IL-6. Ante estos resultados nos propusimos utilizar una herramienta terapeútica que pudiera emplearse clínicamente y por ello decidimos recurrir a las nanopartículas. Realizamos diferentes tratamientos con nanopartículas cargadas con GSE24.2 y GSE4 en las células A-T, obteniendo resultados similares a los obtenidos mediante el uso de lentivirus. Además, hemos encontrado que la expresión del GSE4 en células A-T induce un aumento de la actividad telomerasa y la expresión de TERT, ambas disminuidas en las líneas celulares A-T. Consecuencia de ello es un aumento de la longitud de los telómeros en estas células.

Con esta nueva aproximación terapeútica se podría disminuir los niveles de especies reactivas de oxígeno y con ello el deterioro asociado y relentizar la evolución de la enfermedad con una mejora de la calidad de vida de estos pacientes.

Ataxia Telangiectasia (A-T) is a rare inherited disorder, whose prevalence is 1:100.000 births, with a highly complex phenotype that affects the nervous, immune and other body systems. It is characterized by progressive cerebellar ataxia, radiation sensitivity, telangiectasias, defects in the cell cycle control, genomic instability, recurrent infections and cancer susceptibility (leukemias and lymphomas).

In this thesis, we have approach the use of both GSE24.2 and GSE4 peptides, as a therapeutic treatment in A-T. The GSE24.2 peptide is part of the dyskerin protein, which belongs to the telomerase complex. This peptide and his derivative of smaller size GSE4, reactivates telomerase activity in dyskeratosis congenita cells (DC). Both peptides have been classified as an orphan medication by EMA after evaluate in vitro their eficiency in DC. This disease share with A-T several features like a high oxidative stress, persistent DNA damage, deficiency in antioxidants gene expression. We had previously shown that expression of GSE24.2 or GSE4 in DC cell lines resulted in a decrease in DNA damage, oxidative stress, senescence and a higher proliferative capacity. Based on these results we tested the efficacy of these peptides in A-T cell lines.

Our results showed that infection of patient A-T cells with lentivirus expressing both peptides induced a decrease in DNA damage and oxidative stress, an increase in gene expression of some antioxidant genes, lower senescence and lower expression of IL-6.

With these results in mind we used another alternative therapeutic approach by using nanoparticles to deliver the peptide to cells. We performed different treatments in A-T cells lines with nanoparticles loaded with both peptides, and we concluded that this could be a good therapeutic alternative because the results were very similar to those obtained by lentiviral infection. We have also found that expression of GSE4 in A-T cells increases telomerase activity and TERT expression, both parameters were reduced in A-T cells. As a consequence telomere length of A-T cells increased in GSE4 expressing cells.

The results are very promising, due to the fact that A-T patient cells have a high level of reactive oxygen species, which leads to the loss of Purkinje cells, immunodeficiency and genetic instability, radiosensitivity and cancer. With this new therapeutic approach, it would be possible to reduce the levels of reactive oxygen species and with this, the associated neurological deterioration slowing slow down the evolution of the disease with an improvement in the quality of life of these patients.

ÍNDICE

ABREVIATURAS

- **%TEL/IC**: (*telomerase products /internal control)* productos telomerasa/control interno
- **8-oxoG:** 8 oxo-guanina
- **ABSF: (***aminoethylbenzenesulfonyl fluoride)* fluoruro de aminoetilbencenosulfonilo
- **ADN:** Ácido desoxirribonucleico.
- **ADNc:** Ácido desoxirribonucleico complementaria a la hebra de ARN.
- **ADNg:** Ácido desoxirribonucleico genómico.
- **AEBSF: *(4-(2-aminoethyl)benzenesulfonyl fluoride hydrochloride)*** hidrocloruro de fluoruro de 4-(2-aminoetil) bencenosulfonilo
- **ARN:** Ácido ribonucleico.
- **A-T:** Ataxia telangiectasia.
- **ATCC:** *American Type Culture Collection*.
- **ATM:** Ataxia telangiectasia mutada.
- **ATMi:** Inhibidor de Ataxia telangiectasia mutada
- **ATP:** Adenosin trifosfato.
- **BSA**: (*Bovine Serum Albumin*) Albúmina sérica bovina
- **CAT**: Catalasa
- **CDK**: cinasa dependiente de ciclina
- **CEA**: (*carcinoembryonic antigen*) Antígeno carcino embrionario
- **CHAPS:** 3-{[3-clomidopropil]-dimetil-amonio}-1-propanosulfonato
- **CMV:** Citomegalovirus
- **Ct**: *(cycle threshold)* umbral del ciclo
- **Cys:** cisteína
- **DAPI:** 4,6-Diamino-2-fenil-indol.
- **DC:** Disqueratosis congénita.
- **DCF:** *dichlorofluorescein*
- **DCFH:** *dichlorofluorescin*
- **DCFH-DA:** *Dichloro-dihydro-fluorescein diacetate*
- **DDR:** *(DNA Damage Response)* Respuesta al daño en el ADN
- **DHE:** *dihydroethidium*
- **DIG:** dioxigenina
- **DMEM:** Medio de cultivo *Eagle* modificado por *Dulbecco*.
- **DMSO:** Dimetilsulfóxido.
- **DNAsa:** desoxirribonucleasa
- **dNTPs**: Deoxirribonucleótidos trifosfatados.
- **DSB:** (*Double strand breaks*) Roturas de doble cadena

- **DTT:** Ditiotreitol
- **ECL: (***Enzymatic Chemiluminiscence) Quimioluminiscencia enzimática*
- **EDTA: (***Ethylenediaminetetraacetic acid)* Ácido etilendiaminotetraacético.
- **EGTA: (***Ethylene glycol tetraacetic acid)* Ácido etilenglicol tetraacético
- **EMA:** *(European Medicines Agency*) Agencia Europea del Medicamentos
- **ERK: (***extracellular signal–regulated kinases)* quinasas reguladas por señal extracelular
- **FACs: (***Fluorescence-activated cell sorting)* Selección de células activadas por fluorescencia
- **FBS**: (*Fetal Bovine Serum*) Suero fetal bovino.
- **GAPDH:** gliceraldehído-3-fosfato deshidrogenasa.
- **GFP**: (*Green Fluorescent Protein*) Proteína fluorescente verde
- **GOS:** (*galacto-oligosaccharide)* Galacto-oligosacárido
- **H2A.X:** variante de la histona H2A
- **HEK:** Fibroblastos embrionarios de riñón humano.
- **Hepes:** Ácido 4-(2-hidroxietil)-1-piperazineetanosulfónico.
- **hTERT:** (*Human telomerase reverse transcriptase)* Transcriptasa inversa de la telomerasa humana
- **hTR: (***human telomerase RNA)* ARN de telomerasa humano
- **HU:** hidroxiurea
- **IC50:** Concentración a la que se produce la mitad de la máxima inhibición.
- **ID:** Identificador
- **IDP:** Inmunodeficiencia primaria
- **IF**: Inmunofluorescencia.
- **IFNγ**: Interferón gamma
- **Ig**: Inmunoglobulina
- **IL-6:** Interleuquina 6
- **ILD:** *(Insterticial lung disease)* Enfermedad intersticial pulmonar
- **JNK**: (*c-Jun N-terminal kinase)* quinasa c-Jun N-terminal
- **kDa**: Kilodalton.
- **Kpb**: Kilo pares de bases
- **MAPK: (***Mitogen-Activated Protein Kinases)* Proteína quinasa activada por mitógenos.
- **MEFs**: (*mouse embryonic fibroblasts)* Fibroblastos embrionarios de ratón
- **MMLV-RT: (***Moloney Murine Leukemia Virus Reverse Transcriptase)* Transcriptasa inversa del virus de la leucemia murina de Moloney

- **MMS:** metil, metano, sulfonato
- **MRN:** Mre11-Rad50-NBS1
- **MTS**: 3- (4,5-dimetiltiazol-2-il) -5- (3-carboximetoxifenil) -2- (4-sulfofenil) -2H - tetrazolio
- **MW24**: (*24 wells plate)* placa de 24 pocillos
- **NAC**: N-acetil-cisteína
- **NF-KB:** factor nuclear potenciador de las cadenas ligeras kappa de las células B activadas
- **NPs**: nanopartículas
- **NSCs**: *(neural stem cells)* Células madre neuronales
- **pb**: Pares de bases.
- **PBS:** Tampón fosfato salino.
- **PCR**: (*Polymerase Chain Reaction)* Reacción en cadena de la polimerasa
- **PDL: (***population doubling level)* Nivel de duplicación de la población
- **PI3K:** Fosfoinosítidol-3 quinasa.
- **PLGA/PEI**: ((*poly(lactic-co-glycolic acid)/ Polyethylenimine))* poli (ácido láctico- *co-* glicólico) /polietilenimina
- **PRDX1**: peroxirredoxina 1
- **qPCR**: (*quantitative polymerase chain reaction)* PCR a tiempo real
- **qRT-PCR:** reacción en cadena de la polimerasa con transcriptasa inversa cuantitativa a tiempo real.
- **RB:** Retinoblastoma
- **RNAsa:** Ribonucleasa
- **ROS: (***Reactive oxygen species)* Especies reactivas de oxígeno.
- **rpm:** Revoluciones por minuto.
- **RPMI:** *Roswell Park Memorial Institute*.
- **RQ: (***Relative Quantity)* cantidad relativa, "cambio en veces de expresión génica"
- **SA-β-Gal:** B-Galactosidasa Ácida
- **SASP**: *(s*enescence-associated *secretory phenotype)* fenotipo secretor asociado a senescencia
- **SD**: (standard deviation) desviación estándar
- **SDS**: Dodecil sulfato sódico.
- **Ser**: serina
- **SNC**: sistema nervioso central
- **SOD**: superóxido dismutasa
- **SV40**: *(Simian virus 40)* Virus del simio 40

- **Thr**: treonina
- **TBS**: Tampón tris salino.
- **Thr**: treonina
- **TNF**: *(Tumor necrosis factor)* Factor de necrosis tumoral
- **TOP2:** ADN Topoisomerasa 2
- **TRAP**: (*Telomeric Repeat Amplification Protocol)* Protocolo de Amplificación de las Repeticiones Teloméricas
- **TRF:** (Final restriction fragments) fragmentos de restricción terminal
- **Tyr**: tirosina
- **T/S***: (Telomere/ Single Copy Gene)* Telómeros/Gen de copia única
- **UV**: ultravioleta
- **VS**: versus

INTRODUCCIÓN

1. Ataxia Telangiectasia

1.1. Definición

La ataxia telangiectasia (A-T), también conocida como Síndrome de Louis-Barr, fue descrito por primera vez en 1926 por Sillaba y Hener. Sin embargo, fue la publicación de la neuróloga Denise Louis-Barr en 1941 la que tuvo más repercusión en el medio médico y generó la asociación del síndrome a su nombre. La denominación A-T llegó por fin con la detallada descripción por parte de Boder y Sedywich en 1959. Desde entonces, otros autores han investigado este síndrome cuyo interés ha aumentado en la medida de conocerse su base molecular en 1995.

La A-T es una enfermedad rara, pues la prevalencia es de 1/100.000 habitantes, y es englobada dentro de los síndromes neurocutáneos; afecta a multitud de órganos en el cuerpo, produciendo alteraciones muy importantes tanto en el sistema nervioso central como a nivel sistémico. En la mayoría de los casos la ataxia ocurre en edades tempranas (de 2 a 5 años) mientras que las telangiectasias son detectadas posteriormente o incluso pueden no ser manifestadas en algunos pacientes. Las ataxias son anormalidades neurológicas que tienen como resultado una marcha inestable y, las telangiectasias son la dilatación de los vasos sanguíneos de la piel y de los ojos generalmente, aunque también puede encontrarse en las orejas, cuello y extremidades. Los niños afectados a menudo necesitan silla de ruedas a los 10-12 años (Boder 1985; Lavin and Shiloh 1997; Lee et al. 2013). El pronóstico es grave ya que concurren complicaciones como infecciones respiratorias, inmunodeficiencia variable, neurodegeneración, envejecimiento cutáneo-mucoso acelerado, un mayor riesgo de cáncer y mayor sensibilidad a la radiación ionizante (Biton et al. 2008). Esta enfermedad neurodegenerativa (Shiloh and Kastan 2001), está causada por mutaciones del gen Ataxia Telangiectasia Mutated (ATM), identificado por primera vez en 1988 (Gatti et al. 1988), por un análisis de cosegregación. Está localizado en el brazo largo del cromosoma 11 en 11q22.3-23.1. Durante los siguientes 7 años la región cromosómica fue finamente mapeada por un consorcio internacional e identificado como ATM por Savitsky et al. en 1995. Este gen codifica por una enzima del tipo fosfatidilinositol 3- quinasa involucrada en respuestas celulares a daño genético y control de ciclo celular.

El gen de ATM ocupa 160kb del ADN genómico, codifica un tránscrito de 13kb de 66 exones (Uziel et al. 1996), siendo el producto del gen la proteína ATM (3056aa). ATM es una proteína con localización nuclear, aunque puede encontrarse en

peroxisomas y endosomas (Watters et al. 1999) y tiene un papel importante en el mantenimiento del telómero (Wood et al. 2001).

1.2. Sintomatología

Entre los síntomas más característicos se encuentran:

- Menor desarrollo mental
- Ataxia cerebelosa progresiva, que conlleva a la disminución de la coordinación del movimiento producido por la pérdida de células de Purkinje del cerebelo
- Decoloración en la piel
- Vasos sanguíneos dilatados en la piel y en la esclerótica de los ojos
- Mayor sensibilidad a radiación
- Inmunodeficiencia que les hace más susceptibles a padecer infecciones en las vías respiratorias
- Displasia de la glándula del timo
- Envejecimiento prematuro
- Problemas metabólico-endocrinos como la diabetes

Además, todos estos síntomas van acompañados de un envejecimiento celular acelerado, y presentan una mayor susceptibilidad a manifestar cáncer, particularmente los relacionados con el sistema inmune, tales como linfomas y leucemias (Fang et al. 2010; Byrd et al. 2012).

1.3 Diagnóstico

Durante el embarazo, esta enfermedad puede ser detectada mediante la amniocentesis. Cuando aparece por primera vez tras el nacimiento, la Ataxia Telangiectasia no suele ser visible, y su diagnóstico no se realiza hasta que aparezca algún síntoma, cuando esto sucede, una exploración física puede determinar que el paciente sufre algún tipo de ataxia. La exploración física se puede complementar con una radiografía del timo, y una analítica para comprobar si los niveles de alfafetoproteína (Navratil et al. 2015) o el antígeno carcino embrionario (CEA) en suero están elevados (Kozlov et al. 2006) y si los niveles de IgA, IgG e IgE son bajos pudiendo, de esta manera, realizar un examen genético de la enfermedad, determinando si el gen implicado se encuentra mutado o no. La prueba que confirma la enfermedad consiste en la detección de la proteína ATM, la cual está ausente en el 90% de los pacientes con A-T, 9% presentan niveles bajos mientras que existe un 1% que presentan niveles normales de proteína, pero no suelen presentar actividad

quinasa, por lo que en estos casos hay que evaluar la función de la proteína (Gatti and Perlman 1993).

2. El daño en el ADN

Las células de un organismo se enfrentan continuamente a agresiones que producen lesiones en el material genético que se han relacionado con numerosos aspectos de la fisiología humana. Por un lado el daño en el ADN, se ha relacionado con el envejecimiento de los organismos (Garinis et al. 2008) debido a la pérdida de la capacidad regenerativa de los tejidos producido por una reducción de la tasa proliferativa de las células que los componen. Por otro lado el daño al ADN también se ha relacionado con cáncer (Hanahan and Weinberg 2000) debido a que se puede alterar la función de genes críticos para el control celular. Por tanto, el envejecimiento y el cáncer son dos procesos que producen la desregulación del mantenimiento de la integridad genómica en respuesta a daño exógeno.

Además, el daño en el ADN también se ha relacionado con enfermedades tan diversas como las inmunodeficiencias, la neurodegeneración o la esterilidad. A pesar de todo esto, una de las principales características del ADN es su inmutabilidad a lo largo de las generaciones de cada especie. Esto es así gracias a un complejo sistema de detección, señalización y reparación del daño en el ADN.

2.1 Tipos de daño al ADN

Generalmente las lesiones en el ADN las clasificamos en dos grupos, dependiendo de si la fuente es endógena o exógena, pudiendo ser desde simples mutaciones puntuales sin consecuencias hasta las translocaciones de cromosomas (Figura 1).

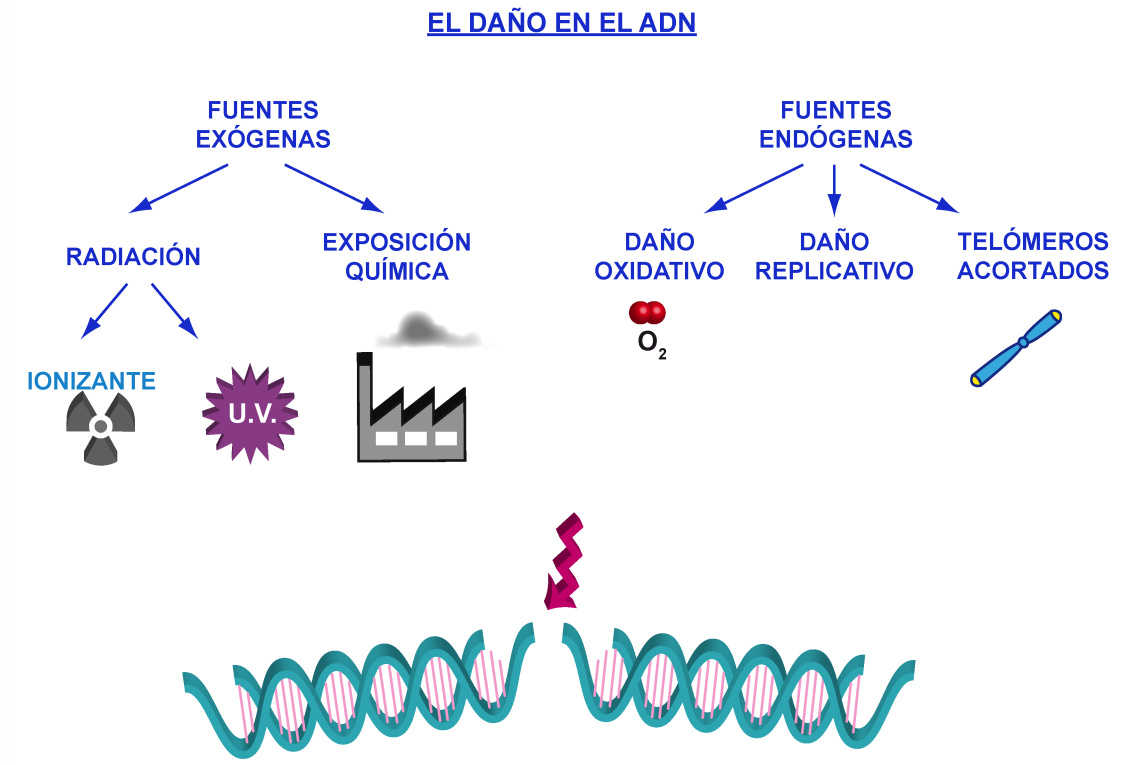

Figura 1. Tipos de daño al ADN. Los daños al ADN pueden ser: endógenos (daño oxidativo, daño replicativo y telómeros acortados) y exógenos (radiación y exposición química).

2.1.1. Daño endógeno

El genoma se encuentra continuamente expuesto a alteraciones causadas por procesos bioquímicos espontáneos, pero, gracias a la estructura de la doble hélice de ADN, se protege a los grupos químicos reactivos de la molécula del daño químico. Aún así, las moléculas de ADN están expuestas a alteraciones químicas. Las bases del ADN pueden modificarse de forma espontánea y pueden tener lugar depurinación, depirimidinación y desaminación de las bases (Lindahl 1993). Sin embargo, la fuente mayoritaria de daño en el ADN proviene del propio metabolismo celular siendo las más peligrosas las especies reactivas de oxígeno: ión superóxido, peróxido de hidrógeno y radical hidroxilo (De Bont and van Larebeke 2004), que se producen en la mitocondria durante el proceso de reducción del oxígeno a agua, generando estos intermediarios altamente reactivos. La consecuencia de estas especies reactivas de oxígeno es la creación de roturas de cadena sencilla y de doble cadena (DSB).

Otra fuente fundamental de lesiones en el ADN es la propia replicación, lo que implica que la aparición de lesiones es intrínseca a la duplicación del material genético. En último lugar, la acción de las topoisomerasas también puede generar

lesiones en el ADN. Las topoisomerasas I y II son enzimas capaces de liberar la tensión provocada por el superenrollamiento que aparece delante de la horquilla durante la replicación. Actúan cortando y ligando una o las dos hebras, proceso que se convierte en una fuente potencial de rupturas si su acción ligadora se bloquea (D'Arpa et al. 1990). Pero, el ADN no se rompe sólo accidentalmente. La misma reparación del ADN, así como algunos procesos biológicos generan selectivamente DSB.

2.1.2. Daño exógeno

Tanto las causas como las respuestas y las consecuencias del daño en el ADN son objeto de numerosos estudios. Para ello, son utilizadas diversas drogas o procedimientos que generan lesiones de diversos tipos, entre ellos se utilizan en tratamientos en el cancer. Son ampliamente utilizados los rayos γ (IR) y la bleomicina para generar DSB en cultivos celulares y en animales de laboratorio. También se usan la hidroxiurea (HU) o la afidicolina para inducir estrés replicativo, al deplecionar los niveles de dNTPs e inhibir las polimerasas respectivamente. Otras drogas ampliamente usadas son la doxorrubicina y cisplatino (agentes intercalantes), el etopósido y la camptotecina (inhibidores de las topoisomerasas II y I) y el MMS (agente alquilante).

El genoma se encuentra bajo el ataque ocasional de mutágenos exógenos y sus metabolitos debido a la interacción con el ambiente. Entre estos agentes se encuentran las radiaciones, como son los rayos X, los rayos gamma (γ) (Hoeijmakers 2001), y la radiación electromagnética que produce liberación de electrones libres al incidir sobre las moléculas de agua de la célula. Todas ellas pueden generar directamente rupturas en una o en ambas cadenas del ADN, así como también especies reactivas de oxígeno (ROS) que a su vez generan más rupturas en las cadenas del ADN. Otro tipo de radiación es la ultravioleta (UV) del sol, que aunque presenta un poder de ionización menor que las anteriores, es la mayor fuente de radiación de la que tiene que protegerse el organismo, pues al incidir y penetrar la luz UV sobre una molécula de ADN en una célula de nuestra piel, puede producir dímeros de pirimidinas entre dos moléculas adyacentes en la misma cadena de ADN (Jiang et al. 2009), siendo altamente estables y mutagénicos. Otra fuente exógena lo componen los carcinógenos ambientales, entre los que se encuentran las drogas utilizadas en quimioterapia, que afecta preferentemente a las células tumorales, mientras que las células sanas al ser menos proliferativas son menos sensibles a los fármacos.

2.2. La respuesta al daño en el ADN

Cuando una célula detecta que su genoma está dañado desencadena una respuesta coordinada cuyo objetivo principal es la reparación del daño y el mantenimiento de la integridad del genoma (Harper and Elledge 2007). La respuesta al daño en el ADN se inicia con la detección de la lesión y se ponen en marcha una serie de mecanismos de reparación, pero, dependiendo del grado de lesión producido pueden desencadenarse mecanismos que permitan la detención del ciclo celular e incluso desencadenar la muerte celular programada (apoptosis) o la senescencia (Mombach et al. 2014). Afortunadamente, la mayoría de las lesiones que se producen son reparadas sin verse afectada la célula, como las modificaciones puntuales en las bases, que son lesiones muy frecuentes. Sin embargo, en la célula ocurren otro tipo de lesiones que provocan la parada del ciclo celular para proceder a la reparación de la misma, produciendo un retraso para iniciar la siguiente fase del ciclo celular y de esta manera, la célula posee más tiempo para repararlo.

Las células han desarrollado complejas redes reguladoras para detectar el daño al ADN y coordinar la replicación del ADN, detención del ciclo celular y la reparación del ADN que está formada por sensores, transductores y efectores. La fosforilación de la variante de histona nucleosómica H2A.X, llevada a cabo por ATM (Guleria and Chandna 2016), está involucrada en la detección y reparación del daño al ADN, generando una descondensación localizada de la cromatina, que proporciona un mayor acceso a los diversos factores y complejos enzimáticos de las vías de reparación y control del ciclo celular (Figura 2) (Ayoub et al. 2009).

Se ha estimado que por cada DSB se fosforilan unas 2000 moléculas de H2A.X. Por lo tanto, una única lesión en el ADN produce una modificación que es amplificada en una extensa región de la cromatina, lo que puede considerarse como la preparación para el reclutamiento y montaje de la maquinaria de reparación (Kinner et al. 2008).

El reclutamiento de proteínas de señalización y reparación en los sitios de lesiones constituye el primer evento de la respuesta celular de daño al ADN. Es sabido que H2A.X interactúa físicamente con NBS1, 53BP1 y MDC1 (Kobayashi et al. 2004). La interacción de MDC1 con H2A.X es el primer paso para la amplificación de la señal y reparación de la DSB. MDC1 también interactúa directamente y de manera dinámica con NBS1, la cual se encuentra formando el complejo MRN (Mre11-Rad50-NBS1) y es necesaria para la activación de ATM, ya que es capaz de interaccionar con ATM a través de su extremo C-terminal (You et al. 2005).

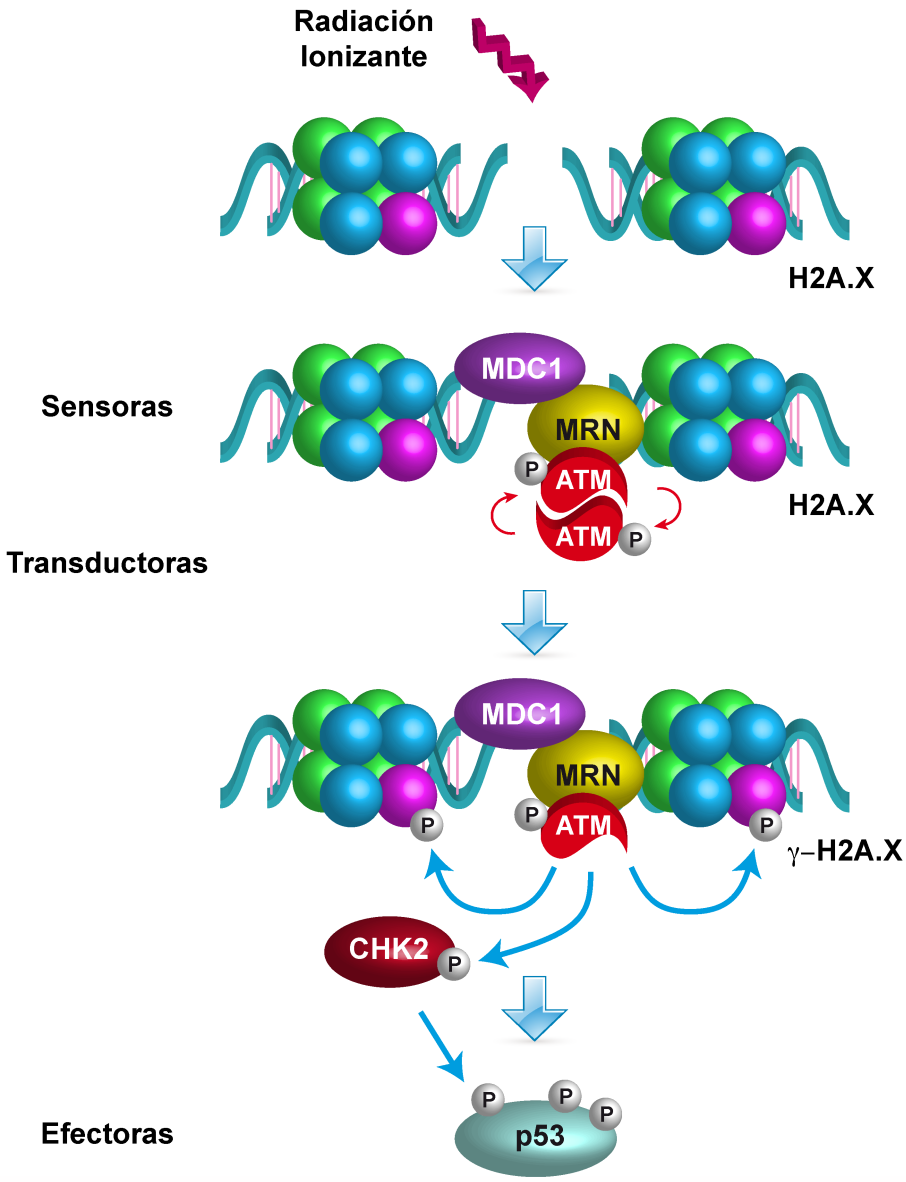

Figura 2. Secuencia de la respuesta a daño en el ADN. Frente a DSB en el ADN, el complejo MRN actúa como sensor y media el reclutamiento de ATM a las DSB, gracias a que MDC1 interactúa directamente con el complejo MRN. ATM se autofosforila para dar lugar a los monómeros/dímeros activos y permite así fosforilar H2A.X y posteriormente se fosforila CHK2, activando así los efectores para que tenga lugar una respuesta celular. Adaptado de (Mirzayans et al. 2013).

Una vez ATM se localiza en el sitio de DSB (Kim et al. 2009), ATM se activa catalíticamente al pasar de un estado dimérico/tetrámero a uno monomérico/dimérico mediante autofosforilación en la serina 1981 (Bakkenist and Kastan 2003) (Figura3). La fosforilación de MDC1 por la caseína quinasa 2 (CK2) promueve la interacción con NBS1. De esta manera se genera una retroalimentación positiva que extiende la fosforilación de H2A.X varias megabases del sitio original de la DSB (Kinner et al. 2008).

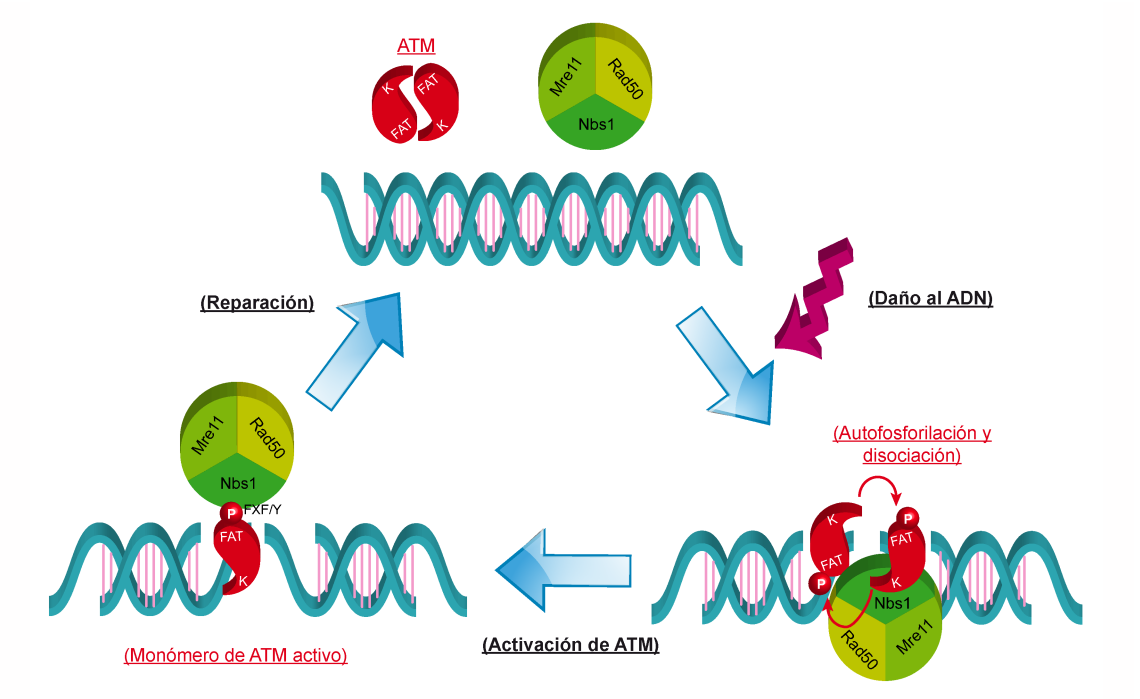

Figura 3: Activación de ATM en los sitios de daño al ADN. El complejo MRN actúa como un sensor y media el reclutamiento de ATM a las DSB. ATM es reclutada como un dímero/tetramero inactivo a los sitios DSB mediante unión al dominio C-terminal de la proteína NBS1. El dominio quinasa de cada molécula de ATM fosforila a la otra en la serina 1981 del dominio FAT. Esta fosforilación provoca la disociación de los dímeros/tetrámeros de ATM en monómeros/dimeros con actividad quinasa. Adaptado de (Guleria and Chandna 2016).

Esto genera un círcuíto de retroalimentación que conduce a más fosforilaciones de H2A.X y a las modificaciones de la cromatina necesarias para el reclutamiento de la proteína 53BP1 que se acumula por la interacción con γ-H2A.X y MDC1. Otras proteínas contribuyen a mantener el estado fosforilado de ATM como 53BP1 y BRCA1. Una vez activada ATM se activa las transducción de la señal a los efectores, ya que fosforila diferentes sustratos de forma dependiente del ciclo celular: en G1-S, fosforila p53 en la serina15, en G2-M fosforila CHK2 en la treonina 68 y en fase intra-S fosforila SMC en la serina957 y serina966.

Posteriormente, la célula debe volver a su estado basal y para ello se requiere la actuación de la fosfatasa PP2A (Bakkenist and Kastan 2004), que defosforila ATM y la devuelve a un estado inactivo (Goodarzi et al. 2004)

2.3. Estrés oxidativo, senescencia e inflamación

Con el incremento en la atmosfera del oxígeno hace 2.3 billones de años, las células han desarrollado mecanismos para mitigar los efectos tóxicos de los radicales de oxígeno que pueden dañar ácidos nucleicos, proteínas o lípidos. El estrés oxidativo es producido cuando existe un desequilibrio entre los oxidantes celulares y los agentes antioxidantes, en el cual la producción de especies reactivas de oxígeno (ROS) es superior a la capacidad antioxidante (Chen et al. 2012). Diariamente ocurren diversos eventos que dañan el ADN, de los cuales las especies reactivas de oxígeno representan una porción importante (Barzilai et al. 2002). Constantemente los ROS son producidos en las células en procesos metabólicos y durante procesos patológicos como la inflamación (Mittal et al. 2014), por ello las células han desarrollado mecanismos de defensa contra el daño oxidativo (Barzilai et al. 2002). El estrés oxidativo puede ser dependiente de la activación de la vía de señalización de p38 MAPK (Son et al. 2011), ya que, en condiciones deficientes de ATM, niveles elevados de ROS activan la ruta p38 MAPK que bloquea la fosforilación de Bmi-1 dependiente de AKT, causando una disminución en supervivencia y proliferación de NSC´s. Las neuronas son particularmente vulnerables al estrés oxidativo y dependen de los astrocitos como soporte de antioxidantes. Los astrocitos muestran una reducida proliferación debido al estrés oxidativo en ausencia de ATM, consecuentemente el soporte de antioxidantes a las neuronas decrece y conlleva a neurodegeneración, como ocurre en las células de Purkinje en A-T.

Los daños producidos en la célula debido a un aumento en los ROS provocan la parada del ciclo celular para que el daño sea reparado. En ausencia de ATM las células presentan niveles elevados de ROS, debido al daño al ADN persistente, y presentan mayor sensibilidad al daño oxidativo, por ello se ha pensado que ATM tiene un papel importante en la defensa celular frente a ROS (Alexander et al. 2010) actuando como sensor de daño oxidativo, además ratones $ATM^{-/-}$ mostraban niveles aumentados de 8-oxoguanina, un marcador de daño oxidativo al ADN, pero, esta inestabilidad genética revertía a niveles normales cuando las dietas de estos ratones era suplementadas con el antioxidante NAC^{-}. En condiciones fisiológicas el aumento de ROS puede activar directamente ATM que se autofosforila (Cys2991) y fosforila sustratos como p53 (ser15) y CHK2 (Thr68). Este proceso de activación es independiente del complejo MRN y otros marcadores como H2A.X no son fosforilados (Guo et al. 2010). Recientemente se ha descrito que la activación de ATM, en condiciones de elevado estrés oxidativo, es mediada por receptores de factores de crecimiento como PDGFRB, se produce la activación por autofosforilación (ser1981) y

ésta se inhibe cuando se utiliza un inhibidor específico de PDGFRB, AG1433 (Kim et al. 2010). Esta activación es protectora en neuronas frente a la excesiva excitación de las neuronas y promueve la autofagia en las neuronas (Kim et al. 2010)

En condiciones de elevado ROS, ATM activa TSC2 que reprime a mTOR1, el cual controla la función oxidativa de la mitocondria a nivel transcripcional y su sobreactivación intensifica la actividad mitocondrial produciendo acumulación de ROS, por lo que ATM media la represión de mTOR que regula los niveles de ROS bajo condiciones de estrés. Por lo tanto, podemos decir que ATM juega un papel fundamental en enfermedades asociadas con estrés oxidativo así como neurodegeneración como ocurre en A-T, y, que, la disfunción mitocondrial en ausencia de ATM es la responsable de niveles de ROS elevados y estrés oxidativo en células A-T (Guleria and Chandna 2016).

3. Papel del estrés oxidativo en el ADN telomérico y la actividad telomerasa

El ADN telomérico se acorta en cada ronda de división celular una media de 50-200pb (Zhao et al. 2009). Este acortamiento continúa hasta que el telómero alcanza una longitud crítica (Hayflick 1965), lo cual a su vez desencadena la parada del ciclo celular, dirigiéndolo a senescencia o apoptosis, siendo esto una característica que permite que los telómeros actúen como un reloj mitótico al restringir la capacidad de las células para la división. Sin embargo, las células germinales y las células madre contrarrestan el acortamiento progresivo de los telómeros con la presencia de telomerasa, una transcriptasa reversa dependiente de ARN, la cual puede sintetizar ADN telomérico de novo. La telomerasa lo forman un núcleo esencial compuesto por la transcriptasa inversa de telomerasa (TERT) para la síntesis de repeticiones teloméricas y el ARN de telomerasa (TERC) que sirve como molde para la elongación del ADN telomérico y por proteínas accesorias (Figura 4). TERT y TERC son necesarios y suficientes para la actividad in vitro de la telomerasa (Ishikawa 1997). Las proteínas accesorias son necesarias para la actividad in vivo y pueden estar involucradas en el ensamblaje del complejo o en la procesividad de la enzima (Mengual Gomez et al. 2014).

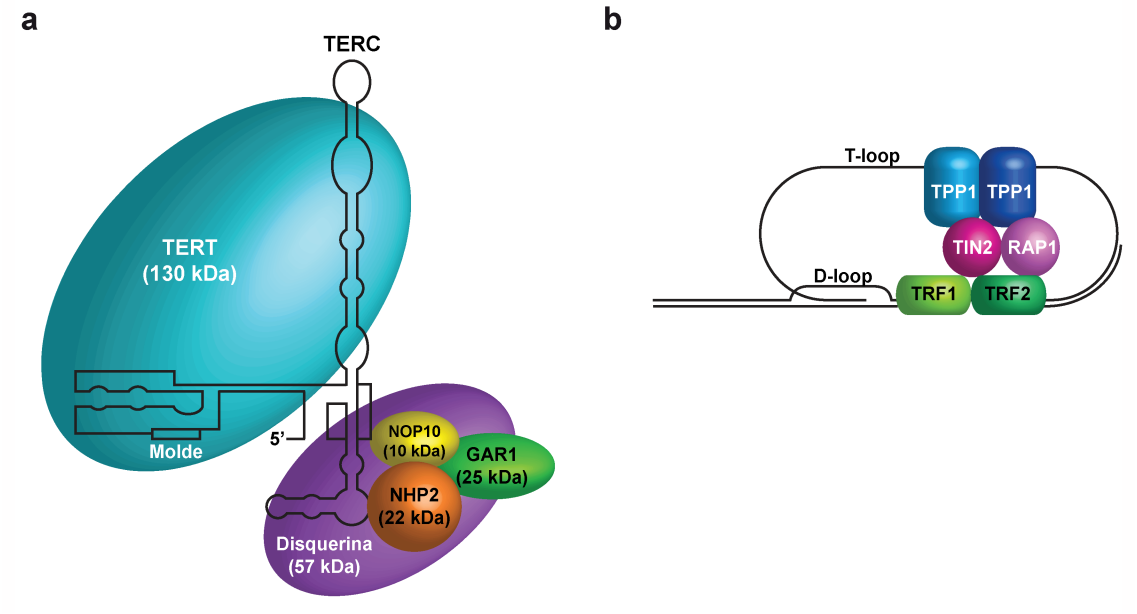

Figura 4: Componentes de los complejos (a) telomerasa (Garcia et al. 2007) y (b) shelterina (Perona et al. 2016). Adaptado de Garcia et al. 2007 y Perona et al. 2016.

El aumento del estrés oxidativo de diferentes fuentes (Figura 5) acelera el acortamiento telomérico (Ahmed et al. 2008) que ocurre en cada ronda de replicación del ADN en ausencia de telomerasa y promueve finalmente senescencia (Forsyth et al. 2003). Hay varias razones por las cuales los telómeros son particularmente vulnerables al estrés oxidativo. En primer lugar con el fin de salvaguardar la estructura de la cromatina, la señalización del daño al ADN y las rutas de reparación de DSB son suprimidas localmente en el telómero, ya que es importante prevenir que los telómeros sean reconocidos como ADN libre y roto, que puede estimular la reorganización cromosomica (Fumagalli et al. 2012). En este contexto, el añadido de bases dañadas por daño oxidativo puede generar roturas en la cadena de ADN. En segundo lugar, estudios in vitro han demostrado que la secuencia 5´-GGG-3´ en las repeticiones telomericas 5´-TTAGGG-3´ es más sensible a la oxidación que otras secuencias en el ADN (Oikawa and Kawanishi 1999). En tercer lugar los telómeros contienen secuencias de cadena única de ADN ya sea en el extremo 3´o internamente en el loop de desplazamiento de la elongación cuando el extremo 3´ invade el ADN telomérico de cadena doble para formar el T-loop (Doksani et al. 2013). Finalmente los telómeros cortos pueden aumentar el estrés oxidativo (Sahin et al. 2011) activando el punto de control del ciclo celular que estabiliza p53 (fosforilación ser15), reprime la expresión de PGC1α y PGC1β, componentes de la estructura de la mitocondria causando la

liberación de radicales de oxígeno y estableciendo un mecanismo de retroalimentación positiva de generación de ROS (Sahin et al. 2011).

Los telómeros cortos pueden inducir fallo cardíaco en el modelo animal de distrofia muscular de Duchenne, el cual el tratamiento con antioxidantes retarda significativamente la aparición de la disfunción cardíaca (Mourkioti et al. 2013). Por otra parte la pérdida de la expresión del gen con capacidad antioxidante *PRDX1* (peroxiredoxina1) en ratón está asociado con el desarrollo de cáncer, anemia hemolítica y acortamiento de la supervivencia celular (Neumann et al. 2003).

Cuando la base oxidada 8-oxoG está en el pool de dNTPs como 8-oxodGTP y la telomerasa utiliza esta base, hay un efecto mutagénico que suprime la elongación de telómero (Fouquerel et al. 2016). La deplección de MTH1 (nudix hydrolase 1), enzima que hidroliza 8-oxo-dGTP, 8-oxo-dATP, 2-hydroxy-dATP y 2-hydroxy rATP, a monofosfatos, inhibe su incorporación en el ADN, aumenta la disfunción telomérica y la muerte celular en células con actividad telomerasa (Fouquerel et al. 2016). En contraste, la existencia de 8-oxoG en la secuencia telomérica estimula la actividad telomerasa desestabilizando la estructura de G-cuadruplex del telómero y esto a su vez inhibe su elongación. Recientemente, en un análisis de la composición de la cromatina telomérica durante el ciclo celular, se ha encontrado que el enzima antioxidante *PRDX1* esta enriquecida en los telómeros durante la fase S del ciclo celular. La delección del gen *PRDX1* genera un severo daño telomérico por estrés oxidativo e interrumpe la elongación del telómero, demostrando que esta proteína tiene una función protectora contra el daño oxidativo en los telómeros.

4. Fenotipo secretor asociado a senescencia

El aumento de ROS puede inducir la inflamación mediante la actuación directa sobre factores de transcripción o indirectamente modulando diferentes procesos tales como la senescencia celular y la expresión de un grupo específico de microRNAs (Lang et al. 2016).

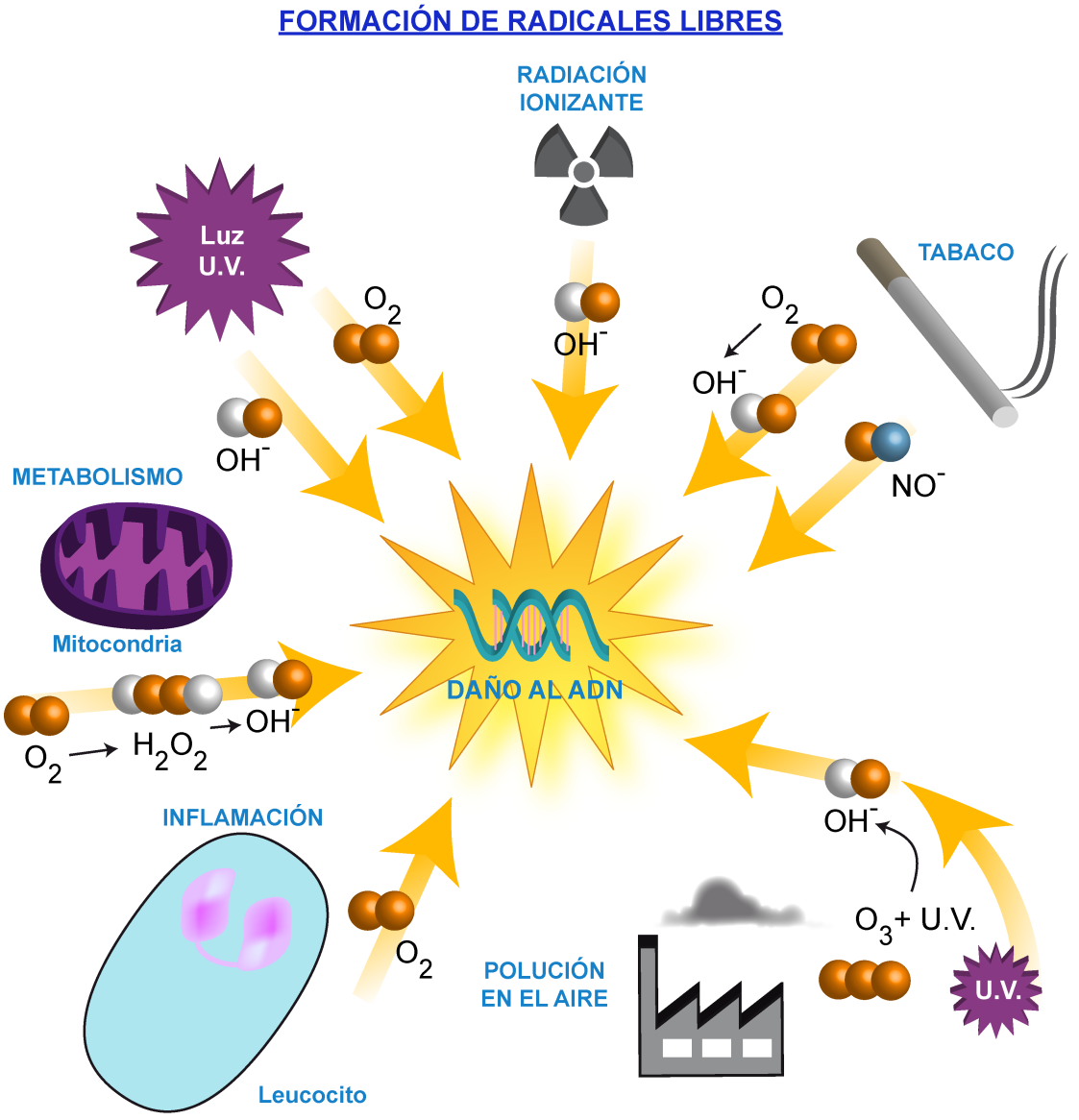

Figura 5: Procesos implicados en la generación de estrés oxidativo. El daño al ADN producido por estrés oxidativo puede producirse por diferentes procesos metabólicos, de inflamación, radiaciones o por la propia contaminación o tabaquismo. Adaptado de (Pendyala et al. 2008).

La senescencia celular puede observarse *in vitro* en cultivos celulares en respuesta a estrés intra o extracelular. El proceso de senescencia mantiene las células en una parada permanente del ciclo celular que previene la transmision del daño a la siguiente generación celular y previene la transformacion maligna. Una variedad de estímulos de estrés inducen senescencia e incluyen la disfunción telomérica resultado de repetidas divisiones celulares (senescencia replicativa), deterioro mitocondrial, estres oxidativo, daño al ADN severo y no reparado (estrés genotóxico) y la expresión de ciertos oncogenes (estrés oncogénico).

El fenotipo senescente no está limitado a una parada de la proliferacion celular. Una célula senescente es una célula que persiste potencialmente en el organismo, con un metabolismo activo y que ha sufrido cambios importantes en la expresión de proteínas y la secreción de factores que dan origen al fenotipo secretor asociado a senescencia (SASP). El SASP incluye la expresión de factores solubles e insolubles que incluyen interleuquinas, chemoquinas y factores de crecimiento, proteasas y componentes insolubles de la matriz extracelular (Coppe et al. 2010). De entre los factores solubles en SASP, la IL-6 es la más relevante. Su secreción se ha asociado a daño en el ADN por estrés oncogénico y parece controlado por la ruta de señalización mediada por ATM y CHK2, pero independiente de p53 (Rodier et al. 2009). La expresión de IL-6 en células senescente puede afectar directamente a las células vecinas que expresan el complejo IL-6R y gp130 en la superficie celular, como son células epiteliales y endoteliales de diferente origen (Coppe et al. 2010).

Las células senescentes se caracterizan morfológicamente por un mayor tamaño y diámetro nuclear y por la expresión de la beta galactosidasa asociada a senescencia (SA-β–gal) (Dimri et al. 1995). La p38 MAPK es un miembro de las MAP quinasas activadas por mitógenos (MAPK). Como otros miembros de esta familia p38 MAPK se activa por fosforilación (Thr180/Tyr182) y ésta ocurre de forma rápida y transitoria (Cuenda and Rousseau 2007). La actividad de p38 MAPK es importante en el proceso de parada del ciclo celular, en senescencia activa la parada de ciclo mediada por p53 y RB/p16. La activación de p38 MAPK es necesaria y suficiente para el desarrollo de un fenotipo SASP. Este efecto lo ejerce regulando principalmente la actividad transcripcional de NFκB que se requiere para la expresión de la mayoría de los factores SASP (Freund et al. 2011).

5. Regulación por ATM en pacientes con A-T

El ciclo celular en eucariotas es una secuencia ordenada de eventos biológicos que se divide en fases separadas por transiciones sometidas a un estricto control. Las fases fundamentales en el metabolismo del ADN son dos: la fase de síntesis o S, donde el ADN es replicado, y la fase de mitosis o M, en la que se produce la segregación de los cromosomas replicados hacia lo que serán las dos células hijas (Norbury and Nurse 1992) (Figura 6). Intercaladas entre estas dos fases se encuentran la fase G1 y la fase G2 durante las cuales la célula se prepara para abordar la síntesis y segregación del material genético respectivamente. En situaciones en las que no se requiere una proliferación continua, la célula entra en fase de reposo o quiescencia llamada G0.

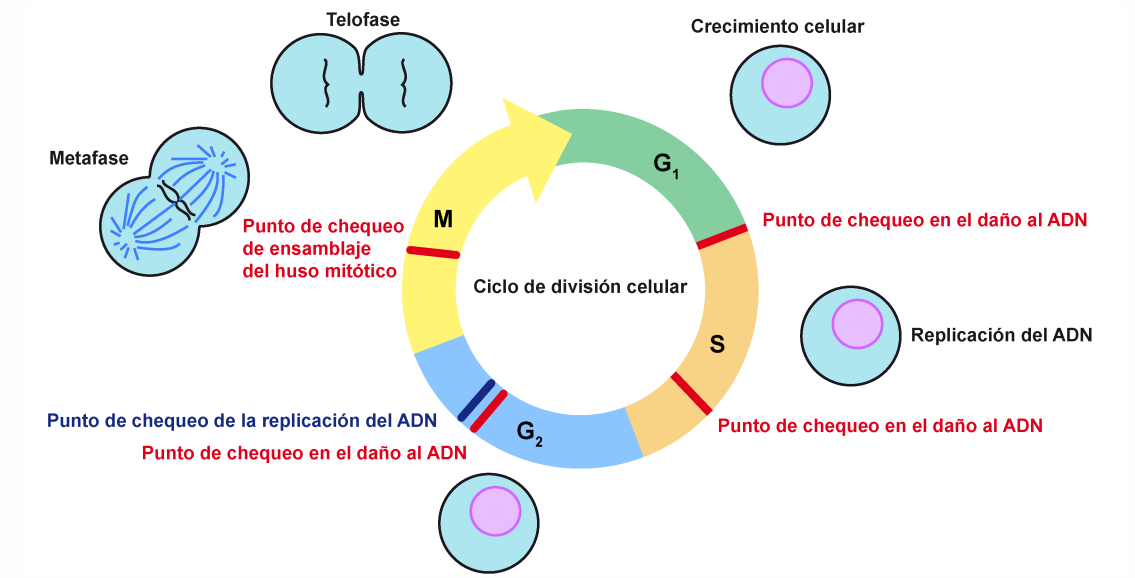

Figura 6: Etapas del ciclo celular. Está dividido en 4 fases: G1 (crecimiento), S (síntesis de ADN), G2 (preparación para dividirse) o M (mitosis). Adaptado de (Chin and Yeong 2010).

Existen complejos mecanismos de control que aseguran la generación de una sóla copia de material genético totalmente fiel al molde original y garantizan el reparto equitativo entre las dos células hijas. En este sentido, juegan un papel muy importante, por un lado, las transiciones entre las fases del ciclo que regulan que una nueva fase no comience hasta que se dan todos los requisitos que definen la terminación de la fase anterior, y por otro, la progresión precisa y ordenada del ciclo que es asegurada por las Cdks (quinasas dependientes de ciclinas) (Morgan 1997). La activación de estas subunidades catalíticas pasa principalmente por su asociación con proteínas reguladoras llamadas ciclinas, cuyos niveles de expresión, a diferencia de los de las Cdks, fluctúan a lo largo del ciclo (Sherr 2004). Gracias a las variaciones en los niveles de ciclinas se consigue una activación secuencial de cada uno de los complejos heterodiméricos Cdk-ciclina, clave para un avance ordenado a lo largo del ciclo.

Los puntos de chequeo del ciclo celular han sido desarrollados en las células como mecanismos de vigilancia para el mantenimiento de la integridad del genoma, pudiendo ser retardado o interrumpido cuando el ADN ha sido dañado. Como consecuencia del control de los puntos de chequeo por ATM, tras exposición de la célula a radiación ionizante, las células en A-T presentan una interrupción de los tres puntos de chequeo (Lavin and Khanna 1999), mediante la fosforilación de las quinasas CHK1 y CHK2. Mientras que, en células normales, si el mecanismo de reparación no funciona de manera correcta, la célula pierde su estabilidad genómica, aumentando

las probablidades de que por otros eventos pueda transformarse en célula cancerosa (Burdak-Rothkamm and Prise 2009).

Los tres puntos de chequeo que se encuentran interrumpidos en AT:

- **G1-S**: en A-T este punto de control se encuentra deficiente, pudiendo ser debido a un defecto en la fosforilación de p53, dependiente de ATM (Kastan et al. 1992), teniendo lugar una respuesta de p53 con cinética reducida y retardada (Kaliberov & Buchsbaum, 2012).
- **Intra-S**: la activación de esta fase es manifestada como un retardo en la síntesis de ADN replicativo en respuesta a lesión en el ADN, evitando que se mantengan rupturas de doble cadena (Osborn et al. 2002).
- **G2-M**: la activación de este punto de control impide la entrada de la célula a la fase M (mitosis), evitando que las anomalías celulares puedan transmitirse a las células hijas. Para activarlo se necesita que las quinasas ATR y ATM estén funcionales, ya que ambas activan muchas proteínas involucradas en la regulación del ciclo. En contraposición de las células normales, las células A-T no son capaces de parar su entrada en la fase M cuando son irradiadas en G2, debido a que ésta estimula la fosforilación y, por ello, la activación de CHK1 y Cds1/Chk2. La activación de Chk2 es dependiente de ATM (Zannini et al. 2014).

6. Alteraciones del sistema inmunológico, función pulmonar y longitud telomérica en A-T

Cerca de dos tercios de los pacientes A-T padecen anormalidades en el sistema inmune. Los defectos más frecuentes son niveles bajos de una o mas clases de inmunoglobulinas (IgA, IgG, IgM o subclases de IgG) fallando la eficiencia en hacer anticuerpos en respuesta a vacunas en infecciones y además la linfopenia afecta severamente los niveles de linfocitos. También hay un número reducido de células B nuevas que abandonan la medula ósea y el de células T que abandonan el timo, un número menor de células B y T no estimuladas y reducido repertorio del receptor de antígenos. En la mayoría de los individuos con A-T las anormalidades inmunológicas no se deterioran con el tiempo pero aproximadamente el 10% de ellos desarrollan problemas severos con la inmunidad humoral.

Los enfermos A-T tienen un alto riesgo de enfermedad crónica inflamatoria que ocurre como un efecto secundario de la inmunodeficiencia. Más del 25% de los pacientes A-T desarrollan enfermedad crónica pulmonar. La tos y la congestión son

síntomas tempranos en los pacientes A-T. Si estos síntomas tempranos no se tratan se produce un empeoramiento severo de la función pulmonar que incluye bronquiectasias, pneumonías recurrentes, fibrosis pulmonar y enfermedad intersticial pulmonar (ILD). La disregulación del sistema inmune lleva a pneumonias recurrentes, bronquiectasias e ILD. Los telómeros cortos y la sensibilidad a radiaciones ionizantes pueden aumentar el riesgo de complicaciones como la fibrosis pulmonar (Rothblum-Oviatt et al. 2016).

7. Mecanismo de acción de los péptidos GSE24.2 y GSE4

Las telomeropatías incluyen todas aquellas enfermedades con mutaciones en los componentes del complejo telomerasa, en el complejo shelterina o proteínas que interactúan directamente con los telómeros. Estarían englobadas diferentes enfermedades como disqueratosis congénita, en su variante más agresiva el síndrome de Hoyeraal-Hreidarsson o la fibrosis pulmonar idiopática. El estudio de estas enfermedades ha permitido profundizar en la investigación sobre las rutas que se encuentran alteradas en estos pacientes además del estudio de los componentes del complejo telomerasa.

El péptido GSE24.2 corresponde con un fragmento interno de la disquerina, proteína cuyo peso molecular de 58 Kda y en humanos está codificada por el gen *DKC1*. La disquerina forma parte del complejo telomerasa junto con TERT, TR, NOP10 y NHP2, entre otros (Figura 4). Las células de los pacientes con telomeropatías presentan una deficiencia en la actividad telomerasa consecuencia de las mutaciones en alguno de los genes que codifican para estas proteínas. Mutaciones en el gen *DKC1* da lugar a disqueratosis congénita ligada al cromosoma X (Bessler et al. 2004), mutaciones en hTR y hTERT están presentes en pacientes con disqueratosis congénita autosómica dominante/recesiva (Heiss et al. 1998) y en fibrosis pulmonar idiopática. Además células obtenidas de estos pacientes presentan una actividad telomerasa y un tamaño telomérico menor que las células de pacientes controles de la misma edad (Trowbridge et al. 1977). Mutaciones en otros genes del complejo telomerasa también han sido descritas, pero son menos frecuentes.

La expresión del GSE24.2 en líneas celulares de disqueratosis congénita induce en estas células mayor viabilidad, menor senescencia y una disminución en el daño al ADN y los niveles de ROS (Manguan-Garcia et al. 2014). Además, cuando se encapsuló el péptido GSE24.2 en nanopartículas biodegradables de PLGA/PEI (Egusquiaguirre et al. 2015), se observó que se veía incrementada la expresión de

ciertos genes del complejo telomerasa que se encontraban disminuidos, *TERT* y *TR*. Finalmente, el péptido GSE24.2 ha sido aceptado como medicamento huérfano por la EMA.

Recientemente ha sido descrito una secuencia peptídica de 11 aminoácidos que corresponde con la región N-terminal de la secuencia peptídica GSE24.2, al que se le conoce como GSE4 (Figura 7), y que presenta la misma actividad que el GSE24.2, en líneas celulares de DC y representa una mejor opción para enfocar posibles terapias en telomeropatías (Iarriccio et al. 2015).

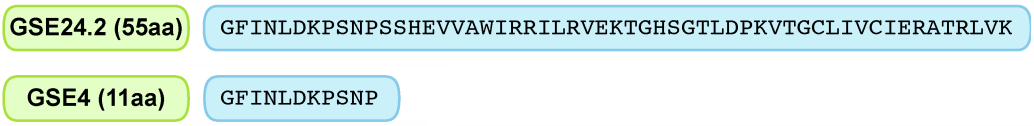

Figura 7: Secuencia de aminoácidos de los péptidos GSE24.2 y GSE4

OBJETIVOS

En objetivo principal de esta tesis es el estudio de la actividad de los péptidos GSE24.2 y GSE4 en células de pacientes de Ataxia Telangiectasia (A-T) para un posible uso como terapia en esta enfermedad.

Para ello nos hemos planteado 4 objetivos:

1. Obtención de líneas celulares de pacientes A-T con expresión estable de los péptidos GSE24.2 y GSE4.

2. Estudio de diferentes procesos celulares que se encuentran alterados en las líneas celulares A-T, tras la expresión de los péptidos GSE24.2 y GSE4.

3. Ensayo de nanopartículas para suministrar los péptidos GSE24.2 y GSE4 a líneas celulares A-T.

4. Estudio de la actividad telomerasa y la longitud telomérica de células A-T y efecto de la expresión del péptido GSE4.

MATERIALES Y MÉTODOS

1. Líneas celulares

1.1 Cultivos celulares

Para el desarrollo de este trabajo se han utilizado las siguientes líneas celulares humanas: HEK293T, células epiteliales inmortalizadas embrionarias de riñón; las líneas celulares controles: C-1787 (fibroblastos) y AT-736-C (linfoblastos), líneas celulares A-T con mutaciones en ATM: AT-3487 (fibroblastos), AT-3189 (linfoblastos), AT-719 (linfoblastos) y L137IIB (linfoblastos). La línea celular 293T fue obtenida de la ATCC y las demás se adquirieron de la empresa Coriell a excepción de la línea celular L137IIB que fue generada previamente en el laboratorio. Los linfoblastos se mantuvieron en cultivo en las condiciones de crecimiento recomendado por Coriell, medio RPMI (Gibco) suplementado al 20% con suero fetal bovino (Gibco), mientras que los fibroblastos se han crecido en medio DMEM (GIBCO) suplementado al 10% de suero fetal bovino, 1X fungizona, 2 mM de glutamina (Lonza), 56 μg/ml de gentamicina (Genta Gobens). Además, todas las células se mantuvieron en condiciones estándar de humedad (95%), presión de CO_2 (5%) y temperatura (37 ºC).

Los cultivos de fibroblastos murinos primarios (MEFs) fueron aislados de los cruces de ratones *Tdp2*$^{-/-}$ y *Atm*$^{-/-}$ y crecidos a 37 ºC, 5% CO_2, 3% O_2 in Dulbecco's Modified Eagle's Medium (DMEM) suplementado con penicilina-estreptomicina, 15% de suero fetal bovino y aminoácidos no esenciales. Los MEFs fueron inmortalizados con vectores retrovirales de T121, un fragmento del antígeno SV40, que antagoniza los miembros de la familia Rb pero no p53 (Alvarez-Quilon et al. 2014).

1.2. Anticuerpos utilizados en este trabajo

Los anticuerpos utilizados para las diferentes técnicas usadas a lo largo del trabajo se encuentran en la tabla 1.

1.3. Producción de plásmidos

Las bacterias se cultivaron durante 24 horas, y posteriormente se centrifugaron a 5000 rpm durante 15 minutos, y con el pellet de bacterias, utilizamos el protocolo del kit Qiagen, para obtener ADN, el cual eluímos en TE 1X.

Los plásmidos lentivirales usados en la producción de virus en este trabajo han sido los siguientes:

- pRRL-CMV-GSE4-IRES-eGFP expresando el GSE4 y la proteína GFP
- pRRL-CMV-24.2-IRES-eGFP expresando el GSE24.2 y la proteína GFP
- pRRL-CMV-IRES-eGFP expresando la proteína GFP

- pCD-NL-BH plásmido que produce proteínas para empaquetamiento de las partículas virales
- pMD2-VSV-G produce la envuelta viral (envuelta glicoproteica del virus de la estomatitis vesicular, VSVg)

ANTICUERPO	DILUCIÓN	TÉCNICA	CASA COMERCIAL
γ-H2A.X	1:100	Inmunofluorescencia	Cell Signaling
53BP1	1:100	Inmunofluorescencia	Cell Signaling
γ-H2A.X	1:1000	Inmunofluorescencia	Millipore
α-tubulina	1:2000	Inmunofluorescencia	Abcam
Vinculin h-VIN-1	1:2000	Inmunofluorescencia	Sigma Aldrich
p-p38 MAPK	1:2000	Western Blot	Cell Signaling
p38 MAPK (C-20)	1:1000	Western Blot	Santa Cruz
γ-H2A.X	1:1000	Western Blot	Cell Signaling
α-tubulina	1:5000	Western Blot	Sigma Aldrich

Tabla 1. **Anticuerpos utilizados en este trabajo**.

1.4. Producción de líneas celulares mediante el uso de lentivirus

Para generar los linfoblastos A-T que expresasen GFP, GSE24.2 o GSE4 se utilizó la infección con lentivirus concentrados; y para los fibroblastos se utilizaron lentivirus no concentrados.

Para la producción de virus se sembraron 1 millón de células HEK293T en placas de 10 cm^2, tras 24 horas se cotransfectaron con los siguientes plásmidos, (citados en el apartado 1.2): 15 μg del plásmido de interés (GFP, GSE24.2 o GSE4), 5 μg del plásmido empaquetador pCD-NL-BH y 5 μg del plásmido de la envuelta, pMD2-

VSV-G usando lipofectamina 2000 (Invitrogen) en medio libre de suero. A las 6 horas se procedió al cambio de medio, sustituyendo este último por medio DMEM suplementado al 10% con suero fetal bovino. A las 24 h se cambió el medio de nuevo, añadiendo 5 ml por placa, y a las 48 h y 72 h de la transfección fueron recogidos los sobrenadantes, con las partículas lentivirales, y se filtraron con un filtro de 0,45 μm y posteriormente se congelaron a -80 ºC para su posterior uso.

Para concentrar los virus se centrifugó el sobrenadante con virus a 25000 rpm durante 1.5 horas a 4 ºC. Se descartó el sobrenadante y el precipitado se resuspendió en 0,3 ml de DMEM con 10% suero. Los virus se mantuvieron en alícuotas a -80 ºC.

Para expresar el GSE24.2 o GSE4 en las diferentes líneas celulares se utilizó la técnica de infección, para ello se sembraron 100.000 células por pocillo en una placa de 24 pocillos, a las 24 h se eliminó el medio y se añadieron los sobrenadantes que contenían las partículas lentivirales, en presencia de 5 μg/ml de polibreno (Sigma) durante 24 h.

Para que la infección fuese más eficiente, se realizó una reinfección a las 24 horas después de la infección primera, únicamente en fibroblastos, y, añadiendo de nuevo polibreno (5 μg/ml) durante 24 horas. Puesto que los lentivirus utilizados no tenían un marcador de selección, las células infectadas se mantuvieron en cultivo hasta que se tuvieron número suficiente de células para realizar los experimentos.

La titulación se determinó en los linfoblastos por citometría de flujo (FACS) y en los fibroblastos se cuantificó el porcentaje de células verdes al microscopio de fluorescencia. Posteriormente se extrajo el ARN de las células y se comprobó mediante qPCR los niveles de expresión del GSE24.2 y del GSE4.

1.5. Tratamiento con nanopartículas

1.5.1. Nanopartículas PLGA-PEI empaquetadas con el péptido GSE24.2 o GSE4

Las nanopartículas PLGA-PEI son nanopartículas biodegradables las cuales en colaboración con el grupo del Dr. Pedraz fueron empaquetadas con los péptidos GSE24.2 o GSE4. Para los tratamientos celulares se sembraron 300.000 células por placa p35 sobre cubreobjetos de 12 mm de diámetro en 2 ml finales del medio correspondiente de las líneas celulares C-1787 (controles) y AT-3487. A las 24 horas fueron tratadas con 7,5 μg/ml de péptido cargado en las nanopartículas PLGA-PEI durante 48 horas (Egusquiaguirre et al. 2015). Transcurrido este tiempo las células fueron lavadas con PBS 1X y posteriormente

fijadas con formaldehido al 3,7% para posteriormente realizar diferentes análisis mediante inmunofluorescencia.

1.5.2. Nanopartículas GOS que contienen el péptido GSE4

Las nanopartículas GOS (Agostini et al. 2012) se basan en una matriz de silicio con una puerta molecular que se degrada por el enzima beta galactosidasa ácida presente en células senescentes (SA-β-gal) liberando así su contenido exclusivamente en estas células. Debido a que estas nanopartículas sólo admiten moléculas de pequeño tamaño sólo se cargaron con el péptido GSE4. Se sembraron 300.000 células/p35 sobre cristales de 12 mm de diámetro en 2 ml finales del medio correspondiente de las líneas celulares C-1787 (controles) y AT-3487, ambas son fibroblásticas y crecen adheridas a las placas. A las 24 horas fueron tratadas con 7,5 μg/ml de péptido cargado en las nanopartículas GOS durante 48 horas. Transcurrido este tiempo las células fueron lavadas con PBS 1X, antes de ser fijadas con formaldehido al 3,7% para posteriormente realizar diferentes análisis mediante inmunofluorescencia.

1.6. Viabilidad celular frente a fármacos

Para llevar a cabo los estudios de viabilidad frente a un fármaco, con células que presentan un crecimiento en suspensión, procedimos a utilizar el método MTS (Promega).

Para llevar a cabo este ensayo, las células se sembraron en placas de 96 pocillos, 1000 células/pocillo, en un volumen final de 50 μl/pocillo. Tras 24 horas de cultivo, las células se trataron con diferentes dosis de bleomicina. A las 72 horas de tratamiento se determinó la supervivencia celular utilizando el método colorimétrico basado en la reducción del compuesto [3-(4,5-dimethylthiazol-2-yl)-5-(3-carboxymethoxyphenyl)-2-(4-sulfophenyl)-2H-tetrazolium; MTS]. Para ello, se añadieron 20 μl de reactivo en cada pocillo y se incubó la reacción durante 3 horas a 37 ºC de temperatura, 95% de humedad y 5% de presión de CO_2. Posteriormente se cuantificó la cantidad de formazan soluble en el medio, originado por la reducción del MTS en las células metabólicamente activas, leyendo la absorbancia a 490 nm en un espectrofotómetro de placas (Molecular devices versamax tunable microplate reader). La viabilidad celular se calculó como el porcentaje de MTS reducido en cada dosis con respecto a las células sin tratamiento, representándose la media de tres experimentos independientes realizados por cuadruplicado con sus correspondientes desviaciones estándar (S.D.)

1.7. Ensayo de senescencia en células tratadas con nanopartículas

Para evaluar la senescencia celular se utilizó el kit Biovision. El ensayo se basa en valorar la actividad del enzima β–galactosidasa ácida (SA-β–gal), cuya expresión se induce en células senescentes. Para ello se sembraron 15.000 células por pocillo en una placa de 6 pocillos. Tras 24 horas se descartó el medio de cultivo y las células se lavaron con PBS 1X. Después se fijaron durante 15 minutos a temperatura ambiente usando la solución de fijación (Biovision). Tras la fijación se lavaron dos veces con PBS 1X, y se añadió 1 ml de la solución de tinción (940 μl de solución de tinción (Biovision), 10 μl del Suplemento (Biovision) y 50 μl de 20 mg/ml X-gal en DMSO por pocillo), incubando 24 horas a 37 ºC. Posteriormente se obtuvieron imágenes (15 por placa) y se cuantificó el número de células azules, que serían las positivas para SA-β–gal frente al número total de células analizadas. Los resultados se expresaron como porcentaje de células azules frente a las totales de cada campo fotografiado. En todos los ensayos se cuantificaron un mínimo de 200 células.

1.8. Estudio de crecimiento de la población de las líneas celulares que crecen en suspensión (PDLs)

Se estudió la capacidad de las células de duplicar la población, para ello se sembraron 400.000 células en un T25 y semanalmente se cuantificó el número de células utilizando Tripan Blue (SIGMA), para evaluar el número de células vivas presentes en la placa. Se volvieron a sembrar 400.000 células en una placa nueva y una semana después se hizo el recuento del número de células, y así sucesivamente hasta 8 semanas.

Se representaron los resultados como crecimiento acumulativo de las células infectadas con respecto a las controles a lo largo del tiempo.

1.9. Determinación del contenido de especies reactivas de oxígeno (ROS)

Este ensayo se realizó para evaluar la capacidad del GSE24.2 o GSE4 de disminuir el estrés oxidativo celular.

1.9.1. 2´,7´-Dichlorofluorescin Diacetate (DCFH-DA)

Es un sensor fluorescente de detección de capacidad oxidante de la célula. DCFH-DA es un colorante no polar, convertido en el derivado polar DCFH por esterasas celulares que son no fluorescentes pero que cambian a DCF altamente fluorescente cuando se oxidan por acción de los radicales reactivos de oxígeno intracelulares (ROS) y otros peróxidos.

Las células se contaron y ajustaron a $1x10^6$ células en 1 ml de medio en 2 tubos y a cada tubo se añadieron 1 dosis de DCFH-DA (10 mM Y 25 mM) (Santa Cruz Biotechnology) durante 25 minutos, transcurrrido este tiempo las células se centrifugaron a 1.500 rpm durante 5 minutos para eliminar el reactivo, se lavaron 2 veces con PBS 1X, y se resuspendieron en 1 ml de PBS 1X. Posteriormente utilizando un citómetro de flujo (FacScanII) se determinó la proporción de células positivas para el 2´,7´Dichlorofluorescin Diacetate, utilizando una longitud de onda de excitación de 502 nm y una longitud de onda de emisión de 523 nm. Los resultados se analizaron utilizando el programa WinMDI. Este compuesto permitió evaluar el estrés oxidativo celular presente de forma basal en las líneas celulares de A-T, pero no se pudo realizar el análisis en esas líneas infectadas, pues el GFP interfería con la señal del compuesto a analizar, por ello, se utilizó el DHE.

1.9.2. Dihidroethidium (DHE)

Este fluoróforo en el citoplasma celular tiene fluorescencia azul, pero por la acción de radicales activos de oxígeno se oxida, dando lugar a etidio, un producto con fluorescencia roja. Las células se contaron y ajustaron a 10^6 células en 1 ml y se añadieron 25 mM de dihidroethidium (DHE) (Life Technologies, Eugene, OR, EEUU.) y se incubaron a 37 ºC durante 25 minutos. Posteriormente se lavaron dos veces con tampón fosfato salino (PBS 1X). La fluorescencia se midió usando el citómetro de flujo FACscan (Becton Dickinson, Franklin Lakes, NJ, EEUU), con una longitud de onda de excitación de 530 nm y una longitud de onda de emisión de 630 nm. Se adquirieron 10.000 eventos por cada condición experimental y la población fue analizada usando los programas de análisis Cell Quest Pro 2.0 (Becton Dickinson) y WinMDI.

1.10. Determinación de expresión de proteínas mediante inmunofluorescencia

Para estos ensayos se sembraron 10.000 células por pocillo en un MW24 (con cubreobjetos). A las 24 horas las células fueron fijadas con una solución de formaldehido 3,7% durante 15 minutos a temperatura ambiente y posteriormente lavadas 3 veces con la solución de lavado (0,05% tritón X-100 + 2% BSA + PBS 1X), y después se incubaron 5 minutos en agitación con la solución de permeabilización (0,1% citrato sódico + 0,5% tritón X-100 + PBS 1X), se lavaron 3 veces con la solución de lavado, y se procedió al bloqueo de las mismas (0,05% tritón X-100 + 2% BSA + 1% suero de cabra + PBS 1X) durante una hora en agitación y se guardaron a 4 ºC para su posterior uso.

Se prepararon las diluciones del anticuerpo primario necesaria (Tabla 1, Cell Signaling) y se incubaron durante 24 horas en una cámara oscura a 4 ºC. Posteriormente, los cubreobjetos fueron lavados 3 veces con la solución de lavado antes de incubarlo durante 45 minutos con el anticuerpo secundario a temperatura ambiente (Alexa 488, Molecular Probes) con una dilución 1:500. Finalmente se lavaron 3 veces con la solución de lavado y se prepararon los portaobjetos. Para ello se preparó 100 μl de vectashield (Vector Laboratories, Inc) con 15 μl de Dapi 1000x y se sellaron los cubreobjetos con laca, y fueron guardados a 4 ºC para su visualización al microscopio confocal.

Para el análisis de los resultados se realizaron las fotos necesarias con el objetivo 63X en el microscopio confocal (Confocal Espectral Leica TCS SP5) para tener un contaje total de 200 células. Las imágenes fueron adquiridas utilizando LAS-AF 1.8.1 Leica y fueron cuantificados el número de focos de los anticuerpos correspondientes en cada célula mediante el uso de programa de imagen ImageJ.

Los resultados fueron representados en tres grupos, en función del número de focos presentes en el núcleo de cada célula de manera que el primer grupo representaba el porcentaje de células sin daño al ADN (lo forman todas las células con un número de focos de 0 a 4), el segundo grupo representaba el porcentaje de células con daño leve al ADN (lo forman todas las células con un número de focos de 5 a 29), y, el último grupo representa el porcentaje de células con mayor daño al ADN (lo forman todas las células con un número de focos mayor de 29).

Para llevar a cabo el estudio de la implicación de los péptidos GSE24.2 y GSE4 en la reparación del ADN mediada por ATM, se procedió a realizar una inmunofluorescencia específica en colaboración con el Dr Ledesma. Para ello las células se crecieron sobre cubres durante 7 días hasta que se llegó a confluencia, en ese momento se trataron con etopósido y posteriormente fijadas con metanol frío durante 10 minutos, después se procedió a la permeabilización (2 min in PBS-0.2% Triton X-100), y bloqueo (30 min in PBS-5% BSA), antes de proceder a la incubación con los anticuerpos primarios (1–3 h in PBS-1% BSA) (Tabla 1, Millipore y Abcam). Se realizaron 3 lavados con PBS-0,1% Tween 20, y se incubaron con los anticuerpos secundarios (1/1,000 dilucion en 1% BSA-PBS), con 3 lavados finales tras esta incubación. Para proceder a preparar los portas, se realizó de la misma manera citada previamente en el ensayo de inmunofluorescencia.

2. Análisis de la expresión de proteínas mediante "Western blotting"

Las células de las distintas líneas celulares, se centrifugaron 5 minutos a 1500 rpm, fueron lavadas 1 vez con PBS 1X, se centrifugaron de nuevo 5 minutos a 1500 rpm, y el pellet fue lisado con el tampón de lisis (tabla 2). Estos lisados se centrifugaron a 13000 rpm durante 15 minutos a 4 ºC. Se recogió el sobrenadante en un tubo nuevo y se procedió a medir la cantidad de proteína en cada extracto por el método del Bradford. Se cargaron 20 μg de proteína en 20 μl totales en geles SDS-poliacrilamida (Biorad) y se transfirieron a membranas de Inmobilon-P (Millipore) mediante transferencia en húmedo. Tras comprobar que la transferencia se había producido correctamente, para lo cual usamos el Rojo Ponceau (Sigma), las membranas se bloquearon con 5% leche ó 5% BSA (Sigma) disueltos en TBS (20 mM Tris-HCl pH 7,5, 150 mM NaCl) al que añadimos 0,1% Tween-20 (Sigma). Las membranas se incubaron durante toda la noche con los anticuerpos primarios correspondientes (ver tabla 1). Los anticuerpos secundarios utilizados anti ratón/conejo (Biorad), conjugados directamente con peroxidasa. Mediante una reacción de quimioluminiscencia con el reactivo ECL (Santa Cruz Biotechnology) se detectaron las bandas por autorradiografía (Konica).

TAMPÓN DE LISIS	INHIBIDORES DE PROTEASAS Y FOSFATASAS
0,2 mM EDTA	
0,3 M NaCl	1 μg/ml Leupeptina
1,5 mM $MgCl_2$	1 μg/ml Aprotinina
25 mM Hepes pH 7,5	0,5 mM DTT
0,1% Tritón X-100	100 mM Na_3VO_4
20 mM β-Glicerofosfato	100 mM ABSF

Tabla 2. Componentes del tampón de lisis y los inhibidores de proteasas y fosfatasas añadidas por ml de tampón. DTT: ditiotreitol. Na3VO4: ortovanadato sódico. ABSF: fluoruro de aminoetilbencenosulfonilo. Todos los inhibidores procedían de Sigma.

3. Análisis de la expresión génica

3.1. Extracción de ARN total de las líneas celulares

El ARN se aisló utilizando el Trizol (Life technologies) siguiendo las instrucciones del fabricante.

La cuantificación se llevó a cabo por espectrofotometría, midiendo la absorbancia a 260 y 280 nm en el espectrofotómetro NanoDrop ND2000. A partir de estos valores, se obtuvo la concentración de ARN en μg/μl. Todas las muestras utilizadas presentaban unos valores de ratio de lecturas dentro del rango óptimo (1.8-2.0).

3.2. Análisis de la expresión génica por qRT-PCR mediante el uso de sondas taqman

La expresión de los genes de interés fue cuantificada mediante la técnica de PCR a tiempo real. Para obtener el ADNc, partimos de 1μg de ARN total que se retrotranscribió a 37 ºC durante 1 hora usando una transcriptasa inversa (MMLV Promega). Para realizar la PCR se utilizó la mezcla de reacción Taqman Universal PCR Master Mix (Applied Biosystems), la información de las sondas taqman utilizadas se describen en la tabla 3.

GEN	ID
β-actina	Hs99999903_m1
catalasa	Hs00156308_m1
DKC1	Hs00154737_m1
GAPDH	Hs99999905_m1
IL-6	Hs00985639_m1
SOD1	Hs00533490_m1
SOD2	Hs00167309_m1
TERC	Hs03454202_s1
TERT	Hs00972650_m1

Tabla 3. Sondas Taqman utilizadas

Para la amplificación génica se utilizó el programa establecido con los siguientes parámetros: 10 minutos a 95 ºC, 40 ciclos de 15 segundos a 95 ºC y un minuto a 60 ºC. La expresión de *β-actina* se utilizó como control interno del ensayo.

La cuantificación relativa de la expresión génica se realizó utilizando el método comparativo 2 -ΔΔCt (Giulietti et al. 2001). Éste consiste en normalizar cada uno de los genes de estudio respecto a la expresión de un gen endógeno de referencia, en nuestro caso se ha utilizado la *β-actina*, y posteriormente en calcular la expresión normalizada de cada gen en la muestra problema respecto a la expresión normalizada del mismo gen en la muestra de referencia, presentándose los datos como el "cambio de veces de expresión (RQ)". Las barras de error se calcularon en base al cálculo máximo (RQMax) y el cálculo mínimo (RQMin) de los niveles de expresión y representamos la desviación estándar de la media del nivel de expresión (RQ).

3.3 Análisis de la expresión génica por qRT-PCR mediante oligonucleótidos

Para la comprobación de la eficiencia de la infección con los lentivirus expresando GSE24.2 o GSE4 se realizó una qPCR con oligos específicos (tabla 4) utilizando Syber Green. El programa de PCR utilizado dependió de los oligonucleótidos a usar. En este caso los programas que se utilizaron para la amplificación fueron los siguientes:

Para el GSE24.2; a) 95 ºC durante 5 min b) 35 ciclos de: 30 s a 94 ºC, 30 s a 60 ºC y 30 s a 72 ºC c) 5 min a 72 ºC.

Para el GSE4: a) 95 ºC durante 5 min b) 28 ciclos de: 40 s a 94 ºC, 60 s a 60 ºC y 40 s a 72 ºC c) 5 min a 72 ºC

Para *GAPDH*: a) 95 ºC durante 5 min b) 28 ciclos de: 40 s a 94 ºC, 60 s a 60 ºC y 40 s a 72 ºC, c) 5 min a 72 ºC

La cuantificación se llevó a cabo de la misma manera en que se ha realizado el análisis de la expresión de genes mediante el uso de sondas taqman.

GEN		OLIGONUCLEÓTIDO (5´-3´)
GSE24.2	DIRECTO	GGGGATCCTTATCGCTTCCGCTTCTTCACCAAGCGAGTGGCTCG
	REVERSO	GCAGTCGACGGTACCGCGGG
GSE4	DIRECTO	GATGGGTTTCATTAATCTTGACAAGCCCTCTAACCCCTAAG
	REVERSO	CCGTCAGATCGCCTGGAGACG
GAPDH	DIRECTO	GAGAGACCCTCACTGTTG
	REVERSO	GATGGTACATGACAAGGTGC

Tabla 4. Secuencia de los oligonucleótidos

4. Estudios específicos relacionados con telómeros

4.1. Obtención de ADN genómico

Se partió de un extracto celular al que después de lavar con PBS 1X se añadió 350 µl de DNAB 1X (150 mM NaCl, 50 mM EDTA, 20 mM Tris-HCL ph 7.6), 40 µl de SDS 10X y 20 µl de proteinasa K. Se incubó esta mezcla 24 horas a 56 ºC. Se procedió a extraer dos veces con igual volumen de fenol-cloroformo-isoamílico, y una vez con igual volumen de cloroformo, se incubaron 5 minutos en movimiento circular a 4 ºC y se centrifugó 5 minutos a 12000 rpm. Se añadió 2,5 volúmenes de etanol frío 100%, se centrifugó 5 minutos a 12000 rpm. Se lavó con etanol frío al 70%, se centrifugó 5 minutos, y tras secar se resuspendió el ADN en TE 1X. La concentración de ADN se determinó en un nanodrop.

4.2. Determinación de longitud telomérica utilizando la técnica de "Southern Blot"

El análisis mediante "Southern Blot" de los fragmentos de restricción terminal (TRF) es la técnica que se ha venido usando desde los primeros estudios de longitud telomérica y sigue siendo un método ampliamente utilizado (Carrillo et al. 2012).

Éste es un ensayo quimioluminiscente no radioactivo para determinar la longitud media telomérica gracias a que permite obtener los TRF mediante la digestión del ADNg. El ADNg purificado es digerido por una mezcla de enzimas de restricción,

Hinf1 y RSA1, que han sido seleccionadas porque no cortan ni el ADN telomérico ni el subtelomérico, mientras que el ADN no telomérico es digerido en fragmentos de muy bajo peso molecular.

Tras la digestión del ADNg, los fragmentos de ADN son separados mediante un gel de electroforesis, y se transfieren por capilaridad utilizando una membrana de nylon. Los fragmentos de ADN se hibridan con una sonda marcada con dioxigenina (DIG) que es específica para las repeticiones teloméricas y luego se incuba con un anticuerpo específico de DIG acoplado covalentemente a fosfatasa alcalina.

Finalmente, la sonda de telómeros inmovilizada se visualiza mediante un sustrato quimioluminiscente altamente sensible para la fosfatasa alcalina, CDP-Star (Figura 8). La longitud media de TRF puede determinarse comparando las señales con un patrón de peso molecular.

Como marcador de peso molecular se utilizó el suministrado por el kit TeloTAGG Telomere Length Assay (Roche) y se siguieron las instrucciones

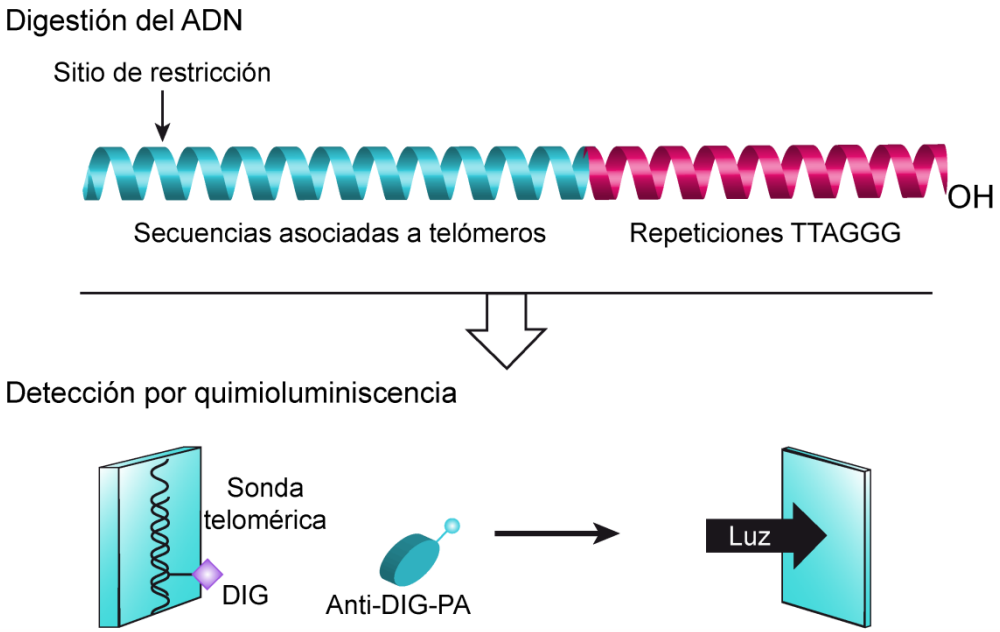

recomendadas.

Figura 8. Esquema del ensayo del "Southern Blot"

4.3. Estudio de longitud telomérica mediante qPCR

El análisis de la longitud telomérica mediante PCR cuantitativa (qPCR) es un método ampliamente utilizado (Cawthon 2002) cuando se dispone de poca cantidad de

ADN, ya que 20 ng de ADN son suficientes para el análisis. A diferencia del análisis de los TRF, el fragmento amplificado no incluye la región subtelomérica.

Para este ensayo se prepararon diluciones de los oligonucleótidos de la tabla indicada (tabla 5) a una concentración de 12 μM para los cebadores TelD y TelR y a una concentración de 4 μM para los cebadores 36B4D y 36B4R.

GEN		OLIGONUCLEÓTIDO (5´-3´)
Tel	DIRECTO	CGGTTTGTTTGGGTTTGGGTTTGGGTTTGGGTTTGGGTT
	REVERSO	GGCTTGCCTTACCCTTACCCTTACCCTTACCCTTACCCT
36B4	DIRECTO	CCCATTCTATCATCATCAACGGGTACAA
	REVERSO	CAGCAAGTGGGAAGGTGTAATCC

Tabla 5. Secuencia de oligonucleótidos para determinación de longitud telomérica mediante q-PCR.

Para este ensayo se realizaron las siguientes operaciones:

a. Preparar diluciones de ADN genómico estándar (a partir de células MCF-7):

A partir de ADN genómico obtenido de la línea celular se prepararon 5 diluciones progresivas (factor de dilución 1:4), partiendo de 8 ng/μl, en agua libre de DNasa/RNasa que se utilizan para realizar la curva estándar.

b. Preparar diluciones de ADN genómico de células:

Según la concentración conocida de ADNg se realizaron diluciones de trabajo de cada muestra en agua libre de DNasa/RNasa a una concentración de 1-2 ng/ml.

c. Medición de longitud telomérica mediante PCR cuantitativa:

Se preparó la mezcla de reacción ("Mix"): Power SYBRGreen PCR Master Mix (2X): 5 μl, Oligonucleótido TelD 12 mM: 0,75 μl, Oligonucleótido TelR 12 mM: 0,75 μl, Agua libre de DNasa/RNasa: 0,5 μl. Se añadieron 7μl de la mezcla de reacción a cada pocillo de la placa de PCR.

Se añadieron 3 μl por pocillo de las diluciones a 1-2 ng/ml del ADNg de las muestra (por triplicado) ó 3 μl por pocillo de cada dilución (D1 a D5) del estándar de ADNg de MCF7 (por duplicado) ó 3 μl de agua para los blancos.

Perfil Térmico de la PCR: a) 95 ºC durante 10 min b) 40 ciclos a: 95 ºC durante 15s, 58 ºC durante 30 s y 72 ºC durante 30 s c) 95 ºC durante 15 s, 55 ºC durante 15 s y 95 ºC durante 15 s.

d. PCR cuantitativa del gen de copia única 36B4 (SCG "Single Copy Gene"):

Se preparó la mezcla de reacción ("Mix"): Power SYBRGreen PCR Master Mix (2X): 5μl, Oligonucleótido 36B4D 4 mM: 0,75 μl, Oligonucleótido 36B4R 4 mM: 0,75 μl y agua libre de DNasa/RNasa: 0,5 μl y se añadieron 7μl de la mezcla de reacción a cada pocillo de la placa de PCR Posteriormente se añadieron 3 μl por pocillo de las diluciones a 1-2 ng/ml del ADNg de las muestra (por triplicado) ó 3 μl por pocillo de cada dilución (D1 a D5) del estándar de ADNg de MCF7 (por duplicado) ó 3 μl de agua para los blancos. El orden de las muestras/estándar en la placa de la PCR cuantitativa del gen 36B4 fue la misma que el orden que se utilizó anteriormente en la placa de la PCR cuantitativa de telómeros para las mismas muestras.

Perfil Térmico de la PCR: a) 95 ºC durante 10 min b) 40 ciclos a: 95 ºC durante 15 s, 58 ºC durante 1 min c) 95 ºC durante 15 s, 55 ºC durante 15 s y 95 ºC durante 15 s.

e. Análisis de los datos para calcular la longitud relativa de los telómeros (T/S):

El análisis de los datos se realizó con el programa ECOTM Software (Version 3.0): Se obtuvo una curva estándar usando las diluciones D1 a D5 del ADN de referencia de las células MCF7. El logaritmo de la concentración del ADN de referencia empleado en la curva estándar se representa frente al Ct obtenido. Se generaron dos curvas estándar, una para el telómero y otra para el gen de copia única. Para calcular la longitud relativa de los telómeros (T/S) de cada muestra se dividió el valor T (número de copias de los telómeros en nanogramos "Tel Mean Qty") entre el valor S (número de copias de gen de copia única en nanogramos "SCG Mean Qty"), determinados al extrapolar los valores de Ct en sus respectivas curvas de calibración. Cada muestra experimental se realizó por triplicado, calculándose los valores de T/S con el promedio de éstos.

4.4. Estudio de actividad telomerasa (TRAPeze Telomerase Detection Kit)

Determinamos la actividad telomerasa usando el protocolo del kit TRAPeze Telomerase Detection Kit, mediante el uso de radioactividad, de acuerdo a las instrucciones del fabricante con las siguientes modificaciones. La actividad telomerasa se determinó mediante la técnica TRAP(Kim et al. 1994), descrita por Kim y cols. Es una técnica derivada de la reacción en cadena de la polimerasa para la amplificación, in vitro, de los productos originados por la actividad ADN polimerasa de la enzima

telomerasa. En el primer paso de la reacción, la telomerasa añade un número de repeticiones teloméricas (GGTTAG) sobre el final 3' de un oligonucleótido sustrato (TS). En el segundo paso, los productos extendidos son amplificados mediante PCR usando primers TS y RP (reverso), generando productos con 6 bases incrementadas empezando 50 nucleótidos (50, 56, 62, etc.) (Figura 9).

Para extraer las proteínas, los extractos celulares se trataron con 200 μl de buffer de lisis CHAPS 1X (3-{[3-clomidopropil]-dimetil-amonio}-1-propanosulfonato), que incluía 0,5% CHAPS, 1 mM de $MgCl_2$, 5 mM de b-mercaptoetanol, 1 mM de EGTA (etilenglicol bis[b-aminoetil eter]-N,N,N',N' ácido tetraacético), 0,1 mM de AEBSF (4-[2-aminoetil]-bencenosulfonil fluoride hidroclorine), 10 mM de Tris-HCl (pH: 7,5) y 10% de glicerol.

Se mantuvieron las muestras en hielo durante 30 min y después se las centrifugó a 13000 x g durante 20 min a 4 ºC. Se retiraron cuidadosamente los sobrenadantes y se determinaron las concentraciones de proteínas mediante el método de Bradford.

El oligonucleótido TS se marcó en el extremo 5´ utilizando [γ- 32P]-ATP usando la enzima T4 polinucleótido quinasa (Promega) (tabla 6). Tras una primera incubación a 37 ºC durante 45 minutos, se procedió a la inactivación de la enzima mediante una incubación a 85 ºC durante 10 minutos. Después del marcaje se realizó la reacción de extensión de la telomerasa (paso 1 de la figura 9) a 30 ºC durante 30 min seguido de desnaturalización de 5 min a 94 ºC y posteriormente, se realizó la amplificación de las repeticiones teloméricas (paso 2 de la figura 9) en 30 ciclos de 94 ºC 30 s y 59 ºC 30 s; y, finalmente 1 minuto a 59 ºC (tabla 7).

Los productos de PCR se separaron en geles de acrilamida no desnaturalizantes al 10% y con cristales de 0,75 mm. La reacción se visualizó por autorradiografía y se analizó utilizando el programa de procesamiento de imágenes Image J. Además la actividad de la telomerasa se normalizó usando el control interno proporcionado en el kit.

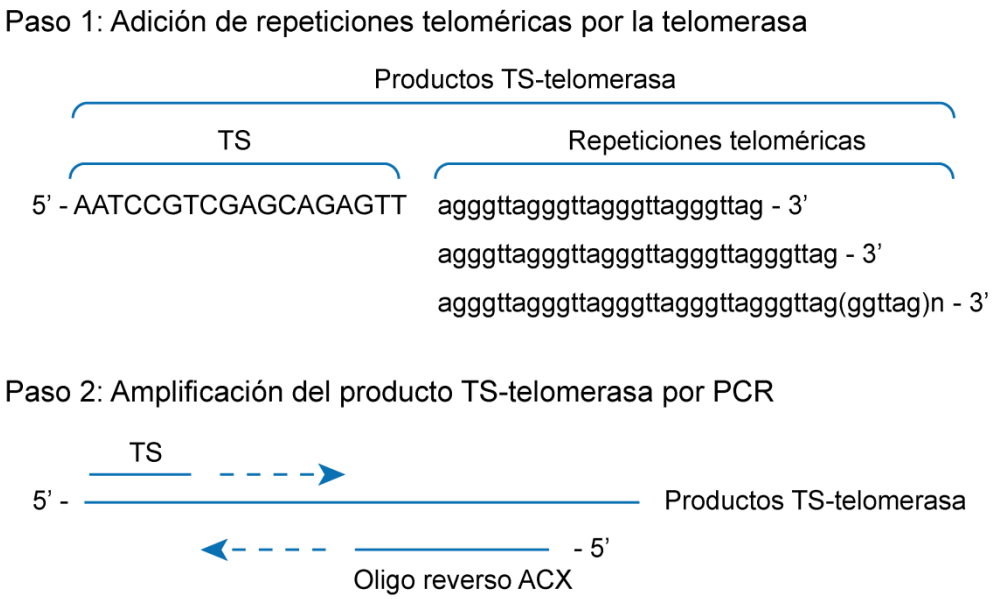

.

Figura 9: Esquema de la reacción de extensión de la telomerasa (Paso 1) **y amplificación de las repeticiones teloméricas** (Paso 2)

Mezcla	Volumen
γ-32P-ATP (10 mCi/ml)	2,5 μl
Oligo TS	10 μl
10x kinase buffer	2 μl
T4 polynucleotide kinase (10 U/μl)	0,5 μl
Agua	5 μl
Volumen final	20 μl

Tabla 6. Marcaje del oligonucleótido TS

Mezcla	Volumen
10x TRAP Reaction Buffer	5 μl
50x dNTP Mix	1 μl
Oligo 32P-TS	2 μl
TRAP Primer Mix	1 μl
Ampli Taq Gold (5 U/ml)	0,4 μl
Agua	38,6 μl
Volumen final	48 μl

Tabla 7. PCR radiactiva

5. Análisis estadísticos

Los datos mostrados en el presente trabajo representan la media ± la desviación estándar (S.D.) de al menos tres experimentos independientes. Para el cálculo de la significación estadística en las líneas celulares se utilizó el test T de Student para distribuciones normales de dos colas y datos no pareados con igualdad de varianzas. Se consideraron estadísticamente significativos valores de p menores de 0,05 (*) y 0,01 (**).

RESULTADOS

Las células de pacientes A-T, debido a la pérdida de actividad de ATM por las mutaciones en este gen, presentan defectos en reparar el daño al ADN de rotura de doble cadena así como incapacidad para compensar el aumento en el daño oxidativo. Por tanto, tienen unos niveles muy altos de radicales libres y daño oxidativo.

El tratamiento en estos pacientes se ha centrado en enlentecer el progreso de la neurodegeneración debido a la pérdida de las células de purkinje en el cerebelo y el mal funcionamiento de otras células neuronales que son la causa de la ataxia. Corregir la pérdida de las células de purkinje es técnicamente complicado, sin embargo, ya que el daño oxidativo contribuye a la muerte de estas células, las terapias diseñadas para disminuir este daño pueden ofrecer una salida terapéutica, frenando el avance de la enfermedad o al menos enlenteciéndolo.

El péptido GSE24.2 y el de menor tamaño GSE4 presentan capacidad de disminuir los niveles de radicales libres y el daño oxidativo en células de pacientes con disqueratosis congénita (Iarriccio et al. 2015). En esta Tesis hemos abordado una estrategia terapéutica en células A-T basado en la posibilidad de que los péptidos GSE24.2 o GSE4 serían capaces de disminuir el daño en el ADN y el estrés oxidativo inducido por la pérdida de función del gen ATM.

1. Generación de líneas celulares con expresión estable de los péptidos GSE24.2 y GSE4

Se adquirieron varias líneas celulares derivadas de pacientes A-T procedentes del instituto Coriell y que portaban diferentes mutaciones del gen ATM. Las líneas celulares de linfoblastos adquiridas fueron: AT-3189 y AT-719 y la fibroblástica AT-3487 y la línea celular control AT-736-C (linfoblástica). La línea celular linfoblástica L137IIB fue obtenida en el laboratorio a partir de un paciente A-T. Se infectaron las tres líneas celulares A-T con lentivirus lentivirus-CMV-eGFP o lentivirus-CMV-GSE24.2-eGFP o CMV-GSE4-eGFP para expresar ambos péptidos o la proteína GFP y se evaluaron los niveles de expresión tanto de GSE24.2 como GSE4 mediante qRT-PCR. Tal como se puede observar en la figura 10, todas ellas expresan los péptidos y por tanto se procedió a realizar los experimentos planificados.

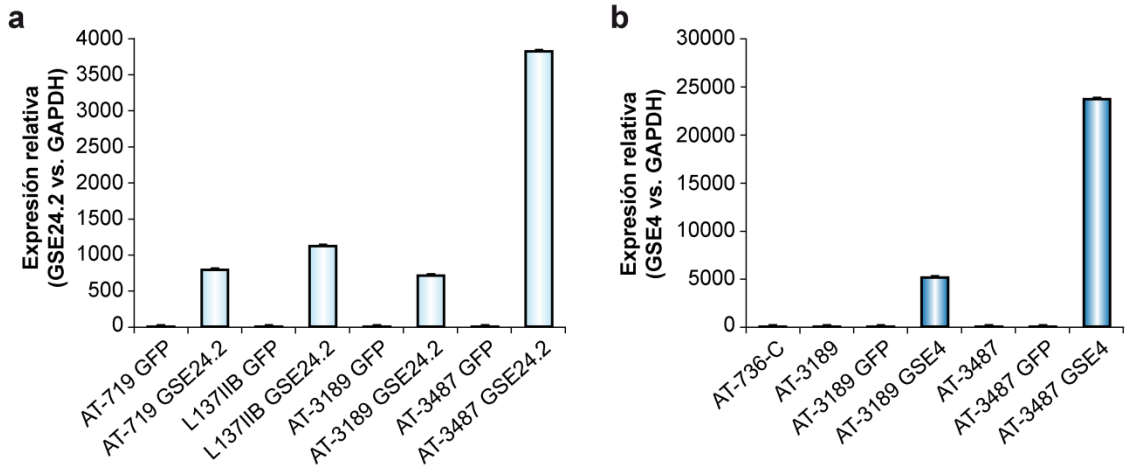

Figura 10. Análisis de la expresión de los péptidos GSE24.2 y GSE4 mediante qPCR. a) Análisis de la expresión del péptido GSE24.2. Después de infectar las líneas celulares de A-T con vectores lentivirales expresando GFP o GSE24.2, se extrajo el ARN, el cual fue retrotranscrito a ADNc, y se determinó la expresión de la secuencia GSE24.2 mediante qPCR utilizando el gen *GAPDH* como referencia. b) Análisis de la expresión del péptido GSE4. Después de infectar las líneas celulares de ataxia AT-3189 y AT-3487 con vectores lentivirales expresando GFP o GSE4, se extrajo el ARN, el cual fue retrotranscrito a ADNc, y se determinó la expresión de la secuencia GSE4 mediante qPCR utilizando el gen *GAPDH* como referencia. Se utilizó la línea AT-736-C como control.

2. Estudio del daño al ADN presente en las líneas celulares A-T y efecto de la expresión de los péptidos GSE24.2 y GSE4.

El estudio del daño al ADN basal presente en las células derivadas de pacientes A-T puede demostrarse analizando si se encuentra activa o no la respuesta al daño en el ADN.

El primer evento que ocurre en respuesta a las roturas de doble cadena (DSB) es la fosforilación de la histona H2A.X (γH2A.X), variante de la histona de la familia H2A, que se fosforila a nivel de la serina 139 en la región terminal del COOH (Rogakou et al. 1998). Dicha fosforilación se ha utilizado para evaluar la formación y reparación de DSB inducidas por diferentes agentes químicos, radiación ionizante y UV (Banath et al. 2004). El número de focos de γH2A.X formados en el ADN es directamente proporcional al número de DSB y su desfosforilación se ha correlacionado con la reparación de las DSB (Keogh et al. 2006). Evaluando mediante microscopía el número de focos nucleares podemos determinar y comparar el grado de daño genético presente en cada situación. El potencial que presenta este método para detectar un foco dentro del núcleo hace que actualmente sea el más sensible para evaluar este parámetro (Ismail et al. 2007).

Resultados anteriores del laboratorio demostraron que la expresión de los péptidos GSE24.2 o GSE4 disminuían el daño genético basal en células de pacientes con disqueratosis congénita. Por tanto se estudió si la expresión de estos péptidos también lo hacía en células A-T.

2.1. Efecto de la expresión del péptido GSE24.2

Se analizó mediante inmunofluorescencia la presencia de proteínas que median esta respuesta al daño al ADN como son la histona H2A.X fosforilada en la serina 139 y la de 53BP1, proteína que es reclutada a los focos de daño tras activarse la cascada de señalización de daño al ADN. Se utilizaron para este ensayo las células AT-3487 expresando GFP o el péptido GSE24.2 y como control la línea fibroblástica C-1787. Tras estudiar el número de focos por célula detectados con anticuerpos contra la histona H2A.X fosforilada o la proteína 53BP1, en las líneas celulares se comprobó que la línea celular AT-3487 expresando GFP presentaba un daño basal elevado indicado por mayor número de focos expresando γH2A.X y 53BP1 (Figura 11a y 11b). Además, se observó que en células de A-T con expresión estable del GSE24.2 había una disminución significativa en el número de focos expresando ambas proteínas.

2.2. Efecto de la expresión de GSE4

Para comprobar si el péptido GSE4 era capaz de inducir una disminución del daño al ADN, de forma similar al GSE24.2, se evaluó la expresión de γ-H2A.X. En este caso, se utilizó una línea celular A-T linfoblástica, AT-3189, y la línea celular control AT-736-C. Ya que en linfoblastos era más fácil evaluar la expresión de γ-H2A.X mediante “western blot” (Figura 12), se utilizó esta técnica. Como control de carga se rehibridaron los filtros con un anticuerpo contra α–tubulina. Se obtuvieron extractos de proteínas de células que habían sido infectadas con GFP o con GSE4. Después de cuantificar la intensidad de las bandas y establecer la relación de expresión entre la histona γ-H2A.X y α-tubulina se encontró que respecto a esta relación en las células AT-3189, las células controles AT-736-C presentaban un valor menor y que las células expresando GFP presentaron el mismo valor que disminuyó en las células expresando GSE4 a niveles similares a los encontrados en las células control AT-736-C.

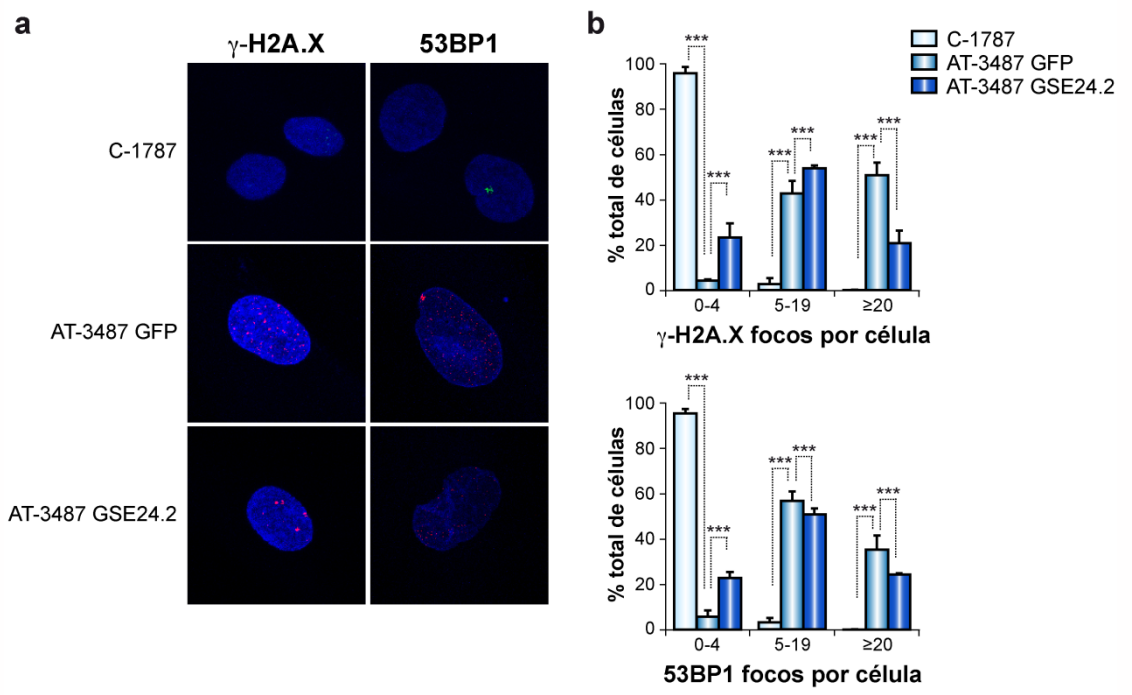

Figura 11. Estudio de la activación de la respuesta al daño en el ADN. Se sembraron 10.000 células AT-3487 con expresión estable de GFP, o GSE24.2 en MW24 sobre cubreobjetos de 12 mm de diámetro y se incubaron con anticuerpos primarios para γ-H2A.X o 53BP1, se incubaron con el correspondiente anticuerpo secundario y se prepararon los portas para tomar imágenes en el microscopio confocal (a). Se cuantificaron 200 células de cada línea celular generada y se agruparon en función del número de focos presentes en el núcleo (b), en el panel superior los resultados obtenidos para la histona γ-H2A.X y en el inferior los correspondientes a 53BP1. Los asteriscos indican diferencias significativas entre las líneas celulares. Los valores y las desviaciones estándar corresponden a dos experimentos independientes. Los experimentos se repitieron tres veces con resultados similares

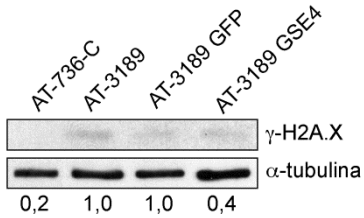

Figura 12. Análisis del daño en el ADN presente en la línea celular AT-3189 con expresión estable de GSE4 mediante "western blot". Los extractos proteicos obtenidos de las líneas celulares AT-736-C, AT-3189 y AT-3189 expresando GFP o GSE4 se analizaron "por western blot" para la expresión de la proteína γ-H2A.X, y como control de expresión se rehibridaron los filtros con un anticuerpo contra α-tubulina. En la figura se indica la relación entre la expresión de γ-H2A.X y α-tubulina. Los experimentos se realizaron tres veces con resultados similares.

2.3. Uso de nanopartículas cargadas con los péptidos GSE24.2 o GSE4

El uso de lentivirus es muy útil para estudiar la expresión de determinados genes, pero es importante poder hacer uso de una alternativa que permita su uso a nivel clínico, por ello, a la vista de los resultados presentados se procedió a evaluar el daño al ADN en la línea celular fibroblástica AT-3487, que se sometió a un tratamiento con nanopartículas de PLGA/PEI vacías o cargadas con el péptido GSE24.2 o GSE4 durante 48 h (Egusquiaguirre et al. 2015). Tras el tratamiento, se estudió la expresión de γ-H2A.X mediante inmunofluorescencia y se cuantificó en 200 células el número de focos expresando γ-H2A.X (Figura 13). Se observó que las células AT-3487 o AT-3487 tratadas con nanopartículas PLGA/PEI vacías presentaron un mayor número de células con más focos de expresión γ-H2A.X (en los grupos de 5-20 focos/célula) y, que estos disminuían significativamente cuando se trataron estas células con nanopartículas cargadas con los péptidos GSE24.2 o GSE4. Estos resultados validaban el uso de las nanopartículas como herramienta de tratamiento en las células A-T para inhibir el daño al ADN.

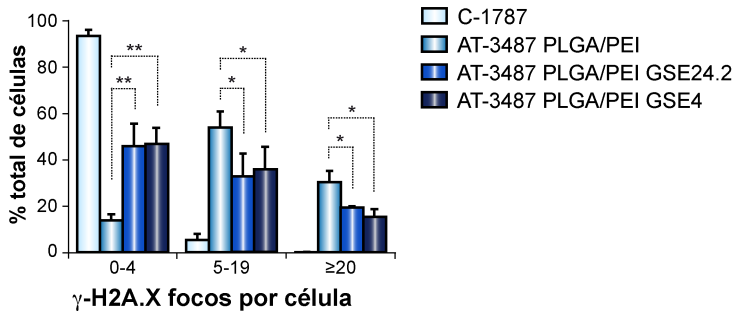

Figura 13: **Estudio del daño en el ADN en células tratadas con nanopartículas PLGA/PEI cargadas con los péptidos GSE24.2 o GSE4.** Las células AT-3487 se trataron con nanopartículas PLGA/PEI vacías o cargadas con 15 µg/2 ml de GSE24.2 o GSE4 durante 48 horas. Se determinó el daño al ADN, analizando la expresión de histona γ-H2A.X mediante inmunofluorescencia. Se estudiaron 200 células por tratamiento y se cuantificó el número de focos por célula con expresión γ-H2A.X. Los asteriscos indican diferencias significativas entre las líneas celulares. Los valores y las desviaciones estándar corresponden a dos experimentos independientes. Los experimentos se repitieron tres veces con resultados similares.

3. Tratamiento con nanopartículas GOS cargadas con el péptido GSE4 en células A-T

Está descrito que el aumento del daño al ADN de forma crónica induce en las células un aumento en el número de células senescentes. En el laboratorio se había descrito un tipo de nanopartículas mesoporosas (GOS) que eran capaces de liberar su contenido en células senescentes (Agostini et al. 2012). Por ello, se procedíó a utilizar estas nanopartículas cargadas con el péptido GSE4 en células A-T. Este tipo de abordaje nos permitía validar con otro tipo de nanopartículas los resultados obtenidos con las nanopartículas PLGA/PEI.

3.1. Evaluación del daño al ADN

Se procedió a evaluar el daño al ADN en la línea celular fibroblástica AT-3487, que se sometió a un tratamiento con nanopartículas GOS vacías o cargadas con el péptido GSE4 durante 48 h. Tras el tratamiento, se estudió la expresión de γ-H2A.X mediante inmunofluorescencia y se cuantificó en 200 células el número de focos correspondientes a γ-H2A.X (Figura 14a). Se observó que las células AT-3487 o AT-3487 tratadas con nanopartículas GOS vacías presentaron un mayor número de células con más focos de expresión γ-H2A.X respecto a las células C-1787 y que éstos disminuían significativamente cuando se trataron estas células con nanopartículas GOS cargadas con el péptido GSE4. Estos resultados indicaban que el daño al ADN en las células AT-3487, más senescentes que las controles, se revertía con el tratamiento con nanopartículas GOS GSE4 (Figura 14a).

3.2. Evaluación del daño oxidativo

El daño al ADN presente en las células A-T, además del producido por la roturas de doble cadena no reparadas, corresponde a daño oxidativo que se produce en los residuos de guanina oxidados que pasan a 8-oxoguanina. Por ello, procedimos a evaluar la presencia de 8-oxoguanina mediante inmunofluorescencia en células tratadas durante 48 h con nanopartículas GOS cargadas o no con GSE4. Los resultados (Figura 14b) muestran que el tratamiento con nanopartículas GOS cargadas con GSE4 en células A-T, era capaz de inducir una disminución del daño oxidativo, ya que se obtuvo una reducción del número de focos de 8-oxoguanina, correlacionado con una disminución en el número de focos de γ-H2A.X, y, por tanto, de daño al ADN. Por tanto, un porcentaje del daño basal y reparado en células A-T como consecuencia de la actividad del GSE4 es, en parte, daño oxidativo.

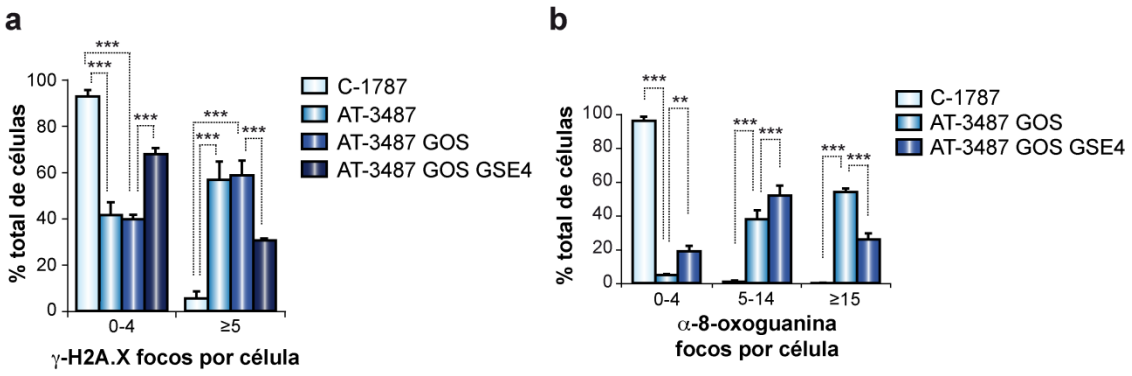

Figura 14: Estudio del uso de nanopartículas GOS cargadas con GSE4 en células A-T. Las células AT-3487 se trataron durante 48 h con nanopartículas GOS vacías o cargadas con GSE4. Se evaluó mediante inmunofluorescencia a) el porcentaje de daño al ADN analizando el número de focos de γ-H2A.X por célula. Se agruparon los resultados en 2 grupos: de 0-4 focos/célula y con 5 o más focos/célula. b) el porcentaje de daño oxidativo analizando el número de focos de 8-oxoguanina por célula. Los resultados se representaron en 3 grupos: de 0-4 focos/célula, de 5-14 focos/célula y más de 14 focos/célula. En ambos casos se utilizó la línea celular control C-1787 y se analizaron 200 células por tratamiento. Los asteriscos indican diferencias significativas entre las líneas celulares. Los valores y las desviaciones estándar corresponden a dos experimentos independientes. Los experimentos se repitieron tres veces con resultados similares.

4. Papel de los péptidos GSE4 o GSE24.2 en la recuperación del daño reparado específicamente por ATM

Tras iniciarse la cascada de señalización del daño al ADN, la proteína ATM es fosforilada en la serina 1981, continuando la activación de otras proteínas que permitirán que se repare el daño celular, que entren en senescencia o apoptosis. Debido a que ATM presenta un papel importante en reparación cuando la célula ha sufrido algún daño, nos planteamos estudiar el papel del GSE24.2 y GSE4 en la reparación de las lesiones inducidas por la pérdida de función de ATM. Para ello, en colaboración con Dr. Ledesma, procedimos a evaluar la activación de la respuesta al daño analizando la formación de focos γ-H2A.X inducido tras el tratamiento con el agente quimioterapeútico etopósido, el cuál genera roturas de doble cadena, que, en ausencia de la enzima TOP2 (Nitiss 2009), resulta en un bloqueo irreversible, requiriendo específicamente la función de ATM (Alvarez-Quilon et al. 2014) para la reparación.

Por ello, procedimos a estudiar, mediante IF, si la expresión del GSE24.2 y GSE4 pueden resctar el daño en respuesta a DSB. Para ello tratamos las células MEFs Tdp2$^{-/-}$ infectadas con los lentivirus-CMV-eGFP o lentivirus-CMV-GSE24.2-eGFP (figura 15a y 15b) o CMV-GSE4-eGFP con etopósido 10 mM durante 30 min en

presencia o no del inhibidor de ATM ku55933 (10 mM), al finalizar los 30 minutos se eliminó el etopósido y se procedió a fijar los cubres a tiempo 0, 3 o 6 horas con formaldehido al 3,7%, continuándose el protocolo de IF para estudiar formación de focos γ-H2A.X citado previamente.

La cuantificación del número de focos γ-H2A.X en células no tratadas y en los diferentes tiempos después de haber eliminado el etopósido se observa en la figura 15b, dónde observamos que la expresión del GSE24.2 o GSE4 no suple la reparación de daño no reparado por ATM, ya que no observamos desaparición de los focos γ-H2A.X en MEFs Tdp2$^{-/-}$ inducidos por etopósido en presencia del inhibidor de ATM, ni incluso 6 horas después de haber eliminado la droga. La reparación de este daño es dependiente de la función de ATM, ya que observamos que en ausencia del inhibidor de ATM el daño es reparado.

Podemos concluir que el efecto del GSE24.2 o GSE4 en la disminución de la acumulación de focos de la histona γ-H2A.X en células A-T es improbable que esté relacionado con la modulación de la señalización de la reparación de roturas de doble cadena que lleva a cabo ATM, pero lo más probable es que esté causado por la disminución en los niveles de daño oxidativo del ADN, que es la otra ruta defectuosa en células A-T.

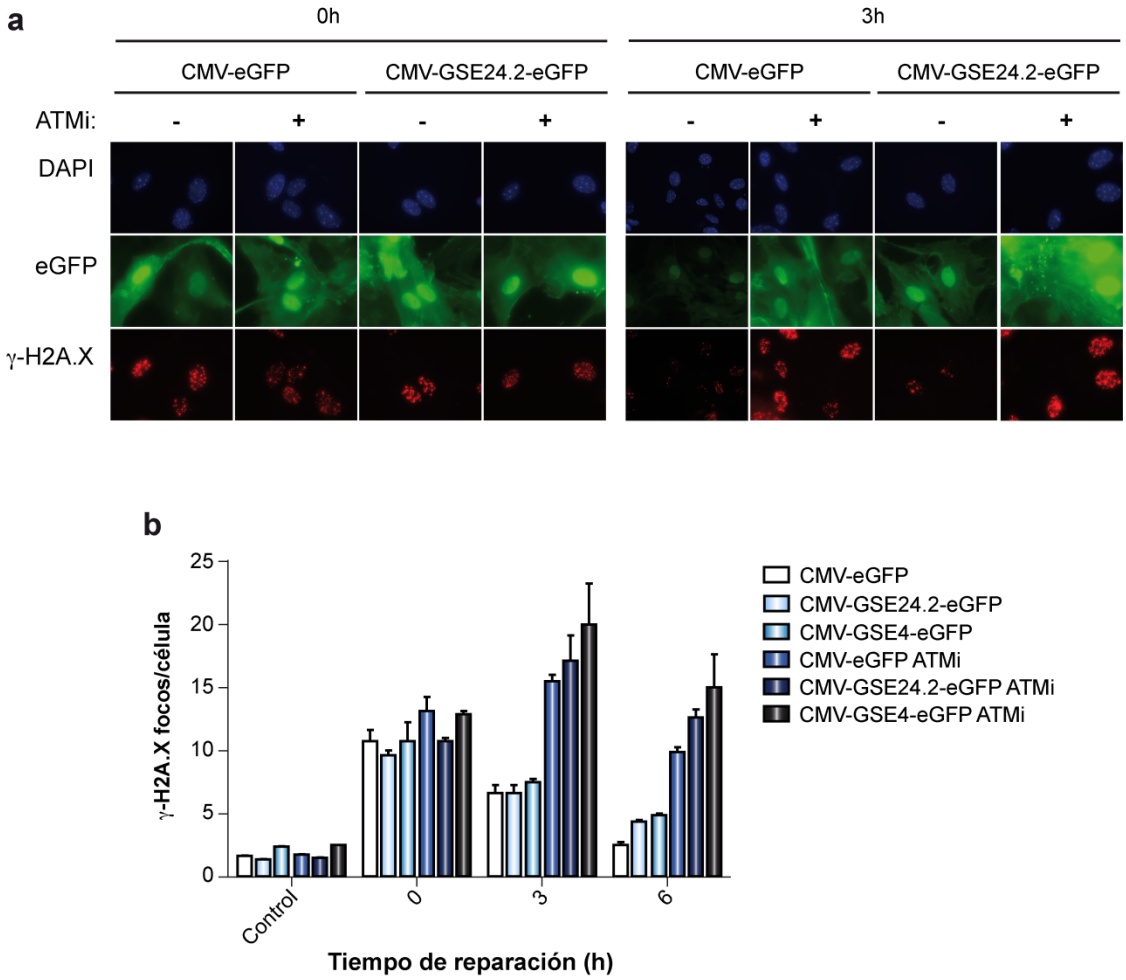

Figura 15. Papel del GSE24.2 y GSE4 en la resolución del daño reparado por ATM. Las células MEFs Tdp2$^{-/-}$ fueron infectadas con lentivirus expresando CMV-eGFP, CMV-GSE24.2-eGFP o CMV-GSE4-eGFP. Posteriormente se trataron con etopósido durante 30 minutos, en presencia o ausencia del inhibidor de ATM (ATMi). Se analizaron los focos positivos para γ-H2A.X mediante inmunofluorescencia a) Imágenes representativas representando los focos de γ-H2A.X (rojo) localizados en el núcleo celular (azul), en células expresando GFP o 24.2 (verdes) al inicio del ensayo y 3 horas después de haber sido eliminado el etopósido. b) Se representó el número medio de focos de la histona γ-H2A.X en las células expresando GFP, GSE24.2 o GSE4, en presencia o no del inhibidor de ATM cuando no habían sido tratadas con etopósido y tras los tiempos indicados después de haber sido eliminado el etopósido en las células. Los valores y las desviaciones estándar corresponden a dos experimentos independientes. Los experimentos se repitieron tres veces con resultados similares.

5. Estudio del estrés oxidativo en células de pacientes A-T expresando GSE24.2 o GSE4

El estrés oxidativo es producto de un desequilibrio entre la producción de especies reactivas de oxígeno (ROS) y la capacidad celular de eliminar rápidamente los reactivos intermedios o reparar el daño resultante. Existen productos que nos permiten evaluar la producción de estas especies reactivas de oxígeno como por ejemplo el Dihidroethidium que es capaz de detectar los radicales superóxido esencialmente.

En estudios recientes se ha mostrado que los pacientes A-T presentan niveles elevados de estrés oxidativo (Maciejczyk et al. 2017), por lo que se quiso comprobar el nivel basal de especies reactivas de oxígeno que presentaban una de estas líneas celulares A-T, AT-3189, que hemos utilizado a lo largo de este trabajo. Ya que se había observado una disminución de los niveles de 8-oxoguanina y de daño al ADN detectado por la fosforilación de H2A.X en células tratadas con GSE4, se quiso analizar si existía o no diferencia de los niveles de ROS en la línea celular AT-3189 y las que se habían obtenido expresando GSE24.2 o GSE4. Para ello se utilizó DHE y mediante citometría de flujo se cuantificaron los niveles de ROS. Se observó que esta línea celular AT-3189 presentaba niveles de radicales libres de oxígeno superiores a la línea celular control AT-736-C, y éstos se veían disminuídos alrededor de un 20% en las líneas que expresan el GSE24.2 o GSE4 con respecto a la que no lo expresa (Figura 16). Estos resultados indicaban que el estrés oxidativo en las células AT-3189 se veía diminuído en aquéllas que expresaban de forma estable el GSE24.2 o GSE4.

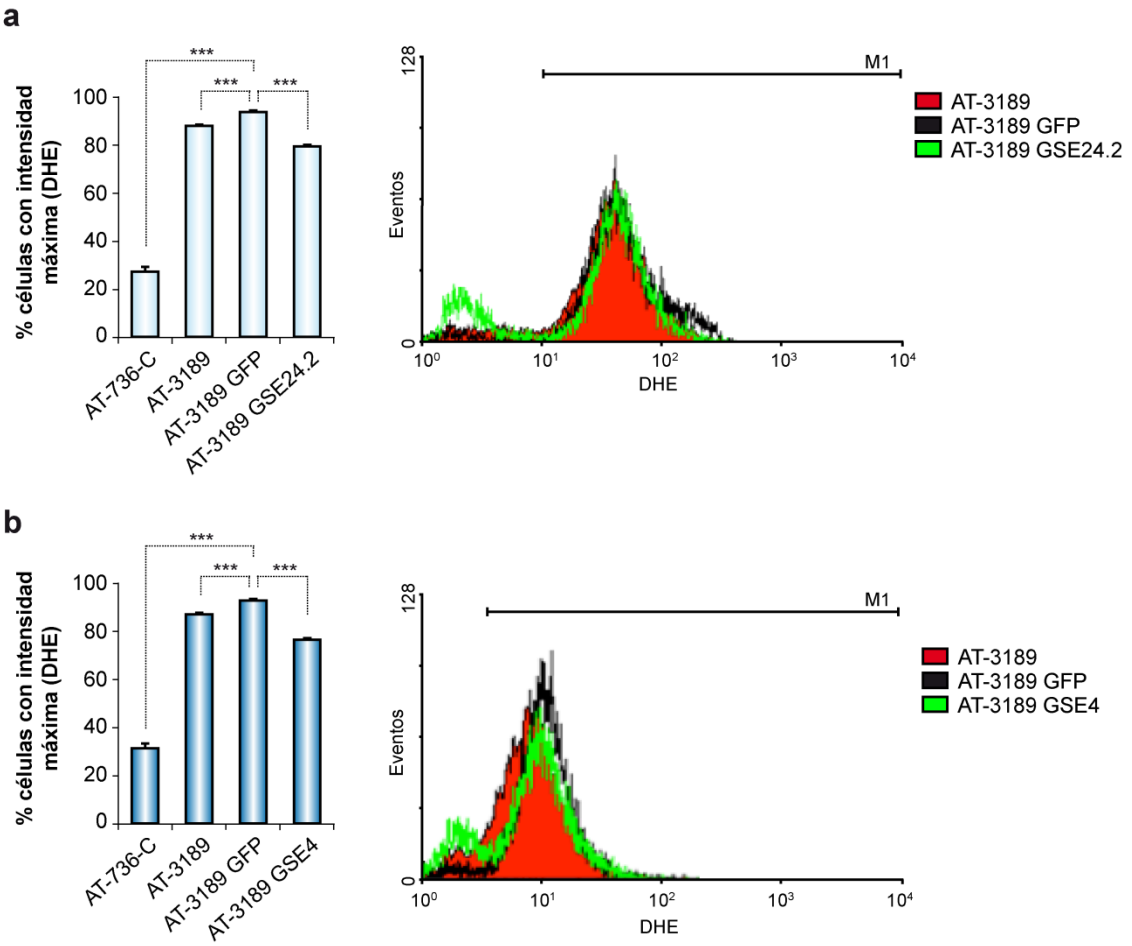

Figura 16. Cuantificación de las especies reactivas de oxígeno en líneas celulares A-T. a) Las células AT-3189 expresando GFP, GSE24.2 o GSE4 o las células control AT-736-C se inicubaron con DHE (5μM 25 minutos). Se evaluó mediante citometría de flujo los niveles de especies reactivas de oxígeno (ROS) a) resultados obtenidos en células expresando GSE24.2 b) o en células expresando GSE4. Los asteriscos indican diferencias significativas entre las líneas celulares. Los valores y las desviaciones estándar corresponden a dos experimentos independientes. Los experimentos se repitieron tres veces con resultados similares.

6. Análisis de la expresión de genes protectores de estrés oxidativo y de citoquinas pro-inflamatorias en células A-T

Una vez determinado que las líneas celulares de A-T presentan niveles elevados de estrés oxidativo y que éstos disminuían tras expresar el GSE24.2 o GSE4, se evaluó in vitro la expresión de algunos genes reguladores del metabolismo oxidativo en líneas celulares de A-T. Para ello, se estudiaron los niveles de expresión de los genes correspondientes a las enzimas antioxidantes como la *catalasa*, *superóxido dismutasas 1 y 2*. Como citoquina pro-inflamatoria nos propusimos estudiar los niveles de expresión de *IL-6* en líneas celulares A-T.

6.1. Expresión de genes *SOD1*, *SOD2* y *catalasa*

El organismo ha adquirido diferentes mecanismos de defensa contra los radicales libres a lo largo de la evolución. Con estos mecanismos se pretende reparar los daños que causan a las macromoléculas o degradar las lesionadas, prevenir su producción y detener o retardar la reacción de oxidación en cadena que desencadena el radical. Los mecanismos antioxidantes actúan de forma coordinada siendo los que constituyen la mejor defensa contra los radicales libres y entre los genes que pueden regular ese proceso están los que corresponden a la *superoxido dismutasa 1* (*SOD1*), *superoxido dismutasa 2* (*SOD2*) y *catalasa* (*CAT*) (Mates et al. 1999). Además, resultados previos indicaban que la expresión, tanto GSE24.2 como GSE4, aumentaban la expresión de estos genes en células DC (Manguan-Garcia et al. 2014; Iarriccio et al. 2015).

Se evaluaron los niveles que presentaban las diferentes líneas celulares de A-T en estos tres genes, y se estudió el efecto de la expresión de GSE24.2 o GSE4. Para ello se extrajo ARN de las células control AT-736-C, y las líneas celulares AT-3189, AT-719, L137IIB expresando GFP o GSE24.2 y las células AT-3189 expresando el GSE4, se retrotranscribió a ADNc y finalmente se evaluó mediante qPCR el nivel de expresión de los genes *SOD1*, *SOD2* y *CAT*. Los estudios demostraron que los niveles de enzimas antioxidantes que presentan las diferentes líneas celulares de A-T eran más bajos que las controles especialmente para *SOD1* y *catalasa*, mientras que no se observaron grandes diferencias en los niveles de expresión de *SOD2* entre las diferentes líneas celulares A-T y la línea control (Figura 17). Estos valores de expresión especialmente en el caso de *SOD1* y *SOD2* se incrementaban en las células con expresión estable del GSE24.2, mientras que en las células con expresión estable del GSE4 se obtuvo un aumento de expresión de los 3 genes estudiados (*SOD1*, *SOD2* y *CAT*).

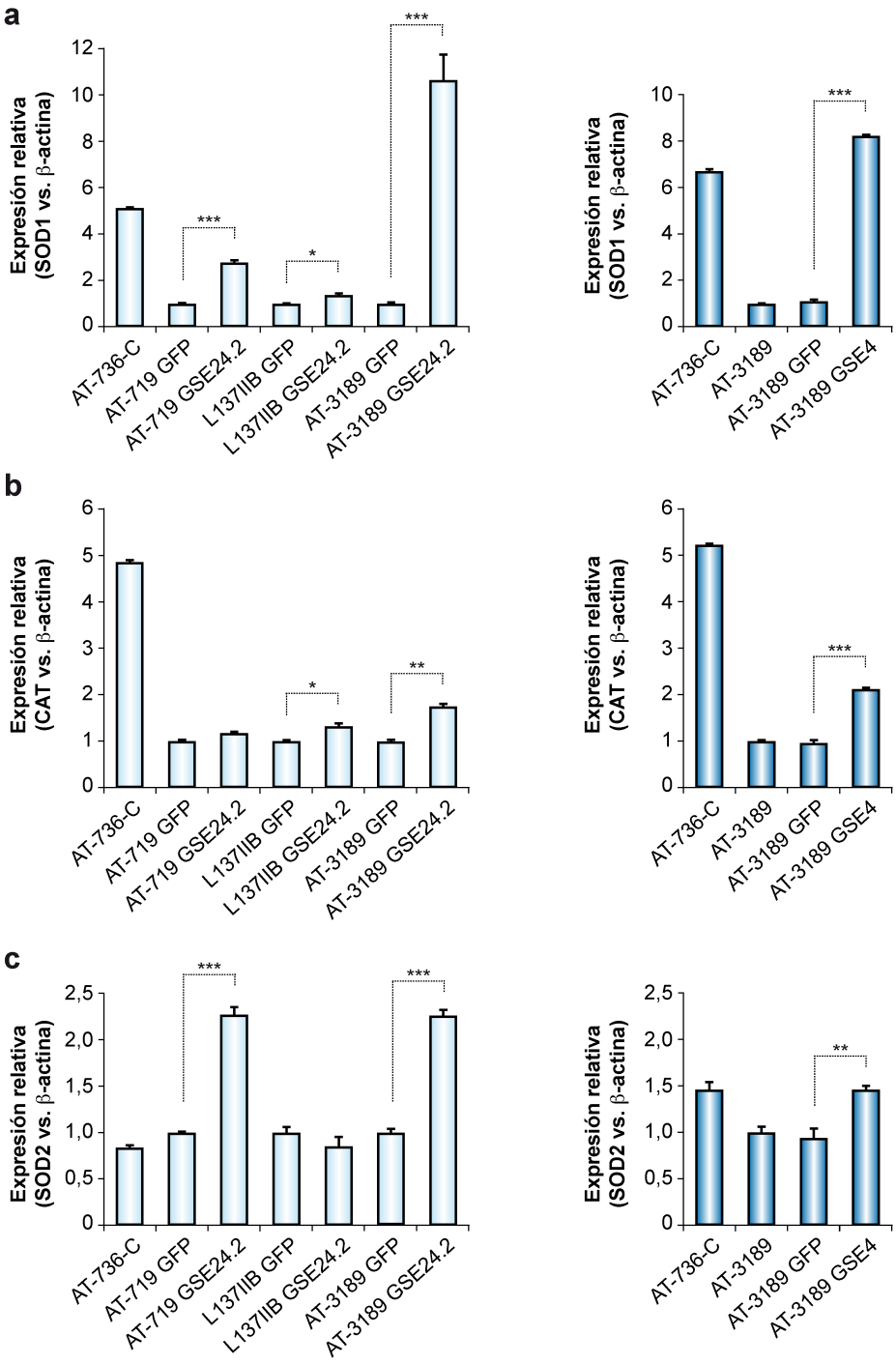

Figura 17. Niveles de expresión de enzimas antioxidantes. Se extrajo ARN de las líneas celulares: control AT-736-C y A-T: AT-3189, AT-719 y L137IIB expresando GFP o GSE24.2 y las células AT-3189 expresando el GSE4. El ARN fue retrotranscrito a ADNc, y se determinó la expresión de las diferentes enzimas antioxidantes a) *SOD1* b) *CAT* y c) *SOD2* mediante qPCR utilizando el gen *β-actina* como referencia y la línea celular AT-736-C como control. En la izquierda se encuentran representados los datos correspondientes a la expresión de estas enzimas antioxidantes en 3 líneas celulares de A-T expresando o no GSE24.2, y, a la derecha está representado la expresión de dichas enzimas en la línea celular AT-3189 expresando o no GSE4. Los asteriscos indican diferencias significativas entre las líneas celulares. Los valores y las desviaciones estándar corresponden a dos experimentos independientes. Los experimentos se repitieron tres veces con resultados similares.

6.2. Expresión de *IL-6* en células A-T

La IL-6 es una citoquina con actividad pro-inflamatoria que se produce en lugares de inflamación aguda o crónica en los cuales se secreta al suero e induce la respuesta inflamatoria a través de la interacción con su receptor alfa. Se ha propuesto que la cascada de señalización que se activa como respuesta a un daño persistente del ADN activa la secreción de citoquinas que incluye IL-6 que son responsables de fenotipo senescente asociado a inflamación (SASP) (Coppe et al. 2010; Campisi et al. 2011).

Ya que el aumento en los radicales libres y la falta de reparación en las roturas de ADN de doble cadena originadas como consecuencia de la falta de actividad de ATM resulta en daño en el ADN, se determinaron los niveles de expresión de *IL-6* en las diferentes líneas celulares A-T. Se extrajo ARN de las líneas celulares: control AT-736-C y A-T: AT-3189 y AT-719, L137IIB expresando GFP o GSE24.2 y las células AT-3189 expresando el GSE4, y mediante qPCR se determinaron los niveles de *IL-6*. En la figura 18a se puede observar que todas las líneas de A-T linfoblásticas que se han utilizado en este trabajo presentan niveles altos de expresión de *IL-6*, siendo la línea celular AT-3189 la que presenta los mayores niveles. Sin embargo, se ha comprobado que estos niveles de *IL-6* se ven disminuídos en aquellas líneas celulares que expresan GSE24.2, presentando la disminución más significativa la línea celular AT-719 (Figura 18a). En la figura 18b se puede observar que la línea celular AT-3189 expresando GSE4 presenta una mayor disminución de expresión de *IL-6* que la observada en la misma línea celular con expresión estable del GSE24.2, llegando a tener casi los valores de expresión de *IL-6* a los de la línea celular control, AT-736-C. Estos resultados podrían indicar que el GSE4 tiene una mayor capacidad de disminuir la expresión de *IL-6* que el GSE24.2.

Estos resultados están de acuerdo con la disminución de los niveles de ROS y del daño al ADN observado en estas líneas celulares A-T expresando ambos péptidos que pueden determinar los niveles más bajos en la expresión de *IL-6*.

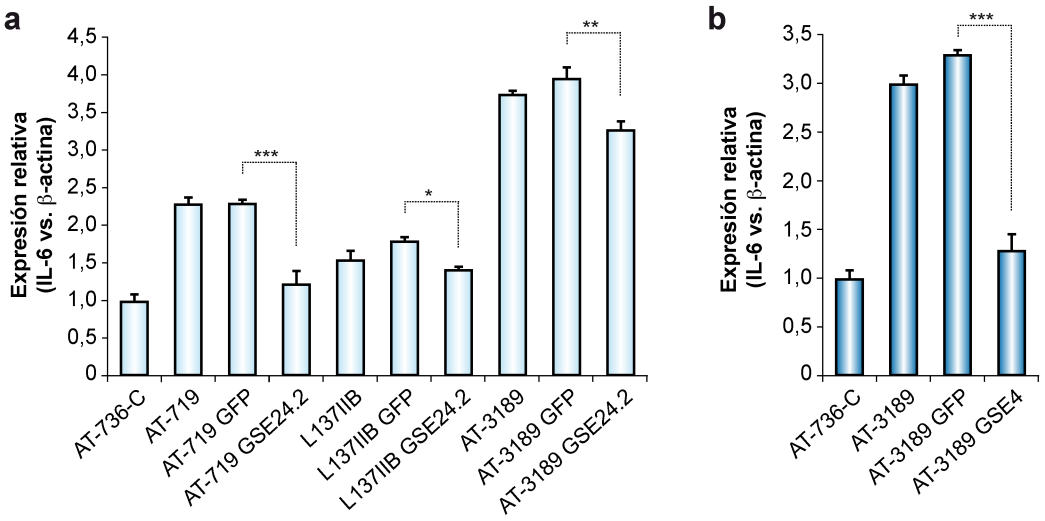

Figura 18. Niveles de expresión de interleuquina 6. Se extrajo ARN de las líneas celulares: control AT-736-C y A-T: AT-3189, AT-719 y L137IIB expresando GFP o GSE24.2 y las células AT-3189 expresando el GSE4. El ARN fue retrotranscrito a ADNc, y se determinó la expresión de la *interleuquina 6* mediante qPCR y utilizando la *β-actina* como gen de referencia a) Niveles de expresión de *IL-6* en las diferentes líneas celulares de A-T con expresión estable o no del GSE24.2 b) Niveles de expresión de *IL-6* en la línea celular AT-3189 con expresión estable o no del GSE4. Los valores y las desviaciones estándar corresponden a dos experimentos independientes. Los experimentos se repitieron tres veces con resultados similares.

7. Evaluación de la senescencia

Los pacientes A-T presentan una disminución de la función de ATM, que está involucrado en regulación del nivel de radicales libres, reparación del daño en el ADN de doble cadena e inducción de senescencia y apoptosis. Se ha encontrado en los apartados anteriores de este trabajo, que la expresión de GSE24.2 o GSE4 disminuye los niveles de radicales libres pero no se observa un aumento en la reparación del ADN mediada por ATM. Con el fin de investigar si la disminución en el daño oxidativo en el ADN y la disminución en los niveles de *IL-6* tenían impacto en la senescencia celular, se estudió si las células A-T expresando el GSE24.2 o GSE4 presentaban un menor número de células senescentes. Para ello se utilizaron en primer lugar nanopartículas GOS cargadas con el péptido GSE4 que descargan su contenido sólo en células senescentes. Para ello se procedió a tratar células AT-3487 con nanopartículas GOS vacías o cargadas con GSE4 durante 48 horas y se evaluó el número de células senescentes como aquéllas que expresaban β-glactosidasa ácida, Sa-β-gal. Se observó que las células AT-3487, presentaban un mayor porcentaje de células senescentes, respecto a las células controles C-1787, además con el tratamiento con nanopartículas GOS había una disminución en las células AT-3487 del

20% de células positivas para el SA-β-Gal en aquellas tratadas con GOS-GSE4 respecto a las tratadas con nanopartículas GOS vacías (Figura 19a).

También se evaluó el porcentaje de células senescentes utilizando células AT-3487 con expresión estable de GSE24.2 o GSE4. En las células infectadas se observa que el porcentaje de células senescentes disminuye tanto en aquellas células AT-3487 que expresaban el GSE24.2 como las que expresaban el GSE4, apreciable en mayor medida según pasaban más días tras la infección (Figura 19b).

Por tanto, se puede concluir que el tratamiento con nanopartículas cargadas con GSE4 o la infección con lentivirus expresando GSE24.2 o GSE4 disminuye el número de células senescentes.

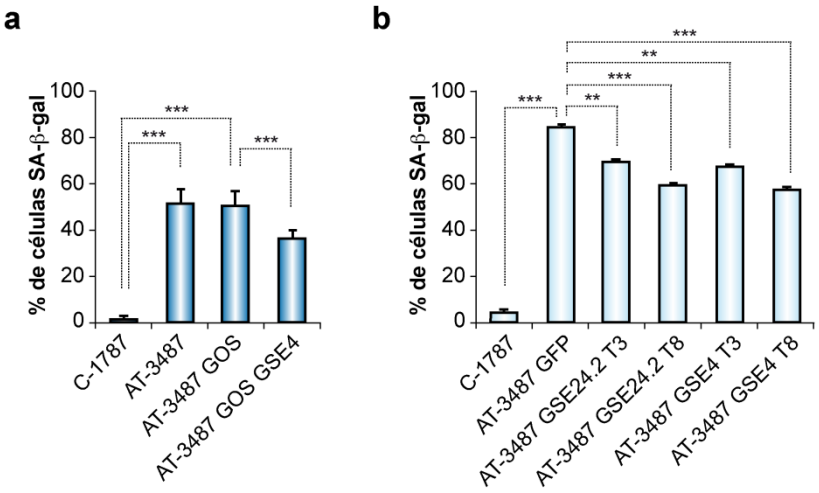

Figura 19. Estudio de senescencia celular mediante un ensayo de SA-β-gal a) la línea celular AT-3487 se trató con nanoparticulas GOS vacías o cargadas con el equivalente de 15 μg/2ml de péptido GSE4 durante 48 h, como línea celular control se utilizó C-1787. Se realizó la tinción de la actividad β-galactosidasa y se determinó el número de células senescentes respecto al total y se representó como porcentaje. b) Determinación de actividad β-galactosidasa en las células AT-3487 expresando GFP, GSE24.2 o GSE4 de forma estable, 3 días u 8 días después de la infección y como control la línea celular C-1787. Se realizó la tinción de la actividad β-galactosidasa y se determinó el número de células senescentes respecto al total y se representó como porcentaje. Los asteriscos indican diferencias significativas entre las líneas celulares. Los valores y las desviaciones estándar corresponden a dos experimentos independientes. Los experimentos se repitieron tres veces con resultados similares

8. Evaluación del crecimiento celular

Tras generar las diferentes líneas celulares con expresión estable del GSE4 o GSE24.2 mediante infección con lentivirus, se procedió a evaluar si la expresión de ambos péptidos podría influir en el crecimiento celular. Tras observar una disminución de estrés oxidativo acompañado de un aumento de expresión de enzimas antioxidantes, y de una disminución del porcentaje de células senescentes nos sugería que se podría observar algún cambio en la capacidad de crecimiento de las líneas celulares.

Para evaluar si la expresión del GSE24.2 o GSE4 estaban incrementando la capacidad de proliferación de los linfoblastos A-T se evalúó el crecimiento celular a lo largo de dos meses. Para ello, se mantuvo en crecimiento la línea celular AT-3189 con expresión estable de GFP, GSE24.2 o GSE4 durante 2 meses después de la infección. Para cuantificar el crecimiento se utilizó un protocolo de cultivo similar al utilizado para estudiar el número de duplicaciones a lo largo del tiempo de una línea celular o PDL. Cada semana se contabilizó el número de células que había en la placa, y se resembraron un número determinado y similar de células cada vez, de manera que al cabo de 2 meses pudimos obtener la relación semanal de incremento de crecimiento entre las células que expresan GFP con respecto a las que expresan GSE24.2 o GSE4. Los datos se representaron como crecimiento acumulativo a los largo del tiempo en cultivo. En la figura 20 se puede observar que durante el primer mes no se produjeron cambios significativos en el crecimiento celular, aunque las células que expresan el GSE24.2 empezaban a presentar un crecimiento más acelerado, mientras que las células que expresan GSE4 no presentaban cambios en el crecimiento con respecto a las células que expresaban GFP. Sin embargo, es durante el segundo mes cuando empezamos a ver claras diferencias de crecimiento con respecto al control, tanto en la línea celular que expresa GSE24.2 como en la que expresa GSE4, probablemente debido a que necesitaban un tiempo para recuperarse del proceso de infección para poder ver cambios a este nivel.

Gracias a este estudio comprobamos que la expresión del GSE24.2 o GSE4 puede ser beneficiosa para el crecimiento de los linfoblastos A-T pues confiere a las células de una mayor capacidad de crecimiento a lo largo del tiempo.

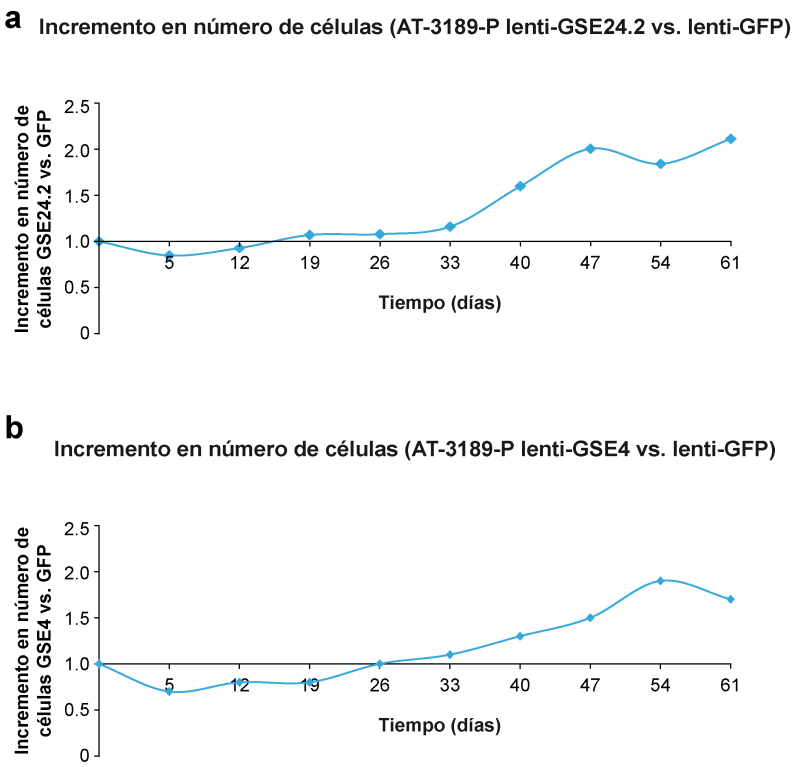

Figura 20. Estudio del crecimiento celular. Durante 2 meses se evaluó la capacidad de multiplicación en varias líneas celulares A-T con expresión de GFP, GSE24.2 o GSE4 a) Ratio de crecimiento de células AT-3189 con expresión de GSE24.2 con respecto a células que no lo expresan. b) Ratio de crecimiento de células AT-3189 con expresión de GSE4 con respecto a células que no lo expresan.

9. Análisis de p38 MAPK

Las proteínas quinasas activadas por mitógeno (MAPK) son una familia de serina/treonina quinasas que participan en procesos celulares tan importantes como el crecimiento celular, proliferación, muerte y diferenciación en respuesta a una serie de estímulos (Pearson et al. 2001). Entre los miembros de la familia MAPK, los mitógenos y factores de crecimiento frecuentemente activan la ruta ERK1/2, mientras que el estrés y procesos inflamatorios constituyen el principal desencadenante de la cascada de JNK y p38 MAPK, algunas veces referidas como “proteínas quinasas activadas por estrés”. Por tanto, median respuestas a choques osmóticos, citoquinas inflamatorias y otras agresiones frecuentemente asociadas con decisiones de supervivencia y apoptosis (Nebreda and Porras 2000).

Debido a que se había observado que las diferentes líneas celulares de A-T presentaban altos niveles ROS e IL-6, ambos parámetros asociados a inflamación, se procedió a estudiar si los niveles de fosforilación de p38 MAPK estaban alterados en

estas líneas celulares, y en tal caso investigar si el tratamiento con GSE24.2 o GSE4 sería capaz de modificarlo.

Para evaluar la fosforilación de p38 MAPK presente en las líneas celulares de A-T con expresión estable de GFP, GSE24.2 o GSE4 se realizó un "western blot" partiendo de extractos celulares de células controles (AT-736-C) o AT-3189 o AT-719 expresando GFP o GSE24.2 y las células AT-3189 GSE4. La fosforilación de p38 MAPK en los residuos Thr180/Tyr182 se evaluó hibridando con un anticuerpo específico y posteriormente los niveles de expresión de p38 MAPK se evaluaron con un anticuerpo contra esta proteína. Se observó un aumento de fosforilación de p38 MAPK en todas las líneas celulares de A-T, al compararlo con la activación de p38 MAPK en la línea celular control, AT-736-C. Por otra parte se observó una disminución en aquellas células A-T que expresaban el péptido GSE24.2 (Figura 21a) o GSE4 (Figura 21b) con respecto a la que la misma línea celular expresando GFP. Por tanto, se puede concluir que en las líneas celulares que expresaban GSE24.2 o GSE4, la menor producción de ROS y menor expresión de *IL-6* podría resultar en una menor activación de p38 MAPK.

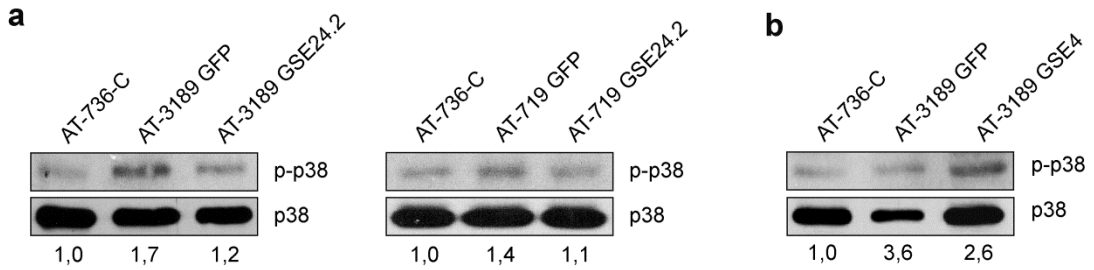

Figura 21. Estudio de la fosforilación de p38 MAPK mediante "western blot". Se obtuvieron extractos proteicos de las diferentes líneas linfoblásticas de A-T comparándolo con la línea control AT-736-C. Los niveles de fosforilación de p38 MAPK se evaluaron utilizando un anticuerpo específico que detecta los residuos Thr180/Tyr182 fosforilados. Posteriormente las membranas se rehibridaron con un anticuerpo contra la proteína p38 MAPK no fosforilada. En la parte inferior de cada carril se representa la relación entre la intensidad de la banda p-p38 MAPK y p38 MAPK. a) Niveles de p-p38 MAPK y p38 MAPK en las líneas linfoblásticas de A-T: AT-3189 y AT-719 expresando GFP o GSE24.2 b) Niveles de p-p38 MAPK en la línea celular AT-3189, expresando GFP o GSE4.

10. Viabilidad celular frente a bleomicina

Las células A-T, debido a que la actividad de la proteína ATM es deficiente en la reparación de roturas de doble cadena en el ADN, son mucho más sensibles a agentes que inducen DSB como radiación ionizante o la bleomicina.

La bleomicina es un glicopéptido con actividad como antibiótico y antitumoral sintetizado por la bacteria Streptomyces verticillus. Este compuesto se une a secuencias en al ADN ricas en guanosina y citosina. Reacciona químicamente con las bases del ADN y produce oxígeno, que produce especies de oxígeno altamente reactivas que inducen roturas de cadena simple en el ADN que posteriormente terminan con la rotura de la segunda cadena. Puesto que la bleomicina puede aumentar los niveles de ROS se planteó la evaluación de la viabilidad de las líneas celulares de A-T a diferentes dosis de bleomicina.

Debido que las líneas celulares linfoblásticas de A-T crecen en suspensión, se evaluó la viabilidad frente a la bleomicina mediante la técnica MTS. Para ello, se hicieron curvas de viabilidad frente a concentraciones crecientes de bleomicina durante 72 horas. Se encontró que en la línea celular AT-3189 expresando GFP hay un menor porcentaje de células viables en relación a las células controles AT-736-C, con una IC50 menor. Por otra parte, las células AT-3189 expresando GSE24.2 o GSE4 presentan una mayor viabilidad frente a bleomicina y en los dos casos intermedia entre la de las células controles y las células A-T expresando GFP (Figura 22 a y b). Se pudo observar que el índice de resistencia de las células AT-3189 GSE24.2 era 18 veces mayor que el de las mismas células expresando GFP. En el caso de las células AT-3189 GSE4 este índice de resistencia era 16.

a

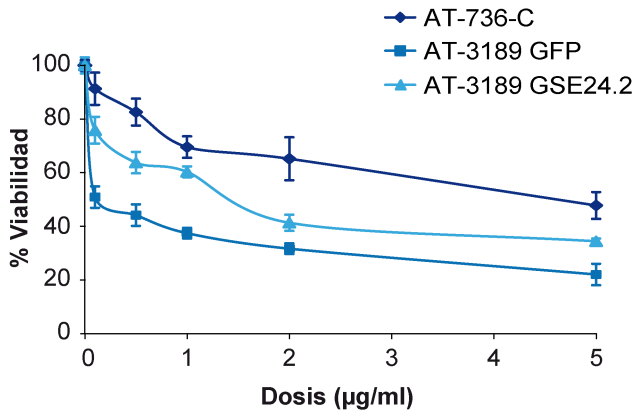

Línea celular	IC50 µg/ml ± DS	Índice resistencia
AT-736-C	5,0 ± 0,03	1
AT-3189 GFP	0,1 ± 0,01	0,02
AT-3189 GSE24.2	1,8 ± 0,01	0,36

b

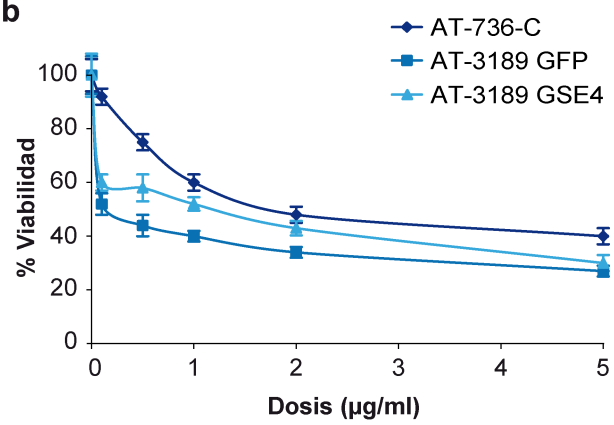

Línea celular	IC50 µg/ml ± DS	Índice resistencia
AT-736-C	2,0 ± 0,04	1
AT-3189 GFP	0,1 ± 0,01	0,05
AT-3189 GSE4	1,6 ± 0,02	0,8

Figura 22. Evaluación de la viabilidad celular mediante MTS tras el tratamiento con diferentes dosis de bleomicina en células A-T. La viabilidad de las líneas celulares A-T expresando GFP, GSE24.2 o GSE4 y la línea celular control AT-736-C se estimó tras incubación con concentraciones crecientes de bleomicina durante 72 horas mediante la técnica MTS a) Viabilidad de la línea celular AT-3189 expresando GFP o GSE24.2 comparándolo con la viabilidad que presenta la línea control AT-736-C a las mismas dosis de bleomicina. b) viabilidad de la línea celular AT-3189 expresando GFP o GSE4 comparándolo con la viabilidad que presenta la línea control AT-736-C a las mismas dosis de bleomicina. Los valores y las desviaciones estándar corresponden a dos experimentos independientes. Los experimentos se repitieron tres veces con resultados similares.

11. Estudio de genes del complejo telomerasa

La expresión de GSE24.2 y GSE4 reactiva la actividad telomerasa a través de un aumento en la expresión de *hTERT* y *hTR* en células de pacientes con disqueratosis congénita (Machado-Pinilla et al. 2008; Iarriccio et al. 2015). En vista de los resultados obtenidos con el tratamiento con estos péptidos a lo largo de esta tesis, se planteó analizar los cambios del complejo telomerasa en células A-T tras expresar GSE4 o GSE24.2.

En primer lugar se evaluaron los niveles de expresión de los genes que se habían observado que aumentaban en DC con la expresión estable de GSE24.2 o GSE4: *hTERT* y *hTR*. Para ello se obtuvo ARN de las líneas celulares AT: L137IIB, AT-719, AT-3189 y la línea control AT-736-C. Los niveles de expresión de ambos genes se evaluó mediante qRT-PCR y se compararon los niveles obtenidos en las células A-T respecto a las células control y en relación a la expresión de un gen control *GAPDH*. Se observó que todas las líneas celulares A-T presentan bajo nivel de expresión de *hTERT* (Figura 23), lo que podría resultar en una inhibición de la actividad telomerasa ya que la expresión de *hTERT*, la actividad transcriptasa inversa, es limitante en el complejo telomerasa. Los niveles de *hTR* son variables entre las líneas celulares A-T y no se observa una inhibición clara de la expresión, pero como se ha comentado, al haber niveles bajos de expresión de *hTERT* no compensarían estos bajos niveles para mantener alta la actividad telomerasa.

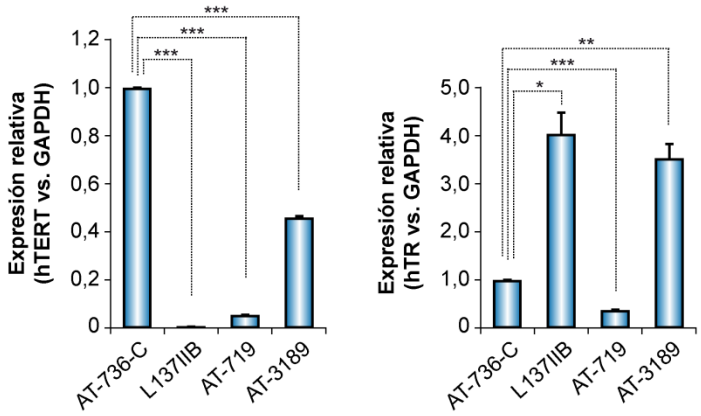

Figura 23: Niveles de expresión de los genes del complejo telomerasa: *hTERT y hTR*. Se aisló ARN de las líneas celulares A-T (AT-3189, AT-719, L137IIB) y la línea celular control AT-736-C. Se analizaron los niveles de expresión de *hTR* y *hTERT* mediante qRT-PCR utilizando *GAPDH* como gen control. Los niveles de expresión de estos dos genes en tres líneas celulares se han comparado con los que se encuentran en la línea celular control. Los asteriscos indican diferencias significativas entre las líneas celulares. Los valores y las desviaciones estándar corresponden a dos experimentos independientes. Los experimentos se repitieron tres veces con resultados similares.

Se decidió entonces estudiar si se producía algún cambio a nivel de expresión de estos genes *hTR* y *hTERT* en las líneas A-T linfoblásticas con expresión estable del GSE24.2 o GSE4. Se aisló ARN de estas líneas celulares y mediante qRT-PCR se estudió el nivel de expresión de dichos genes en relación a las líneas celulares expresando GFP.

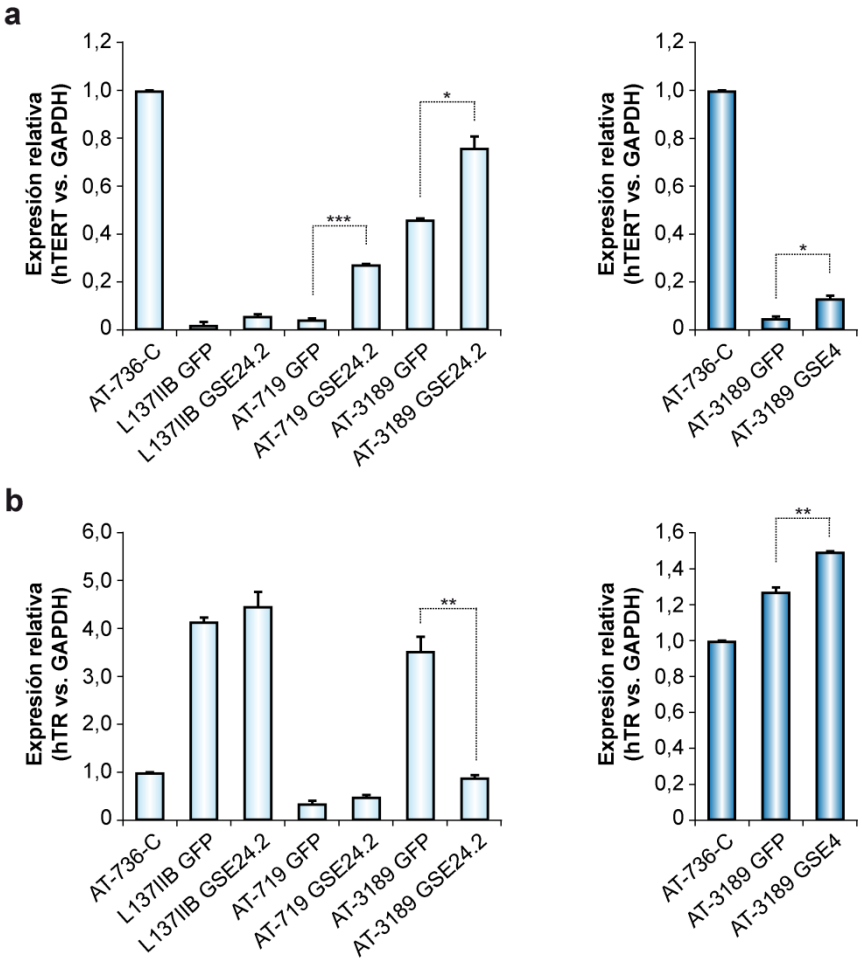

Figura 24. Análisis de los niveles de expresión de los genes del complejo telomerasa *hTERT* y *hTR* en las líneas celulares linfoblásticas de A-T con expresión estable del GSE24.2 o GSE4. Se aisló ARN de las líneas celulares A-T: (AT-3189, AT-719, L137IIB) y la línea celular control AT-736-C expresando GFP, GSE24.2 o GSE4. Mediante qRT-PCR se estudió el nivel de expresión de *hTR* y *hTERT*, usando como referencia el gen *GAPDH*. a) Niveles de expresión del gen *hTERT* en 3 líneas celulares linfoblásticas de A-T, comparándolo con los niveles de expresión de la línea control AT-736-C. b) Niveles de expresión del gen *hTR* en 3 líneas celulares linfoblásticas de A-T, comparándolo con los niveles de expresión de la línea control AT-736-C. Los asteriscos indican diferencias significativas entre las líneas celulares. Los valores y las desviaciones estándar corresponden a dos experimentos independientes. Los experimentos se repitieron tres veces con resultados similares.

Cuando se evaluaron los niveles de expresión de *hTERT* se observó con diferente magnitud, un aumento en la expresión de *hTERT* al expresar GSE24.2 o GSE4 (Figura 24a). Los resultados mostraron que la expresión estable del GSE24.2 o GSE4 no alteraba en gran medida la expresión de *hTR* a excepción de la línea celular AT-3189 en la que se observó un pequeño aumento de expresión de *hTR* (Figura 24b). Estos resultados indicaban que en las líneas celulares A-T que expresan GSE24.2 o GSE4 se podría producir una recuperación de la actividad telomerasa gracias a un aumento en la expresión de *hTERT* al igual que ocurre en diferentes líneas celulares DC (Machado-Pinilla et al. 2008; Iarriccio et al. 2015).

12. Estudio de la longitud telomérica

Se ha descrito que las células A-T tienen una respuesta anómala a los agentes que inducen ROS, respuesta que está asociada a acortamiento telomérico (Tchirkov and Lansdorp 2003). Por otra parte, el acortamiento telomérico induce la respuesta al daño en el ADN, senescencia, y, el mantenimiento fisiológico de la longitud telomérica es esencial para la viabilidad celular. Finalmente, el acortamiento prematuro en la longitud de los telómeros están asociados con la generación de enfermedades degenerativas, una de las cuales es A-T (Opresko and Shay 2017).

Tras haber evaluado que las líneas utilizadas de A-T, presentan una inhibición en los niveles de expresión de *hTERT*, y que esto podría afectar los niveles de actividad telomerasa y por tanto producir un acortamiento del telómero se planteó evaluar el tamaño medio telomérico, de las líneas celulares linfoblásticas que se han utilizado mediante dos metodologías complementarias, “southern blot” y qPCR

Utilizando la técnica de “southern blot” se pudo comprobar que las 2 líneas de A-T presentan tamaños teloméricos muy diferentes, la línea celular AT-3189 presenta un tamaño telomérico aproximado de 5kpb, la línea AT-719 de 8kpb y la línea celular control AT-736-C, de 12kpb (Figura 25).

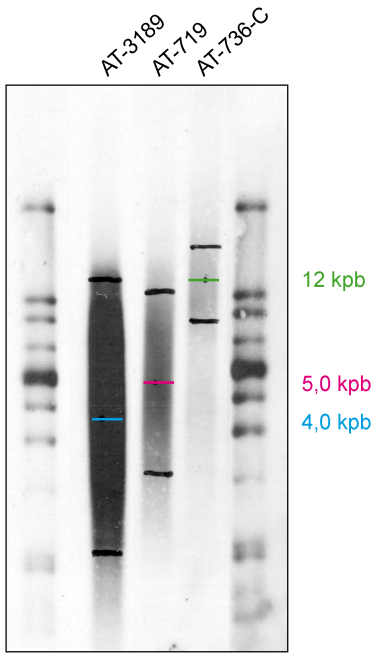

Figura 25. Estudio del tamaño medio telomérico de líneas celulares A-T. Se obtuvo ADN genómico de las tres líneas celulares AT-3189, AT-719 y la línea celular control AT-736-C y utilizando la técnica de southern blot se estudió el tamaño medio telomérico. La figura indica en tamaño medio telomérico para las tres líneas celulares.

Finalmente, se quiso evaluar si se producía algún cambio en el tamaño medio telomérico en líneas celulares que expresasen el GSE24.2 o GSE4. Se eligió para ello la línea celular AT-3189, expresando el GSE4 en relación a la misma línea celular expresando GFP. Se eligió la línea celular con menor tamaño medio telomérico, la AT-3189, porque de existir una mejoría sería en la que más fácil sería observarlo. Se utilizaron líneas celulares recién infectadas y tras dos meses después de haber realizado la infección (Figura 26). Utilizamos este péptido ya que es el que se había decidido utilizar en el tratamiento de disqueratosis congénita. Tras analizar los resultados del "southern blot" no encontramos diferencias obvias en el tamaño medio telomérico (Figura 26a). Por tanto se procedió a evaluar la longitud telomérica mediante qPCR (Figura 26b). Mediante esta técnica, esta vez, si se observó un pequeño incremento de 0,5kpb, dos meses después de la infección, en la línea celular AT-3189 que expresaba GSE4.

a

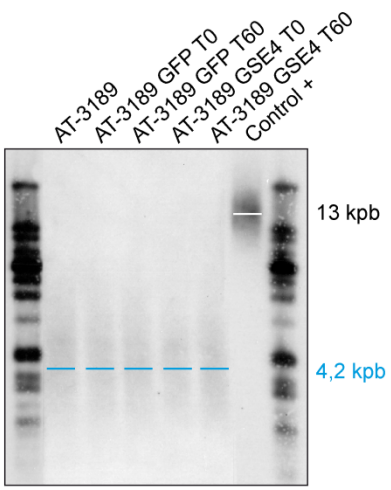

b

ADN	Longitud relativa telómero (ratio T/S)	±DS Longitud relativa telómero (T/S)	Longitud telómero kpb (1T/S=4,8kpb)	±DS Longitud telómero (kpb)
C-1787	1,689	±0,110	8,111	±0,55
AT-3189	0,912	±0,010	4,380	±0,05
AT-3189 GFP T60	0,934	±0,052	4,486	±0,25
AT-3189 GSE4 T60	1,040	±0,036	4,989	±0,17

Figura 26. Estudio del tamaño medio telomérico de la línea celular AT-3189 tras dos meses (T60) expresando de forma estable el péptido GSE4. Se obtuvo ADN genómico de la línea celular AT-3189 expresando GFP, GSE4 o sin infectar y la línea celular control C-1787 y se estudió el tamaño telomérico mediante (a) southern blot y (b) qPCR.

13. Actividad telomerasa en líneas celulares A-T

El papel de la actividad telomerasa y la longitud del telómero en A-T aún no ha sido bien establecido, sin embargo recientemente (Tong et al. 2015) se ha descrito que la actividad de ATM es necesaria para el reclutamiento de la telomerasa al telómero. Resultados presentados en los apartados anteriores indican que en células A-T, hay una disminución en la expresión *TERT* y un acortamiento telomérico, esto ultimo podría deberse a una disminución de la actividad telomerasa por lo que se estudiaron los niveles de la actividad de la telomerasa en las líneas celulares A-T, que presentan disfunción de ATM.

Ya que en la línea celular AT-3189 se había observado un importante acortamiento telomérico, se evaluó la actividad telomerasa presente en esta línea celular. Para ello se obtuvieron extractos proteicos y, mediante el método TRAP se evaluaron los niveles de actividad telomerasa. Los resultados demostraron que había una inhibición en la actividad telomerasa de un 40% con respecto a la línea celular control AT-736-C (Figura 27).

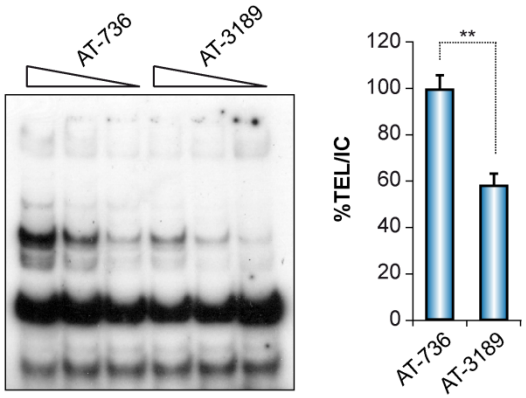

Figura 27: Actividad telomerasa en la línea celular AT-3189. Se obtuvieron extractos proteicos de las líneas celulares AT-736-C y AT-3189. Tras realizase el ensayo TRAP los productos de reacción se separaron en un gel de acrilamida. Para cada línea celular se realizaron reacciones con 3 cantidades de extracto (panel izquierdo). La cuantificación de la actividad telomerasa se representa en el panel derecho, con respecto a la línea control y al control interno de reacción de cada dilución. Se realizaron dos ensayos diferentes con resultados similares.

Puesto que la expresión del GSE4 en la línea celular AT-3189 fue capaz de inducir una elongación del telómero, se estudió si había un aumento en la actividad telomerasa. Para ello se realizó un ensayo TRAP para evaluar la actividad telomerasa en las células AT-3189, sin infectar, y tras 60 días expresando GFP o el GSE4. Los resultados demostraron que las células expresando GSE4 presentaron un aumento de un 60% en la actividad telomerasa respecto a aquellas que expresan GFP (Figura 28).

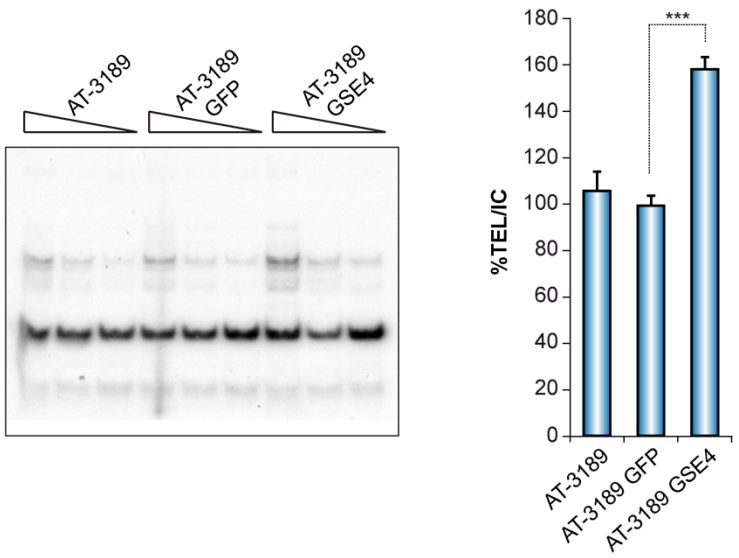

Figura 28. Estudio de la actividad telomerasa en células AT-3189 expresando GSE4. Se obtuvieron extractos proteicos de las líneas celulares AT-3189, expresando GFP y GSE4. Tras realizarse el ensayo TRAP los productos de reacción se separaron en un gel de acrilamida. Para cada línea celular se realizaron reacciones con 3 cantidades de extracto (panel izquierdo). La cuantificación de la actividad telomerasa se representa en el panel derecho, con respecto a la línea AT-3189 sin infectar y al control interno de reacción de cada dilución. Se realizaron dos ensayos diferentes con resultados similares.

DISCUSIÓN

La integridad del genoma frente a daños externos y la correcta transmisión de la información genética es custodiada por un gran número de proteínas, siendo una de ellas la proteína ATM. El gen que codifica para esta proteína se encuentra mutado en los pacientes con Ataxia Telangiectasia. Los sustratos de la quinasa ATM están implicados en los puntos de control del ciclo celular, de este modo, si las células sufren daño en el ADN, la progresión del ciclo celular se detendrá para reparar el daño (Langerak and Russell 2011). Como consecuencia de las mutaciones en ATM que alteran la función de la proteína, los pacientes A-T presentan fallos en los puntos de control del ciclo celular. Además, hay un componente muy importante de la enfermedad como es la falta de control en los niveles de radicales libres consecuencia también de la falta de función del gen ATM. Este aumento en el nivel de radicales libres es el responsable de la muerte de las células de purkinje causantes de la ataxia progresiva en A-T.

La Ataxia telangiectasia también está clasificada como una inmunodeficiencia primaria (IDP) junto con un grupo de casi 200 enfermedades de origen genético en las que existe una alteración cuantitativa y/o funcional de los diferentes mecanismos implicados en la respuesta inmunológica. Las inmunodeficiencias primarias asociadas a defectos en la reparación de daño al ADN como A-T, suelen estar relacionadas a manifestaciones clínicas como radiosensibilidad, defectos en el desarrollo y predisposición a cáncer (Slatter and Gennery 2010).

Actualmente no existe cura para la A-T. Sin embargo, se han diseñado diferentes estrategias como tratamiento paliativo para los efectos sobre los diferentes órganos como intestino, pulmones y sistema inmune. También se han diseñado estrategias con agentes antioxidantes pero ninguno de ellos ha demostrado hasta ahora una eficiencia terapéutica o al menos retrasar el avance de la enfermedad.

Estudios previos en el laboratorio han permitido describir un péptido derivado de la disquerina, formado por 55 aa y conocido como GSE24.2 y otro de menor tamaño, de 11 aminoácidos, al que se le denominó GSE4, y que en células de pacientes con DC producían disminución del estrés oxidativo, de daño al ADN y de la senescencia, acompañado de un incremento de la actividad telomerasa (Iarriccio et al. 2015). En vista a estos resultados y debido a que ambas enfermedades son IDP y comparten algunas alteraciones celulares como aumento de ROS, daño al ADN,o senescencia hemos desarrollado el presente trabajo, centrado en el papel de los péptidos GSE24.2 y GSE4 en una posible terapia para A-T.

1. Papel de los péptidos GSE24.2 y GSE4 en procesos celulares alterados en A-T

1.1. Análisis de los cambios en expresión génica tras sobreexpresar los péptidos GSE24.2 y GSE4 en células de pacientes A-T

Los análisis de expresión génica obtenidos tras sobreexpresar GSE24.2 y GSE4 en diferentes líneas celulares A-T, sugieren la participación de estos péptidos en los procesos de reversión del estrés oxidativo y en el consecuente daño al ADN, lo cual se valoró mediante diferentes ensayos in vitro.

El cambio patológico más relevante que presentan los pacientes A-T es la pérdida específica de las células de Purkinje debido a niveles de estrés oxidativo elevado. Es conocido que la mayoría de ROS intracelular es producido por la cadena respiratoria en la mitocondria, por lo que se han llevado a cabo diferentes estudios en A-T relacionados con la regulación de los niveles de ROS, que son capaces de causar daño a lípidos y proteínas y son capaces de generar lesiones en el ADN (Ambrose and Gatti 2013). En otros estudios en A-T han observando una disfunción mitocondrial (Ambrose et al. 2007), y otras anormalidades como la expresión alterada de algunos genes cuyos productos son dirigidos a la mitocondria, como la topoisomerasa I y *SOD2* (Pallardo et al. 2010), además, en otros tipos de ataxia también se han descrito disminución de expresión del enzima SOD2 (Sandi et al. 2014). Varias enzimas son responsables de detoxificar específicamente ROS: entre ellas *SOD (1 y 2)* que convierten los radicales superóxido en H_2O_2 y O_2 y la *catalasa* que es específica del peróxido de hidrógeno (Kamsler et al. 2001) por lo que en este trabajo se evaluó los niveles de enzimas antioxidantes *SOD2*, *SOD1* y *CAT*.

Nosotros hemos comprobado que todas las líneas celulares A-T utilizadas a lo largo de este trabajo presentaban niveles bajos de expresión de enzimas antioxidantes. Se ha observado la downregulación de los niveles de expresión de genes antioxidantes, sobre todo *SOD1* y *CAT*, sin embargo, estos niveles de expresión se vieron incrementados en estas líneas celulares A-T con expresión estable del GSE24.2 o GSE4, tal como se ha descrito en células DC expresando el péptido GSE24.2 (Manguan-Garcia et al. 2014) y esto puede contribuir a disminuir el estrés oxidativo presente en las células.

En las células A-T la falta de ATM funcional resulta en un incremento del daño no reparado en el ADN (Barlow et al. 1996) y de un estado de estrés oxidativo crónico, aún en ausencia de agentes inductores de daño oxidativo (Rotman and Shiloh 1997). Por ello, quisimos comprobar si la expresión de los péptidos GSE4 y GSE24.2

contribuían o no a disminuir el estrés oxidativo presente en las células. Nuestros resultados nos confirmaron que las líneas celulares expresando constitutivamente GSE24.2 o GSE4 presentaban menores niveles de ROS, y por lo tanto, menor estrés oxidativo.

Una consecuencia del continuo estado de estrés oxidativo y el aumento en daño genético que ello conlleva en la célula es un aumento en expresión de citoquinas pro-inflamatorias, como *IL-1 beta, IL-6, IL-8, TNF-alfa e IFN-gamma* (Rodier et al. 2009). En pacientes A-T se ha descrito una asociación entre los niveles elevados de *IL-6* con una disminución de la función de los pulmones, de esta manera se podrían usar marcadores como la *IL-6* para identificar individuos A-T con mayor riesgo de presentar enfermedades en las vías respiratorias (McGrath-Morrow et al. 2016). En vista de la evidencia en la literatura quisimos estudiar los niveles de *IL-6* presentes en estas líneas celulares A-T. Encontramos que la línea de A-T estudiada, AT-3189, presentaba valores de expresión de *IL-6* muy elevados. Este aumento se conseguía disminuir cuando expresaban GSE24.2 o GSE4.

Por lo tanto, podemos concluir que el aumento de estrés oxidativo generado por la deficiencia de ATM, el cual participa en muchas funciones celulares, se ve disminuído cuando las células expresan GSE24.2 o GSE4, que las protege, probablemente debido una mayor expresión de enzimas antioxidantes y ello desencadena una disminución de la expresión de citoquinas pro-inflamatorias como *IL-6*.

1.2 Implicación de los péptidos GSE24.2 y GSE4 en daño y reparación del ADN y disminución de la senescencia

Las histonas juegan un papel importante en el contexto de la respuesta celular a las roturas de doble cadena en el ADN (van Attikum and Gasser 2005). Concretamente la fosforilación de la histona H2A.X es uno de los primeros eventos que tienen lugar en esta respuesta (Kuo and Yang 2008). La fosforilación es llevada a cabo por ATM, y favorecería el reclutamiento y el mantenimiento de las distintas moléculas implicadas en la reparación en el sitio donde se produjo la rotura o modificación en el ADN (Celeste et al. 2003). 53BP1 es una de las proteínas que continúa activando la ruta, debido a que es reclutada en la zona del daño al ADN (Schultz et al. 2000). Es conocido que la detección en la localización de estas proteínas mediante inmunofluorescencia nos permite cuantificar los procesamientos de las roturas de doble cadena (Kinner et al. 2008). Por tanto, el análisis microscópico de los focos γH2A.X, que se forman después de la fosforilación de H2A.X en la Ser-139

en respuesta a roturas de doble cadena del ADN, se ha convertido en una herramienta indispensable. En este trabajo hemos analizado la presencia de γH2A.X y 53BP1 en líneas celulares A-T para evaluar la activación de la ruta del daño al ADN, comprobándose que las células A-T presentaban elevado el daño genético basal debido al número elevado de focos en el núcleo celular al analizar ambas proteínas. Estudios previos en la literatura han demostrado una respuesta enlentecida a radiación ionizante en líneas de modelos murinos A-T (Dar et al. 2006).

Además hemos comprobado que las líneas celulares A-T con expresión estable de GE24.2 o GSE4 presentaban menor daño basal, posiblemente debido a que el estrés oxidativo que presentan es menor y ello conlleva a menor activación de la ruta de activación de daño al ADN.

El regulador más importante de la respuesta celular a DSB es ATM (Khanna et al. 2001), ya que regula los tres puntos de control del ciclo celular, G1/S intra-S y G2M. Las roturas en el ADN tienen que repararse de forma eficiente y exacta, ya que de lo contrario pueden generarse problemas degenerativos o disparar procesos tumorales (Alvarez-Quilon et al. 2014).

Una vez comprobado que la expresión de GSE24.2 o GSE4 en las líneas celulares A-T producían una disminución en el daño al ADN, quisimos estudiar si estos péptidos estarían implicados en el proceso de reparación de las lesiones genómicas reparadas específicamente por ATM, por lo que inhibiendo ATM en células en ausencia de la enzima TOP2 podríamos saber si estos péptidos estaban implicados o no en este proceso de reparación (Alvarez-Quilon et al. 2014).

Tras generar roturas de doble cadena con etopósido para producir daño persistente en el ADN (Schonn et al. 2010), se procedió a utilizar inhibidores de vías específicas de reparación del ADN, en concreto, se usaron inhibidores de ATM, bloqueando la reparación del ADN (Rimkus et al. 2008), reproduciendo de esta manera lo que ocurre en los pacientes A-T y, determinamos que los péptidos GSE24.2 y GSE4 no están implicados en el proceso de reparación de las lesiones reparadas específicamente por ATM, ya que en estas condiciones experimentales no observamos disminución en el número de focos de γ-H2A.X.

La correcta reparación del daño al ADN es muy importante ya que una acumulación de mutaciones puede conducir a la célula a un estado de senescencia, a la síntesis de proteínas aberrantes o a la apoptosis cuando ésta no puede llevarse a cabo. La senescencia celular es un programa que limita la proliferación de las células y

en la mayoría de los casos esto va asociado a un acortamiento telomérico (Hayflick 1965).

Las células que están en riesgo de transformación celular también pueden entrar en senescencia, imponiendo un programa de parada irreversible del crecimiento celular. Las células normales entran en un programa de senescencia en respuesta a un severo e irreparable daño en el ADN especialmente debido a roturas de doble cadena (Herbig et al. 2004). Es un proceso fisiológico y patológico inducido por numerosos factores, durante los cuales cesa el crecimiento y altera la expresión génica, de manera que protege contra el desarrollo de cáncer y juega un papel importante en la reparación de tejidos (Gonzalez et al. 2016). Aunque es un potente mecanismo supresor de tumores, la senescencia ha sido implicada en varios procesos patológicos incluyendo muchos otros procesos como el envejecimiento y la enfermedad neurodegenerativa (van Deursen 2014). Las células senescentes también desarrollan un complejo fenotipo secretor asociado a senescencia denominada SASP a través del cual las células senescentes aumentan la secreción de citoquinas proinflamatorias, quimiocinas, factores de crecimiento y proteasas, y este mecanismo que se encuentra incrementado en las enfermedades neurodegenerativas como A-T (Chinta et al. 2015), afectando tanto a las células senescentes como al microambiente que las rodea (Kang et al. 2015).

Las células senescentes presentan marcadores específicos como la expresión de SA-β-gal (Cho and Hwang 2012). Nosotros habíamos encontrado que las células AT-3189 expresaban altos niveles de *IL-6* que disminuía cuando expresábamos de forma estable GSE24.2 o GSE4. Por ello decidimos estudiar si esta disminución en los niveles de *IL-6* estaba asociada a una disminución de la senescencia. Por ello evaluamos la senescencia celular presente en las líneas A-T fibroblásticas estudiando la expresión de SA-β-gal, ya que se había descrito que los fibroblastos de A-T presentaban menor vida media que las líneas celulares controles junto con signos de senescencia celular temprana (Shiloh et al. 1982).

De acuerdo con lo escrito en la literatura encontramos que la línea celular fibroblástica AT-3487 presentaba niveles elevados de expresión de SA-β-gal, que disminuía un 20% en las células con expresión estable de GSE24.2 o GSE4. De acuerdo con una inhibición en el proceso de senescencia, por la expresión de GSE24.2 y GSE4, encontramos que la línea linfoblastica AT-3189 expresando GSE4 o GSE24.2 tenía más capacidad de proliferación que las célulasexpresando el virus control. Ademas las células A-T, que expresan mayores niveles de p-p38 MAPK que

las células controles, la cual esta asociada a mayor senescencia, expresan menor activación de esta quinasa cuando se expresa el GSE24.2 o GSE4.

1.3. Modulación de la respuesta a bleomicina por los péptidos GSE24.2 y GSE4

En células normales la integridad genómica es mantenida monitorizando con la maquinaria celular, el daño al ADN y reparándolo, evitando la transmisión de ADN no reparado a las células hijas. Entre los diferentes tipos de daño al ADN, las DSB, las cuales son principalmente inducidas mediante radiación ionizante o drogas radiomiméticas, son considerados como una gran amenaza para la estabilidad genómica de las células de mamíferos, ya que pueden conducir a la muerte celular si están parcial o totalmente no reparados (Harrison and Haber 2006).

Los pacientes A-T son más sensibles a la radiación ionizante (Gilad et al. 1998) y a químicos radiomiméticos como la bleomicina (Taylor et al. 1979), no activándose los puntos de control del ciclo celular después del tratamiento con estos agentes (Guerra et al. 2014).

Nosotros hemos comprobado que las células A-T presentan mayor sensibilidad frente a la bleomicina, y que las células que expresaban GSE24.2 o GSE4 presentaban mayor resistencia a este compuesto aunque la reversión a niveles de las células controles no es total. Por tanto, ya que la expresión de GSE4 o GSE24.2 no incrementa el DSB, es posible que esta mayor viabilidad a bleomicina sea debida a la disminución de los niveles de daño oxidativo, que tambien es tóxica cuando se induce DSB.

2. Reparación de los telómeros en células A-T por los péptidos GSE24.2 y GSE4

. El acortamiento de los telómeros está relacionado con la senescencia celular prematura y podría ser un marcador de la patología celular en enfermedades neurológicas.

Los telómeros son estructuras nucleoproteicas especializadas que constituyen los extremos de los cromosomas y cuya longitud predice la capacidad replicativa de las células (Allsopp et al. 1992). Ya que la telomerasa, es la enzima que sintetiza el ADN telomérico y, por tanto, controla la elongación de los telómeros y juega un papel importante en el proceso de inmortalización de las células, quisimos comprobar los niveles de expresión de los dos genes que controlan la actividad catalitica de la telomerasa *TERT* y *TR* en las líneas celulares A-T. Encontramos que la mayoría de las líneas linfoblásticas A-T presentaban niveles bajos de expresión de *TERT*, y niveles de

expresión aumentados de *TR*, a excepción de la línea celular AT-719 que lo presenta disminuido. Los niveles de expresión de *TERT* aumentaban en las células tras la expresión del GSE24.2 o GSE4.

Por lo tanto, es de esperar que si las líneas celulares de A-T presentan bajos los niveles de expresión de *TERT*, implicará que hay una menor actividad telomerasa (Saldanha et al. 2003; Cifuentes-Rojas and Shippen 2012). Mediante ensayos TRAP hemos comprobado que hay efectivamente una disminución en la actividad telomerasa en células A-T. Además, se observó que las líneas celulares con expresión estable GSE4 presentaron también mayor actividad telomerasa que las que no lo expresaban al igual que se ha descrito en células DC (Iarriccio et al. 2015).

En las células A-T se ha reportado un considerable acortamiento de los telómeros y el aumento de las fusiones cromosómicas en comparación con la que presentan las células controles (Smilenov et al. 1997). La expresión ectópica de la unidad catalítica de la telomerasa (TERT) en fibroblastos A-T fue capaz de invertir los fenotipos de senescencia prematura (Wood et al. 2001). Esto se corroboró en estudios en ratones, en los que al generar el modelo de ratón nulo doble de $ATM^{-/-}$ y $TERC^{-/-}$ observaron mayor acortamiento en los telómeros e inestabilidad genómica, sugiriéndonos que la enfermedad A-T está vinculada al estado funcional de los telómeros o al menos su progresión (Barlow et al. 1996) y también mostraron mayor número de fusiones cromosómicas y mayor muerte de células germinales al compararlas con ratones knockout único, lo cual tambien sugiriere que la deficiencia de ATM acentúa la disfunción telomérica (Qi et al. 2003). Además se ha descrito que la frecuencia de repeticiones teloméricas es variable en las líneas celulares A-T (4,3 a 8,2 kpb), comparándolo con las líneas celulares controles (9.6 a 12 kpb) y se observó una correlación inversa entre la longitud de los telómeros y las fusiones de los extremos cromosómicos (Pandita et al. 1995).

A la vista de estos estudios, nos propusimos estudiar la longitud media telomérica que presentaban las líneas celulares A-T mediante “southern blot” (Gabellini et al. 2003). Observamos que las líneas celulares A-T utilizadas presentaban acortamiento telomérico pues presentaban menos de 5 kpb como media en comparación con la 12 kpb de la linea control. Tras expresar el GSE4 durante dos meses, encontramos, un aumento de la longitud media telomérica de 0,5 kpb. Este aumento de la longitud del telómero debe de ser consecuencia del incremento en la actividad telomerasa en las células que expresan GSE4.

Basados en nuestros resultados, podemos concluir que el estrés oxidativo promueve daño particularmente en las regiones teloméricas en las células A-T, resultando en el acortamiento del telómero con cada división celular lo cual puede resultar en senescencia prematura (Passos et al. 2007). Además, debido al daño oxidativo persistente se induciría la activación de p38 MAPK y la secreción de IL-6 reforzando el fenotipo senescente de las células, dando lugar a la pérdida de células funcionales. En las células A-T con expresión de GSE24.2 o GSE4 se produce un triple efecto que va mediado por: 1) incrementan los niveles de expresión de *TERT* lo que conlleva a una mayor estabilidad del complejo telomerasa, y a una mayor actividad catalítica y elongación de los telómeros, 2) una disminución del nivel de ROS debido a una regulación de la expresión de enzimas antioxidantes y 3) una disminución del daño oxidativo y producción del fenotipo secretor (menores niveles de IL-6 y p-p38 MAPK) que disminuiría la senescencia existente en las células A-T permitiendo que recuperen parte de su capacidad de dividirse (Figura 29).

3. Uso de la nanopartículas como tratamiento terapeútico

A la vista de los resultados obtenidos con células que expresaban los péptidos de forma estable, nos planteamos qué metodología podríamos usar para tratar a pacientes A-T, y por ello procedimos a hacer uso de nanopartículas como terapia, ya que este sistema permite la protección y liberación controlada de moléculas de interés terapeútico, como el GSE24.2 o GSE4. Esta alternativa emergente podría actuar sobre las células madre residentes del sistema nervioso central (SNC) para la reparación de las lesiones inducidas por estrés oxidativo (Santos et al. 2012).

La A-T, al ser un síndrome multisistémico requiere de un grupo multidisciplinar de especialistas con experiencia en estas enfermedades y un tratamiento multisistémico de los pacientes. En la actualidad no existe un tratamiento curativo de la A-T, por lo que la actitud terapéutica se basa en el tratamiento sintomático de las diferentes manifestaciones clínicas (Perlman et al. 2003). Las principales complicaciones que llevan a la muerte de los pacientes con A-T son en un 46% las infecciones pulmonares, por lo que en los pacientes con A-T, se recomienda inicio de tratamiento precoz con terapia para el asma, broncodilatadores y glucocorticoides, ya que podrían prevenir el deterioro de la función pulmonar y mejorar su pronóstico (Berkun et al. 2010), en un 21% las neoplasias malignas y en un 28% la combinación de las dos anteriores (Teive et al. 2015).

La ataxia progresiva es la manifestación más invalidante que sufren los pacientes con A-T y es probablemente el área en donde los distintos tratamientos

obtienen los resultados más variables. Para el tratamiento de los transtornos del movimiento se requiere fisioterapia osteomuscular para prevenir la rigidez muscular y mantener la movilidad funcional. La amantadina se considera una droga efectiva y bien tolerada para los síntomas motores de la A-T (Nissenkorn et al. 2013). Las alteraciones en el equilibrio, el lenguaje y la coordinación podrían beneficiarse del tratamiento con amantadina, fluoxetina o buspiron. El temblor se controla frecuentemente con gabapentina, clonacepam o propanolol.

Con el objetivo de enlentecer la progresión de la neurodegeneración se han realizado varios estudios con tratamientos antioxidantes, con resultados variables La administración de antioxidantes está recomendada en todos los pacientes con A-T, principalmente la vitamina E o el ácido alfa lipoico, el cual mejora la función mitocondrial en células de pacientes con A-T (Ambrose et al. 2007), otro antioxidante que también se podría administrar es N-acetilcisteína para prevenir fundamentalmente linfomas (Reliene and Schiestl 2008). Por otra parte, los antioxidantes sintéticos, especialmente las porfirinas de manganeso MnTnHex-2-PyP y MnMx-2-PyPCalbio, podrían tener un efecto radioprotector ya que tienen la capacidad de imitar a la enzima superóxido dismutasa reduciendo y oxidando los radicales superóxido. En pacientes con A-T, éstas y otras porfirinas de manganeso pueden ser de utilidad para reducir los efectos neurodegenerativos.

Con nuestro trabajo se plantearía un tratamiento que conllevaría una mejora a nivel sistémico, pues con las nanopartículas GOS o PLGA/PEI cargadas con estos péptidos permitían disminuir el daño oxidativo y el daño persistente al ADN a nivel periferico y que conlleva, una disminución del número de células senescentes en estos pacientes. Con este tratamiento se solventaría a nivel periférico problemas que presentan las células de estos pacientes sobre todo a nivel pulmonar. Resultados aún sin publicar de nuestro grupo demuestran que el péptido GSE4 suministrado en nanopartículas PLGA/PEI es capaz de revertir la fibrosis pulmonar inducida por bleomicina en un modelo de rata (manuscrito en preparación). Sin embargo, debido a que el problema principal en A-T radica en la pérdida de las células de Purkinje, dando lugar a neurodegeneración, el objetivo final sería utilizar unas nanopartículas poliméricas biodegradables que puedan ser formuladas para cruzar la barrera hematoencefálica (Metcalfe et al. 2016) permitiendo la entrada sostenida de los péptidos GSE24.2 o GSE4, durante suficiente tiempo para restablecer la homeostasis neuro-inmune, para poder actuar disminuyendo el estrés oxidativo presente, reduciendo por tanto la pérdida de las células de Purkinje.

El modelo que proponemos con el tratamiento con estas nanopartículas cargadas con el péptido GSE4 se basa fundamentalmente en nuestros resultados in vitro obtenidos para la A-T. El suministro de nanopartículas PLGA/PEI (ya aprobadas por la FDA y la EMA en protocolos clínicos) podría por una parte prevenir y tratar la inmunodeficiencia y la fibrosis pulmonar, ya que ha demostrado eficiencia en el tratamiento en un modelo de fibrosis pulmonar en rata y eficiencia en el tratamiento de linfoblastos DC y A-T. En la actualidad se están ensayando nanoparticulas PLGA/PEI con modificacines que permitan que atraviesen la barrera hematoencefálica y éstas serían utiles para el tratameinto del problema neurológico en A-T. Con estas nanopartículas podríamos demostrar la validez de nuestro abordaje en modelos murinos de A-T.

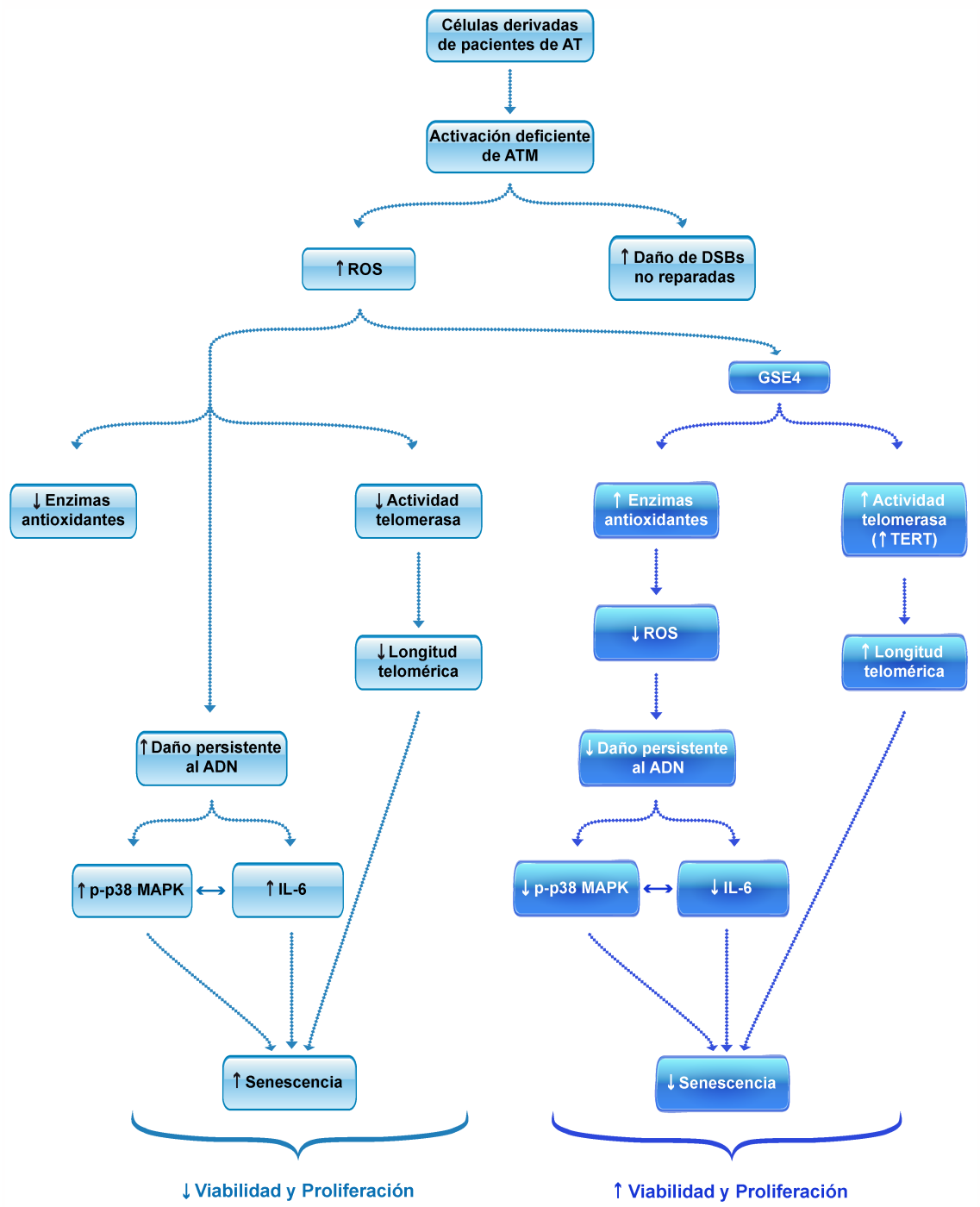

Figura 29: Esquema global de los procesos estudiados alterados en A-T y el efecto del péptido GSE4 en dichos procesos.

CONCLUSIONES

1. Las líneas celulares A-T con expresión estable del GSE24.2 o GSE4 presentan una disminución significativa del daño al ADN, analizado por la presencia de la histona γ-H2A.X. Estas líneas celulares tratadas con nanopartículas PLGA/PEI cargadas con los péptidos GSE24.2 o GSE4 mostraban una disminución similar del daño al ADN a la obtenida con células infectadas con lentivirus expresando estos péptidos, indicándo que este tratamiento podría ser una alternativa terapeútica.

2. La expresión del GSE24.2 o GSE4, no restablece la capacidad de ATM de reparar roturas de doble cadena en el ADN.

3. Las líneas celulares A-T presentan niveles elevados de daño oxidativo en el ADN, determinado por los niveles de 8-oxoguanina que disminuye cuando son tratadas con nanopartículas GOS cargadas con GSE4.

4. Las líneas celulares A-T presentan un aumento en los niveles de ROS y disminución en la expresión de algunos enzimas antioxidantes. La expresión estable del GSE24.2 o GSE4 disminuye los niveles de ROS y aumenta los niveles de algunos enzimas antioxidantes.

5. La expresión del GSE24.2 y GSE4 en células A-T induce una disminución en los niveles de *IL-6* con respecto a las células no tratadas, presentan una menor actividad p38 MAPK, una disminución en el número de células senescentes así como un aumento en la proliferación.

6. El tratamiento con bleomicina induce una disminución de la viabilidad celular en líneas celulares A-T en relación a células normales y la expresión de GSE24.2 o GSE4 induce supervivencia respecto a las células parentales A-T indicando que la expresión de estos péptidos podría actuar como radioprotector.

7. Las líneas celulares A-T presentan niveles disminuidos de actividad telomerasa que va asociado a una menor expresión de *TERT*. La expresión de GSE24.2 o GSE4 induce un aumento en la expresión de *TERT* y un aumento en la actividad telomerasa. Esta disminución de actividad telomerasa en células A-T va asociado a una menor longitud de los telómeros. La expresión de GSE4 en células A-T induce un aumento medio telomérico de 0,5kpb tras dos meses de la infección.

8. Como conclusión general, los resultados obtenidos en este trabajo sugieren que la expresión de los péptidos GSE24.2 o GSE4 confieren a las células A-T ventajas in vitro, que incluyen inhibición de daño oxidativo, disminución de la senescencia asociada a un fenotipo secretor, aumento de la viabilidad celular, disminución de la radiosensibilidad, reactivación de la actividad telomerasa y elongación de los telómeros. Por tanto, estos péptidos representan una alternativa terapeútica para inhibir algunos de los efectos patológicos en líneas A-T.

BIBLIOGRAFÍA

Agostini, A., L. Mondragon, A. Bernardos, R. Martinez-Manez, M. D. Marcos, F. Sancenon, J. Soto, A. Costero, C. Manguan-Garcia, R. Perona, M. Moreno-Torres, R. Aparicio-Sanchis and J. R. Murguia (2012). "Targeted cargo delivery in senescent cells using capped mesoporous silica nanoparticles." Angew Chem Int Ed Engl **51**(42): 10556-60.

Ahmed, S., J. F. Passos, M. J. Birket, T. Beckmann, S. Brings, H. Peters, M. A. Birch-Machin, T. von Zglinicki and G. Saretzki (2008). "Telomerase does not counteract telomere shortening but protects mitochondrial function under oxidative stress." J Cell Sci **121**(Pt 7): 1046-53.

Alexander, A., S. L. Cai, J. Kim, A. Nanez, M. Sahin, K. H. MacLean, K. Inoki, K. L. Guan, J. Shen, M. D. Person, D. Kusewitt, G. B. Mills, M. B. Kastan and C. L. Walker (2010). "ATM signals to TSC2 in the cytoplasm to regulate mTORC1 in response to ROS." Proc Natl Acad Sci U S A **107**(9): 4153-8.

Allsopp, R. C., H. Vaziri, C. Patterson, S. Goldstein, E. V. Younglai, A. B. Futcher, C. W. Greider and C. B. Harley (1992). "Telomere length predicts replicative capacity of human fibroblasts." Proc Natl Acad Sci U S A **89**(21): 10114-8.

Alvarez-Quilon, A., A. Serrano-Benitez, J. A. Lieberman, C. Quintero, D. Sanchez-Gutierrez, L. M. Escudero and F. Cortes-Ledesma (2014). "ATM specifically mediates repair of double-strand breaks with blocked DNA ends." Nat Commun **5**: 3347.

Ambrose, M. and R. A. Gatti (2013). "Pathogenesis of ataxia-telangiectasia: the next generation of ATM functions." Blood **121**(20): 4036-45.

Ambrose, M., J. V. Goldstine and R. A. Gatti (2007). "Intrinsic mitochondrial dysfunction in ATM-deficient lymphoblastoid cells." Hum Mol Genet **16**(18): 2154-64.

Ayoub, N., A. D. Jeyasekharan, J. A. Bernal and A. R. Venkitaraman (2009). "Paving the way for H2AX phosphorylation: chromatin changes in the DNA damage response." Cell Cycle **8**(10): 1494-500.

Bakkenist, C. J. and M. B. Kastan (2003). "DNA damage activates ATM through intermolecular autophosphorylation and dimer dissociation." Nature **421**(6922): 499-506.

Bakkenist, C. J. and M. B. Kastan (2004). "Phosphatases join kinases in DNA-damage response pathways." Trends Cell Biol **14**(7): 339-41.

Banath, J. P., S. H. Macphail and P. L. Olive (2004). "Radiation sensitivity, H2AX phosphorylation, and kinetics of repair of DNA strand breaks in irradiated cervical cancer cell lines." Cancer Res **64**(19): 7144-9.

Barlow, C., S. Hirotsune, R. Paylor, M. Liyanage, M. Eckhaus, F. Collins, Y. Shiloh, J. N. Crawley, T. Ried, D. Tagle and A. Wynshaw-Boris (1996). "Atm-deficient mice: a paradigm of ataxia telangiectasia." Cell **86**(1): 159-71.

Barzilai, A., G. Rotman and Y. Shiloh (2002). "ATM deficiency and oxidative stress: a new dimension of defective response to DNA damage." DNA Repair (Amst) **1**(1): 3-25.

Berkun, Y., D. Vilozni, Y. Levi, S. Borik, D. Waldman, R. Somech, A. Nissenkorn and O. Efrati (2010). "Reversible airway obstruction in children with ataxia telangiectasia." Pediatr Pulmonol **45**(3): 230-5.

Bessler, M., D. B. Wilson and P. J. Mason (2004). "Dyskeratosis congenita and telomerase." Curr Opin Pediatr **16**(1): 23-8.

Biton, S., A. Barzilai and Y. Shiloh (2008). "The neurological phenotype of ataxia-telangiectasia: solving a persistent puzzle." DNA Repair (Amst) **7**(7): 1028-38.

Boder, E. (1985). "Ataxia-telangiectasia: an overview." Kroc Found Ser **19**: 1-63.

Burdak-Rothkamm, S. and K. M. Prise (2009). "New molecular targets in radiotherapy: DNA damage signalling and repair in targeted and non-targeted cells." Eur J Pharmacol **625**(1-3): 151-5.

Byrd, P. J., V. Srinivasan, J. I. Last, A. Smith, P. Biggs, E. F. Carney, A. Exley, C. Abson, G. S. Stewart, L. Izatt and A. M. Taylor (2012). "Severe reaction to radiotherapy for breast cancer as the presenting feature of ataxia telangiectasia." Br J Cancer **106**(2): 262-8.

Campisi, J., J. K. Andersen, P. Kapahi and S. Melov (2011). "Cellular senescence: a link between cancer and age-related degenerative disease?" Semin Cancer Biol **21**(6): 354-9.

Carrillo, J., P. Martinez, J. Solera, C. Moratilla, A. Gonzalez, C. Manguan-Garcia, M. Aymerich, L. Canal, M. Del Campo, J. L. Dapena, L. Escoda, J. M. Garcia-Sagredo, S. Martin-Sala, S. Rives, J. Sevilla, L. Sastre and R. Perona (2012). "High resolution melting analysis for the identification of novel mutations in DKC1 and TERT genes in patients with dyskeratosis congenita." Blood Cells Mol Dis **49**(3-4): 140-6.

Cawthon, R. M. (2002). "Telomere measurement by quantitative PCR." Nucleic Acids Res **30**(10): e47.

Celeste, A., O. Fernandez-Capetillo, M. J. Kruhlak, D. R. Pilch, D. W. Staudt, A. Lee, R. F. Bonner, W. M. Bonner and A. Nussenzweig (2003). "Histone H2AX phosphorylation is dispensable for the initial recognition of DNA breaks." Nat Cell Biol **5**(7): 675-9.

Chen, L. Y., S. Redon and J. Lingner (2012). "The human CST complex is a terminator of telomerase activity." Nature **488**(7412): 540-4.

Chin, C. F. and F. M. Yeong (2010). "Safeguarding entry into mitosis: the antephase checkpoint." Mol Cell Biol **30**(1): 22-32.

Chinta, S. J., G. Woods, A. Rane, M. Demaria, J. Campisi and J. K. Andersen (2015). "Cellular senescence and the aging brain." Exp Gerontol **68**: 3-7.

Cho, S. and E. S. Hwang (2012). "Status of mTOR activity may phenotypically differentiate senescence and quiescence." Mol Cells **33**(6): 597-604.

Cifuentes-Rojas, C. and D. E. Shippen (2012). "Telomerase regulation." Mutat Res **730**(1-2): 20-7.

Coppe, J. P., P. Y. Desprez, A. Krtolica and J. Campisi (2010). "The senescence-associated secretory phenotype: the dark side of tumor suppression." Annu Rev Pathol **5**: 99-118.

Cuenda, A. and S. Rousseau (2007). "p38 MAP-kinases pathway regulation, function and role in human diseases." Biochim Biophys Acta **1773**(8): 1358-75.

D'Arpa, P., C. Beardmore and L. F. Liu (1990). "Involvement of nucleic acid synthesis in cell killing mechanisms of topoisomerase poisons." Cancer Res **50**(21): 6919-24.

Dar, I., S. Biton, Y. Shiloh and A. Barzilai (2006). "Analysis of the ataxia telangiectasia mutated-mediated DNA damage response in murine cerebellar neurons." J Neurosci **26**(29): 7767-74.

De Bont, R. and N. van Larebeke (2004). "Endogenous DNA damage in humans: a review of quantitative data." Mutagenesis **19**(3): 169-85.

Dimri, G. P., X. Lee, G. Basile, M. Acosta, G. Scott, C. Roskelley, E. E. Medrano, M. Linskens, I. Rubelj, O. Pereira-Smith and et al. (1995). "A biomarker that identifies senescent human cells in culture and in aging skin in vivo." Proc Natl Acad Sci U S A **92**(20): 9363-7.

Doksani, Y., J. Y. Wu, T. de Lange and X. Zhuang (2013). "Super-resolution fluorescence imaging of telomeres reveals TRF2-dependent T-loop formation." Cell **155**(2): 345-56.

Egusquiaguirre, S. P., C. Manguan-Garcia, L. Pintado-Berninches, L. Iarriccio, D. Carbajo, F. Albericio, M. Royo, J. L. Pedraz, R. M. Hernandez, R. Perona and M. Igartua (2015). "Development of surface modified biodegradable polymeric nanoparticles to deliver GSE24.2 peptide to cells: a promising approach for the treatment of defective telomerase disorders." Eur J Pharm Biopharm **91**: 91-102.

Fang, Z., S. Kozlov, M. J. McKay, R. Woods, G. Birrell, C. N. Sprung, D. F. Murrell, K. Wangoo, L. Teng, J. H. Kearsley, M. F. Lavin, P. H. Graham and R. A. Clarke (2010). "Low levels of ATM in breast cancer patients with clinical radiosensitivity." Genome Integr **1**(1): 9.

Forsyth, N. R., A. P. Evans, J. W. Shay and W. E. Wright (2003). "Developmental differences in the immortalization of lung fibroblasts by telomerase." Aging Cell **2**(5): 235-43.

Fouquerel, E., J. Lormand, A. Bose, H. T. Lee, G. S. Kim, J. Li, R. W. Sobol, B. D. Freudenthal, S. Myong and P. L. Opresko (2016). "Oxidative guanine base damage regulates human telomerase activity." Nat Struct Mol Biol **23**(12): 1092-1100.

Freund, A., C. K. Patil and J. Campisi (2011). "p38MAPK is a novel DNA damage response-independent regulator of the senescence-associated secretory phenotype." EMBO J **30**(8): 1536-48.

Fumagalli, M., F. Rossiello, M. Clerici, S. Barozzi, D. Cittaro, J. M. Kaplunov, G. Bucci, M. Dobreva, V. Matti, C. M. Beausejour, U. Herbig, M. P. Longhese and F. d'Adda di Fagagna (2012). "Telomeric DNA damage is irreparable and causes persistent DNA-damage-response activation." Nat Cell Biol **14**(4): 355-65.

Gabellini, C., A. Antonelli, P. Petrinelli, A. Biroccio, L. Marcucci, G. Nigro, G. Russo, G. Zupi and R. Elli (2003). "Telomerase activity, apoptosis and cell cycle progression in ataxia telangiectasia lymphocytes expressing TCL1." Br J Cancer **89**(6): 1091-5.

Garcia, C. K., W. E. Wright and J. W. Shay (2007). "Human diseases of telomerase dysfunction: insights into tissue aging." Nucleic Acids Res **35**(22): 7406-16.

Garinis, G. A., G. T. van der Horst, J. Vijg and J. H. Hoeijmakers (2008). "DNA damage and ageing: new-age ideas for an age-old problem." Nat Cell Biol **10**(11): 1241-7.

Gatti, R. and S. Perlman (1993). Ataxia-Telangiectasia. GeneReviews(R). R. A. Pagon, M. P. Adam, H. H. Ardinger, S. E. Wallace, A. Amemiya, L. J. H. Bean, T. D. Bird, N. Ledbetter, H. C. Mefford, R. J. H. Smith and K. Stephens. Seattle (WA).

Gatti, R. A., I. Berkel, E. Boder, G. Braedt, P. Charmley, P. Concannon, F. Ersoy, T. Foroud, N. G. Jaspers, K. Lange and et al. (1988). "Localization of an ataxia-telangiectasia gene to chromosome 11q22-23." Nature **336**(6199): 577-80.

Gilad, S., L. Chessa, R. Khosravi, P. Russell, Y. Galanty, M. Piane, R. A. Gatti, T. J. Jorgensen, Y. Shiloh and A. Bar-Shira (1998). "Genotype-phenotype relationships in ataxia-telangiectasia and variants." Am J Hum Genet **62**(3): 551-61.

Giulietti, A., L. Overbergh, D. Valckx, B. Decallonne, R. Bouillon and C. Mathieu (2001). "An overview of real-time quantitative PCR: applications to quantify cytokine gene expression." Methods **25**(4): 386-401.

Gonzalez, L. C., S. Ghadaouia, A. Martinez and F. Rodier (2016). "Premature aging/senescence in cancer cells facing therapy: good or bad?" Biogerontology **17**(1): 71-87.

Goodarzi, A. A., J. C. Jonnalagadda, P. Douglas, D. Young, R. Ye, G. B. Moorhead, S. P. Lees-Miller and K. K. Khanna (2004). "Autophosphorylation of ataxia-telangiectasia mutated is regulated by protein phosphatase 2A." EMBO J **23**(22): 4451-61.

Guerra, B., K. Iwabuchi and O. G. Issinger (2014). "Protein kinase CK2 is required for the recruitment of 53BP1 to sites of DNA double-strand break induced by radiomimetic drugs." Cancer Lett **345**(1): 115-23.

Guleria, A. and S. Chandna (2016). "ATM kinase: Much more than a DNA damage responsive protein." DNA Repair (Amst) **39**: 1-20.

Guo, Z., S. Kozlov, M. F. Lavin, M. D. Person and T. T. Paull (2010). "ATM activation by oxidative stress." Science **330**(6003): 517-21.

Hanahan, D. and R. A. Weinberg (2000). "The hallmarks of cancer." Cell **100**(1): 57-70.

Harper, J. W. and S. J. Elledge (2007). "The DNA damage response: ten years after." Mol Cell **28**(5): 739-45.

Harrison, J. C. and J. E. Haber (2006). "Surviving the breakup: the DNA damage checkpoint." Annu Rev Genet **40**: 209-35.

Hayflick, L. (1965). "The Limited in Vitro Lifetime of Human Diploid Cell Strains." Exp Cell Res **37**: 614-36.

Heiss, N. S., S. W. Knight, T. J. Vulliamy, S. M. Klauck, S. Wiemann, P. J. Mason, A. Poustka and I. Dokal (1998). "X-linked dyskeratosis congenita is caused by mutations in a highly conserved gene with putative nucleolar functions." Nat Genet **19**(1): 32-8.

Herbig, U., W. A. Jobling, B. P. Chen, D. J. Chen and J. M. Sedivy (2004). "Telomere shortening triggers senescence of human cells through a pathway involving ATM, p53, and p21(CIP1), but not p16(INK4a)." Mol Cell **14**(4): 501-13.

Hoeijmakers, J. H. (2001). "Genome maintenance mechanisms for preventing cancer." Nature **411**(6835): 366-74.

Iarriccio, L., C. Manguan-Garcia, L. Pintado-Berninches, J. M. Mancheno, A. Molina, R. Perona and L. Sastre (2015). "GSE4, a Small Dyskerin- and GSE24.2-Related Peptide, Induces Telomerase Activity, Cell Proliferation and Reduces DNA Damage, Oxidative Stress and Cell Senescence in Dyskerin Mutant Cells." PLoS One **10**(11): e0142980.

Ishikawa, F. (1997). "Regulation mechanisms of mammalian telomerase. A review." Biochemistry (Mosc) **62**(11): 1332-7.

Ismail, I. H., T. I. Wadhra and O. Hammarsten (2007). "An optimized method for detecting gamma-H2AX in blood cells reveals a significant interindividual variation in the gamma-H2AX response among humans." Nucleic Acids Res **35**(5): e36.

Jiang, Y., M. Rabbi, M. Kim, C. Ke, W. Lee, R. L. Clark, P. A. Mieczkowski and P. E. Marszalek (2009). "UVA generates pyrimidine dimers in DNA directly." Biophys J **96**(3): 1151-8.

Kamsler, A., D. Daily, A. Hochman, N. Stern, Y. Shiloh, G. Rotman and A. Barzilai (2001). "Increased oxidative stress in ataxia telangiectasia evidenced by alterations in redox state of brains from Atm-deficient mice." Cancer Res **61**(5): 1849-54.

Kang, C., Q. Xu, T. D. Martin, M. Z. Li, M. Demaria, L. Aron, T. Lu, B. A. Yankner, J. Campisi and S. J. Elledge (2015). "The DNA damage response induces inflammation and senescence by inhibiting autophagy of GATA4." Science **349**(6255): aaa5612.

Kastan, M. B., Q. Zhan, W. S. el-Deiry, F. Carrier, T. Jacks, W. V. Walsh, B. S. Plunkett, B. Vogelstein and A. J. Fornace, Jr. (1992). "A mammalian cell cycle checkpoint pathway utilizing p53 and GADD45 is defective in ataxia-telangiectasia." Cell **71**(4): 587-97.

Keogh, M. C., J. A. Kim, M. Downey, J. Fillingham, D. Chowdhury, J. C. Harrison, M. Onishi, N. Datta, S. Galicia, A. Emili, J. Lieberman, X. Shen, S. Buratowski, J. E. Haber, D. Durocher, J. F. Greenblatt and N. J. Krogan (2006). "A phosphatase complex that dephosphorylates gammaH2AX regulates DNA damage checkpoint recovery." Nature **439**(7075): 497-501.

Khanna, K. K., M. F. Lavin, S. P. Jackson and T. D. Mulhern (2001). "ATM, a central controller of cellular responses to DNA damage." Cell Death Differ **8**(11): 1052-65.

Kim, N. W., M. A. Piatyszek, K. R. Prowse, C. B. Harley, M. D. West, P. L. Ho, G. M. Coviello, W. E. Wright, S. L. Weinrich and J. W. Shay (1994). "Specific association of human telomerase activity with immortal cells and cancer." Science **266**(5193): 2011-5.

Kim, T. S., M. Kawaguchi, M. Suzuki, C. G. Jung, K. Asai, Y. Shibamoto, M. F. Lavin, K. K. Khanna and Y. Miura (2010). "The ZFHX3 (ATBF1) transcription factor induces PDGFRB, which activates ATM in the cytoplasm to protect cerebellar neurons from oxidative stress." Dis Model Mech **3**(11-12): 752-62.

Kim, Y. C., G. Gerlitz, T. Furusawa, F. Catez, A. Nussenzweig, K. S. Oh, K. H. Kraemer, Y. Shiloh and M. Bustin (2009). "Activation of ATM depends on chromatin interactions occurring before induction of DNA damage." Nat Cell Biol **11**(1): 92-6.

Kinner, A., W. Wu, C. Staudt and G. Iliakis (2008). "Gamma-H2AX in recognition and signaling of DNA double-strand breaks in the context of chromatin." Nucleic Acids Res **36**(17): 5678-94.

Kobayashi, J., A. Antoccia, H. Tauchi, S. Matsuura and K. Komatsu (2004). "NBS1 and its functional role in the DNA damage response." DNA Repair (Amst) **3**(8-9): 855-61.

Kozlov, S. V., M. E. Graham, C. Peng, P. Chen, P. J. Robinson and M. F. Lavin (2006). "Involvement of novel autophosphorylation sites in ATM activation." EMBO J **25**(15): 3504-14.

Kuo, L. J. and L. X. Yang (2008). "Gamma-H2AX - a novel biomarker for DNA double-strand breaks." In Vivo **22**(3): 305-9.

Lang, A., S. Grether-Beck, M. Singh, F. Kuck, S. Jakob, A. Kefalas, S. Altinoluk-Hambuchen, N. Graffmann, M. Schneider, A. Lindecke, H. Brenden, I. Felsner, H. Ezzahoini, A. Marini, S. Weinhold, A. Vierkotter, J. Tigges, S. Schmidt, K. Stuhler, K. Kohrer, M. Uhrberg, J. Haendeler, J. Krutmann and R. P. Piekorz (2016). "MicroRNA-15b regulates mitochondrial ROS production and the senescence-associated secretory phenotype through sirtuin 4/SIRT4." Aging (Albany NY) **8**(3): 484-505.

Langerak, P. and P. Russell (2011). "Regulatory networks integrating cell cycle control with DNA damage checkpoints and double-strand break repair." Philos Trans R Soc Lond B Biol Sci **366**(1584): 3562-71.

Lavin, M. F. and K. K. Khanna (1999). "ATM: the protein encoded by the gene mutated in the radiosensitive syndrome ataxia-telangiectasia." Int J Radiat Biol **75**(10): 1201-14.

Lavin, M. F. and Y. Shiloh (1997). "The genetic defect in ataxia-telangiectasia." Annu Rev Immunol **15**: 177-202.

Lee, P., N. T. Martin, K. Nakamura, S. Azghadi, M. Amiri, U. Ben-David, S. Perlman, R. A. Gatti, H. Hu and W. E. Lowry (2013). "SMRT compounds abrogate cellular phenotypes of ataxia telangiectasia in neural derivatives of patient-specific hiPSCs." Nat Commun **4**: 1824.

Lindahl, T. (1993). "Instability and decay of the primary structure of DNA." Nature **362**(6422): 709-15.
Machado-Pinilla, R., I. Sanchez-Perez, J. R. Murguia, L. Sastre and R. Perona (2008). "A dyskerin motif reactivates telomerase activity in X-linked dyskeratosis congenita and in telomerase-deficient human cells." Blood **111**(5): 2606-14.

Maciejczyk, M., B. Mikoluc, B. Pietrucha, E. Heropolitanska-Pliszka, M. Pac, R. Motkowski and H. Car (2017). "Oxidative stress, mitochondrial abnormalities and antioxidant defense in Ataxia-telangiectasia, Bloom syndrome and Nijmegen breakage syndrome." Redox Biol **11**: 375-383.

Manguan-Garcia, C., L. Pintado-Berninches, J. Carrillo, R. Machado-Pinilla, L. Sastre, C. Perez-Quilis, I. Esmoris, A. Gimeno, J. L. Garcia-Gimenez, F. V. Pallardo and R. Perona (2014). "Expression of the genetic suppressor element 24.2 (GSE24.2) decreases DNA damage and oxidative stress in X-linked dyskeratosis congenita cells." PLoS One **9**(7): e101424.

Mates, J. M., C. Perez-Gomez and I. Nunez de Castro (1999). "Antioxidant enzymes and human diseases." Clin Biochem **32**(8): 595-603.

McGrath-Morrow, S. A., J. M. Collaco, B. Detrick and H. M. Lederman (2016). "Serum Interleukin-6 Levels and Pulmonary Function in Ataxia-Telangiectasia." J Pediatr **171**: 256-61 e1.

Mengual Gomez, D. L., R. G. Armando, H. G. Farina and D. E. Gomez (2014). "[Telomerase and telomere: their structure and dynamics in health and disease]." Medicina (B Aires) **74**(1): 69-76.

Metcalfe, S. M., S. Bickerton and T. Fahmy (2016). "Neurodegenerative Disease: A Perspective on Cell-Based Therapy In The New Era of Cell-Free Nano-Therapy." Curr Pharm Des.

Mirzayans, R., B. Andrais, A. Scott, Y. W. Wang and D. Murray (2013). "Ionizing radiation-induced responses in human cells with differing TP53 status." Int J Mol Sci **14**(11): 22409-35.

Mittal, M., M. R. Siddiqui, K. Tran, S. P. Reddy and A. B. Malik (2014). "Reactive oxygen species in inflammation and tissue injury." Antioxid Redox Signal **20**(7): 1126-67.

Mombach, J. C., C. A. Bugs and C. Chaouiya (2014). "Modelling the onset of senescence at the G1/S cell cycle checkpoint." BMC Genomics **15 Suppl 7**: S7.

Morgan, D. O. (1997). "Cyclin-dependent kinases: engines, clocks, and microprocessors." Annu Rev Cell Dev Biol **13**: 261-91.

Mourkioti, F., J. Kustan, P. Kraft, J. W. Day, M. M. Zhao, M. Kost-Alimova, A. Protopopov, R. A. DePinho, D. Bernstein, A. K. Meeker and H. M. Blau (2013). "Role of telomere dysfunction in cardiac failure in Duchenne muscular dystrophy." Nat Cell Biol **15**(8): 895-904.

Navratil, M., V. Duranovic, B. Nogalo, A. Svigir, I. Dumbovic Dubravcic and M. Turkalj (2015). "Ataxia-Telangiectasia Presenting as Cerebral Palsy and Recurrent Wheezing: A Case Report." Am J Case Rep **16**: 631-6.

Nebreda, A. R. and A. Porras (2000). "p38 MAP kinases: beyond the stress response." Trends Biochem Sci **25**(6): 257-60.

Neumann, C. A., D. S. Krause, C. V. Carman, S. Das, D. P. Dubey, J. L. Abraham, R. T. Bronson, Y. Fujiwara, S. H. Orkin and R. A. Van Etten (2003). "Essential role for the peroxiredoxin Prdx1 in erythrocyte antioxidant defence and tumour suppression." Nature **424**(6948): 561-5.

Nissenkorn, A., S. Hassin-Baer, S. F. Lerman, Y. B. Levi, M. Tzadok and B. Ben-Zeev (2013). "Movement disorder in ataxia-telangiectasia: treatment with amantadine sulfate." J Child Neurol **28**(2): 155-60.

Nitiss, J. L. (2009). "Targeting DNA topoisomerase II in cancer chemotherapy." Nat Rev Cancer **9**(5): 338-50.

Norbury, C. and P. Nurse (1992). "Animal cell cycles and their control." Annu Rev Biochem **61**: 441-70.

Oikawa, S. and S. Kawanishi (1999). "Site-specific DNA damage at GGG sequence by oxidative stress may accelerate telomere shortening." FEBS Lett **453**(3): 365-8.

Opresko, P. L. and J. W. Shay (2017). "Telomere-associated aging disorders." Ageing Res Rev **33**: 52-66.

Osborn, A. J., S. J. Elledge and L. Zou (2002). "Checking on the fork: the DNA-replication stress-response pathway." Trends Cell Biol **12**(11): 509-16.

Pallardo, F. V., A. Lloret, M. Lebel, M. d'Ischia, V. C. Cogger, D. G. Le Couteur, M. N. Gadaleta, G. Castello and G. Pagano (2010). "Mitochondrial dysfunction in some oxidative stress-related genetic diseases: Ataxia-Telangiectasia, Down Syndrome, Fanconi Anaemia and Werner Syndrome." Biogerontology **11**(4): 401-19.

Pandita, T. K., S. Pathak and C. R. Geard (1995). "Chromosome end associations, telomeres and telomerase activity in ataxia telangiectasia cells." Cytogenet Cell Genet **71**(1): 86-93.

Passos, J. F., G. Saretzki and T. von Zglinicki (2007). "DNA damage in telomeres and mitochondria during cellular senescence: is there a connection?" Nucleic Acids Res **35**(22): 7505-13.

Pearson, G., F. Robinson, T. Beers Gibson, B. E. Xu, M. Karandikar, K. Berman and M. H. Cobb (2001). "Mitogen-activated protein (MAP) kinase pathways: regulation and physiological functions." Endocr Rev **22**(2): 153-83.

Pendyala, G., B. Thomas and S. Kumari (2008). "The challenge of antioxidants to free radicals in periodontitis." J Indian Soc Periodontol **12**(3): 79-83.

Perlman, S., S. Becker-Catania and R. A. Gatti (2003). "Ataxia-telangiectasia: diagnosis and treatment." Semin Pediatr Neurol **10**(3): 173-82.

Perona, R., L. Iarriccio, L. Pintado-Berninches, J. Rodriguez-Centeno, C. Manguan-Garcia, E. Garcia, B. López-Ayllón and L. Sastre (2016). Molecular Diagnosis and Precision Therapeutic Approaches for Telomere Biology Disorders. Telomere - A Complex End of a Chromosome. M. L. Larramendy, Intech**:** 77-117.

Qi, L., M. A. Strong, B. O. Karim, M. Armanios, D. L. Huso and C. W. Greider (2003). "Short telomeres and ataxia-telangiectasia mutated deficiency cooperatively increase telomere dysfunction and suppress tumorigenesis." Cancer Res **63**(23): 8188-96.

Reliene, R. and R. H. Schiestl (2008). "Experimental antioxidant therapy in ataxia telangiectasia." Clin Med Oncol **2**: 431-6.

Rimkus, S. A., R. J. Katzenberger, A. T. Trinh, G. E. Dodson, R. S. Tibbetts and D. A. Wassarman (2008). "Mutations in String/CDC25 inhibit cell cycle re-entry and neurodegeneration in a Drosophila model of Ataxia telangiectasia." Genes Dev **22**(9): 1205-20.

Rodier, F., J. P. Coppe, C. K. Patil, W. A. Hoeijmakers, D. P. Munoz, S. R. Raza, A. Freund, E. Campeau, A. R. Davalos and J. Campisi (2009). "Persistent DNA damage signalling triggers senescence-associated inflammatory cytokine secretion." Nat Cell Biol **11**(8): 973-9.

Rogakou, E. P., D. R. Pilch, A. H. Orr, V. S. Ivanova and W. M. Bonner (1998). "DNA double-stranded breaks induce histone H2AX phosphorylation on serine 139." J Biol Chem **273**(10): 5858-68.

Rothblum-Oviatt, C., J. Wright, M. A. Lefton-Greif, S. A. McGrath-Morrow, T. O. Crawford and H. M. Lederman (2016). "Ataxia telangiectasia: a review." Orphanet J Rare Dis **11**(1): 159.

Rotman, G. and Y. Shiloh (1997). "Ataxia-telangiectasia: is ATM a sensor of oxidative damage and stress?" Bioessays **19**(10): 911-7.

Sahin, E., S. Colla, M. Liesa, J. Moslehi, F. L. Muller, M. Guo, M. Cooper, D. Kotton, A. J. Fabian, C. Walkey, R. S. Maser, G. Tonon, F. Foerster, R. Xiong, Y. A. Wang, S. A. Shukla, M. Jaskelioff, E. S. Martin, T. P. Heffernan, A. Protopopov, E. Ivanova, J. E. Mahoney, M. Kost-Alimova, S. R. Perry, R. Bronson, R. Liao, R. Mulligan, O. S. Shirihai, L. Chin and R. A. DePinho (2011). "Telomere dysfunction induces metabolic and mitochondrial compromise." Nature **470**(7334): 359-65.

Saldanha, S. N., L. G. Andrews and T. O. Tollefsbol (2003). "Analysis of telomerase activity and detection of its catalytic subunit, hTERT." Anal Biochem **315**(1): 1-21.

Sandi, C., M. Sandi, H. Jassal, V. Ezzatizadeh, S. Anjomani-Virmouni, S. Al-Mahdawi and M. A. Pook (2014). "Generation and characterisation of Friedreich ataxia YG8R mouse fibroblast and neural stem cell models." PLoS One **9**(2): e89488.

Santos, T., R. Ferreira, J. Maia, F. Agasse, S. Xapelli, L. Cortes, J. Braganca, J. O. Malva, L. Ferreira and L. Bernardino (2012). "Polymeric nanoparticles to control the differentiation of neural stem cells in the subventricular zone of the brain." ACS Nano **6**(12): 10463-74.

Schonn, I., J. Hennesen and D. C. Dartsch (2010). "Cellular responses to etoposide: cell death despite cell cycle arrest and repair of DNA damage." Apoptosis **15**(2): 162-72.

Schultz, L. B., N. H. Chehab, A. Malikzay and T. D. Halazonetis (2000). "p53 binding protein 1 (53BP1) is an early participant in the cellular response to DNA double-strand breaks." J Cell Biol **151**(7): 1381-90.
Sherr, C. J. (2004). "Principles of tumor suppression." Cell **116**(2): 235-46.

Shiloh, Y. and M. B. Kastan (2001). "ATM: genome stability, neuronal development, and cancer cross paths." Adv Cancer Res **83**: 209-54.

Shiloh, Y., E. Tabor and Y. Becker (1982). "Colony-forming ability of ataxia-telangiectasia skin fibroblasts is an indicator of their early senescence and increased demand for growth factors." Exp Cell Res **140**(1): 191-9.

Slatter, M. A. and A. R. Gennery (2010). "Primary immunodeficiencies associated with DNA-repair disorders." Expert Rev Mol Med **12**: e9.

Smilenov, L. B., S. E. Morgan, W. Mellado, S. G. Sawant, M. B. Kastan and T. K. Pandita (1997). "Influence of ATM function on telomere metabolism." Oncogene **15**(22): 2659-65.

Son, Y., Y. K. Cheong, N. H. Kim, H. T. Chung, D. G. Kang and H. O. Pae (2011). "Mitogen-Activated Protein Kinases and Reactive Oxygen Species: How Can ROS Activate MAPK Pathways?" J Signal Transduct **2011**: 792639.

Taylor, A. M., C. M. Rosney and J. B. Campbell (1979). "Unusual sensitivity of ataxia telangiectasia cells to bleomycin." Cancer Res **39**(3): 1046-50.

Tchirkov, A. and P. M. Lansdorp (2003). "Role of oxidative stress in telomere shortening in cultured fibroblasts from normal individuals and patients with ataxia-telangiectasia." Hum Mol Genet **12**(3): 227-32.

Teive, H. A., A. Moro, M. Moscovich, W. O. Arruda, R. P. Munhoz, S. Raskin and T. Ashizawa (2015). "Ataxia-telangiectasia - A historical review and a proposal for a new designation: ATM syndrome." J Neurol Sci **355**(1-2): 3-6.

Tong, A. S., J. L. Stern, A. Sfeir, M. Kartawinata, T. de Lange, X. D. Zhu and T. M. Bryan (2015). "ATM and ATR Signaling Regulate the Recruitment of Human Telomerase to Telomeres." Cell Rep **13**(8): 1633-46.

Trowbridge, A. A., C. Sirinavin and J. W. Linman (1977). "Dyskeratosis congenita: hematologic evaluation of a sibship and review of the literature." Am J Hematol **3**: 143-52.

Uziel, T., K. Savitsky, M. Platzer, Y. Ziv, T. Helbitz, M. Nehls, T. Boehm, A. Rosenthal, Y. Shiloh and G. Rotman (1996). "Genomic Organization of the ATM gene." Genomics **33**(2): 317-20.

van Attikum, H. and S. M. Gasser (2005). "The histone code at DNA breaks: a guide to repair?" Nat Rev Mol Cell Biol **6**(10): 757-65.

van Deursen, J. M. (2014). "The role of senescent cells in ageing." Nature **509**(7501): 439-46.

Watters, D., P. Kedar, K. Spring, J. Bjorkman, P. Chen, M. Gatei, G. Birrell, B. Garrone, P. Srinivasa, D. I. Crane and M. F. Lavin (1999). "Localization of a portion of extranuclear ATM to peroxisomes." J Biol Chem **274**(48): 34277-82.

Wood, L. D., T. L. Halvorsen, S. Dhar, J. A. Baur, R. K. Pandita, W. E. Wright, M. P. Hande, G. Calaf, T. K. Hei, F. Levine, J. W. Shay, J. J. Wang and T. K. Pandita (2001). "Characterization of ataxia telangiectasia fibroblasts with extended life-span through telomerase expression." Oncogene **20**(3): 278-88.

You, Z., C. Chahwan, J. Bailis, T. Hunter and P. Russell (2005). "ATM activation and its recruitment to damaged DNA require binding to the C terminus of Nbs1." Mol Cell Biol **25**(13): 5363-79.

Zannini, L., D. Delia and G. Buscemi (2014). "CHK2 kinase in the DNA damage response and beyond." J Mol Cell Biol **6**(6): 442-57.

Zhao, Y., A. J. Sfeir, Y. Zou, C. M. Buseman, T. T. Chow, J. W. Shay and W. E. Wright (2009). "Telomere extension occurs at most chromosome ends and is uncoupled from fill-in in human cancer cells." Cell **138**(3): 463-75.

ANEXO I:

Artículos que no forman parte de la tesis

- **Jaime Carrillo, Oriol Calvete, Laura Pintado-Berninches, Cristina Manguan-Garcia, Julian Sevilla Navarro, Elena G Arias-Salgado, Leandro Sastre, Guliiermo Guenechea, Eduardo López Granados, Jean-Pierre de Vallartay, Patrick Revy, Javier Benitez, Rosario Perona (2017).**
Mutations in XLF/NHEJ1/CERNUNNOS gene results in downregulation of Telomerase genes expression and telomere shortening. Human Molecular Genetics (in press).

- **R. Montejano, N. Stella Ascariz, S. Monge, J.I. Bernardino, I. Pérez-Valero, M. Montes, J. Mingorance, L. Pintado-Berninches, R. Perona, J.R. Arribas (2017).**
Impact of antiretroviral treatment containing tenofovir difumarate on the telomere length of aviremic HIV-infected patients. JAIDS (in press).

- **Natalia Stella-Ascariz, Rocío Montejano, Laura Pintado-Berninches, Susana Monge, José I. Bernardino, Ignacio Pérez Valero, María L. Montes, Jesús Mingorance, Rosario Perona and José R. Arribas. (2017)**.
Differential effects of Tenofovir, Abacavir, Emtricitabine, and Duranavir on Telomerase Activity in vitro. JAIDS.

- **Rosario Perona, Laura Iarriccio, Laura Pintado-Berninches, Javier Rodriguez-Centeno, Cristina Manguan-Garcia, Elena Garcia, Blanca Lopez-Ayllón and Leandro Sastre (2016).**
Molecular Diagnosis and Precision Therapeutic Approaches for Telomere Biology Disorders. Chapter from the book Telomere - A Complex End of a Chromosome (77-117).

- **Laura Iarriccio, Cristina Manguán-García, Laura Pintado-Berninches, José Miguel Mancheño, Antonio Molina, Rosario Perona, Leandro Sastre (2015)**.
GSE4, a Small Dyskerin- and GSE24.2-Related Peptide, Induces Telomerase Activity, Cell Proliferation and Reduces DNA Damage, Oxidative Stress and Cell Senescence in Dyskerin Mutant Cells. PLOS ONE.

- **Cristina Manguan-Garcia, Laura Pintado-Berninches, Jaime Carrillo, Rosario Machado-Pinilla, Leandro Sastre, Carme Pe ´rez-Quilis, Isabel Esmoris, Amparo Gimeno, Jose Luis García-Giménez, Federico V. Pallardó, Rosario Perona (2014).**
Expression of the Genetic Suppressor Element 24.2 (GSE24.2) Decreases DNA Damage and Oxidative Stress in X-Linked Dyskeratosis Congenita Cells. PLOS ONE.

- **Susana P. Egusquiaguirre, Cristina Manguán-García, Laura Pintado-Berninches, Laura Iarriccio, Daniel Carbajo, Fernando Albericio, Miriam Royo, José Luís Pedraz, Rosa M. Hernández, Rosario Perona, Manuela Igartua (2014).**
Development of surface modified biodegradable polymeric nanoparticles to deliver GSE24.2 peptide to cells: A promising approach for the treatment of defective telomerase disorders. European Journal of Pharmaceutics and Biopharmaceutics.

- **J. Carrillo, A. González, C. Manguán-García, L. Pintado-Berninches, R. Perona (2013)**.
p53 pathway activation by telomere attrition in X-DC primary fibroblasts occurs in the absence of ribosome biogenesis failure and as a consequence of DNA damage. Clinical and Translational Oncology.

Differential Effects of Tenofovir, Abacavir, Emtricitabine, and Darunavir on Telomerase Activity In Vitro

Natalia Stella-Ascariz, MS, Rocío Montejano, MD,† Laura Pintado-Berninches, MS,‡ Susana Monge, MD,§ José I. Bernardino, MD,† Ignacio Pérez-Valero, MD,† María L. Montes, MD,† Jesús Mingorance, PhD,* Rosario Perona, PhD,‡ and José R. Arribas, MD†*

Abstract: In vitro, tenofovir and abacavir induced a significant dose-dependent inhibition of telomerase activity at therapeutic concentrations in peripheral blood mononuclear cells of healthy subjects. Median inhibition of telomerase activity by tenofovir at 0.5 and 1 μM was 29% [Interquartile range (IQR) 29%–34%, $P = 0.042$] and 28% (IQR 28%–41%, $P = 0.042$), respectively. Abacavir inhibition was 12% (IQR 9%–13%, $P = 0.043$) at 3 μM and 14% (IQR 10%–29%, $P = 0.043$) at 10 μM. Tenofovir and abacavir did not change human telomerase reverse transcriptase (hTERT) levels or mRNA levels of other telomerase complex genes. Exposure to emtricitabine or darunavir did not affect telomerase activity, hTERT protein levels, or mRNA levels of telomerase/shelterin genes.

Key Words: HIV infection, antiretroviral therapy, telomerase, telomere, hTERT

(*J Acquir Immune Defic Syndr* 2017;74:91–94)

INTRODUCTION

There is growing concern about the issue of aging of HIV-infected patients. It is well established that HIV-infected patients have an increased risk for several "non-AIDS" complications (cardiovascular disease, malignancy, liver disease, kidney disease, bone disease, and neurocognitive decline) that are classically associated with the normal aging process.[1] It remains unclear if the higher risk of these complications is expression of an "accelerated" aging process, complications occurring at earlier ages, or of an "accentuated" aging process—higher prevalence of complications at every age strata.[2,3] It is also unknown if this accentuated or accelerated aging is caused by the proinflammatory state associated with even well-controlled HIV infection, traditional risk factors (such as smoking) that are more prevalent among HIV-infected people, or other still unknown causes.[4]

Another potential cause of accelerated or accentuated aging in HIV-infected patients could be telomere shortening caused by antiretroviral drugs.[5] There is a close association between shortened telomere length (TL) in peripheral blood mononuclear cells (PBMCs) and diseases of aging, including increased cardiovascular diseases and dementia.[6,7]

Telomerase is a ribonucleoprotein enzyme complex with a RNA template (TERC), a human telomerase reverse transcriptase (hTERT) subunit, and other regulatory proteins that together with the shelterin complex maintains telomere structure.[8] Telomerase adds repetitive TTAGGG sequences to the ends of chromosomes, compensating for the progressive telomeric loss occurring at each cell division. Because of structural and mechanistic similarity to HIV reverse transcriptase, nucleoside/nucleotide reverse transcriptase inhibitors [N(t)RTI] can inhibit telomerase.[9] Zidovudine (AZT), stavudine (d4T), didanosine (ddI), and abacavir (ABC) can inhibit telomerase activity in replicating cell lines in vitro, leading to accelerated shortening of TL.[10,11] This inhibition is not observed with nonnucleoside reverse transcriptase inhibitors.[12] Recently, Leeansyah and collaborators reported that tenofovir (TFV)[13] at therapeutic concentrations is a potent inhibitor of telomerase

Received for publication May 24, 2016; accepted July 29, 2016.

From the *Microbiology Service, Hospital Universitario La Paz, IdiPAZ, Madrid, Spain; †HIV Unit, Internal Medicine Service, Hospital Universitario La Paz, IdiPAZ, Madrid, Spain; ‡Instituto de Investigaciones Biomédicas CSIC/UAM, IdiPAZ, Biomarkers and New Therapies and CIBER de Enfermedades Raras (CIBERER), Madrid, Spain; and §Universidad de Alcalá de Henares, Centro de Investigación Biomédica en Red de Epidemiología y Salud Pública (CIBERESP), Madrid, Spain.

Supported by Grant PI13/01467 and PI14/01495 from Fondo de Investigaciones Sanitarias (supported by FEDER funds). Instituto de Salud Carlos III.

Presented as a poster in the 23th Conference on Retrovirus and Opportunistic Infections, February 22–25, 2016, Boston, MA.

N.S. is supported by a predoctoral fellowship from Fondo de Investigaciones Sanitarias. R.M. is supported by a Río Hortega fellowship from Fondo de Investigaciones Sanitarias. J.I.B. has received payment for lectures including service on the speaker's bureau from ViiV Healthcare and Janssen and currently received payment for expert testimony from Gilead Sciences and MSD. I.P.V. is supported by a Grant from Instituto de Salud Carlos III and Gilead Sciences and he has received payment for consultancy and payment for lectures including service on the speaker's bureau from Janssen Cilag, Gilead and VIIV and Gilead Sciences, Janssen Cilag, VIIV, BMS and MSD, respectively. M.L.M. is currently receiving payment for board membership and for development of educational presentations from Janssen and Abbvie and Gilead, respectively. Also, she has received payment for consultancy from Janssen, Abbvie, ViiV, for expert testimony from Abbvie, Brsitol, Janssen and for lectures including service on the speaker's bureau from Bristol, Janssen, ViiV, Abbvie. J.R.A. is currently receiving payment for board membership and for consultancy from Viiv, Janssen, Abbvie, BMS, Gilead, MSD and Viiv, Janssen, BMS, Gilead, and MSD, respectively. Also, he is receiving payment for lectures including service on the speaker's bureau from Viiv, Janssen, Abbvie, BMS, Gilead, and MSD. The remaining authors have no funding or conflicts of interest to disclose.

R.P. and J.R.A. equal contribution to this manuscript.

Supplemental digital content is available for this article. Direct URL citations appear in the printed text and are provided in the HTML and PDF versions of this article on the journal's Web site (www.jaids.com).

Correspondence to: José R. Arribas, MD, PhD, Consulta Medicina Interna 2, Hospital La Paz, IdiPAZ, Castellana 261, 28046 Madrid, Spain (e-mail: joser.arribas@salud.madrid.org).

activity, causing telomere shortening in vitro. In Leeansyah et al study, lamivudine (3 TC) and emtricitabine (FTC) also inhibited telomerase activity although only at high concentrations. This finding is surprising because, being cytidine analogues, 3 TC and FTC should not act as chain terminators and therefore other mechanism of telomerase inhibition by 3 TC and FTC could be operating.

Two studies have reported that saquinavir, a protease inhibitor (PI), is able to increase telomerase activity in PBMCs[14,15] and demonstrated that telomerase up-regulation appeared to be the result of enhanced expression of hTERT in human T leukemia cells in vitro.[16] Saquinavir is no longer a preferred protease inhibitor in expert guidelines. Darunavir (DRV) boosted with ritonavir is the recommended protease inhibitor in the majority of expert guidelines. The impact of DRV on telomerase activity is currently unknown.

The main objective of our study was to confirm if ABC, FTC and especially TFV, at therapeutic concentrations, inhibit telomerase activity in vitro in activated-PBMCs. Secondly, we assayed if DRV is able to increase telomerase activity in vitro. Finally, we wanted to evaluate the possible impact of these antiretrovirals on mechanisms of telomerase inhibition different from chain termination such as expression of telomerase genes.

METHODS

Culture of PBMCs In Vitro With Antiretrovirals

PBMCs from healthy volunteers were isolated from whole blood by density gradient centrifugation using Ficoll-Pague PLUS (GE Healthcare). PBMCs were cultured in RPMI medium with 10% FBS supplemented with phytohemaglutinin, M form (PHA-M) (1% vol/vol; Gibco—Life Technologies), and human recombinant interleukin 2 (IL-2) (5 ng/mL; Gibco—Life Technologies) for 72 hours. Subsequently, 4×10^6 activated PBMCs were treated with increased concentrations of TFV, ABC, FTC or DRV (National Institute of Health AIDS Research and Reference Reagent Program) in fresh medium plus PHA-M/IL-2 for another 72 hours. Concentrations used for ABC and FTC were 0; 1; 3; 10; 50; and 100 μM, for TFV were 0; 0.1; 0.5; 1; 3; and 5 μM and for DRV were 0; 0.5; 1; 5; 10; 50 μM. Concentrations were calculated based on the pharmacokinetic parameters summarized in http://www.hiv-druginteractions.org/fact_sheets website of University of Liverpool.

Measurement of Telomerase Activity

We determined telomerase activity according to the Telomeric Repeat Amplification Protocol (TRAP) by TRAPeze Telomerase Detection kit (EMD Millipore, Billerica, MA) using radioisotopic detection according to the manufacturer's instructions with following modifications: radioactive end-labeling of the TS Primer[17] was incubated 30 minutes at 37°C and 10 minutes at 85°C, telomerase extension reaction was performed with 3 serial dilutions of cell extract at 30°C for 30 minutes followed by 5 minutes denaturation at 94°C, and amplification of the telomeric repeats was done in 30 cycles. The reaction was visualized by autoradiography and was analyzed using the image-processing program ImageJ (http://imagej.nih.gov/ij/). Telomerase activity was normalized using the internal control provided in the kit and expressed relative to untreated PBMCs.

Western Blot Analysis of hTERT Expression

20 μg of total cellular protein was subjected to 8% SDS-PAGE and transferred to polyvinylidene fluoride membranes (Immobilon-P; Millipore). Membranes were then blocked with 5% milk and incubated with rabbit anti-hTERT antibody (1:1000) (cat no. sc-7212; Santa Cruz Biotechnology, Santa Cruz, CA) at 4°C overnight, followed by incubation with a secondary anti-rabbit antibody (1:1000) conjugated with horseradish peroxidase at room temperature for 30 minutes. Membranes were rehybridized with α-tubulin antibody as a housekeeping expressed control protein. Membrane antibody binding was detected by enhanced chemiluminescence (ECL; Santa Cruz Biotechnology). Image quantifications were performed using ImageJ software.

Measurement of Gene Expression of the Telomerase/Shelterin Complex

Total RNA was isolated from cells using Tri Reagent (Sigma) and was quantified spectrophotometrically. First-strand cDNA was synthesized from 1 μg of total RNA by reverse transcriptase in a volume of 20 μL containing 200 U of Moloney murine leukemia virus reverse transcriptase (M-MLV RT) (Promega), 1X M-MLV 5X reaction buffer (Promega), 20 U of RNase OUT (Invitrogen), 0.5 μg random primer (Promega), and 0.5 mM dNTPs. The reaction was performed for 60 minutes at 37°C and cDNA was stored at −80°C until use.

The mRNA expression level of the genes coding for the different telomerase or shelterin complex subunits (*hTERT*, *TERC*, *DKC1*, *TINF2*, *TRF1* and *TRF2*) was quantified by quantitative real-time PCR (qPCR) using TaqMan Gene Expression Assay (Applied Biosystem). To normalize the amount of total mRNA present in each reaction, we amplified an endogenous housekeeping gene encoding for glyceraldehyde-3-phosphate dehydrogenase (*GAPDH*). qPCR was performed with 100 ng of cDNA in a total volume of 20 μL containing 1X TaqMan Universal Master Mix II, no UNG and 1X TaqMan Gene Expression Assay of each gene (Applied Biosystem) (see Table 1, Supplemental Digital Content, http://links.lww.com/QAI/A880). Samples were performed in duplicate using a Real Time Stratagene MX3000P. The thermal cycling conditions included preincubation for 10 minutes at 95°C, followed by 40 cycles of 15 seconds at 95°C and 30 seconds at 60°C.

Statistical Analysis

Statistic evaluation was performed with STATA v12 (Stata Corporation, College Station, Texas). Statistical significance for telomerase activity, levels of hTERT protein, and expression of telomerase complex subunits genes were calculated using

Wilcoxon signed-rank test. P values < 0.05 were considered statistically significant.

The institutional review board of Hospital La Paz approved the study and samples were obtained after written informed consent.

RESULTS

TFV and ABC Inhibit Telomerase Activity In Vitro

We analyzed the effect of 3 N(t)RTIs (TFV, ABC and FTC) and 1 PI (DRV) on telomerase activity in PHA-activated PBMCs from healthy volunteers after 72 hours of treatment. We performed 5 independent experiments with all N(t)RTIs and 6 independent experiments with DRV. Telomerase activity was expressed relative to untreated PBMCs.

Of the N(t)RTIs tested, only TFV and ABC induced a significant dose-dependent decrease of telomerase activity within the therapeutic concentration range. Median inhibition induced by TFV at 0.5 and 1 μM was 29% (IQR: 29%–34%; range: 12%–39%; $P = 0.042$) and 28% (IQR: 28%–41%; range: 25%–47%; $P = 0.042$), respectively. For ABC at 3 and 10 μM, median inhibition was 12% (IQR: 9%–13%; range: 8%–17%; $P = 0.043$) and 14% (IQR: 10%–29%; range: 7%–40%; $P = 0.043$), respectively. Exposure to FTC or DRV did not affect telomerase activity even at concentrations above the therapeutic plasma level range (Fig. 1A).

No Changes in Levels of hTERT Protein or Expression of the Telomerase/Shelterin Complex Genes.

Experiments were performed to establish whether reduction of telomerase activity mediated by TFV and ABC was the consequence of a decrease in the amount of hTERT protein. We determined the levels of hTERT after treatment for 72 hours with ABC, FTC and DRV (4 experiments each) and TFV (5 experiments). We did not find differences in the amount of hTERT between untreated and treated PBMCs (Fig. 1B). In addition, we measured the expression levels of the genes coding for the different telomerase and shelterin complex subunits (*hTERT*, *TERC*, *DKC1*, *TINF2*, *TRF1*, and *TRF2*). We measured the levels of mRNA after treatment for 72 hours with TFV, ABC, and DRV (6 experiments each) and FTC (5 experiments). We did not detect changes in expression of the genes that code for the catalytic subunit hTERT of the telomerase complex (Fig. 1C) or other telomerase subunits.

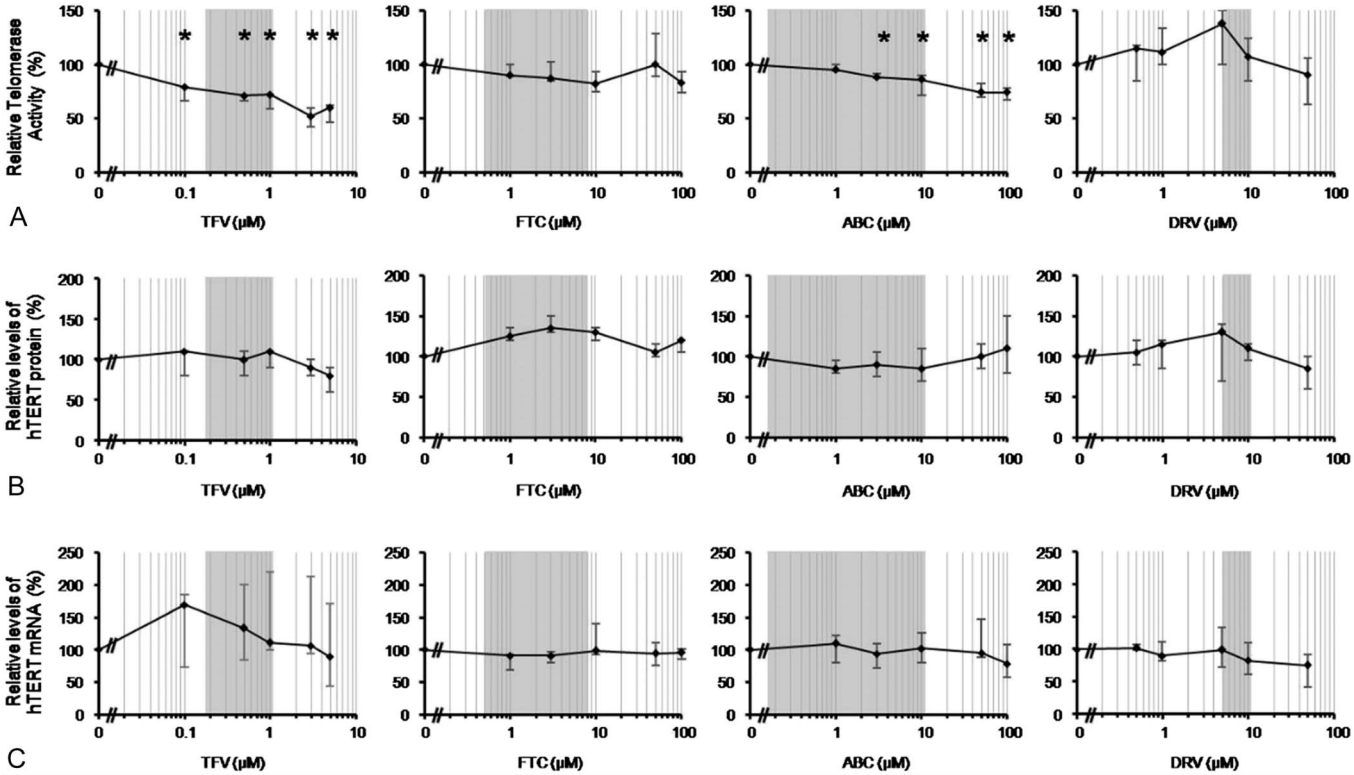

FIGURE 1. The effect of nucleos(t)ide reverse transcriptase inhibitors and darunavir on telomerase activity (A), levels of hTERT protein (B), and hTERT mRNA (C) in activated PBMCs. Closed circles represent the median, error bars represent interquartile range, and gray area represents the expected plasma levels in vivo for each antiretroviral (boosted DRV therapeutic range was assumed for DRV). The data are represented as percentage telomerase activity, levels of hTERT protein, and amount of hTERT mRNA of untreated cells. For telomerase activity (A), results are shown for TFV, ABC, and FTC (n = 5) and for DRV (n = 6). For levels of hTERT protein (B), results are shown for TFV (n = 5) and ABC, FTC, and DRV (n = 4). For levels of hTERT, mRNA results are shown for TFV, ABC, and DRV (n = 6) and FTC (n = 5). *$P < 0.05$.

DISCUSSION

In our study, we explored if N(t)RTIs could play a role in the aging process of HIV-infected patients by means of inhibition of telomerase activity and whether DRV could have a similar effect. We have found that TFV and ABC, but not FTC, produced a significant dose-dependent decrease of telomerase activity in PHA-activated PBMCs within the therapeutic concentration range in vivo. After 72 hours of treatment, telomerase inhibition caused by TFV was more than double the inhibition caused by ABC: 29% and 12%, respectively. The observed decrease in telomerase activity caused by TFV and ABC was not associated with a decrease in hTERT protein level, or a change in the expression of *hTERT* gene or the other genes that code for the subunits of the telomerase/shelterin complexes. Furthermore, we have shown that DRV did not affect telomerase activity, *hTERT* gene expression, or hTERT protein levels.

The active forms of TFV, ABC, and FTC compete with the intracellular dATP, dGTP and dCTP pools, respectively, and the incorporation of these nucleotide analogs causes viral DNA chain termination. Telomeres are made up of hexamer repeat TTAGGG sequences. Telomerase binds to the 3' end of the telomeres through its own RNA template and adds TTAGGG polynucleotides to the extreme, whereas the complementary strand is filled in by DNA polymerase later on. Consequently, inhibition of the reverse transcriptase activity of hTERT by the chain termination mechanism would be possible with TFV and ABC but not with FTC. Leeansyah and collaborators[13] have previously shown that TFV was the only N(t)RTI that at therapeutic concentrations in vitro significantly inhibited telomerase activity and enhanced shortening of TL. However, in their study, ABC and FTC were also able to inhibit telomerase activity at concentrations above the therapeutic range, but only ABC enhanced shortening of TL. Probably, our study underestimates the inhibition of activity telomerase with ABC and FTC because we performed measurements of telomerase activity after 72 hours of treatment with a single dose of each drug, in contrast to Leeansyah study in which N(t)RTIs were replenished every 48 hours. This difference could account for the lack of effect of FTC on telomerase activity observed in our study. Moreover, another limitation of our study is that we cannot determine whether the main effects of NRTIs were on $CD4^+$ or $CD8^+$ T cells, or specific subsets of T cells or non–T-cell population.

The in vivo relevance of the differential effects of TFV, ABC, FTC, and DRV on telomerase activity remains to be elucidated. Although Leeansyah and colleagues reported that in vivo telomere length was significantly inversely associated with the total duration of treatment with any N(t)RTI, other studies have not found this association. In a substudy of the MONET clinical trial[18] comparing darunavir/ritonavir monotherapy versus darunavir/ritonavir and 2 N(t)RTIs for maintenance of virological suppression, there were not significant differences between 2 arms after 3 years of follow-up in telomerase activity or mean change per year of telomere length.

Our results provide more evidence about the inhibition caused by some NRTI on telomerase activity. We have confirmed that TFV and ABC inhibit telomerase activity in activated PBMCs in vitro at therapeutic concentrations and that TFV is the most potent inhibitor. Telomerase activity inhibition caused by N(t)RTIs is probably due to inhibition of hTERT activity leading to chain termination and does not involve changes in expression levels of telomerase genes or hTERT protein. In addition, we did not find that DRV affects telomerase activity, *hTERT* gene expression, or hTERT protein levels. To our knowledge, ours is the first study showing a lack of implication of hTERT proteins levels and mRNA expression. The in vivo relevance of these findings remains to be elucidated.

REFERENCES

1. High KP, Brennan-Ing M, Clifford DB, et al. HIV and aging: state of knowledge and areas of critical need for research. A report to the NIH Office of AIDS Research by the HIV and Aging Working Group. *J Acquir Immune Defic Syndr.* 2012;60(suppl 1):S1–S18.
2. Rasmussen LD, May MT, Kronborg G, et al. Time trends for risk of severe age-related diseases in individuals with and without HIV infection in Denmark: a nationwide population-based cohort study. *Lancet HIV*. 2015;2:e288–e298.
3. Althoff KN, McGinnis KA, Wyatt CM, et al. Comparison of risk and age at diagnosis of myocardial infarction, end-stage renal disease, and non-AIDS-defining cancer in HIV-infected versus uninfected adults. *Clin Infect Dis.* 2015;60:627–638.
4. Hunt PW. HIV and aging: emerging research issues. *Curr Opin HIV AIDS.* 2014;9:302–308.
5. Bollmann FM. Telomerase inhibition may contribute to accelerated mitochondrial aging induced by anti-retroviral HIV treatment. *Med Hypotheses.* 2013;81:285–287.
6. Haycock PC, Heydon EE, Kaptoge S, et al. Leucocyte telomere length and risk of cardiovascular disease: systematic review and meta-analysis. *BMJ*. 2014;349:g4227.
7. Honig LS, Kang MS, Schupf N, et al. Association of shorter leukocyte telomere repeat length with dementia and mortality. *Arch Neurol.* 2012; 69:1332–1339.
8. Hodes RJ, Hathcock KS, Weng N. Telomeres in T and B cells. *Nat Rev Immunol.* 2002;2:699–706.
9. Peng Y, Mian IS, Lue NF. Analysis of telomerase processivity: mechanistic similarity to HIV-1 reverse transcriptase and role in telomere maintenance. *Mol Cell.* 2001;7:1201–1211.
10. Strahl C, Blackburn EH. Effects of reverse transcriptase inhibitors on telomere length and telomerase activity in two immortalized human cell lines. *Mol Cell Biol.* 1996;16:53–65.
11. Tendian SW, Parker WB. Interaction of deoxyguanosine nucleotide analogs with human telomerase. *Mol Pharmacol.* 2000;57:695–699.
12. Hukezalie KR, Thumati NR, Côté HCF, et al. In vitro and ex vivo inhibition of human telomerase by anti-HIV nucleoside reverse transcriptase inhibitors (NRTIs) but not by non-NRTIs. *PLoS One*. 2012;7:e47505.
13. Leeansyah E, Cameron PU, Solomon A, et al. Inhibition of telomerase activity by human immunodeficiency virus (HIV) nucleos(t)ide reverse transcriptase inhibitors: a potential factor contributing to HIV-associated accelerated aging. *J Infect Dis.* 2013;207:1157–1165.
14. Franzese O, Lombardi A, Comandini A, et al. Effect of saquinavir on proliferation and telomerase activity of human peripheral blood mononuclear cells. *Life Sci.* 2001;69:1509–1520.
15. Comandini FA, Lombardi A, Saponiero A, et al. Saquinavir up-regulates telomerase activity in lymphocytes activated with monoclonal antibodies against CD3/CD28. *J Chemother.* 2001;13:384–388.
16. Adamo R, Comandini A, Aquino A, et al. The antiretroviral agent saquinavir enhances hTERT expression and telomerase activity in human T leukaemia cells in vitro. *J Exp Clin Cancer Res.* 2013;32:38.
17. Manguan-Garcia C, Pintado-Berninches L, Carrillo J, et al. Expression of the genetic suppressor element 24.2 (GSE24.2) decreases DNA damage and oxidative stress in X-linked dyskeratosis congenita cells. *PLoS One.* 2014;9:e101424.
18. Solomon A, Tennakoon S, Leeansyah E, et al. No difference in the rate of change in telomere length or telomerase activity in HIV-infected patients after three years of darunavir/ritonavir with and without nucleoside analogues in the MONET trial. *PLoS One.* 2014;9:e109718.

Chapter 5

Molecular Diagnosis and Precision Therapeutic Approaches for Telomere Biology Disorders

Rosario Perona, Laura Iarriccio, Laura Pintado-Berninches, Javier Rodriguez-Centeno, Cristina Manguan-Garcia, Elena Garcia, Blanca Lopez-Ayllón and Leandro Sastre

Additional information is available at the end of the chapter

http://dx.doi.org/10.5772/65353

Abstract

Telomeres are nucleo-protein structures located at the end of chromosomes that protect them from degradation. Telomeres length is maintained by the activity of the telomerase complex. These structures are protected by a specialized protein complex named shelterin. In the absence of telomerase activity and/or protection telomeres are shortened after each round of DNA replication. When a critical size is reached, telomeres are recognized as damaged DNA by the cell p53-dependent DNA-repair system. Persistent activation of this pathway finally results in cell apoptosis or senescence.

There are a number of rare hereditary diseases caused by the presence of shortened telomeres, collectively named telomeropathies or telomere biology disorders. In these diseases, cell proliferation is impaired, which results in premature aging and dysfunction of highly proliferative tissues (bone morrow, skin and other epithelia). Among them are Dyskeratosis congenita, the Hoyeraal-Hreidarsson, Revesz and Coats plus syndromes, Aplastic anemia, Idiopathic pulmonary fibrosis and nonalcoholic, noninfectious liver disease. Mutations present in the genes coding for component of the telomerase and shelterin complexes and other proteins involved in telomere replication are the cause of these diseases. Clinical manifestations, causative mutations, diagnosis and possible therapeutic approaches to these diseases will be discussed in this chapter.

Keywords: telomere, telomere biology disorders, telomeropathies, pulmonary fibrosis, bone marrow failure

1. Introduction

Eukaryotic chromosomes are capped at their ends by specialized nucleo-protein structures, named telomeres that protect them from degradation. Human telomeres have a specific nucleotide sequence composed by thousand of repetitions of the TTAGGG hexanucleotide [1]. A protein complex, named shelterin associates to this DNA region to form the telomere-specific chromatin structure. Telomeres protects the chromosomal ends from degradation and are, therefore, essential for chromosomal and genome stability [2]. In their absence chromosomal ends are recognized as damaged DNA by the cell and can be degraded or recombined with other chromosomal ends resulting in the fusion and reorganization of chromosomes [3]. The maintenance of telomeres is, therefore, of critical importance for the genetic stability of cells and organisms.

Replication of telomeric DNA requires the contribution of a specific enzymatic machinery. DNA polymerases responsible for replication of the rest of the chromosomal DNA cannot completely synthesize telomeric DNA. DNA polymerases always require a primer molecule that cover the 5′ end of the DNA and are not able to complete the synthesis of the lagging strand of lineal DNA molecules, such as chromosomes. This end-replication problem results in the shortening of each telomere by 50-100 nucleotides at each DNA replication cycle and, therefore, at each cell division [4]. In most eukaryotic organisms, including humans, telomere length is maintained by the activity of the telomerase complex that elongates the telomeres by a replication-independent mechanism [5]. The complex is formed by a protein with reverse-transcriptase activity (TERT) and one RNA with a region of homology to the telomere DNA that is used as template for elongation [6]. Telomerase activity is, therefore, required for unlimited cell proliferation. Telomerase components and, in particular the TERT gene, are expressed to high relative levels during embryonic development allowing high cell proliferation rates. Expression of the TERT gene is, however, repressed in most human adult cells [7]. TERT expression is found only in germinal cells, in stem cells, specially in those of highly proliferative tissues such as bone marrow and epithelia and in lymphocytes [8]. The rest of the cells express very low TERT levels and their telomeres get progressively shorter after each cell division. When telomeres reach a critical size get unprotected and are recognized as damaged DNA. The ATM and ATR kinases, that regulate cellular responses to DNA damage are recruited to critically-short telomeres and activate the p53-dependent pathway that results in cell cycle arrest [3]. Prolonged arrest would finally induce apoptotic cell death or cellular senescence. Actually, most tissue-specific stem cells do not express enough TERT protein to completely replicate their telomeres at each cell division and their proliferative capacity decreases with the age of the organism [9]. With time, stem cell exhaustion impairs tissue renewal. Because of this reason, telomere shortening has been recognized as one of the hallmarks of human aging [10].

Telomere replication is also involved in the acquisition of the unlimited proliferative capacity that characterizes tumor cells [7]. Telomerase expression and activity is induced in about 85% of tumors, which allows tumor cells to completely elongate their telomeres at each cell division. In the other about 15% of tumors, telomeres length is maintained by a telomerase-independent

http://dx.doi.org/10.5772/65353

mechanism, know as Alternative Lengthening of the Telomeres (ALT) that elongates telomeres through DNA recombination mechanisms [11].

The importance of telomere homeostasis is further enforced by the existence of a number of rare hereditary diseases that are caused by the presence of shortened telomeres, collectively named telomeropathies, short telomere syndromes or telomere biology disorders [12]. These diseases are caused by mutations in genes coding for proteins involved in telomere lengthening (telomerase complex and related proteins) or in the maintenance of telomere structure (shelterin complex). These diseases are commonly characterized by the presence of very short telomeres in the cells of the affected patients. The molecular pathology of these diseases, their diagnosis and emerging therapies will be summarized in this chapter. It is necessary to enforce the importance of telomere homeostaxis for healthy life since excessively long telomeres are also causative of disease. Recent reports have associated the presence of long telomeres to increased frequency of cancers such as melanoma or glioma [13]. Mutations in the promoter region of the TERT gene that increase gene expression are frequently found in these and other tumors [14, 15]. In addition, mutations in the coding region of genes coding for protein of the shelterin complex have been found in human tumors [16, 17].

2. Main body

2.1. Telomere structure

Telomeres have a very specialized chromatin structure that is required to protect chromosome ends from degradation and to avoid telomere-telomere fusions [2]. The general structure will be briefly summarized in this section of the chapter and is schematically shown in the upper panel of Figure 1 where the genes mutated in telomere biology disorders are indicated by asterisks. Telomere structure has been the subject of several recent excellent reviews [2, 12, 18, 19]. The nucleotide sequence of telomeres is composed for multiple repetitions of the TTAGGG hexanucleotide in humans and several other animals. The length of these regions is variable in different organisms. In humans, telomeres have and average size of 8-14 kb in peripheral blood cells in new born children [20]. The size decreases with age so that the average size in a 90-years old person is of 3-7 kb [12]. In contrast, most mice strains used in research have an average telomere length of 50-100 kb which has made more difficult the development of mouse models of telomere biology disorders [21, 22].

Telomere ends are not formed by blunt-ended double-stranded DNA, as might be expected. Instead, the 3′ strand is about 75-300 bases longer than the 5′ end strand forming an overhanging single-stranded DNA fragment (Fig 1, upper panel) [1]. The overhanging strand contains the TTAGGG sequence and is, therefore, known as the G-rich strand. The complementary strand contains the complementary CCCTAA repeats and is named the C-rich strand. The overhanging strand is not unstructured. Instead, it turns over the telomere DNA and intercalates in the neighbouring double-stranded DNA forming a loop, named the T-loop, as schematically shown in the upper panel of Figure 1 [23]. Looping results in the formation of a

triple stranded DNA region known as D-loop that is required for the stability of the terminal telomeric DNA region [24].

Telomeres are further stabilized by the presence of a specific protein complex, the shelterin complex. It is composed by six different proteins: TRF1, TRF2, RAP1, TIN2, TPP1 and POT1 (upper panel of Figure 1] [2]. TRF1 (telomeric repeat binding factor 1, encoded by the TERF1 gene) binds to telomeric double-stranded DNA as a dimmer [25]. TRF2 (telomeric repeat binding factor 2, encoded by the TERF2 gene) also binds double-stranded DNA as a dimmer and associates with TRF1 [26]. The TIN2 protein (TRF1-interacting protein 2] interacts with TRF1 and TRF2 [27] and recruits the POT1(Protection of telomeres protein 1]/TPP1(POT1-interacting protein 1] heterodimer [28]. POT1 binds with high affinity to the G-rich strand overhang [29]. RAP1 (repressor-activator protein 1] incorporates to the shelterin complex via TRF2 interaction [28]. In addition, telomeres and subtelomeric regions are enriched in heterochromatin components including the association of HP1 proteins and histone 3 Lysine 9 and histone 4 lysine 20 trimethylation which further contributes to their stability [30].

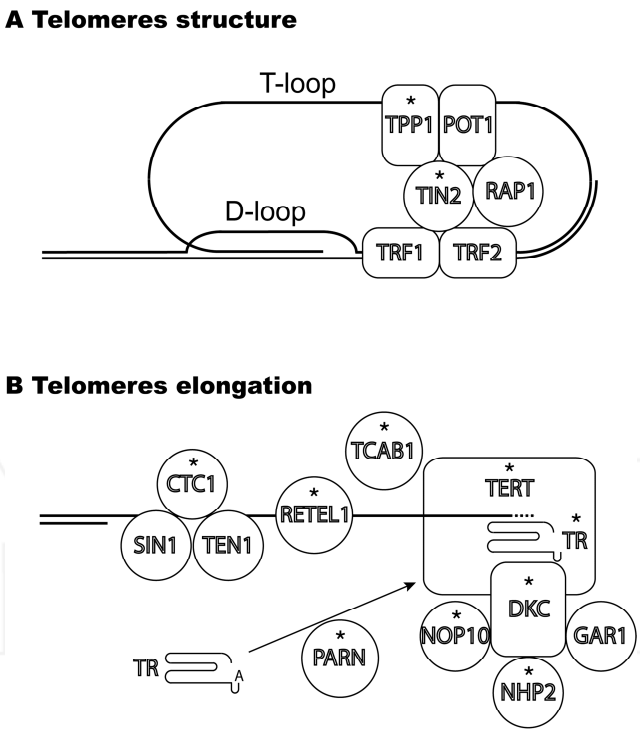

Figure 1. Telomere structure and elongation mechanism.

The shelterin complex is required for telomere maintenance and function and prevents the recognition of telomeres as damaged DNA. TRF2 inhibits the ATM kinase that induces the

http://dx.doi.org/10.5772/65353

canonical non-homologous-end-joining DNA repair pathway that would result in telomere-telomere fusions [31]. In addition, POT1 inhibits signalling by the ATR kinase in response to DNA damage by double-strand and single-strand breaks and alkylating agents [32]. POT1 also inhibits sister-telomere associations [33].

Telomere structure is schematically shown in upper panel A of the figure. Telomeric DNA is formed by repetitions of the TTAGGG hexanucleotide and is represented as two lines in the figure. The upper line represents the leading, G-rich strand. The 3′ end of this strand is single-stranded and forms a loop (T-loop) to hybridize to a region of the upstream double-stranded DNA forming a smaller loop (D-loop). The lower line represents the lagging DNA strand. Proteins of the shelterin complex, which binds to telomeric DNA, are represented as boxes. Asterisks indicate the proteins whose encoding gene have been found mutated in patients with telomere biology disorders. Panel B represent the components involved in telomere elongation. DNA is represented as two lines and proteins as boxes, as indicated on panel A. The DNA leading strand is the upper one and the DNA being synthesized is represented as a broken line. The components of the telomerase complex that catalyzes telomere elongation are represented on the right of the panel. Telomerase complex is composed by the TERT, DKC, NOP10, NHP2 and GAR1 proteins and the RNA molecule TR. The protein TCAB1 is required for telomerase recruitment to telomeres. PARN is required for TR RNA processing. The RETEL1 helicase and the CTC1/SIN1/TEN1 complex facilitate telomere elongation by disrupting DNA secondary structures. Asterisks indicate the proteins whose encoding genes have been found mutated in patients with telomere biology disorders.

2.2. Telomere elongation

In this section a brief summary of the telomere elongation process and its regulation will be presented because many of the proteins involved are related to telomere biology disorders. A schematic representation of the process is shown at the lower panel of Figure 1. Genes mutated in telomere biology disorders, as described in next sections, are indicated by asterisks. Telomere replication has been reviewed recently by several authors [18, 19, 34-36]. Cellular DNA polymerases cannot complete the replication of DNA double-strand ends which is know as the end-replication problem [37], as mentioned in the Introduction section. In mammals, telomere DNA 3′ ends are elongated by the telomerase complex through reverse transcription. The catalytic activity of the complex resides in the TERT (telomerase reverse transcriptase) protein [6] while the 454 nucleotides long TR (telomerase RNA, encoded by the TERC gene) is used as template [38] (Figure 1, lower panel) [36]. This is because TR has an internal region complementary to the TTAGGG repeats that allows hybridization to the 3′ end of the telomere DNA [36]. The TR RNA has similarity to other small nucleolar RNAs and contains a H/ACA motif [39]. It is transcribed by RNA polymerase II and contains a Cap structure and its 5′end and a 3′ oligo-Adenosine tail [40]. It has been recently shown that the 3′ end of TR has to be processed through exonuclease cleavage and that the Poly(A)-specific ribonuclease (PARN) is required for this maturation process [41].

Additional proteins form part of the telomerase complex and are required for its assembly and stability. Among them, dyskerin (encoded by the DKC1 gene) binds to TR through its inter-

action with the dyskerin PUA RNA binding domain [42]. Dyskerin binding is required for TR stability and for its recruitment to the telomerase complex. The proteins NHP2 and NOP10 associate to dyskerin and are also required for telomerase assembly [43].

Telomerase activity is dependent on TERT gene expression that is tissue-dependent and developmentally regulated, as mentioned in the Introduction section. In addition, it is dependent on protein-protein interactions that regulate telomerase-complex assembly and its recruitment to telomeres. One of the proteins involved is TCAB1 (encoded by the WRAP53 gene) that is an essential component of the subnuclear Cajal body structures. TACB1associates to TR, contributing to telomerase assembly in these structures [44]. Depletion of TCAB1 results in a relocation of the telomerase complex to the nucleolus and reduced recruitment to telomeres [44]. The shelterin-complex component TPP1 is also required for the recruitment of telomerase to telomeres. The TEL patch of TPP1, rich in Glutamate and Leucine residues, interacts with the TEN domain of TERT to mediate telomerase recruitment [45]. This interaction also promotes the telomerase ability to catalyze repeated cycles of DNA synthesis at the telomeres [46].

After elongation of the G-rich overhanging strand by the telomerase complex the C-rich strand is synthesized by the activity of the primase/DNA polymerase complex [35]. Proteins with helicase activity are required to facilitate telomere elongation through disruption of DNA structures that impair telomerase and DNA polymerase activity. The G-rich nature of the overhanging strand favours the formation of secondary structures such as G-quartets [47]. In addition, the D-loop structure of telomeres can also impair DNA synthesis. One of the proteins involved in solving DNA structures at the telomeres is RETEL1 (regulator of telomere length 1], a DNA helicase with D-loop-disrupting activity that has been proposed to facilitate T loop unwinding and to counteract the formation of G-quartets [48, 49]. In addition, RETEL1 has additional functions at other DNA loci [50]. The CST complex, formed by the CTC1, STN1 and TEN1 proteins promotes the initiation of the lagging C-rich strand synthesis [51]. CTC1 binds to the single-stranded G-rich DNA strand and recruits the initiator Polα primase complex to accomplish C-rich strand synthesis [52].

Once DNA synthesis is completed at telomeres, DNA is further processed to generate the G-strand overhangs [35]. This is a highly regulated process so that G-strands overhangs are between 30 and 400 nucleotides long and the C-rich strand ends at the 3′-CCAATC-5′ sequence in most telomeres [53]. Processing requires the activity of several factors: the Apollo/SNMB1 nuclease, Exonuclease I, the CST complex and two shelterin proteins, POT1 and TRF2 [54].

It is important to enforce that although telomere structure and replication have been presented separately for simplicity they are highly interconnected processes. For example, proteins of the shelterin complex play essential roles in telomere elongation through recruitment of the telomerase complex and proteins involved in the regulation of telomere length.

2.3. Telomere biology disorders

Several diseases related to telomere biology will be described in this section. The clinical manifestations of each disease will be described together with their molecular bases. These

http://dx.doi.org/10.5772/65353

diseases are multisystem genetic disorders that share many of the affected genes (see [12, 13, 18, 19, 55-58] for recent reviews). They also have in common the presence of very short telomeres in the affected patients. However, time of onset, phenotype and clinical severity of these diseases are very heterogeneous. Some of the disorders manifest in young children as it is the case of Dyskeratosis congenita, Hoyeraal-Hreidarsson syndrome, Revesz syndrome and Coats plus syndrome that are rare diseases presented with very low frequency in the population. Other diseases that manifest at older ages, generally in adults, are less severe and more frequent in the population. Among these are Aplastic anemia, Lung disease and Non-alcoholic, non-infectious liver disease. A summary of these diseases, their clinical manifestations, time of presentation and the genes that have been found mutated is shown in Table 1.

Disease	**Symptoms**	**Presentation time**	**Mutated genes (inheritance)***
Dyskeratosis congenita	Nail dysplasia	Childhood	DKC1 (XL)
	Abnormal skin pigmentation		TERT (AD,AR)
	Oral leukoplakia		TERC (AD)
	Bone marrow failure		TINF2 (AD)
	Pulmonary fibrosis		WRAP53 (AR)
	Liver abnormalities		NOP10 (AR)
	Avascular necrosis of the hips		NHP2 (AR)
	Stenosis of the exophagus, lacrimal ducts and/or uretra		CTC1 (AR)
	Increased cancer risk		RTEL1 (AD,AR)
	Osteopenia, risk of bone fractures		PARN (AR)
	Psychiatric disorders		
Hoyeraal-Hreidarsson syndrome	Intrauterine growth retardation	Early childhood	DKC1 (XL)
	Microcephaly		TINF2 (AD)
	Cerebellar hypoplasia		TERT (AR)
	Thrombocytopenia		RTEL1 (AR)
	Immunodeficiency		TPP1 (AR)
	Nonspecific enteropathies		PARN (AR)
	Bone marrow failure		
Revesz syndrome	Bilateral exudative retinopathy	Early childhood	TINF2 (AD)
	Bone marrow failure		
	Intrauterine growth retardation		
	Intracraneal calcifications		

Disease	Symptoms	Presentation time	Mutated genes (inheritance)*
	Developmental delay		
	Fine, sparse hair		
	Nail dystrophy		
Coats plus syndrome	Bilateral exudative retinopathy	Early childhood	CTC1 (AR)
	Retinal telangiectasias		
	Intrauterine growth retardation		
	Bone abnormalities with poor healing		
	Gastrointestinal vascular ectasias		
Aplastic anemia	Bone marrow failure	Middle age	TERC (AD) TERT (AD)
Idiopathic pulmonary fibrosis	Pulmonary fibrosis	Middle age	TERC (AD)
	Emphysema		TERT (AD)
	Interstitial pneumonitis		PARN (AD)
	Honeycombing in high resolution computarized tomography		RTEL1 (AD)
Nonalcoholic, noninfectious liver disease	Hepatic fibrosis	Middle age	TERC (AD)
	Noncirrhotic portal hypertension		TERT (AD)
	Hepatopulmonary syndrome		

*XL: X-linked; AD: autosomal dominant; AR: Autosomal recesive

Table 1. Clinical characteristics of telomere biology disorders.

2.3.1. Dyskeratosis congenita

Dyskeratosis congenita (DC) was the first telomere biology disease described in early 1900s [59]. It is an inherited disorder that is usually diagnosed in early childhood. The most characteristic clinical feature is a triad of mucocutaneous features: leukoplakia, reticulated skin pigmentation and nail dystrophy, as shown in Table 1. Lacy reticular pigmentation use to be observed at neck and upper chest. However, DC symptoms have variable expressivity and/or incomplete penetrance and this triad is not always present. Some patients worsen with age and the triad might not be evident in the firsts examinations. The median age of appearance of the triad is approximately 8 years [59]. The variability in the nail phenotype can go from ridging to complete nail loss and can involve both the finger and toenails. The skin may be hyper or hypo pigmented. Leukoplakia may affect other mucosa surfaces. However, additional

http://dx.doi.org/10.5772/65353

reports expanded the phenotype and it is now recognized as a multisystem disease. One of the most common haematological manifestations is bone marrow failure that is the most significant cause of mortality in DC patients, up to 60-70% [60]. Patients present hypocellular bone marrow and severe cytopenias.

DC patients frequently show other skin manifestations, some of them are atrophy of the dorsal surface of hands and feet,hyperhydrosis and hyperkeratosis of palms and soles. Other mucosal surfaces can also be affected leading to stenosis of the oesophagus, urethra or lacrimal duct. Oesophageal strictures and non-specific enteropathies are common. Dental abnormalities can be also observed including extensive caries in 13-17% of the patients [61]. Early greying and loss of hair also occur. Skeletal abnormalities are also observed in up to 5% of the patients [62] including osteoporosis and avascular necrosis. Osteoporosis resembles that seen in natural aging and can led to fractures [63].

Respiratory abnormalities are also a significant cause of morbidity and mortality and cause the death of 10-15% of DC patients [64]. The main clinical manifestation is pulmonary fibrosis that usually is posterior to the mucocutaneous or bone marrow features. Hepatic disease can be also observed including cirrhosis, fibrosis, portal hypertension and portal vein thrombosis and several cases of non-alcoholic, non-infectious liver diseases have been reported [65].

Neuropsychiatric disorders were recently described in 55% of children and 75% of adult DC patients [66]. These disorders include mood, anxiety, psychotic and adjustment disorders, attention deficit/hyperactivity, intellectual disability, learning disabilities and pervasive developmental disorders.

DC patients also present increased risk of cancer development. Co-occurrence of Myelodysplastic syndrome (MDS), Acute myelogenous leukemia (AML) and head and neck squamous cell cancer has been described. A literature review reported a 11-fold increased risk of cancer in DC patients including AML, MDS, tongue cancer, cervical squamous cell carcinoma and non-Hodgkin's lymphoma, with a risk of 40% of developing any cancer by the age of 50 [67].

This diversity in clinical manifestations makes the diagnosis of DC challenging. When the mucocutaneous triad is observed the diagnosis is relatively clear but this is not always the case. Vulliamy et al proposed in 2006 clinical criteria for the diagnosis of DC [68]. These criteria require the presence of the three components of the mucocutaneous triad or one feature of the triad, bone marrow failure and two other clinical manifestations usually found in DC patients, as described above. However, the diagnosis of some patients can still be difficult because the triad might evolve late in time and other clinical manifestations might not be associated to DC because of their diversity.

2.3.1.1. Dyskeratosis congenita as a telomere biology disease, implications in diagnosis

Dyskeratosis congenita may have X-linked inheritance which allowed the identification of one X-chromosome gene that presented missense mutations in several unrelated DC patient. The encoded protein was named dyskerin and the gene DKC1 [60, 69]. Dyskerin was characterized as a highly conserved protein with possible nucleolar functions [60]. Soon afterwards, fibroblasts derived from DC patients were shown to have very short telomeres [70]. These cells

also presented reduced telomerase activity and decreased levels of TERC expression. The correlation between Dyskeratosis and telomere length was strengthened when a large family was found carrying an autosomal dominant mutation in the TERC gene [71].

The recognition of DC as a telomere biology disease helped to understand the biology of this disease. As mentioned in the Introduction, critically short telomeres are recognized as damaged DNA by DNA-damage response pathways that involve the ATM and ATR protein kinases and the p53 protein. Activation of these pathways induces apoptotic cell death and cellular senescence. Telomere shortening is associated to DNA replication, which is specially relevant in cells that have impaired systems of telomere elongation and protection, as is the case of DC patients cells. Therefore, highly proliferative cells are expected to be the firstly affected by telomere shortening. Some of these highly proliferative cells are the stem cells of tissues with high capacity of renewal such epithelia, bone marrow cells and lymphocytes. These cells types are characterized by the expression of high telomerase activity in healthy individuals. Depletion of these stem cell populations can explain the main clinical manifestations of DC patients. Among them are the deficit observed in epithelial tissues such as different mucosa and skin that could be due to insufficient cell renewal because of exhaustion of stem cell populations. Impaired proliferation of bone marrow stem cells also could explain the existence of hypocellular bone marrow and severe cytopenia. Pulmonary alveolar stem cell failure has also been recently described in patients with telomere dysfunction [72]. The reduction in the number and proliferative capacity of stem cells can also explain the premature aging of DC patients as manifested by hair loss and early greying. These data would recognize DC as a stem cell disease.

A second clinical characteristic associated to progressive telomere shortening is the existence of genetic anticipation. It is defined by the occurrence of increasing disease severity and early onset with successive generations, as observed in multigenerational families with autosomal dominant DC [73-75]. Genetic anticipation is due, in these diseases, to non-complete telomere replication in germinal cells due to impaired telomerase activity. Successive generations inherit progressively short telomeres and, therefore, critically short telomeres appear at an early age in highly proliferative tissues of the affected patients.

The identification of telemere shortening also provides one important diagnostic criteria. DC patients are characterized by the presence of very short telomeres in peripheral blood cells. Usually bellow the 1% of the telomere size of control populations of the same age as the patient. Measuring telomere length provides one differential diagnostic criteria for telomere biology diseases. The length of telomeres can be determined by different methods in patient samples [76] and compared with controls of the same age. Variation of telomere length with ethnicity has also been described [77]. One of the methods estimates telomere length by Southern blot. Purified DNA is digested with a restriction enzyme that has recognition sites close to the telomeres (sub-telomeric region) but not at the telomere. Digestion products are separated in agarose gels and blotted to membranes that are hybridized to telomere-specific probes. The distribution of telomeres size and average length can be determined by comparison to the migration of DNA molecular weight markers. The use of this technique requires relatively high amounts of pure DNA.

Telomere length can also be determined by quantitative PCR methods from clinical samples. Some of these methods use telomere-specific oligonucleotides to determine the amount of telomeric DNA in comparison to non-telomeric DNA in each sample. This method has the advantage that a large number of samples can be easily analyzed but it gives and average length of all the cellular telomeres. However, variation in the length of individual chromosomes can be also important in disease progression [78]. Telomeres rearrangements can also have a large effect on the cell [79] and would not be detected by measuring average telomeric DNA content. A PCR-based method that determines single telomere length (Single telomere length assay, STELA) has also been developed [80]. Telomere length can also be determined by flow fluorescence in situ hybridization (flow-FISH) using peripheral blood lymphocytes [81]. This technique can be used in clinical settings and has been shown to be highly sensitive and specific in identifying patients with DC from their unaffected relatives and healthy controls [81, 82]. Flow-FISH is presently the only clinically certified test for DC.

2.3.1.2. Molecular genetics of Dyskeratosis congenita

DC is a rare inherited disease caused by mutations in genes coding for proteins involved in telomere synthesis and protection. Mutations in ten genes have been identified to date in DC patients [55]. Mutations in these genes explain about 60% of the cases of DC so that there are many cases where the causative gene has not been identified. Until few years ago, molecular diagnosis was made through PCR amplification and DNA sequencing of each exon of the candidate genes, pre-analyzed by High Resolution Melting [83]. Discovery of new genes involved in DC and related telomeropathies required positional cloning and were challenging projects. The development of techniques of massive parallel DNA sequencing makes now possible to sequence either all the genes of a patient (genome sequencing) or all the gene exons (exome sequencing) [84]. Analyses of massive sequencing data greatly facilitates molecular diagnosis as well as the discovery of genes whose causative relationship with the disease was previously unknown. One example is the recent identification of mutations in the PARN gene, coding for a Poly(A)-specific ribonuclease in DC patients [85]. The genetic mutations found in DC patients will be reviewed in this section of the chapter and have been described in recent reviews [18, 86]. A summary is also presented in Table 1. Detailed updated information on the nucleotide variants found in DC-related genes can also be found at the Telomerase Database (http://telomerase.asu.edu/diseases.html).

2.3.1.2.1 Dyskerin (DKC1]

Dyskerin is a 524 amino acids long protein that is highly conserved during evolution. It is an essential nucleolar protein that is expressed in all tissues [42]. Dyskerin participates in two very relevant cellular activities, telomere maintenance and RNA pseudouridylation. The first activity has been described in the Telomere elongation section of this chapter (section 2.2]. For the second activity dyskerin binds to small nucleolar RNAs containing the H/ACA box to form small nucleolar RNP (snoRNP) complexes. The proteins NHP2, NOP10 and GAR1, involved in telomerase assembly are also part of these complexes [42]. Small nucleolar RNAs guide snoRNPs to specific uridine residues that are converted to pseudouridines by dyskerin. Pseudouridylation takes place in many cellular RNAs including ribosomal RNAs but also

small nuclear and nucleolar RNAs and mRNAs, as recently described [87]. This modification is important for folding and processing of these RNAs [88]. One subset of snoRNPs (Cajal body RNPs, scaRNPs) is directed to Cajal bodies by the TCAB1 protein [89]. The telomerase RNA, TR, assembles as a typical scaRNP, which is important for TR stability and telomerase recruitment [39, 70] as previously indicated (section 2.1]. Because of this pseudouridylation activity of rRNAs, dyskerin is important for ribosome biogenesis and function, and dyskerin mutations could impair protein synthesis. However, human cells obtained from X-linked DC patients showed intact or only slightly affected ribosome biogenesis and function and very reduced TR levels [90, 91]. These data support the hypothesis that impaired TR stability and telomerase activity are the main cause of DC. However, Bellodi et al. have reported that impaired protein synthesis could contribute to the cancer predisposition of DC patients [92].

Sequence analyses in the Pfam databank identified three functional domains in dyskerin: the dyskerin-like domain (amino acids 48-106] with a yet unknown function; the TruB pseudouridine synthase catalytic domain (aa 110-126], and the PUA RNA binding domain (aa 297-370]. To date, over 50 different DKC1 mutations have been found in association with DC. Many of them were inherited but there were some that were generated de novo in the patients. Not all these mutations show the same severe phenotype and 13 of them cause the Hoyeraal-Hreidarsson syndrome, a more severe manifestation that will be described in the section 2.3.2 of this chapter. Two of the DKC1 mutations are only found in this syndrome. Most DKC1 mutations cluster in two regions of the gene: the region coding amino acids 2-72, at the N-terminus of the protein, and the region coding amino acids 314-420, at the PUA domain [68, 86]. These two domains are contiguous in the three-dimensional structure of the protein and might form a binding site for other proteins [93]. Some disease-causing mutations have been show to alter dyskerin-TR binding because they affect binding of the RNP assembly factor SHQ1 [94]. N-terminal DKC1 mutations overlap a SUMOylation motif and Brault et al have shown that impaired SUMOylation leads to reduced dyskerin, and TR, levels [95]. A mutation in the promoter region of DKC1 that affected dyskerin expression was also identified in a DC patient [96] suggesting that protein levels could have an important role in DC pathogenesis. DKC1 is encoded in the X-chromosome and dyskerin mutations have X-linked transmission with affected males and carrier mothers. In most of the cases carriers do not show any clinical manifestation but carriers of some mutations can manifest late onset diseases such as pulmonary fibrosis that will be described in section 2.3.6.

2.3.1.2.2 Telomerase Reverse Transcriptase (TERT)

The catalytic protein component of the telomerase complex is one 1132 amino acid long protein that contains three major functional domains conserved trough evolution [97]. The telomerase essential N-terminal (TEN) domain is highly conserved among vertebrate proteins and has been implicated in telomere DNA binding upstream of the primer-template interaction [98]. The TEN domain contains a DAT motif involved in telomerase recruitment to the telomeres through interaction with the TEL patch of TPP1 shelterin component. The TERT RNA-binding domain (TRBD) is located next to the TEN domain and precedes the reverse transcriptase domain, which contains the active site for reverse

http://dx.doi.org/10.5772/65353

transcription. In addition, the reverse transcriptase motif also participates in TR RNA binding ensuring the maintenance of a stable telomerase complex [99]. Finally, TERT contains a less-conserved C-terminal extension region.

Comparative analysis of the TERT gene in healthy individuals and telomere biology disorder patients has shown a high degree of nucleotide variation. More than 200 distinct missense nucleotide variants are described in the TERT gene at the Exome Aggregation Consortium (ExAC) database (http://exac.broadinstitute.org/). This database compiles all the nucleotides variants found in the different Exome sequencing projects and presently accumulates information from about 60.700 individuals [121.400 alleles for each gene). Data from both healthy individuals and patients from different diseases are incorporated to this database. Over 75 TERT mutations, most of them novel, have been reported in telomere biology disorders diseases [100], including missense, stop gain, frameshift and splice site mutations. However, the existence of a given mutation in a patient does not imply that it is causative of the disease. It might be a mutation that does not affect protein functionality. The existence of a familiar history showing a strong correlation between the presence of the mutation and disease manifestation would support the causative role of this mutation. However, if it is a novel mutation, or the family history is short, experimental assay of the activity of the mutated protein is required to ascertain the possible causal role. For this purpose, mutated TERT proteins are expressed in cells that have very low telomerase activity, if any. The activity of the mutated protein can be consequently tested on this background using the telomere repeat amplification protocol (TRAP) or primer extension assays (see Collopy et al [101] for a recent example).

TERT mutations associated with DC and other telomere biology disorders are found all over the protein although their frequency is higher at the reverse transcriptase domain. Most reported patients with TERT mutations are monoallelic heterozygous. The telomerase activity found in cells from these patients is an average of homozygous wild type and mutant cells and might indicate that haploinsufficiency is the cause of the clinical phenotype [74, 102, 103].

2.3.1.2.3 Telomerase RNA, TR (TERC)

The RNA component of the telomerase complex is 454 nucleotides in length and is encoded by the TERC gene. This RNA provides the template sequence for reverse transcription and is involved in assemblage of the RNP complex [104]. The interaction between TR and TERT regulates the catalytic activity, processivity and telomere-binding activity of the telomerase complex [105]. TR presents domains conserved through evolution that are involved in RNA stabilization, accumulation, subcellular localization and telomerase assembly. They are the template/pseudoknot domain and the CR4/5 motif [106]. These two domains are sufficient to restore telomerase activity when combined with TERT [107, 108]. An additional H/ACA domain at the 3′ end of TR allows binding of the proteins required for telomerase biogenesis dyskerin, NOP10, NHP2 and GAR1 [43].

Mutations in TERC are less frequent than in TERT in DC patients and approximately 60 different mutations have been reported [100]. Nucleotide variants are also less frequent in the general population and only 62 are reported in ExAC exomes database. Among the mutations

found in DC patients some deleted large segments that affect functional domains while others are nucleotide substitutions. Mutations are particularly frequent at the pseudoknot domains and present an autosomal dominant inheritance (http://telomerase.asu.edu/diseases.html). As indicated for TERT, the functional significance of TERC mutations, specially nucleotide substitutions, has to be determined experimentally. A relevant example determined functional properties such as TR stability, TERT interaction, telomerase activity and processivity of 13 TR mutations [109].

2.3.1.2.4 TERF1- interacting nuclear factor 2 (TINF2]

The gene TINF2 codes for the protein TIN2, component of the shelterin complex that protect the telomere and regulates telomerase recruitment and activity. TIN2 links the double-stranded DNA binding proteins TRF1and TRF2 to the single-stranded DNA binding proteins TPP-1 and POT1 within the shelterin complex. TIN2 also interacts with heterochromatin protein 1 gamma (HP1γ) [110] through the canonical PTVML binding site [111] which is crucial for sister telomere cohesion.

Over 20 mutations in TINF2 have been described in DC patients. Many of them are novel mutations and results in early-onset disease. Familiar mutations are usually inherited in autosomal-dominant manner [111, 112]. All TINF2 mutations reported to date cluster in a segment coding for 34 amino acids centrally located in the gene. The function of this short protein fragment is not clear at the present time. One of the functions affected in some TINF2 mutants is HP1γ binding [110] which could be explained because the PTVML binding site is located within the mutation cluster [111]. Impaired HP1γ binding resulted in reduced sister telomere cohesion. On the contrary, the interaction of TIN2 with TERF1 is not affected in most of the mutated proteins [112, 113]. Impairment of telomerase recruitment to telomeres in a TIN2 mutant has been reported [114]. However, the telomere shortening observed in a mouse model of TINF2 mutation was recently reported to be telomerase independent [115].

2.3.1.2.5 TCAB1: Driving telomerase to Cajal bodies (WRAP53]

The protein TCAB1 (encoded by the WRAP53 gene) [116] binds to the telomerase RNA, TR, through the 4 nucleotides CAB box, present on small Cajal body-associated RNAs. Telomerase recruitment to Cajal Bodies is required for consequent assembly on the telomeres [44, 117].

Compound heterozygous mutations in WRAP53 have been identified in DC patients [118]. Telomerase localization to Cajal Bodies was disrupted in this patients leading to TR accumulation in the nucleoli. Mutations map to a region that mediates interaction between TCAB1 and the TCP-1 Ring Complex (TRiC) that is required for TCAB1 folding.

2.3.1.2.6 Nucleolar protein 10 (NOP10, Nola3]

Nucleolar protein 10 (NOP10] is encoded by the Nola3 gene (nucleolar protein family A, member 3]. This protein is a H/ACA snoRNA-binding protein that binds the TR RNA in association with dyskerin and NHP2 [43]. One homozygous mutation has been found in a DC patient that impaired TR binding and RNP assembly [119].

2.3.1.2.7 NHP2 ribonucleoprotein (Nola 2]

Similarly to NOP10, the NHP2 protein, encoded by the NHP2 gene, also named Nola2, is a H/ACA snoRNA-binding protein that associates to TR together with dyskerin [43]. One homozygous missense mutation in the NHP2 gene was described in a patient with severe DC while compound heterozygous mutations were described in a second DC patient [120]. These patients had decreased TR levels and short telomeres because of impaired telomerase assembly and stability [119].

2.3.1.2.8 Conserved telomere maintenance component 1 (CTC1]

The protein CTC1 is one of the components of the CST complex (CTC1, STN1, TEN1] that promotes re-start of the telomere lagging strand synthesis and fill-in C-rich strand synthesis at the telomeres [51, 52]. CTC1 binds to single-stranded DNA at telomeres and associates with the replication initiator polα primase complex.

Biallelic, compound heterozygous, CTC1 mutations were identified in a group of DC patients [121, 122]. These mutations impaired the association of CSC1 with STN1, TEN1 and polα primase, telomeric DNA binding and cellular localization [123]. To date, 10 CTC1 mutations have been associated with DC patients [122].

2.3.1.2.9 Regulator of telomere elongation helicase 1 (RTEL1]

Regulator of telomere elongation helicase 1 is an essential DNA helicase that belongs to a small family of these proteins involved in different genomic instability diseases [124]. At telomeres, RTEL1 disrupts the D-loops resolving the T-loop structure [48]. RTEL1 is recruited to telomeres by TRF2 in late S phase and is essential to prevent nuclease-dependent excision of telomere T-circles [49]. RTEL1 also show G-quartet unwinding activity required for telomeric DNA replication although this activity is independent of TRF2 [50]. In addition, RTEL1 has important non-telomeric functions in processes such as DNA-replication, DNA repair and homologous recombination [125].

Whole-exome sequencing in DC patients and their families identified RTEL1 mutations that could cause DC and related telomere biology disease such as the Hoyeraal–Hreidarsson syndrome and Pulmonary Fibrosis, that will be described later (sections 2.3.2 and 2.3.6] [126-128]. To date almost 30 RTEL1 variants have been reported in telomere biology diseases patients. Most RTEL1 mutations are transmitted in autosomal recessive manner but autosomal dominance has been also reported [126]. Some mutations map to functional protein domains such as the helicase, harmonin homology or the C4C4 metal-binding motifs [129]. The RTEL1 R1264H mutation, that impairs RTEL1 interaction with TRF2, has been found in 1% of the Ashkenazi Jewish population [130].

2.3.1.2.10 Poly(A)-specific 3′ exoribonuclease (PARN)

Poly(A)-specific 3′ exoribonuclease is a widely expressed protein with Poly(A) deadenylase activity that participates in the regulation of global mRNA levels during development [131]. In addition, PARN also deadenylates small nucleolar RNAs [40]. A recent exome sequencing study linked PARN mutations with pulmonary fibrosis and telomere shortening [128].

A subsequent study, also based on exome sequencing, identified bialelic mutations in the PARN gene in three families with individuals exhibiting severe DC [85]. Two of the families were homozygous for one missense variant and one Splicing-altering variant, respectively. The third affected patient was a compound heterozygous. These patients exhibited reduced TERC, DKC1, RTEL1 and TERF1 mRNA levels. Cells from these patients showed activated DNA-damage response associated to nuclear p53 regulation, cell-cycle arrest and reduced cell viability upon UV treatment [85]. These results supported a potential link between PARN, the p53-dependent pathway and telomere shortening [132]. A subsequent study using cells derived from these patients has shown that PARN is required for the 3'-maturation of the telomerase RNA component [41]. Specifically, PARN is required for removal of the oligo(A) tails post-transcriptionally added to the TR 3' end and that target nuclear RNAs for degradation.

2.3.2. Hoyeraal-Hreidarsson syndrome

The Hoyeraal-Hreidarsson syndrome (HH) is frequently considered a severe variant of DC, typically presented in infancy [133]. The first patients with this syndrome were described by Hoyeraal et al [134] and Hreidarsson et al [135]. However, the eponym was first proposed in 1995 in a case report of a child with clinical features very similar to those described by Hoyeraal and Hreidarsson [136]. About 50 cases of HH have been reported since the first description [86]. HH is a multisystem genetic disorder and represents the extreme phenotype of the telomere biology disorders. Peripheral blood cells from these patients present very short telomeres, below the first percentile for their age. Clinical manifestations typically present early in childhood. These patients present developmental problems such as cerebellar hypoplasia, microcephaly, developmental delay and intrauterine growth retardation (IUGR). In addition, typically present immunodeficiency and progressive bone marrow failure. In addition to these specific symptoms, HH patients can also present clinical manifestations found in DC patients. For example, the typical triad of mucocutaneous alterations shown in DC patients can also be present at diagnosis or develop with time in HH patients. Other DC-associated symptoms that are also present in some HH patients include immunodeficiency, prematurity, dysmorphology, gastrointestinal features and neurological symptoms. Among these symptoms, cerebellar hypoplasia is considered a requirement for the diagnosis of HH [75, 137]. Other neurological complications include impaired myelination, seizures, hypoplastic corpus callosum and intracranial calcifications (reviewed in Glousker et al. [86]). Immunodeficiency is observed in a large proportion of HH patients with increased susceptibility to life-threatening infections. Over half of the patients present with lymphopenia [86]. The T cell compartment is less frequently affected although abnormalities of T cell proliferation have been observed [138]. There are also some reports of severe combined immunodeficiency [139]. Therefore, any child presenting with humoral deficiency or combined immunodeficiency and neurological features (microcephaly, cerebellar hypoplasia) should be considered a possible HH patient. Digestive tract anomalies are frequent in HH patients and include oesophageal strictures, severe enteropathy and colitis [140]. Other clinical complications include skeletal malformations [141], urinary tract abnormalities [136, 142], and ophthalmological signs [136, 142].

2.3.2.1. Molecular genetics of Hoyeraal-Hreidarsson syndrome

As mentioned above, HH can be considered as severe form of DC and, in agreement with this consideration, some of the genes mutated in DC are also found mutated in HH patients [86]. The specific mutations present in HH patients can be different to those found in DC so that mutations that affect more importantly protein function are associated to HH. In other cases the difference is found in allele composition so that some mutations are found in homozygosis or compound heterozygosis in HH and in heterozygosis in DC. The mutations presently associated to HH will be briefly described in the following paragraphs and the genes affected are indicated in Table 1.

2.3.2.1.1 Dyskerin (DKC1]

DKC1 mutations cause DC and also HH so that 13 out of the over 50 different mutations presently known cause DC and HH and two of them are only found in HH (T49M and S304N) [68, 143]. No clear correlation has been found between the location of the mutation on dyskerin functional domains and the severity of the disease. Indeed, some mutations are associated with variable severity from mild DC to HH, like the A353V mutation [144]. The two HH-associated mutations are located to the catalytic TruB domain suggesting that pseudouridylation activity is important for telomerase function [143].

2.3.2.1.2 Telomerase Reverse Transcriptase (TERT)

Mutations in the TERT gene have been found in HH patients but not as frequently as in DC patients. From the more than 50 TERT mutations related to telomere biology disorders only five are implicated in HH. Four of them cause HH in homozygosis (T567M, R901W) [145, 146] or compound heterozygosis (P530L, A880T) [147]. Carriers of these mutations have short telomeres without reported clinical manifestations. The A880T and R901W mutations fall into the TERT catalytic reverse transcriptase domain and the T576M mutation in the RNA-binding domain. These mutations greatly impair telomerase activity and processivity, respectively [146]. Only one autosomal dominant TERT mutation has been associated with HH (F1127L) but it was also found in the healthy mother with could indicate the presence of a second, paternal, mutation or disease anticipation [148].

2.3.2.1.3 TERF1- interacting nuclear factor 2 (TINF2]

The shelterin component TIN2 is encoded by the gene TINF2 and has an important role by interacting with the double-stranded DNA binding proteins TRF1/TRF2 and the single-stranded DNA binding heterodimer TPP1/POT1, as mentioned above. Three of the over 20 DC-associated TINF2 mutations have been found in HH patients. These mutations were de novo or inherited in an autosomal-dominant manner [100, 111].

2.3.2.1.4 Regulator of telomere elongation helicase 1 (RTEL1]

The RTEL1 protein is a DNA helicase required for telomere replication, as mentioned above. Presently, 18 RTEL1 mutations have been described in 17 HH patients. Most RTEL1 mutations were biallelic, with either homozygous or compound heterozygous recessive inheritance. The mutations were located in domains involved in protein-protein interaction or ubiquitin transfer [127, 142].

2.3.2.1.5 TPP1 (ACD)

The protein TPP1 (TINT1, PTOP, PIP1] is encoded by the Adrenocortical Dysplasia Homolog (ACD) gene and is a component of the shelterin complex, as previously described (Section 2.1]. Three functional domains have been identified in this protein. The N-terminal OB domain is involved in the interaction of TPP1 with TERT that participates in the recruitment of the telomerase complex to telomeres through the TEL patch and increases telomerase processivity [45, 46]. The central domain is required for heterodimer formation with POT1 [28, 149]. The C-terminal domain binds TIN2 to form the shelterin complex, as mentioned above [150]. Whole exome sequencing discovered a mutation at the TEL patch of TPP1 together with a missense mutation in this same gene in a compound heterozygous HH patient [151]. The TEL patch mutation was a single amino acid deletion and resulted in a reduction of telomerase processivity and recruitment to telomeres. This same mutation has been identified in a family with aplastic anemia and other DC symptoms and was transmitted in a dominant inheritance manner [152].

2.3.2.1.6 Poly(A)-specific 3′ exoribonuclease PARN

The Poly(A)-specific 3′ exoribonuclease is involved in processing of the telomerase RNA, TR, as mentioned above. A recent work identified PARN mutations in three families with individuals exhibiting severe DC [85]. Actually, some of these patients had a disease classified as HH syndrome associating PARN mutations to this disease [132]. These patients presented biallelic mutations in the PARN gene indicating a recessive manner of inheritance.

2.3.3. Revesz syndrome

The syndrome of Revesz (RS) is a telomere biology disorder that affects young children. This disease was first reported by Revesz et al as a case of a 6-month-old children with bilateral exudative retinopathy that developed a severe bone marrow failure [153]. This and subsequent reports indicated the following symptoms, summarized in Table 1: intrauterine growth retardation, intracranial calcifications, developmental delay, fine spare hair and nail dystrophy. The clinical presentations have several symptoms in common with DC and the specific diagnosis of RS requires identification of bilateral exudative retinopathy [154]. Besides common manifestations, the relation of RS with DC and other telomere biology disorders was confirmed because RS patients have very short telomeres and present mutations in the TINF2 gene, that encodes the TIN2 shelterin component [111].

2.3.4. Coats plus syndrome/CRMCC

The Coats plus syndrome (CPS) is also known as cerebroretinal microangiopathy with calcifications and cysts (CRMCC). Coats plus patients have bilateral exudative retinopathy, retinal telangiectasias, intrauterine growth retardation, intracranial calcifications, bone abnormalities with poor healing, and gastrointestinal vascular ectasias (Table 1). Some patients also present DC-related features such as dystrophic nails, sparse or greying hair and anemia. Intracranial calcifications and bilateral exudative retinopathy are also present in RS patients but Coats plus patients also present cerebellar and hematologic manifestations [12, 56].

http://dx.doi.org/10.5772/65353

Autosomal recessive compound heterozygous mutations in CTC1 have been described in CPS identifying this syndrome as a telomere biology disorder [155-157]. As mentioned above, the protein Conserved telomere maintenance component 1 (CTC1] is required for telomere elongation. Actually, mutations in CTC1 probably account for most of the CTS cases. In addition, telomeres that are bellow the first percentile for age have been found in CTS patients and telomeres from heterozygous carriers have a length bellow average [155].

2.3.5. Aplastic anemia

Aplastic anemia is one of the clinical manifestations of telomere biology disorders in adults usually associated to mutations in TERT and TERC. Symptoms in these patients are milder than in children and mucocutaneous features are infrequent [12, 56]. Aplastic anemia can have very different causes and there are inherited and acquired forms of the disease. Acquired forms can be related to environmental exposures and infectious, among other factors, and is immune-mediated. Inherited aplastic anemia has been reported to occur in patients with Fanconi anemia, Shwachman-Diamond syndrome and other inherited bone marrow failures, including DC. It has been described that approximately 10% of patients with isolated aplastic anemia have mutations in TERC and TERT genes [158]. These mutations usually present an autosomal dominant manner of inheritance. Telomere length in these patients is usually bellow the 10% percentile for age [159]. The existence of symptoms related to telomere biology disorders in relatives of these patients, such as pulmonary fibrosis, mild cytopenias, leukemia and squamous cell cancer, can be of great help for their diagnosis [12].

2.3.6. Pulmonary fibrosis

Idiopathic pulmonary fibrosis (IPF) is a lung disease characterized by progressive interstitial fibrosis that has a poor prognosis (median survival time of 2-3 years) [160]. Diagnosis of pulmonary fibrosis, also known as interstitial pneumonia, is made by the presence of honeycombing on high-resolution computarized tomography (HRCT). In addition to pulmonary fibrosis, these patients can present a range of pulmonary pathologies, including bronchiolitis, obliterans organizing pneumonia, chronic hypersensitive pneumonia and emphysema alone or combined with pulmonary fibrosis (Table 1) [56]. Familial forms of pulmonary fibrosis have been also described and might represent up to 20% of the cases [161]. The study of these familial forms identified mutations in TERT and TERC in 8-15 % of the cases [162, 163], establishing IPF as a telomere biology disorder. IPF is inherited in these families as an autosomal dominant trail. This observation is supported by animal models since TERT null mice have decreased number or alveolar epithelial cells [164]. TRF1 deletion in type II alveolar cells also causes pulmonary fibrosis in mice [165].

Heterozygous mutations in genes coding for telomere-related proteins have been found in 15-20% of IPF families without a history of DC [162, 163, 166] and 1-3% of sporadic cases of IPF [167]. In addition, 20% of patients with DC develop pulmonary fibrosis [57, 58]. In agreement with these observations, IPF patients have significantly shorter telomeres than age-matched controls. Actually, IPF is the most common manifestation of telomere biology disorders since DC and AA have much lower prevalence [168]. IPF due to telomere disfunction

presents in adulthood, into middle age [164]. The gene most frequently mutated in IPF patients is TERT [8-15% of familial cases) but mutations have been also found in TERC (<1%), DKC1 (<1%)[169], TINF2 (<1%)[170], RTEL1 [5%)[128, 166] and PARN [4%) [128]. TERT mutations have been also found in smokers with severe emphysema at a frequency of 1% [171]. Telomere dysfunction due to these genetic mutations can originate irreversible alveolar stem cell failure that would be at the origin of pulmonary fibrosis and emphysema [72, 162]. IPF patients that carry mutations in telomere-related genes can also present extra-pulmonary manifestations related to telomere biology disorders such as bone marrow failure including red blood cells, single lineage cytopenias or aplastic anemia [164]. Actually, the complex syndrome of IPF and bone marrow failure predicted the presence of TERT or TERC mutations in 10 families that presented these diseases in consecutive generations [172].

Short telomere length is a common finding in IPF patients, even in those without mutations in telomere-related genes [167]. These results could indicate that IPF may be more likely to develop in those individuals that naturally present shorter telomeres in the general population. These individuals might also have increased incidence of other telomere-related disorders such as cryptogenic liver cirrhosis and diabetes [58].

2.3.7. Liver disease

The study of five families with liver disease in combination with hematologic and autoimmune disorders identified mutations in TERT and TERC [65]. A subsequent study of patients with idiopathic live cirrhosis also found an increased frequency of TERT and TERC mutations [3.7% vs 0,85% in the control population) [173]. Affected patients presented reduced telomerase activity and short telomere length in peripheral blood cells. They also have increased probability to progress to end-stage liver disease. In addition, liver disease, including hepatic fibrosis, noncirrhotic portal hypertension, and hepatopulmonary syndrome has been reported in DC patients (Table 1) [62, 64].

2.4. Treatment of telomere biology disorders

Treatment of diseases with several organs potentially compromised has many practical complications. Presently, there are no curative therapies for many of the clinical manifestations of telomere biology disorders. The major causes of decease in these patients are bone marrow failure and pulmonary fibrosis and in this section we will summarize the present treatment of these pathologies. In the second part we will describe some of the experimental strategies that are being used to generate new therapies for telomere biology disorders.

2.4.1. Present treatment of telomere biology diseases

Hematopoietic stem cells transplantation (HSCT) is the only treatment than can cure bone marrow failure in these patients. Donor's selection requires special attention in telomere biology disorders since relatives might be silent carriers of the mutations, given the clinical heterogeneity of these diseases. This circumstance has been reported in two cases and there was a failure either to engraft or to mobilize stem cells from the graft [174]. Analysis of the

outcome of 34 DC patients transplanted with bone marrow indicated higher rates of mortality and morbidity due to respiratory complications and graft failure [175]. Best results were obtained transplanting grafts from HLA-matched siblings but the 10-year probability of survival was 30% in this study. Conditioning of transplanted DC patients may also contribute to long-term development of pulmonary fibrosis and liver disease. Therefore, the use of reduced intensity conditioning, avoiding radiotherapy, busulfan and high dose of cyclophosphamide might benefit to these patients [176].

Androgen therapy has been also used for telomere biology disorder patients with bone marrow failure. These patients seem to be responsive to male hormones [177]. The mechanism involved seems to be that male hormones modulate TERT gene expression and increase telomerase activity [178]. In a retrospective analysis of 16 DC patients treated with androgens, 11 achieved clinically significant hematologic response [179]. Telomere elongation after androgen treatment has been reported in one case [180]. However, androgens can have side effects such as masculinisation, liver function abnormalities, hyperlipidemia and splenic peliosis (when androgens are used in conjunction with GCSF) and telomere biology disorders patients can be specially sensitive to these effects [181]. The androgen-stimulating hormone Danazol has less masculinising side effects and has been also used for treatment of DC patients [182].

Treatment of idiopathic pulmonary fibrosis is presently mainly supportive with pulmonary rehabilitation therapy and the administration of supplemental oxygen. Recently, two pharmacological agents, pirfenidone [183] and nintedanib [184] were shown to reduce lung function decline in IPF patients. Danazol administration has also been described to slow down the progression of pulmonary fibrosis in DC patients [182]. However, lung transplantation is the only curative strategy available. Lung transplantation was successfully used in a patient after HSCT [185]. The study of a small series of IPF patients with TERC or TERT mutations showed a favourable short term output with 7 of 8 patients alive after a median follow-up of 1,9 years. However, frequent haematological, renal and infectious complications were observed [186].

Because of the lack of curative therapies, telomere biology disorder's management are presently based on supportive measures and close follow-up for medium and long term complications [55]. Regular clinical review to monitor organ-specific disease progression, such as haematological analysis and pulmonary function testing must be performed. Surveillance for the appearance of dermatological and digestive tumours is important for early detection and complete surgical resection. Preventive measures such as avoidance of potential carcinogens (tobacco smoke, sun exposure) and adequate dental hygiene are also very important.

2.4.2. Experimental strategies for treatment of telomere biology disorders

Important efforts for the development of mice models of telomere biology disorders aimed to the development of novel therapies have been made in the last years [187]. However, the existence of very long telomeres in the mice strains used for experimentation [50-100 kb) has made of this a difficult task. Mice strains with defective telomerase activity have been generated [187, 188] but they have to be crossed for 4-5 generations before their telomeres are sufficiently short to manifest telomere-associated defects [189]. The use of mice with short

telomeres to generate telomerase-deficient strains provided a better experimental model [190]. Mouse models carrying mutations in DKC1 have been also generated [191]. More recently, tissue-specific inactivation of genes related to telomere biology has been used to generate mice models of these diseases. For example, mice models of bone marrow failure and pulmonary fibrosis were generated by deleting the TRF1 gene in the hematopoietic compartment and type II alveolar cells, respectively [165, 192]. However, these mouse models did not completely reproduce the human disease and telomere size was not reduced [190, 191]. Mice lacking the p53 C-terminal domain had short telomeres and suffer from aplastic anemia and pulmonary fibrosis and could be a useful model for the study of telomere biology disorders [193].

Telomere biology disorders are caused by mutations in a single gene in most patients and could be, therefore, amenable for gene therapy strategies. An important caveat is that telomere length is narrowly controlled and excessively long telomeres increase the probability of developing some cancers such as melanoma [13]. Mice over-expressing TERT also develop a large number of tumors unless the tumor-suppressor protein p53 is also overexpressed [194]. Raval et al recently showed that inducible reactivation of telomerase activity could reverse defective hematopoiesis caused by telomere shortening in TERT-deleted mice [189] opening new perspectives to gene therapy approaches. Transient expression of TERT also extends telomeres in human cells [195]. Recent reports indicate that TERT plays roles beyond telomeres and contributes to stem cells maintenance and cell reprogramming which might offer new therapeutics targets for telomere biology disorders [196].

Telomere shortening results in the accumulation of DNA damage at telomeres and the activation of the p53 pathway, as mention above. A DC mouse model in which mice carries a DKC1 exon 15 deletion demonstrated that mutant cells had a growth retardation compared to wild-type cells [191]. Mutant cells accumulated increased levels of DNA damage. In addition, these cells are hypersensitive to oxygen and accumulate reactive oxygen species. Treatment of these cells with the antioxidant N-acetyl cysteine increased cell growth, both in vitro and in vivo. Competitive bone marrow repopulation studies showed that the DCK1 mutation is associated with a functional stem cell defect consistent with accelerated senescence. This stem cell defect was partially reverted by N-acetyl cystein treatment of the animals [197]. These results suggest that antioxidant treatment may prevent or delay some DC manifestations.

A new therapeutic opportunity came from the observation that a dyskerin motif, corresponding to the TruB domain of the protein (GSE24.2], reactivated telomerase activity in DC-patients and human telomerase-deficient cells [198]. This peptide activated human TERT promoter in a c-myc expression-dependent manner. GSE24.2 rescued DC-fibroblasts from premature senescence. The peptide also increased the telomerase RNA, TR, expression trough stabilization of the molecule [199]. DC-cells presented increased DNA damage at the telomeres and increased levels of oxidative stress. Expression of GSE24.2 decreased both DNA damage and oxidative stress of the cells that expressed a DKC1 mutant protein [200]. Subsequent studies demonstrated that a shorter fragment of GSE24.2, named GSE4, maintained the same biological activity and induced telomerase activity and cell proliferation of DKC-mutant cells. In addition, DNA damage, oxidative stress and cell senescence were reduced upon expression of GSE4 [201]. GSE24.2 could be delivered to cells using surface modified biodegradable

polymeric nanoparticles, which might facilitate their administration to patients [202]. These results open a new therapeutic opportunity for the treatment of telomere biology disorders and GSE24.2 was recently approved by the EMA as an orphan drug for DC treatment (EU/3/12/1070-EMA/OD/136/11].

2.5. Conclusion

Telomere biology disorders, also named telomeropathies, compose a group of diseases with diverse clinical presentations, affecting several systems, but a common genetic etiology. Telomere maintenance or protection is defective in the patients affected by these diseases and, as a consequence, they present short telomeres. Critically short telomeres induce cell death or senescence impairing cell proliferation. Cell renewal in adult tissues depends on the proliferation of stem cells. In patients with defects in telomere biology, telomeres of stem cells are shortened after each cell cycle and get exhausted much earlier than in healthy individuals which impairs tissue renewal. This effect is specially important in highly proliferative tissues such as bone marrow, lymphocytes and epithelial tissues, including lung alveolar epithelia, that are the tissues mainly affected in patients with telomere biology disorders.

The severity of the disease seems to be dependent on the functional alterations that each mutation causes in the biological activity of the corresponding protein. The genetic doses is also very important since patients that are homozygous for the mutation or compound heterozygous for more than one mutation usually present more severe symptoms of the disease that manifest at an early age. These forms of the disease are inherited in a recessive or X-linked manner. Heterozygous patients might be healthy carriers but they can also present milder forms of the disease that present at an older age, generally in adults. These disease manifestations are inherited in an autosomal dominant manner. There is also an association between the severity of the disease and the tissues affected. High-turnover tissues are affected in younger patients and as a more severe disease. For example, the main manifestation in infancy is severe immunodeficiency affecting B cells, T cells and NK cells that have high replication rates. Bone marrow defects manifests later in children and young adults as isolated cytopenias and aplastic anemia. The gastrointestinal epithelium is also affected in children and young adults. In contrast, telomere phenotypes predominantly manifest in slow-turnover tissues such as lung and liver in adults [9]. There is also a strong correlation between the size of the telomeres, as determined in peripheral blood cells, the severity of the disease and the time of presentation so that patients younger and with more severe presentation have shorter telomeres [12].

Genetic anticipation can also have a relevant influence in the presentation and evolution of these diseases. As previously described, patients and healthy carriers of telomere biology disease can transmit shortened telomeres to their descendants. If descendants are affected by the disease, their stem cells will present critically short telomeres at an early age that the previous generation, anticipating the time of onset and increasing the severity of the disease [74]. For example, a large family has been described with several patients manifesting IPF, bone marrow failure or a combined phenotype. There seemed to be a difference of several

decades in the onset of the disease between generations with IPF manifesting in older individuals (mean 51 years) and bone marrow failure in younger ones [14 years) [172].

The heterogeneous presentation of telomere biology diseases make difficult their diagnosis as already mentioned in the description of DC (section 2.3.1]. In addition, some of the symptoms also occur in patients with other diseases. For example, inherited bone marrow failure is also observed in patients with Fanconi anemia, Shwachmann-Diammond syndrome and other inherited BMFs. However, differentiating DC-associated BMF is important for patient management since, for example, these patients often do not respond to immunosuppressive therapy. One important criterion for diagnosis of telomere biology disorders is the presence of short telomeres in comparison to the aged healthy population, usually lower than the 1% percentile. However, some IPF patients present short telomeres even in the absence of mutations in telomere biology related genes [167]. Therefore, an accurate diagnosis requires establishing the molecular basis of the disease, identifying the causative mutation. Molecular diagnosis can be done sequencing the exons contained in the genes presently known to be mutated in telomere biology disorders. However, the high number of candidate genes and the large number of exons present in some of them makes this approach time-consuming and expensive. Alternatively, sequencing by exome sequencing techniques all exons of patients and close relatives is becoming a more attractive, faster and cheaper method [84]. In addition, exome sequencing allows the identification of mutations in genes that have not been previously related to telomere biology (see [128] for a recent example).

These diseases can be considered and example of the importance of precision medicine for diagnosis but also for patient managing and genetic counselling. The importance in diagnosis is enforced by the elevated heterogeneity of the clinical presentations in several systems that can create some uncertainty until a genetic analysis is performed. The importance for patient management derives from the possible progressive alteration of different organs, as mentioned above. This progression with time is very characteristic of telomerase biology disorders and can only be predicted by a precise molecular diagnosis. Disease progression also determines the therapeutic treatment. As mentioned above, the only curative alternatives are organ transplantation, either hematopoietic stem cell transplantation (HSCT) or lung transplantation. However, in telomere biology disorders both transplants have specific complications. Reduced intensity conditioning is advised and patients frequently present graft failure. In the case of HSCT respiratory complications have been described. In contrast, haematological, renal and infectious complications were observed after lung transplantation. Both complications could be expected for the multi-systemic nature of these diseases.

Precision medicine is also important for genetic counselling in telomere biology disorders [12]. Depending on the mutation, these diseases can have different manners of inheritance. The phenotypic penetrance of each mutation can be different. Heterozygous clinically silent carriers can be found whose long-term evolution is not yet understood. Patients treated for a symptom can develop a different one later on. As mentioned above, supportive measures and close follow-up of patients and carrier relatives is also very important. All these characteristics, specific to these diseases, might be difficult to transmit to the patients and their relatives what

http://dx.doi.org/10.5772/65353

makes even more important to provide appropriate genetic education and counselling to the families.

As mentioned above, presently there are no really curative alternatives for these diseases. Lung transplantation and HSCT are important therapeutic interventions but, unfortunately, with a short time of survival. Some experimental therapies are promising but new curative therapies are urgently needed and should be the focus of intensive research in the near future.

Acknowledgements

This work was supported by grant PI1401495 from Fondo de Investigaciones Sanitarias, Instituto de Salud Carlos III, Spain, supported by FEDER funds. CM-G is supported by the CIBER de Enfermedades Raras (CIBERER).

Author details

Rosario Perona[1,2,3*], Laura Iarriccio[1,4], Laura Pintado-Berninches[1,4], Javier Rodriguez-Centeno[1,4], Cristina Manguan-Garcia[1,2], Elena Garcia[4], Blanca Lopez-Ayllón[1,3] and Leandro Sastre[1,2,3]

*Address all correspondence to: lsastre@iib.uam.es

1 Instituto de Investigaciones Biomedicas, CSIC/UAM, Madrid, Spain

2 CIBER de Enfermedades Raras (CIBERER), Valencia, Spain

3 Biomarkers and Experimental Therapeutics in Cancer, IdiPaz, Madrid, Spain

4 Advanced Medical Projects, Madrid, Spain

References

[1] McElligott R, Wellinger RJ. The terminal DNA structure of mammalian chromosomes. EMBO J. 1997 Jun 16;16(12):3705-14.

[2] de Lange T. Shelterin: the protein complex that shapes and safeguards human telomeres. Genes Dev. 2005 Sep 15;19(18):2100-10.

[3] Karlseder J, Broccoli D, Dai Y, Hardy S, de Lange T. p53- and ATM-dependent apoptosis induced by telomeres lacking TRF2. Science. 1999 Feb 26;283(5406):1321-5.

[4] Harley CB, Futcher AB, Greider CW. Telomeres shorten during ageing of human fibroblasts. Nature. 1990 May 31;345(6274):458-60.

[5] Blackburn EH, Greider CW, Szostak JW. Telomeres and telomerase: the path from maize, Tetrahymena and yeast to human cancer and aging. Nat Med. 2006 Oct;12(10): 1133-8.

[6] Greider CW, Blackburn EH. Identification of a specific telomere terminal transferase activity in Tetrahymena extracts. Cell. 1985 Dec;43(2 Pt 1):405-13.

[7] Kim NW, Piatyszek MA, Prowse KR, Harley CB, West MD, Ho PL, et al. Specific association of human telomerase activity with immortal cells and cancer. Science. 1994 Dec 23;266(5193):2011-5.

[8] Wright WE, Piatyszek MA, Rainey WE, Byrd W, Shay JW. Telomerase activity in human germline and embryonic tissues and cells. Dev Genet. 1996;18(2):173-9.

[9] Armanios M. Telomeres and age-related disease: how telomere biology informs clinical paradigms. J Clin Invest. 2013 Mar;123(3):996-1002.

[10] Lopez-Otin C, Blasco MA, Partridge L, Serrano M, Kroemer G. The hallmarks of aging. Cell. 2013 Jun 6;153(6):1194-217.

[11] Nabetani A, Ishikawa F. Alternative lengthening of telomeres pathway: recombination-mediated telomere maintenance mechanism in human cells. J Biochem. 2010 Jan; 149(1):5-14.

[12] Savage SA. Human telomeres and telomere biology disorders. Prog Mol Biol Transl Sci. 2014;125:41-66.

[13] Stanley SE, Armanios M. The short and long telomere syndromes: paired paradigms for molecular medicine. Curr Opin Genet Dev. 2015 Aug;33:1-9.

[14] Horn S, Figl A, Rachakonda PS, Fischer C, Sucker A, Gast A, et al. TERT promoter mutations in familial and sporadic melanoma. Science. 2013 Feb 22;339(6122):959-61.

[15] Huang FW, Hodis E, Xu MJ, Kryukov GV, Chin L, Garraway LA. Highly recurrent TERT promoter mutations in human melanoma. Science. 2013 Feb 22;339(6122):957-9.

[16] Aoude LG, Pritchard AL, Robles-Espinoza CD, Wadt K, Harland M, Choi J, et al. Nonsense mutations in the shelterin complex genes ACD and TERF2IP in familial melanoma. J Natl Cancer Inst. 2015 Feb;107(2):pli:dju408.

[17] Bainbridge MN, Armstrong GN, Gramatges MM, Bertuch AA, Jhangiani SN, Doddapaneni H, et al. Germline mutations in shelterin complex genes are associated with familial glioma. J Natl Cancer Inst. 2015 Jan;107(1):384.

[18] Bertuch AA. The Molecular Genetics of the Telomere Biology Disorders. RNA Biol. 2016; 13(8):696-706.

[19] Giardini MA, Segatto M, da Silva MS, Nunes VS, Cano MI. Telomere and telomerase biology. Prog Mol Biol Transl Sci. 2014;125:1-40.

[20] Aubert G, Baerlocher GM, Vulto I, Poon SS, Lansdorp PM. Collapse of telomere homeostasis in hematopoietic cells caused by heterozygous mutations in telomerase genes. PLoS Genet. 2012;8(5):e1002696.

[21] Kipling D, Cooke HJ. Hypervariable ultra-long telomeres in mice. Nature. 1990 Sep 27;347(6291):400-2.

[22] Blasco MA. Telomeres and human disease: ageing, cancer and beyond. Nat Rev Genet. 2005 Aug;6(8):611-22.

[23] de Lange T, Shiue L, Myers RM, Cox DR, Naylor SL, Killery AM, et al. Structure and variability of human chromosome ends. Mol Cell Biol. 1990 Feb;10(2):518-27.

[24] de Lange T. T-loops and the origin of telomeres. Nat Rev Mol Cell Biol. 2004 Apr; 5(4):323-9.

[25] Cooper JP, Nimmo ER, Allshire RC, Cech TR. Regulation of telomere length and function by a Myb-domain protein in fission yeast. Nature. 1997 Feb 20;385(6618): 744-7.

[26] Broccoli D, Smogorzewska A, Chong L, de Lange T. Human telomeres contain two distinct Myb-related proteins, TRF1 and TRF2. Nat Genet. 1997 Oct;17(2):231-5.

[27] Ye JZ, Donigian JR, van Overbeek M, Loayza D, Luo Y, Krutchinsky AN, et al. TIN2 binds TRF1 and TRF2 simultaneously and stabilizes the TRF2 complex on telomeres. J Biol Chem. 2004 Nov 5;279(45):47264-71.

[28] Liu D, O'Connor MS, Qin J, Songyang Z. Telosome, a mammalian telomere-associated complex formed by multiple telomeric proteins. J Biol Chem. 2004 Dec 3;279(49): 51338-42.

[29] Chen LY, Redon S, Lingner J. The human CST complex is a terminator of telomerase activity. Nature. 2012 Aug 23;488(7412):540-4.

[30] Garcia-Cao M, O'Sullivan R, Peters AH, Jenuwein T, Blasco MA. Epigenetic regulation of telomere length in mammalian cells by the Suv39h1 and Suv39h2 histone methyltransferases. Nat Genet. 2004 Jan;36(1):94-9.

[31] Karlseder J, Hoke K, Mirzoeva OK, Bakkenist C, Kastan MB, Petrini JH, et al. The telomeric protein TRF2 binds the ATM kinase and can inhibit the ATM-dependent DNA damage response. PLoS Biol. 2004 Aug;2(8):E240.

[32] Wu L, Multani AS, He H, Cosme-Blanco W, Deng Y, Deng JM, et al. Pot1 deficiency initiates DNA damage checkpoint activation and aberrant homologous recombination at telomeres. Cell. 2006 Jul 14;126(1):49-62.

[33] Diotti R, Loayza D. Shelterin complex and associated factors at human telomeres. Nucleus. 2011 Mar-Apr;2(2):119-35.

[34] Nandakumar J, Cech TR. Finding the end: recruitment of telomerase to telomeres. Nat Rev Mol Cell Biol. 2013 Feb;14(2):69-82.

[35] Martinez P, Blasco MA. Replicating through telomeres: a means to an end. Trends Biochem Sci. 2015 Sep;40(9):504-15.

[36] Schmidt JC, Cech TR. Human telomerase: biogenesis, trafficking, recruitment, and activation. Genes Dev. 2015 Jun 1;29(11):1095-105.

[37] Watson JD. Origin of concatemeric T7 DNA. Nat New Biol. 1972 Oct 18;239(94): 197-201.

[38] Greider CW, Blackburn EH. A telomeric sequence in the RNA of Tetrahymena telomerase required for telomere repeat synthesis. Nature. 1989 Jan 26;337(6205):331-7.

[39] Mitchell JR, Cheng J, Collins K. A box H/ACA small nucleolar RNA-like domain at the human telomerase RNA 3' end. Mol Cell Biol. 1999 Jan;19(1):567-76.

[40] Berndt H, Harnisch C, Rammelt C, Stohr N, Zirkel A, Dohm JC, et al. Maturation of mammalian H/ACA box snoRNAs: PAPD5-dependent adenylation and PARN-dependent trimming. RNA. 2012 May;18(5):958-72.

[41] Moon DH, Segal M, Boyraz B, Guinan E, Hofmann I, Cahan P, et al. Poly(A)-specific ribonuclease (PARN) mediates 3'-end maturation of the telomerase RNA component. Nat Genet. 2015 Dec;47(12):1482-8.

[42] Angrisani A, Vicidomini R, Turano M, Furia M. Human dyskerin: beyond telomeres. Biol Chem. 2014 Jun;395(6):593-610.

[43] Egan ED, Collins K. Specificity and stoichiometry of subunit interactions in the human telomerase holoenzyme assembled in vivo. Mol Cell Biol. 2010 Jun;30(11): 2775-86.

[44] Venteicher AS, Abreu EB, Meng Z, McCann KE, Terns RM, Veenstra TD, et al. A human telomerase holoenzyme protein required for Cajal body localization and telomere synthesis. Science. 2009 Jan 30;323(5914):644-8.

[45] Zhong FL, Batista LF, Freund A, Pech MF, Venteicher AS, Artandi SE. TPP1 OB-fold domain controls telomere maintenance by recruiting telomerase to chromosome ends. Cell. 2012 Aug 3;150(3):481-94.

[46] Nandakumar J, Bell CF, Weidenfeld I, Zaug AJ, Leinwand LA, Cech TR. The TEL patch of telomere protein TPP1 mediates telomerase recruitment and processivity. Nature. 2012 Dec 13;492(7428):285-9.

[47] Williamson JR, Raghuraman MK, Cech TR. Monovalent cation-induced structure of telomeric DNA: the G-quartet model. Cell. 1989 Dec 1;59(5):871-80.

[48] Vannier JB, Pavicic-Kaltenbrunner V, Petalcorin MI, Ding H, Boulton SJ. RTEL1 dismantles T loops and counteracts telomeric G4-DNA to maintain telomere integrity. Cell. 2012 May 11;149(4):795-806.

[49] Sarek G, Vannier JB, Panier S, Petrini JH, Boulton SJ. TRF2 recruits RTEL1 to telomeres in S phase to promote t-loop unwinding. Mol Cell. 2015 Feb 19;57(4):622-35.

[50] Vannier JB, Sandhu S, Petalcorin MI, Wu X, Nabi Z, Ding H, et al. RTEL1 is a replisome-associated helicase that promotes telomere and genome-wide replication. Science. 2013 Oct 11;342(6155):239-42.

[51] Stewart JA, Wang F, Chaiken MF, Kasbek C, Chastain PD, 2nd, Wright WE, et al. Human CST promotes telomere duplex replication and general replication restart after fork stalling. EMBO J. 2012 Aug 29;31(17):3537-49.

[52] Wang F, Stewart JA, Kasbek C, Zhao Y, Wright WE, Price CM. Human CST has independent functions during telomere duplex replication and C-strand fill-in. Cell Rep. 2012 Nov 29;2(5):1096-103.

[53] Sfeir AJ, Chai W, Shay JW, Wright WE. Telomere-end processing the terminal nucleotides of human chromosomes. Mol Cell. 2005 Apr 1;18(1):131-8.

[54] Wu P, Takai H, de Lange T. Telomeric 3' overhangs derive from resection by Exo1 and Apollo and fill-in by POT1b-associated CST. Cell. 2012 Jul 6;150(1):39-52.

[55] Barbaro P, Ziegler DS, Reddel RR. The wide-ranging clinical implications of the Short Telomere Syndromes. Intern Med J. 2016; 46(4):393-403.

[56] Townsley DM, Dumitriu B, Young NS. Bone marrow failure and the telomeropathies. Blood. 2014 Oct 30;124(18):2775-83.

[57] Kropski JA, Blackwell TS, Loyd JE. The genetic basis of idiopathic pulmonary fibrosis. Eur Respir J. 2015 Jun;45(6):1717-27.

[58] Armanios M. Telomerase and idiopathic pulmonary fibrosis. Mutat Res. 2012 Feb 1;730(1-2):52-8.

[59] Dokal I. Dyskeratosis congenita in all its forms. Br J Haematol. 2000 Sep;110(4): 768-79.

[60] Heiss NS, Knight SW, Vulliamy TJ, Klauck SM, Wiemann S, Mason PJ, et al. X-linked dyskeratosis congenita is caused by mutations in a highly conserved gene with putative nucleolar functions. Nat Genet. 1998 May;19(1):32-8.

[61] Atkinson JC, Harvey KE, Domingo DL, Trujillo MI, Guadagnini JP, Gollins S, et al. Oral and dental phenotype of dyskeratosis congenita. Oral Dis. 2008 Jul;14(5):419-27.

[62] Ballew BJ, Savage SA. Updates on the biology and management of dyskeratosis congenita and related telomere biology disorders. Expert Rev Hematol. 2013 Jun;6(3): 327-37.

[63] Pignolo RJ, Suda RK, McMillan EA, Shen J, Lee SH, Choi Y, et al. Defects in telomere maintenance molecules impair osteoblast differentiation and promote osteoporosis. Aging Cell. 2008 Jan;7(1):23-31.

[64] Dokal I. Dyskeratosis congenita. Hematology Am Soc Hematol Educ Program. 2011;2011:480-6.

[65] Calado RT, Regal JA, Kleiner DE, Schrump DS, Peterson NR, Pons V, et al. A spectrum of severe familial liver disorders associate with telomerase mutations. PLoS One. 2009;4(11):e7926.

[66] Rackley S, Pao M, Seratti GF, Giri N, Rasimas JJ, Alter BP, et al. Neuropsychiatric conditions among patients with dyskeratosis congenita: a link with telomere biology? Psychosomatics. 2012 May-Jun;53(3):230-5.

[67] Alter BP, Giri N, Savage SA, Rosenberg PS. Cancer in dyskeratosis congenita. Blood. 2009 Jun 25;113(26):6549-57.

[68] Vulliamy TJ, Marrone A, Knight SW, Walne A, Mason PJ, Dokal I. Mutations in dyskeratosis congenita: their impact on telomere length and the diversity of clinical presentation. Blood. 2006 Apr 1;107(7):2680-5.

[69] Knight SW, Heiss NS, Vulliamy TJ, Greschner S, Stavrides G, Pai GS, et al. X-linked dyskeratosis congenita is predominantly caused by missense mutations in the DKC1 gene. Am J Hum Genet. 1999 Jul;65(1):50-8.

[70] Mitchell JR, Wood E, Collins K. A telomerase component is defective in the human disease dyskeratosis congenita. Nature. 1999 Dec 2;402(6761):551-5.

[71] Vulliamy T, Marrone A, Goldman F, Dearlove A, Bessler M, Mason PJ, et al. The RNA component of telomerase is mutated in autosomal dominant dyskeratosis congenita. Nature. 2001 Sep 27;413(6854):432-5.

[72] Alder JK, Barkauskas CE, Limjunyawong N, Stanley SE, Kembou F, Tuder RM, et al. Telomere dysfunction causes alveolar stem cell failure. Proc Natl Acad Sci U S A. 2015 Apr 21;112(16):5099-104.

[73] Vulliamy T, Marrone A, Szydlo R, Walne A, Mason PJ, Dokal I. Disease anticipation is associated with progressive telomere shortening in families with dyskeratosis congenita due to mutations in TERC. Nat Genet. 2004 May;36(5):447-9.

[74] Armanios M, Chen JL, Chang YP, Brodsky RA, Hawkins A, Griffin CA, et al. Haploinsufficiency of telomerase reverse transcriptase leads to anticipation in autosomal dominant dyskeratosis congenita. Proc Natl Acad Sci U S A. 2005 Nov 1;102(44):15960-4.

[75] Savage SA, Bertuch AA. The genetics and clinical manifestations of telomere biology disorders. Genet Med. 2010 Dec;12(12):753-64.

[76] Aubert G, Hills M, Lansdorp PM. Telomere length measurement-caveats and a critical assessment of the available technologies and tools. Mutat Res. 2012 Feb 1;730(1-2): 59-67.

[77] Diez Roux AV, Ranjit N, Jenny NS, Shea S, Cushman M, Fitzpatrick A, et al. Race/ethnicity and telomere length in the Multi-Ethnic Study of Atherosclerosis. Aging Cell. 2009 Jun;8(3):251-7.

[78] Hemann MT, Strong MA, Hao LY, Greider CW. The shortest telomere, not average telomere length, is critical for cell viability and chromosome stability. Cell. 2001 Oct 5;107(1):67-77.

[79] Letsolo BT, Rowson J, Baird DM. Fusion of short telomeres in human cells is characterized by extensive deletion and microhomology, and can result in complex rearrangements. Nucleic Acids Res. 2010 Apr;38(6):1841-52.

[80] Baird DM, Rowson J, Wynford-Thomas D, Kipling D. Extensive allelic variation and ultrashort telomeres in senescent human cells. Nat Genet. 2003 Feb;33(2):203-7.

[81] Alter BP, Baerlocher GM, Savage SA, Chanock SJ, Weksler BB, Willner JP, et al. Very short telomere length by flow fluorescence in situ hybridization identifies patients with dyskeratosis congenita. Blood. 2007 Sep 1;110(5):1439-47.

[82] Alter BP, Rosenberg PS, Giri N, Baerlocher GM, Lansdorp PM, Savage SA. Telomere length is associated with disease severity and declines with age in dyskeratosis congenita. Haematologica. 2012 Mar;97(3):353-9.

[83] Carrillo J, Martinez P, Solera J, Moratilla C, Gonzalez A, Manguan-Garcia C, et al. High resolution melting analysis for the identification of novel mutations in DKC1 and TERT genes in patients with dyskeratosis congenita. Blood Cells Mol Dis. 2012 Oct 15-Dec 15;49(3-4):140-6.

[84] Sastre L. Exome sequencing:what clinicians need to know. Advances in Genomics and Genetics. 2014;4:15-27.

[85] Tummala H, Walne A, Collopy L, Cardoso S, de la Fuente J, Lawson S, et al. Poly(A)-specific ribonuclease deficiency impacts telomere biology and causes dyskeratosis congenita. J Clin Invest. 2015 May;125(5):2151-60.

[86] Glousker G, Touzot F, Revy P, Tzfati Y, Savage SA. Unraveling the pathogenesis of Hoyeraal-Hreidarsson syndrome, a complex telomere biology disorder. Br J Haematol. 2015 Aug;170(4):457-71.

[87] Schwartz S, Bernstein DA, Mumbach MR, Jovanovic M, Herbst RH, Leon-Ricardo BX, et al. Transcriptome-wide mapping reveals widespread dynamic-regulated pseudouridylation of ncRNA and mRNA. Cell. 2014 Sep 25;159(1):148-62.

[88] Kiss T, Fayet-Lebaron E, Jady BE. Box H/ACA small ribonucleoproteins. Mol Cell. 2010 Mar 12;37(5):597-606.

[89] Tycowski KT, Shu MD, Kukoyi A, Steitz JA. A conserved WD40 protein binds the Cajal body localization signal of scaRNP particles. Mol Cell. 2009 Apr 10;34(1):47-57.

[90] Wong JM, Collins K. Telomerase RNA level limits telomere maintenance in X-linked dyskeratosis congenita. Genes Dev. 2006 Oct 15;20(20):2848-58.

[91] Carrillo J, Gonzalez A, Manguan-Garcia C, Pintado-Berninches L, Perona R. p53 pathway activation by telomere attrition in X-DC primary fibroblasts occurs in the absence of ribosome biogenesis failure and as a consequence of DNA damage. Clin Transl Oncol. 2013 Jun;16(6):529-38.

[92] Bellodi C, Kopmar N, Ruggero D. Deregulation of oncogene-induced senescence and p53 translational control in X-linked dyskeratosis congenita. EMBO J. 2010 Jun 2;29(11):1865-76.

[93] Walbott H, Machado-Pinilla R, Liger D, Blaud M, Rety S, Grozdanov PN, et al. The H/ACA RNP assembly factor SHQ1 functions as an RNA mimic. Genes Dev. 2011 Nov 15;25(22):2398-408.

[94] Grozdanov PN, Fernandez-Fuentes N, Fiser A, Meier UT. Pathogenic NAP57 mutations decrease ribonucleoprotein assembly in dyskeratosis congenita. Hum Mol Genet. 2009 Dec 1;18(23):4546-51.

[95] Brault ME, Lauzon C, Autexier C. Dyskeratosis congenita mutations in dyskerin SUMOylation consensus sites lead to impaired telomerase RNA accumulation and telomere defects. Hum Mol Genet. 2013 Sep 1;22(17):3498-507.

[96] Salowsky R, Heiss NS, Benner A, Wittig R, Poustka A. Basal transcription activity of the dyskeratosis congenita gene is mediated by Sp1 and Sp3 and a patient mutation in a Sp1 binding site is associated with decreased promoter activity. Gene. 2002 Jun 26;293(1-2):9-19.

[97] Lingner J, Hughes TR, Shevchenko A, Mann M, Lundblad V, Cech TR. Reverse transcriptase motifs in the catalytic subunit of telomerase. Science. 1997 Apr 25;276(5312):561-7.

[98] Moriarty TJ, Ward RJ, Taboski MA, Autexier C. An anchor site-type defect in human telomerase that disrupts telomere length maintenance and cellular immortalization. Mol Biol Cell. 2005 Jul;16(7):3152-61.

[99] Bryan TM, Goodrich KJ, Cech TR. Telomerase RNA bound by protein motifs specific to telomerase reverse transcriptase. Mol Cell. 2000 Aug;6(2):493-9.

[100] Podlevsky JD, Bley CJ, Omana RV, Qi X, Chen JJ. The telomerase database. Nucleic Acids Res. 2008 Jan;36(Database issue):D339-43.

[101] Collopy LC, Walne AJ, Cardoso S, de la Fuente J, Mohamed M, Toriello H, et al. Triallelic and epigenetic-like inheritance in human disorders of telomerase. Blood. 2015 Jul 9;126(2):176-84.

[102] Xin ZT, Beauchamp AD, Calado RT, Bradford JW, Regal JA, Shenoy A, et al. Functional characterization of natural telomerase mutations found in patients with hematologic disorders. Blood. 2007 Jan 15;109(2):524-32.

[103] Zaug AJ, Crary SM, Jesse Fioravanti M, Campbell K, Cech TR. Many disease-associated variants of hTERT retain high telomerase enzymatic activity. Nucleic Acids Res. 2013 Oct;41(19):8969-78.

[104] Stone MD, Mihalusova M, O'Connor C M, Prathapam R, Collins K, Zhuang X. Stepwise protein-mediated RNA folding directs assembly of telomerase ribonucleoprotein. Nature. 2007 Mar 22;446(7134):458-61.

[105] Lai CK, Miller MC, Collins K. Roles for RNA in telomerase nucleotide and repeat addition processivity. Mol Cell. 2003 Jun;11(6):1673-83.

[106] Chen JL, Opperman KK, Greider CW. A critical stem-loop structure in the CR4-CR5 domain of mammalian telomerase RNA. Nucleic Acids Res. 2002 Jan 15;30(2):592-7.

[107] Tesmer VM, Ford LP, Holt SE, Frank BC, Yi X, Aisner DL, et al. Two inactive fragments of the integral RNA cooperate to assemble active telomerase with the human protein catalytic subunit (hTERT) in vitro. Mol Cell Biol. 1999 Sep;19(9):6207-16.

[108] Mitchell JR, Collins K. Human telomerase activation requires two independent interactions between telomerase RNA and telomerase reverse transcriptase. Mol Cell. 2000 Aug;6(2):361-71.

[109] Robart AR, Collins K. Investigation of human telomerase holoenzyme assembly, activity, and processivity using disease-linked subunit variants. J Biol Chem. 2009 Feb 12;285(7):4375-86.

[110] Canudas S, Houghtaling BR, Bhanot M, Sasa G, Savage SA, Bertuch AA, et al. A role for heterochromatin protein 1gamma at human telomeres. Genes Dev. 2011 Sep 1;25(17):1807-19.

[111] Walne AJ, Vulliamy T, Beswick R, Kirwan M, Dokal I. TINF2 mutations result in very short telomeres: analysis of a large cohort of patients with dyskeratosis congenita and related bone marrow failure syndromes. Blood. 2008 Nov 1;112(9):3594-600.

[112] Sasa GS, Ribes-Zamora A, Nelson ND, Bertuch AA. Three novel truncating TINF2 mutations causing severe dyskeratosis congenita in early childhood. Clin Genet. 2012 May;81(5):470-8.

[113] Xin ZT, Ly H. Characterization of interactions between naturally mutated forms of the TIN2 protein and its known protein partners of the shelterin complex. Clin Genet. 2012 Mar;81(3):301-2.

[114] Yang D, He Q, Kim H, Ma W, Songyang Z. TIN2 protein dyskeratosis congenita missense mutants are defective in association with telomerase. J Biol Chem. 2011 Jul 1;286(26):23022-30.

[115] Frescas D, de Lange T. A TIN2 dyskeratosis congenita mutation causes telomerase-independent telomere shortening in mice. Genes Dev. 2014 Jan 15;28(2):153-66.

[116] Henriksson S, Farnebo M. On the road with WRAP53beta: guardian of Cajal bodies and genome integrity. Front Genet. 2015;6:91.

[117] Stern JL, Zyner KG, Pickett HA, Cohen SB, Bryan TM. Telomerase recruitment requires both TCAB1 and Cajal bodies independently. Mol Cell Biol. 2012 Jul;32(13): 2384-95.

[118] Zhong F, Savage SA, Shkreli M, Giri N, Jessop L, Myers T, et al. Disruption of telomerase trafficking by TCAB1 mutation causes dyskeratosis congenita. Genes Dev. 2011 Jan 1;25(1):11-6.

[119] Trahan C, Martel C, Dragon F. Effects of dyskeratosis congenita mutations in dyskerin, NHP2 and NOP10 on assembly of H/ACA pre-RNPs. Hum Mol Genet. 2009 Mar 1;19(5):825-36.

[120] Vulliamy T, Beswick R, Kirwan M, Marrone A, Digweed M, Walne A, et al. Mutations in the telomerase component NHP2 cause the premature ageing syndrome dyskeratosis congenita. Proc Natl Acad Sci U S A. 2008 Jun 10;105(23):8073-8.

[121] Keller RB, Gagne KE, Usmani GN, Asdourian GK, Williams DA, Hofmann I, et al. CTC1 Mutations in a patient with dyskeratosis congenita. Pediatr Blood Cancer. 2012 Aug;59(2):311-4.

[122] Walne AJ, Bhagat T, Kirwan M, Gitiaux C, Desguerre I, Leonard N, et al. Mutations in the telomere capping complex in bone marrow failure and related syndromes. Haematologica. 2013 Mar;98(3):334-8.

[123] Chen LY, Majerska J, Lingner J. Molecular basis of telomere syndrome caused by CTC1 mutations. Genes Dev. 2013 Oct 1;27(19):2099-108.

[124] White MF. Structure, function and evolution of the XPD family of iron-sulfur-containing 5'-->3' DNA helicases. Biochem Soc Trans. 2009 Jun;37(Pt 3):547-51.

[125] Uringa EJ, Lisaingo K, Pickett HA, Brind'Amour J, Rohde JH, Zelensky A, et al. RTEL1 contributes to DNA replication and repair and telomere maintenance. Mol Biol Cell. 2012 Jul;23(14):2782-92.

[126] Ballew BJ, Yeager M, Jacobs K, Giri N, Boland J, Burdett L, et al. Germline mutations of regulator of telomere elongation helicase 1, RTEL1, in Dyskeratosis congenita. Hum Genet. 2013 Apr;132(4):473-80.

[127] Le Guen T, Jullien L, Touzot F, Schertzer M, Gaillard L, Perderiset M, et al. Human RTEL1 deficiency causes Hoyeraal-Hreidarsson syndrome with short telomeres and genome instability. Hum Mol Genet. 2013 Aug 15;22(16):3239-49.

[128] Stuart BD, Choi J, Zaidi S, Xing C, Holohan B, Chen R, et al. Exome sequencing links mutations in PARN and RTEL1 with familial pulmonary fibrosis and telomere shortening. Nat Genet. 2015 May;47(5):512-7.

[129] Stanley SE, Noth I, Armanios M. What the genetics "RTEL"ing us about telomeres and pulmonary fibrosis. Am J Respir Crit Care Med. 2015 Mar 15;191(6):608-10.

[130] Fedick AM, Shi L, Jalas C, Treff NR, Ekstein J, Kornreich R, et al. Carrier screening of RTEL1 mutations in the Ashkenazi Jewish population. Clin Genet. 2014 Aug;88(2): 177-81.

[131] Korner CG, Wahle E. Poly(A) tail shortening by a mammalian poly(A)-specific 3'-exoribonuclease. J Biol Chem. 1997 Apr 18;272(16):10448-56.

[132] Mason PJ, Bessler M. mRNA deadenylation and telomere disease. J Clin Invest. 2015 May;125(5):1796-8.

[133] Ohga S, Kai T, Honda K, Nakayama H, Inamitsu T, Ueda K. What are the essential symptoms in the Hoyeraal-Hreidarsson syndrome? Eur J Pediatr. 1997 Jan;156(1): 80-1.

[134] Hoyeraal HM, Lamvik J, Moe PJ. Congenital hypoplastic thrombocytopenia and cerebral malformations in two brothers. Acta Paediatr Scand. 1970 Mar;59(2):185-91.

[135] Hreidarsson S, Kristjansson K, Johannesson G, Johannsson JH. A syndrome of progressive pancytopenia with microcephaly, cerebellar hypoplasia and growth failure. Acta Paediatr Scand. 1988 Sep;77(5):773-5.

[136] Aalfs CM, van den Berg H, Barth PG, Hennekam RC. The Hoyeraal-Hreidarsson syndrome: the fourth case of a separate entity with prenatal growth retardation, progressive pancytopenia and cerebellar hypoplasia. Eur J Pediatr. 1995 Apr;154(4):304-8.

[137] Savage SA, Alter BP. Dyskeratosis congenita. Hematol Oncol Clin North Am. 2009 Apr;23(2):215-31.

[138] Sznajer Y, Baumann C, David A, Journel H, Lacombe D, Perel Y, et al. Further delineation of the congenital form of X-linked dyskeratosis congenita (Hoyeraal-Hreidarsson syndrome). Eur J Pediatr. 2003 Dec;162(12):863-7.

[139] Cossu F, Vulliamy TJ, Marrone A, Badiali M, Cao A, Dokal I. A novel DKC1 mutation, severe combined immunodeficiency (T+B-NK- SCID) and bone marrow transplantation in an infant with Hoyeraal-Hreidarsson syndrome. Br J Haematol. 2002 Dec;119(3):765-8.

[140] Borggraefe I, Koletzko S, Arenz T, Fuehrer M, Hoffmann F, Dokal I, et al. Severe variant of x-linked dyskeratosis congenita (Hoyeraal-Hreidarsson Syndrome) causes significant enterocolitis in early infancy. J Pediatr Gastroenterol Nutr. 2009 Sep;49(3): 359-63.

[141] Malbora B, Avci Z, Ozbek N. Aplastic anemia and Hoyeraal-Hreidarsson syndrome. Skinmed. 2014 Mar-Apr;12(2):117-8.

[142] Ballew BJ, Joseph V, De S, Sarek G, Vannier JB, Stracker T, et al. A recessive founder mutation in regulator of telomere elongation helicase 1, RTEL1, underlies severe immunodeficiency and features of Hoyeraal Hreidarsson syndrome. PLoS Genet. 2013 Aug;9(8):e1003695.

[143] Knight SW, Heiss NS, Vulliamy TJ, Aalfs CM, McMahon C, Richmond P, et al. Unexplained aplastic anaemia, immunodeficiency, and cerebellar hypoplasia (Hoyeraal-Hreidarsson syndrome) due to mutations in the dyskeratosis congenita gene, DKC1. Br J Haematol. 1999 Nov;107(2):335-9.

[144] Lai W, Deng WP, Liu X, Chen HM, Dai Sh X. A recurrent p. A353V mutation in DKC1 responsible for different phenotypes of dyskeratosis congenita in a Chinese family. J Dermatol Sci. 2011 Aug;63(2):122-4.

[145] Marrone A, Sokhal P, Walne A, Beswick R, Kirwan M, Killick S, et al. Functional characterization of novel telomerase RNA (TERC) mutations in patients with diverse clinical and pathological presentations. Haematologica. 2007 Aug;92(8):1013-20.

[146] Gramatges MM, Qi X, Sasa GS, Chen JJ, Bertuch AA. A homozygous telomerase T-motif variant resulting in markedly reduced repeat addition processivity in siblings with Hoyeraal Hreidarsson syndrome. Blood. 2013 May 2;121(18):3586-93.

[147] Vogiatzi P, Perdigones N, Mason PJ, Wilson DB, Bessler M. A family with Hoyeraal-Hreidarsson syndrome and four variants in two genes of the telomerase core complex. Pediatr Blood Cancer. 2013 Jun;60(6):E4-6.

[148] Vulliamy TJ, Walne A, Baskaradas A, Mason PJ, Marrone A, Dokal I. Mutations in the reverse transcriptase component of telomerase (TERT) in patients with bone marrow failure. Blood Cells Mol Dis. 2005 May-Jun;34(3):257-63.

[149] Ye JZ, Hockemeyer D, Krutchinsky AN, Loayza D, Hooper SM, Chait BT, et al. POT1-interacting protein PIP1: a telomere length regulator that recruits POT1 to the TIN2/TRF1 complex. Genes Dev. 2004 Jul 15;18(14):1649-54.

[150] Takai KK, Kibe T, Donigian JR, Frescas D, de Lange T. Telomere protection by TPP1/POT1 requires tethering to TIN2. Mol Cell. 2011 Nov 18;44(4):647-59.

[151] Kocak H, Ballew BJ, Bisht K, Eggebeen R, Hicks BD, Suman S, et al. Hoyeraal-Hreidarsson syndrome caused by a germline mutation in the TEL patch of the telomere protein TPP1. Genes Dev. 2014 Oct 1;28(19):2090-102.

[152] Guo Y, Kartawinata M, Li J, Pickett HA, Teo J, Kilo T, et al. Inherited bone marrow failure associated with germline mutation of ACD, the gene encoding telomere protein TPP1. Blood. 2014 Oct 30;124(18):2767-74.

[153] Revesz T, Fletcher S, al-Gazali LI, DeBuse P. Bilateral retinopathy, aplastic anaemia, and central nervous system abnormalities: a new syndrome? J Med Genet. 1992 Sep; 29(9):673-5.

[154] Tsilou ET, Giri N, Weinstein S, Mueller C, Savage SA, Alter BP. Ocular and orbital manifestations of the inherited bone marrow failure syndromes: Fanconi anemia and dyskeratosis congenita. Ophthalmology. 2010 Mar;117(3):615-22.

[155] Anderson BH, Kasher PR, Mayer J, Szynkiewicz M, Jenkinson EM, Bhaskar SS, et al. Mutations in CTC1, encoding conserved telomere maintenance component 1, cause Coats plus. Nat Genet. 2012 Mar;44(3):338-42.

[156] Polvi A, Linnankivi T, Kivela T, Herva R, Keating JP, Makitie O, et al. Mutations in CTC1, encoding the CTS telomere maintenance complex component 1, cause cerebroretinal microangiopathy with calcifications and cysts. Am J Hum Genet. 2012 Mar 9;90(3):540-9.

[157] Savage SA. Connecting complex disorders through biology. Nat Genet. 2012 Mar; 44(3):238-40.

[158] Yamaguchi H, Baerlocher GM, Lansdorp PM, Chanock SJ, Nunez O, Sloand E, et al. Mutations of the human telomerase RNA gene (TERC) in aplastic anemia and myelodysplastic syndrome. Blood. 2003 Aug 1;102(3):916-8.

[159] Scheinberg P, Cooper JN, Sloand EM, Wu CO, Calado RT, Young NS. Association of telomere length of peripheral blood leukocytes with hematopoietic relapse, malignant transformation, and survival in severe aplastic anemia. JAMA. 2010 Sep 22;304(12):1358-64.

[160] Kim HJ, Perlman D, Tomic R. Natural history of idiopathic pulmonary fibrosis. Respir Med. 2015 Jun;109(6):661-70.

[161] Loyd JE. Pulmonary fibrosis in families. Am J Respir Cell Mol Biol. 2003 Sep;29(3 Suppl):S47-50.

[162] Armanios MY, Chen JJ, Cogan JD, Alder JK, Ingersoll RG, Markin C, et al. Telomerase mutations in families with idiopathic pulmonary fibrosis. N Engl J Med. 2007 Mar 29;356(13):1317-26.

[163] Tsakiri KD, Cronkhite JT, Kuan PJ, Xing C, Raghu G, Weissler JC, et al. Adult-onset pulmonary fibrosis caused by mutations in telomerase. Proc Natl Acad Sci U S A. 2007 May 1;104(18):7552-7.

[164] Diaz de Leon A, Cronkhite JT, Katzenstein AL, Godwin JD, Raghu G, Glazer CS, et al. Telomere lengths, pulmonary fibrosis and telomerase (TERT) mutations. PLoS One. 2010;5(5):e10680.

[165] Povedano JM, Martinez P, Flores JM, Mulero F, Blasco MA. Mice with Pulmonary Fibrosis Driven by Telomere Dysfunction. Cell Rep. 2015 Jul 14;12(2):286-99.

[166] Cogan JD, Kropski JA, Zhao M, Mitchell DB, Rives L, Markin C, et al. Rare variants in RTEL1 are associated with familial interstitial pneumonia. Am J Respir Crit Care Med. 2015 Mar 15;191(6):646-55.

[167] Alder JK, Chen JJ, Lancaster L, Danoff S, Su SC, Cogan JD, et al. Short telomeres are a risk factor for idiopathic pulmonary fibrosis. Proc Natl Acad Sci U S A. 2008 Sep 2;105(35):13051-6.

[168] Armanios M. Syndromes of telomere shortening. Annu Rev Genomics Hum Genet. 2009;10:45-61.

[169] Kropski JA, Mitchell DB, Markin C, Polosukhin VV, Choi L, Johnson JE, et al. A novel dyskerin (DKC1) mutation is associated with familial interstitial pneumonia. Chest. 2014 Jul;146(1):e1-7.

[170] Fukuhara A, Tanino Y, Ishii T, Inokoshi Y, Saito K, Fukuhara N, et al. Pulmonary fibrosis in dyskeratosis congenita with TINF2 gene mutation. Eur Respir J. 2013 Dec; 42(6):1757-9.

[171] Stanley SE, Chen JJ, Podlevsky JD, Alder JK, Hansel NN, Mathias RA, et al. Telomerase mutations in smokers with severe emphysema. J Clin Invest. 2015 Feb;125(2): 563-70.

[172] Parry EM, Alder JK, Qi X, Chen JJ, Armanios M. Syndrome complex of bone marrow failure and pulmonary fibrosis predicts germline defects in telomerase. Blood. 2011 May 26;117(21):5607-11.

[173] Calado RT, Brudno J, Mehta P, Kovacs JJ, Wu C, Zago MA, et al. Constitutional telomerase mutations are genetic risk factors for cirrhosis. Hepatology. 2011 May;53(5): 1600-7.

[174] Fogarty PF, Yamaguchi H, Wiestner A, Baerlocher GM, Sloand E, Zeng WS, et al. Late presentation of dyskeratosis congenita as apparently acquired aplastic anaemia due to mutations in telomerase RNA. Lancet. 2003 Nov 15;362(9396):1628-30.

[175] Gadalla SM, Sales-Bonfim C, Carreras J, Alter BP, Antin JH, Ayas M, et al. Outcomes of allogeneic hematopoietic cell transplantation in patients with dyskeratosis congenita. Biol Blood Marrow Transplant. 2013 Aug;19(8):1238-43.

[176] Ayas M, Nassar A, Hamidieh AA, Kharfan-Dabaja M, Othman TB, Elhaddad A, et al. Reduced intensity conditioning is effective for hematopoietic SCT in dyskeratosis congenita-related BM failure. Bone Marrow Transplant. 2013 Sep;48(9):1168-72.

[177] Islam A, Rafiq S, Kirwan M, Walne A, Cavenagh J, Vulliamy T, et al. Haematological recovery in dyskeratosis congenita patients treated with danazol. Br J Haematol. 2013 Sep;162(6):854-6.

[178] Calado RT, Yewdell WT, Wilkerson KL, Regal JA, Kajigaya S, Stratakis CA, et al. Sex hormones, acting on the TERT gene, increase telomerase activity in human primary hematopoietic cells. Blood. 2009 Sep 10;114(11):2236-43.

[179] Khincha PP, Wentzensen IM, Giri N, Alter BP, Savage SA. Response to androgen therapy in patients with dyskeratosis congenita. Br J Haematol. 2014 May;165(3): 349-57.

[180] Ziegler P, Schrezenmeier H, Akkad J, Brassat U, Vankann L, Panse J, et al. Telomere elongation and clinical response to androgen treatment in a patient with aplastic anemia and a heterozygous hTERT gene mutation. Ann Hematol. 2012 Jul;91(7):1115-20.

[181] Giri N, Pitel PA, Green D, Alter BP. Splenic peliosis and rupture in patients with dyskeratosis congenita on androgens and granulocyte colony-stimulating factor. Br J Haematol. 2007 Sep;138(6):815-7.

[182] Zlateska B, Ciccolini A, Dror Y. Treatment of dyskeratosis congenita-associated pulmonary fibrosis with danazol. Pediatr Pulmonol. 2015 50(12):48-51.

[183] Noble PW, Albera C, Bradford WZ, Costabel U, du Bois RM, Fagan EA, et al. Pirfenidone for idiopathic pulmonary fibrosis: analysis of pooled data from three multinational phase 3 trials. Eur Respir J. 2015 Jan;47(1):243-53.

[184] Richeldi L, du Bois RM, Raghu G, Azuma A, Brown KK, Costabel U, et al. Efficacy and safety of nintedanib in idiopathic pulmonary fibrosis. N Engl J Med. 2014 May 29;370(22):2071-82.

[185] Giri N, Lee R, Faro A, Huddleston CB, White FV, Alter BP, et al. Lung transplantation for pulmonary fibrosis in dyskeratosis congenita: Case Report and systematic literature review. BMC Blood Disord. 2011;11:3.

[186] Silhan LL, Shah PD, Chambers DC, Snyder LD, Riise GC, Wagner CL, et al. Lung transplantation in telomerase mutation carriers with pulmonary fibrosis. Eur Respir J. 2014 Jul;44(1):178-87.

[187] Blasco MA, Lee HW, Hande MP, Samper E, Lansdorp PM, DePinho RA, et al. Telomere shortening and tumor formation by mouse cells lacking telomerase RNA. Cell. 1997 Oct 3;91(1):25-34.

[188] Lee HW, Blasco MA, Gottlieb GJ, Horner JW, 2nd, Greider CW, DePinho RA. Essential role of mouse telomerase in highly proliferative organs. Nature. 1998 Apr 9;392(6676):569-74.

[189] Raval A, Behbehani GK, Nguyen le XT, Thomas D, Kusler B, Garbuzov A, et al. Reversibility of Defective Hematopoiesis Caused by Telomere Shortening in Telomerase Knockout Mice. PLoS One. 2015;10(7):e0131722.

[190] Herrera E, Samper E, Martin-Caballero J, Flores JM, Lee HW, Blasco MA. Disease states associated with telomerase deficiency appear earlier in mice with short telomeres. EMBO J. 1999 Jun 1;18(11):2950-60.

[191] Gu BW, Bessler M, Mason PJ. A pathogenic dyskerin mutation impairs proliferation and activates a DNA damage response independent of telomere length in mice. Proc Natl Acad Sci U S A. 2008 Jul 22;105(29):10173-8.

[192] Beier F, Foronda M, Martinez P, Blasco MA. Conditional TRF1 knockout in the hematopoietic compartment leads to bone marrow failure and recapitulates clinical features of dyskeratosis congenita. Blood. 2012 Oct 11;120(15):2990-3000.

[193] Simeonova I, Jaber S, Draskovic I, Bardot B, Fang M, Bouarich-Bourimi R, et al. Mutant mice lacking the p53 C-terminal domain model telomere syndromes. Cell Rep. 2013 Jun 27;3(6):2046-58.

[194] Garcia-Cao I, Garcia-Cao M, Martin-Caballero J, Criado LM, Klatt P, Flores JM, et al. "Super p53" mice exhibit enhanced DNA damage response, are tumor resistant and age normally. EMBO J. 2002 Nov 15;21(22):6225-35.

[195] Ramunas J, Yakubov E, Brady JJ, Corbel SY, Holbrook C, Brandt M, et al. Transient delivery of modified mRNA encoding TERT rapidly extends telomeres in human cells. FASEB J. 2015 May;29(5):1930-9.

[196] Maida Y, Masutomi K. Telomerase reverse transcriptase moonlights: Therapeutic targets beyond telomerase. Cancer Sci. 2015 106(11):1486-92.

[197] Gu BW, Fan JM, Bessler M, Mason PJ. Accelerated hematopoietic stem cell aging in a mouse model of dyskeratosis congenita responds to antioxidant treatment. Aging Cell. 2011 Apr;10(2):338-48.

[198] Machado-Pinilla R, Sanchez-Perez I, Murguia JR, Sastre L, Perona R. A dyskerin motif reactivates telomerase activity in X-linked dyskeratosis congenita and in telomerase-deficient human cells. Blood. 2008 Mar 1;111(5):2606-14.

[199] Machado-Pinilla R, Carrillo J, Manguan-Garcia C, Sastre L, Mentzer A, Gu BW, et al. Defects in mTR stability and telomerase activity produced by the Dkc1 A353V mutation in dyskeratosis congenita are rescued by a peptide from the dyskerin TruB domain. Clin Transl Oncol. 2012 Oct;14(10):755-63.

[200] Manguan-Garcia C, Pintado-Berninches L, Carrillo J, Machado-Pinilla R, Sastre L, Perez-Quilis C, et al. Expression of the genetic suppressor element 24.2 (GSE24.2) decreases DNA damage and oxidative stress in X-linked dyskeratosis congenita cells. PLoS One. 2014;9(7):e101424.

[201] Iarriccio L, Manguan-Garcia C, Pintado-Berninches L, Mancheno JM, Molina A, Perona R, et al. GSE4, a Small Dyskerin- and GSE24.2-Related Peptide, Induces Telomerase Activity, Cell Proliferation and Reduces DNA Damage, Oxidative Stress and Cell Senescence in Dyskerin Mutant Cells. PLoS One. 2015;10(11):e0142980.

http://dx.doi.org/10.5772/65353

[202] Egusquiaguirre SP, Manguan-Garcia C, Pintado-Berninches L, Iarriccio L, Carbajo D, Albericio F, et al. Development of surface modified biodegradable polymeric nanoparticles to deliver GSE24.2 peptide to cells: a promising approach for the treatment of defective telomerase disorders. Eur J Pharm Biopharm. 2015 Apr;91:91-102.

PLOS ONE

RESEARCH ARTICLE

GSE4, a Small Dyskerin- and GSE24.2-Related Peptide, Induces Telomerase Activity, Cell Proliferation and Reduces DNA Damage, Oxidative Stress and Cell Senescence in Dyskerin Mutant Cells

Laura Iarriccio[1,5], Cristina Manguán-García[1,2,3], Laura Pintado-Berninches[1], José Miguel Mancheño[4], Antonio Molina[5], Rosario Perona[1,2,3,6‡], Leandro Sastre[1,2,3,6‡]*

1 Instituto de Investigaciones Biomédicas CSIC/UAM, Madrid, Spain, **2** CIBER de Enfermedades Raras, Valencia, Spain, **3** IdiPaz, Madrid, Spain, **4** Instituto de Química-Física "Rocasolano" CSIC, Madrid, Spain, **5** Advanced Medical Projects, Madrid, Spain, **6** Biomarkers and Experimental Therapeutics in Cancer, IdiPaz, Hospital Universitario La Paz, Madrid, Spain

‡ RP and LS are joint senior authors on this work.
* lsastre@iib.uam.es

OPEN ACCESS

Citation: Iarriccio L, Manguán-García C, Pintado-Berninches L, Mancheño JM, Molina A, Perona R, et al. (2015) GSE4, a Small Dyskerin- and GSE24.2-Related Peptide, Induces Telomerase Activity, Cell Proliferation and Reduces DNA Damage, Oxidative Stress and Cell Senescence in Dyskerin Mutant Cells. PLoS ONE 10(11): e0142980. doi:10.1371/journal.pone.0142980

Editor: Arthur J. Lustig, Tulane University Health Sciences Center, UNITED STATES

Received: August 28, 2015

Accepted: October 29, 2015

Published: November 16, 2015

Data Availability Statement: All relevant data are within the paper and its Supporting Information files.

Funding: This work was supported by grants PI1401495 (supported by FEDER funds) and ER15PR07ACC114/757 (Fondo de Investigaciones Sanitarias, Instituto de Salud Carlos III. Spain), 201320E075 (Consejo Superior de Investigaciones Científicas) and IPT-2012-0674-090000 (Ministerio de Economía y Competitividad. Spain). CM-G is supported by the CIBER de Enfermedades Raras.

Abstract

Dyskeratosis congenita is an inherited disease caused by mutations in genes coding for telomeric components. It was previously reported that expression of a dyskerin-derived peptide, GSE24.2, increases telomerase activity, regulates gene expression and decreases DNA damage and oxidative stress in dyskeratosis congenita patient cells. The biological activity of short peptides derived from GSE24.2 was tested and one of them, GSE4, that probed to be active, was further characterized in this article. Expression of this eleven amino acids long peptide increased telomerase activity and reduced DNA damage, oxidative stress and cell senescence in dyskerin-mutated cells. GSE4 expression also activated c-myc and TERT promoters and increase of c-myc, TERT and TERC expression. The level of biological activity of GSE4 was similar to that obtained by GSE24.2 expression. Incorporation of a dyskerin nuclear localization signal to GSE24.2 did not change its activity on promoter regulation and DNA damage protection. However, incorporation of a signal that increases the rate of nucleolar localization impaired GSE24.2 activity. Incorporation of the dyskerin nuclear localization signal to GSE4 did not alter its biological activity. Mutation of the Aspartic Acid residue that is conserved in the pseudouridine synthase domain present in GSE4 did not impair its activity, except for the repression of c-myc promoter activity and the decrease of c-myc, TERT and TERC gene expression in dyskerin-mutated cells. These results indicated that GSE4 could be of great therapeutic interest for treatment of dyskeratosis congenita patients.

Competing Interests: The authors have declared that no competing interest exists.

Introduction

Telomere maintenance alterations are in the origin of an increasing number of diseases such as dyskeratosis congenita, aplastic anemia or pulmonary fibrosis (recently reviewed by S.A. Savage [1]). Telomeres are structures located at the end of the chromosomes that play essential roles in chromosome replication and stability [2, 3]. The sequence of their DNA consists of hundreds of repeats of the TTAGGG motif. The DNA replication machinery cannot complete the synthesis of the chromosome ends that is accomplished by a RNA-protein complex with reverse transcriptase activity named telomerase [4]. The telomerase protein with reverse transcriptase activity is encoded by the TERT gene and uses as template the RNA molecule encoded by the TERC (also named TR) gene that is another component of the telomerase complex [5]. A third essential component is dyskerin, encoded by the dkc1 gene [6, 7]. Additional components of the telomerase complex include the proteins NOP10, GAR and NHP2 [8]. Telomeres acquire a very specialized structure since the terminal region of the DNA stays single-stranded and folds back to get inter winged with a close telomere region to form a circular structure (T-circle) [9]. In addition, the telomere DNA binds to a specific protein complex, named shelterin complex, which protects telomeres from degradation [10]. This structure also avoids the recognition of telomeres as damaged DNA by the DNA-repair signalling system. The correct structure of the telomeres is therefore essential for the maintenance of chromosome integrity and cell cycle progression [11]. Telomere shortening that occurs during proliferation of non-stem or transformed cells results in genome instability, the fusion of chromosomes and induces apoptotic cell death or senescence [11].

Mutations in the genes coding for components of the telomerase (TERT, TERC, DKC, NOP10, NH2) or shelterin (TINF2) complexes cause a number of diseases known as telomeropathies or Telomere Biology Disorders. Among them are dyskeratosis congenita, premature aging syndromes, aplastic anemia, pulmonary fibrosis and cancer (see Savage, S.A. [1] and Glousker, G. et al [12] for recent reviews).

Dyskeratosis congenita is a rare disorder characterized by bone marrow failure and increased susceptibility to cancer [13]. Mutations in DKC1 produce the predominant X-linked form of this disease. The encoded protein, dyskerin, is a pseudouridine synthase required for the postranscriptional modification of ribosomal, small nuclear and nucleolar RNAs and some mRNAs [7, 14] [15, 16]. In addition, is an essential component of the telomerase complex as previously indicated. Dyskerin has three conserved domains, the Dyskerin Like Domain (DKLD), the pseudouridine synthase domain (TRUB domain) and the RNA binding domain (PUA domain) [7]. Mutations in these domains produce X-linked dyskeratosis congenita [7, 17]. We have previously described that a 55 amino acids-long fragment of the dyskerin TRUB domain, named GSE24.2, has protective effects on cells derived from dyskeratosis congenita patients [18]. GSE24.2 treatment increases telomerase activity of patient cells. This peptide also protects cells from treatment with the anticancer drug cisplatin, that induces intra- and inter-strand DNA bridges, and from telomerase inhibitors. Expression of GSE24.2 from plasmid or viral vectors or direct transfection of cells with the peptide, produced in bacteria or chemically synthesized, have similar effects [19]. GSE24.2 increases TERT and c-myc expression through transcriptional activation and stabilizes TERC RNA in dyskerin mutant cells [19]. This peptide protects cells from basal DNA damage, which is increased in dyskeratosis congenita patients [20]. These activities make of GSE24-2 a good candidate for a therapeutic approach to dyskeratosis congenita and related telomeropathies. Actually, the EMA recently approved GSE24.2 as an orphan drug for dyskeratosis congenita treatment (EU/3/12/1070-EMA/OD/136/11).

In this article we describe that a smaller peptide of just eleven amino acids, named GSE4, corresponding to the N-terminal region of GSE24.2, maintains the same capacity to regulate

gene expression, to protect cells from DNA damage and to decrease oxidative stress as GSE24.2. In addition, GSE24.2 and GSE4 protect dyskeratosis congenita patient's cell from cell senescence.

Materials and Methods

Cell culture and transfection

The previously described F9 and dyskerin-mutated F9 cells (F9-A353V) [19, 21], were cultured in Dulbecco Modified Eagle Medium (DMEM) supplemented with 10% foetal bovine serum, 2 mM glutamine (Gibco) and 1.5 gr/ml of sodium bicarbonate. HEK293T cells (ATCC) were cultured in DMEM media supplemented with 10% foetal bovine serum and 2 mM glutamine. DC-C and DC-3 cells (Coriell Cell Repository) were cultured in Roswell Park Memorial Institute (RPMI) media supplemented with 20% foetal bovine serum and 2 mM glutamine. XDC-1787-C (Corriel Cell Repository) and F26IIB cells (generated in our laboratory), were cultured in Minimum Essential Medium Eagle (MEM) media supplemented with 15% foetal bovine serum and 2 mM glutamine. Cells were transfected with 10 μg of DNA/10^6 cells using lipofectamine plus (Invitrogene, Carlsbad, USA) or the K2 transfection kit (Biontex Lab, Planegg/Martinsried, GE) according to the manufacturers' instructions. 15 μg of peptides per 35 mm dish were transfected using the ProteoJuice Protein Transfection Reagent (Merck Millipore, Billerica, MA, USA) or the K2 transfection kit.

Peptide production and purification

The GSE24.2 peptide was produced in E. coli DH5α transformed with pGATEV GSE24.2 as previously described [20]. HPLC-purified synthetic peptides were obtained from Peptide 2.0 Inc (Chantilly, USA) and China Peptides Co. Ltd. (Shanghai, China).

Vector constructions and in vitro mutagenesis

The localization signal KRKR (amino acids 446–449) was incorporated to the 3' end of the GSE 24.2 expression vector by PCR using the oligonucleotides 5'-GGGAATTCTGGTTTGATTAATCTTGACAAGC-3' and 5'-GGTCTAGACTCGCTTCCGCTTCTTCACCAAGCGAGTGGCTCG-3'. The amplified product was cloned between the EcoRI and XbaI sites of the pcDNA3-myc vector to generate the GSE24.2-NLS1.3 vector. The localization signal KKEKKKSKK (amino acids 467–476) was introduced using the oligonucleotides: 5'-GGGAATTCTGGTTTGATTAATCTTGACAAGC-3' and 5'-GGTCTAGACCTTCTTACTCTTCTTCTTTTCCTTCTTCTTCACCAAGCGAGTGGCTCG-3' and cloned in pcDNA3-myc to generate GSE24.2-NLS2.3. The fragments GSE24.2, GSE24.2-NLS1.3 and GSE24.2-NLS2.3 were also cloned in the pRRL-CMV-IRES-GFP vector using the PstI and BamHI restriction sites. GSE4 and derived fragment were cloned between the PstI and BamHI restriction sites of pRRL-CMV as double-stranded oligonucleotides obtained by hybridization of the following oligonucleotides: GSE4, 5'-GATGGGTTTCATTAATCTTGACAAGCCCTCTAACCCCTAAG-3' and 5'-GATCCTTAGGGGTTAGAGGGCTTGTCAAGATTAATGAAACCCATCTGCA-3'; GSE4-NLS1: 5'-GATGGGTTTCATTAATCTTGACAAGCCCTCTAACCCCAAGCGGAAGCGATAAG-3' and 5'-GATCCTTATCGCTTCCGCTTGGGGTTAGAGGGCTTGTCAAGATTAATGAAACCCATCTGCA-3'; GSE4-NLS1-DA (incorporating the GAC to GCC change): 5'-GATGGGTTTCATTAATCTTGCCAAGCCCTCTAACCCCAAGCGGAAGCGATAAG-3' and 5'-GATCCTTATCGCTTCCGCTTGGGGTTAGAGGGCTTGGCAAGATTAATGAAACCCATCTGCA-3'.

Gene-reporter assays

Cells were transfected with 10 μg/10^6 cells of expression vectors for GSE24.2, GSE4 and derived peptides and the corresponding luciferase reporter vectors (1 μg/10^6 cells). The TERT and c-myc (px3.2) promoter constructs have been described previously [18, 22]. Twenty four hours after transfection protein extracts were prepared and luciferase activity determined using a commercial kit (Promega Corporation, Madison, WI, USA). Luciferase activity was expressed as arbitrary units by μg of protein concentration, determined with the Bradford Reagent (BioRad, Berkeley, CA, USA).

Immunofluorescence and immunocytochemistry

Cells were grown on coverslips, fixed, permeabilized and incubated with the corresponding antibodies as previously described [20]. Nucleoli were stained incubating the cells for 20 min with 0,5 μM of the SYTO RNA Select Green Fluorescent Cell Stain (Molecular Probes). DNA damage foci were identified by the presence of γH2AX as previously described [20]. Oxidative stress was determined using the anti-8-oxoguanine antibody, clone 483.15 (MAB3560, Merck-Millipore). Images were acquired using a Zeiss Confocal microscope and processed using ZEN 2011 Light Edition and ImageJ software. DNA synthesis was determined by immunocytochemistry using anti-Ki67 antibodies (RM9106-50; NeoMarkers Inc. Fremont, CA, USA).

Telomeric Repeat Amplification Protocol (TRAP) assay

The TRAPeze kit (Millipore, Billerica, MA, USA) [23] was used to determine telomerase activity. The activity of each sample was normalized using the internal control provided in the kit.

Determination of reactive oxygen species (ROS) content with dihydroethidium

Cells were washed 2 times with pre-warmed PBS medium, dihydroethidium (Dihydroethidium, D7008-Sigma, St. Louis, MI. USA) was added and the cells incubated at 37°C for 25 min. The fluorescence was measured using FACS SCAN II (BD, USA), with 530 nm of excitation wavelength and 630 nm of emission wavelength.

Determination of cell senescence

Cells were plated on 6-well plates at a density of 1x10^4 cells/well. After 4 days of culture cells were fixed and the acid-β-galactosidase activity detected using the Senescence Detection Kit (BioVision, USA). Six images were taken from each well using a Nikon Eclipse TS100 microscope (Nikon, USA) and the percentage of senescent cells calculated for each of them.

Protein expression analyses

Whole-cell extracts were obtained and analyzed by Western blot as previously described [24].

Antibodies

Primary antibodies used for γH2AX and phosporylated Chk2 detection were from Cell Signalling Technology (2577, Cell Signalling Technology, Danvers, MA, USA), and those used for α-tubulin detection from Sigma-Aldrich (T9026, Sigma-Aldrich, St. Louis, MO, USA). Secondary antibodies were purchased from BioRad (Berkeley, CA, USA) and Cell Signalling Technology.

Quantitative RT-PCR analyses of gene expression

Total RNA was obtained from the cell cultures using the Trizol Reagent (Invitrogen, Carlsbad, CA, USA). One microgram of RNA was converted to cDNA using random primers and the High-Capacity cDNA Archive Kit (Applied Biosystems, Foster City, CA, USA). Quantitative PCR was done using the Power SYBR Green kit (Applied Biosystems, Foster City, CA, USA). The programs used have been described by Machado-Pinilla, et al. [19]. SOD1(Cu/Zn SOD) and SOD2 (Mn SOD) mRNA levels were determined using the TaqMan Universal PCR Master Mix. The StepOne Plus Real Time PCR System (Applied Biosystems, Foster City, CA, USA) was used for analyses of the PCR products. Relative gene expression was calculated according to the comparative threshold cycle method [25] using β-actin as endogenous control.

Primers used for quantitative RT-PCR

The following primers were used: m-cmyc-S: 5'-GAGCTGTTTGAAGGCTGGATTT-3'; m-cmyc-AS: 5'-TCCTGTTGGTGAAGTTCACGTT-3'; m-TERT-S: 5'-AGATCAAGAGCAG TAGTCGCCAG-3'; m-TERT-AS: 5'-TTTACAGCACACCGACCCAGAG-3'; m-TR-S: 5': GCTGTGGGTTCTGGTCTTTTGTTC-3'; m-TR-AS: 5'-CGTTTGTTTTTGAGGCTCGGG-3'; β-actin-S: 5'- GGTATGGAATCCTGTGGCATCCATGAAA-3'; β-actin-AS: 5'-GTGTA AAACGCAGCTCAGTAACAGTCCG-3'.

Statistical analyses

Experiments were repeated, at least, three times with triplicate samples. Statistical significance was calculated using the Unpaired t-test (two- tailed). The significance has been considered at $^{*}p<0.05$, $^{**}p<0.01$ and $^{***}p<0.001$. GraphPad software v5.0 was used for statistical analysis and graphic representations.

Results

1. Functional study of the GSE24.2-derived peptide GSE4 on DNA damage rescue, telomerase activity and cell proliferation in dyskeratosis congenita cells

Many of the previous functional studies were done with GSE24.2 peptides produced in E. coli. The analysis of these preparations by mass spectroscopy indicated the presence of several smaller peptides probably originated by GSE24.2 partial degradation. The more abundant peptide was an eleven amino acids long peptide corresponding to the N-terminal region of GSE24.2 (GSE4, Fig 1A). The functional activity of this peptide was compared to that of GSE24.2 in several analyses. We have previously reported that the GSE24.2 peptide reduced DNA damage [20]. We transfected F9 or the F9-derived dyskerin-mutant F9A353V cells with pRRL-CMV-IRES-GFP vector, either empty (vector) or expressing GSE24.2 or GSE4 to study their possible effect on basal DNA damage by measuring γH2AX phosphorylation (Fig 1A). We found that the amount of γH2AX in F9A353V cells decreased to similar levels after transfecting both peptides (40 and 30%, respectively). The possible effect of GSE4 expression on telomerase activity was assayed on the fibroblastoid cell line F26IIB, derived from a dyskeratosis congenita patient carrying the Ala2Val hemizygous mutation [26]. Cells were transfected with the above-mentioned vectors and their telomerase activity determined, as shown in Fig 1B. Quantification of the extension products indicated a significant increase in telomerase activity upon GSE24.2 and GSE4 expression. The proliferation capacity of the transfected cells was estimated by the expression of the Ki67 nucleolar protein, as shown in

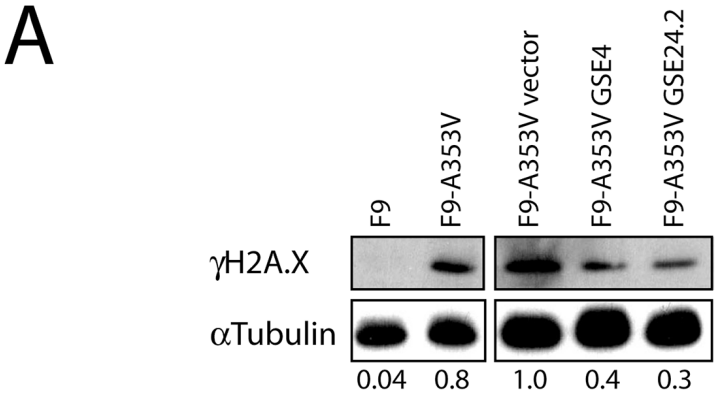

GSE24.2: GFINLDKPSNPSSHEVVAWIRRILRVEKTGHSGTLDPKVTGCLIVCIERATRLVK
GSE4: GFINLDKPSNP

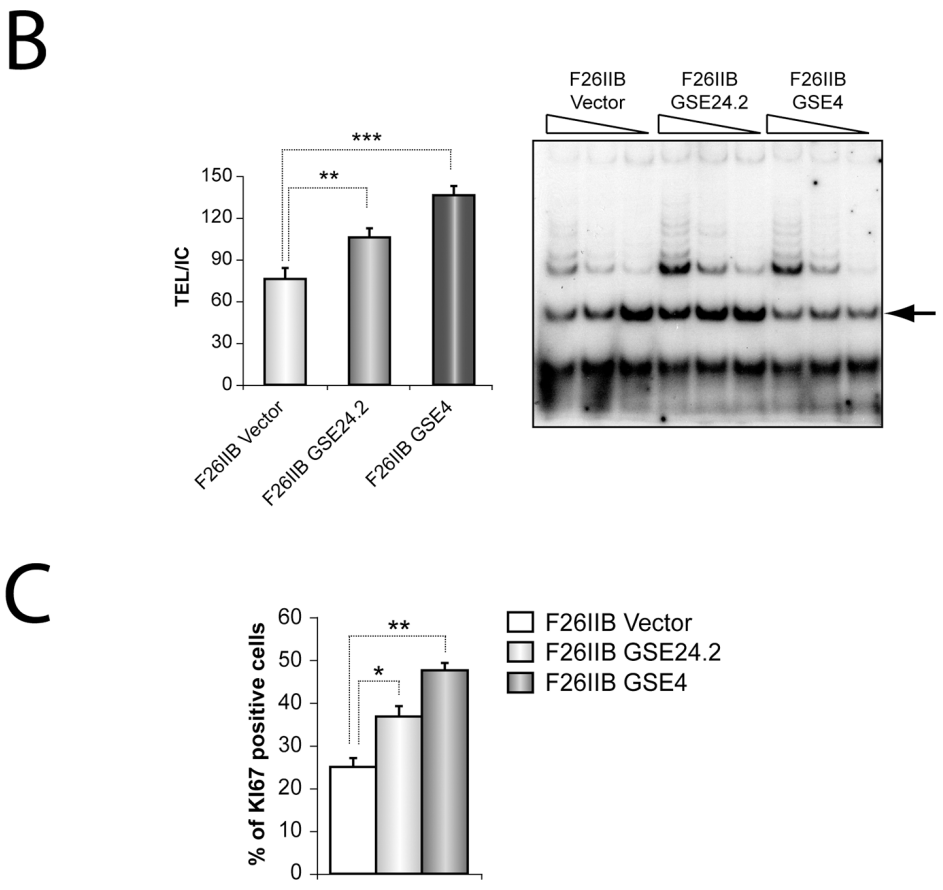

Fig 1. DNA-damage protective effect, telomerase activation and cell proliferation induction of one small peptide, GSE4, derived from GSE24.2. Panel A. One small peptide derived from GSE24.2, GSE4, and GSE24.2 were expressed in F9_A353V cells that were transfected with the pRRL-CMV-IRES-EGFP vector, either empty (Vector) or expressing GSE24.2 or GSE4. Twenty four hours later cells were lysed and the presence of γH2AX and α-tubulin (loading control) analyzed by western blot. Un-transfected F9 and F9-A353V cells were used as controls. The values at the bottom of the panel indicate the estimated ratio between γH2AX and α-tubulin expression levels referred to those found in cells transfected with the empty vector (F9-A353V vector). The amino acid sequences of GSE24.2 and GSE4 are indicated at the lower part

of the panel. Panel B. The telomerase activity of F26IIB cells transfected with the pRRL-CMV-IRES-GFP vector empty (vector), expressing GSE24.2 (GSE24.2) or GSE4 (GSE4) was determined using the Telomeric Repeat Amplification Protocol (TRAP) assay. The amplification products obtained using three decreasing amounts of cell extracts for each cell line are shown in the right panel. Quantification of the amplification products, normalized to the internal control provided in the assay (indicated by an arrow at the right panel) is shown in the left panel. Panel C. Expression of Ki67 was determined by immunocytochemistry in F26IIB cells transfected as described in panel B. The percentage of cells expressing Ki67 is represented for each type of transfected cells. The experiments were repeated three times with similar results. Asterisks indicated the statistical significance (* $p<0.05$, ** $p<0.01$, *** $p<0.001$).

doi:10.1371/journal.pone.0142980.g001

Fig 1C. A significantly higher percentage of cells expressing GSE24.2 and GSE4 were positive for Ki67 expression, indicative of higher proliferation rates.

2. Oxidative stress and senescence are decreased in X-DC cells by GSE4 expression

Oxidative stress is one of the causes of DNA damage producing both single-strand breaks (SSBs) and double-strand breaks (DSBs). Cells obtained from dyskeratosis congenita patients showed high levels of oxidative stress and reactive oxygen species (ROS) production that decreased upon treatment with GSE24.2 [20]. We therefore tested the activity of GSE4 on oxidative stress on a cellular model of dyskeratosis congenita. Oxidative stress was first determined by the presence of α-8-oxoguanine on the cellular DNA. F9-A353V cells were transfected with the pRRL-CMV-IRES-GFP vector expressing GSE24.2, GSE4 or the empty vector and the amount of α-8-oxoguanine present on the cells determined by immunohistochemistry. F9 cells that do not carry any DKC mutation were used as control. The quantification of α-8-oxoguanine expression is shown in Fig 2A. Expression of GSE24.2 and GSE4 decreased α-8-oxoguanine levels of F9-A353V cells. Oxidative stress was also measured in cells derived from dyskeratosis congenita patients (DC-3, carrying the Thr66Ala mutation in dkc1) and healthy relatives (DC-C) by determining ROS levels using dihydroethidium, as shown in Fig 2B. Dyskeratosis- congenita patient cells infected with the empty vector showed higher levels of ROS than those of the healthy controls. Expression of GSE24.2 and GSE4 in the patient cells significantly decreased ROS levels. ROS production is associated with decreased expression of antioxidant enzymes such as the Cu/Zn- and Mn-dependent Superoxide Dismutases (SOD) [20]. The expression levels of the mRNAs coding for these two enzymes was determined by RT-qPCR, as shown in Fig 2C. Patient cells expressing the empty vector (DC-3 vector) showed decreased levels of both mRNAs, as compared to cells from the healthy control (Control cells). Expression of GSE24-2 and GSE4 greatly increased Cu/Zn SOD and Mn SOD mRNA expression levels in agreement with their capacity to decrease ROS production.

Telomere shortening has been described to result in cell senescence [27]. Therefore, the possible effect of GSE24.2 and GSE4 expression in senescence of dyskeratosis congenita patient's cells has been studied. One fibroblastoid cell line established from a dyskeratosis congenita patient (F26IIB) was transfected with the pRRL-CMV-IRES-GFP vector, either empty or expressing GSE24.2 or GSE4. After four days of culture senescent cells were identified by the expression of acidic β-galactosidase and the percentage of senescent (SA-β-gal) cells determined, as shown in Fig 2D. A fibroblastoid cell line established from a healthy relative of a DC patient (XDC-1787-C) was used as internal control. Expression of GSE4 and GSE24.2 significantly decreased cell senescence.

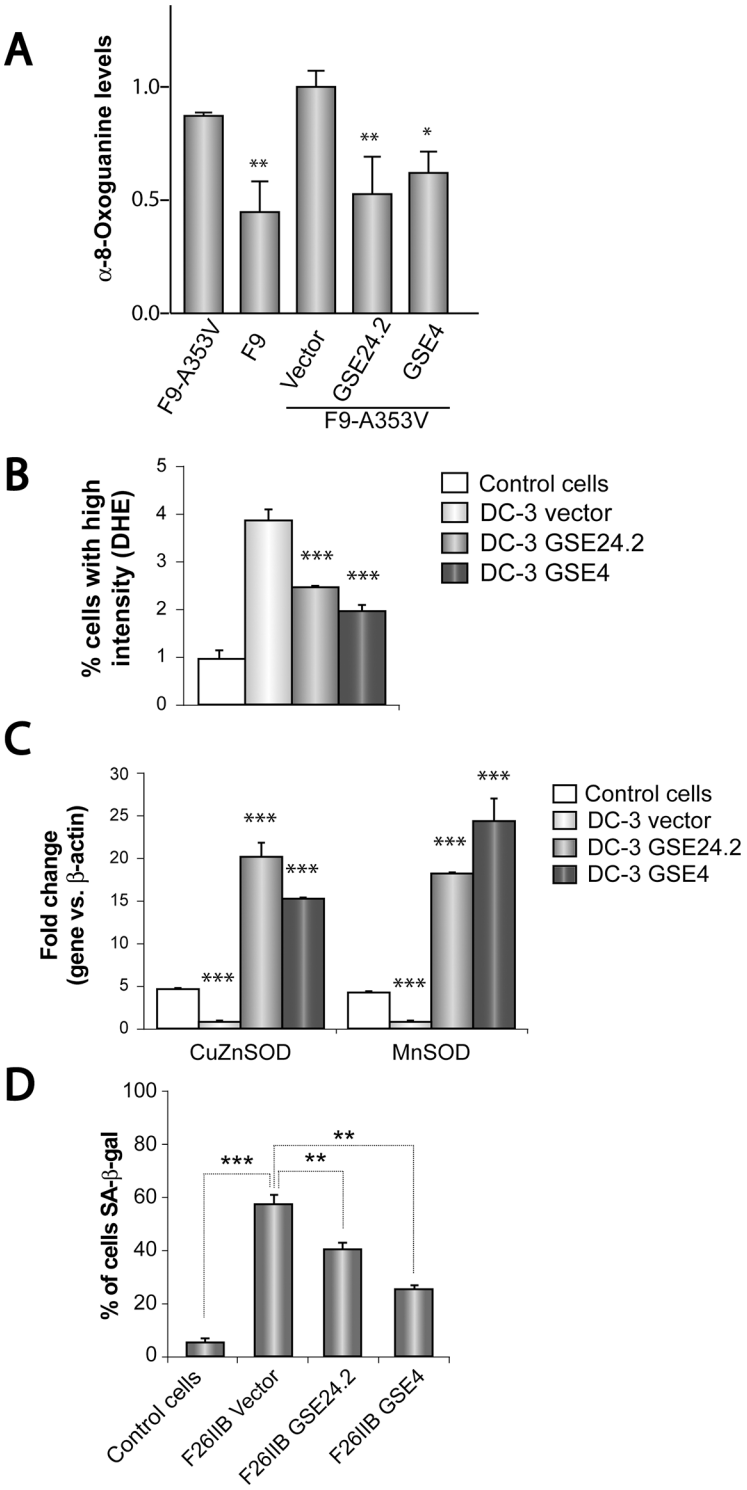

Fig 2. Effects of GSE24 and GSE4 peptides on oxidative stress and cell senescence. Panel A. F9-A353V cells were transfected with the pRRL-CMV-IRES-EGFP vector empty (Vector), expressing GSE24.2 (GSE24.2) or GSE4 (GSE4) (10 μg DNA per million cells). After 24 hours of transfection cells were fixed and incubated with an anti-α-8-Oxoguanine antibody. The amount of antibody bound was determined using a Zeiss Confocal microscope and quantified with the ImageJ program. Untransfected F9 and F9-A353V cells were used as controls. Average α-8-Oxoguanine expression and standard deviations are shown. Panel B. The amount of Reactive Oxygen Species (ROS) of control cells derived from healthy relative controls

(DC-C) and cells derived form a dyskeratosis congenita patient (DC-3) infected with the pRRL-CMV-IRES-EGFP vector, either empty (DC-3 vector) or expressing GSE24.2 (DC-3 GSE24.2) or GSE4 (DC-3 GSE4) was determined using dihydroethidium (DHE). The average percentage of cells with high intensity of DHE and standard deviation are represented. Panel C. Cells obtained from dyskeratosis congenita patients and healthy relatives were transfected as described in panel B. The expression of the mRNAs coding for Cu/Zn Superoxide dismutase (CuZnSOD) and Mn Superoxide dismutase (MnSOD) were determined by quantitative RT-PCR. Panel D. The presence of senescent cells in the cell cultures was determined by the assay of the β-Galactosidase activity using the X-Gal substrate. Fibroblasts obtained from a dyskeratosis congenita patient (F26IIB) were transfected as described above using the empty vector (F26IIB vector) or those expressing GSE24.2 (F26IIB GSE24.2) or GSE4 (F26IIB GSE4). Control cells isolated from a healthy relative (XDC-1787C) were used as control. The percentage of cells expressing β-Galactosidase activity (SA-β-gal) is represented for each cell line. Average values and standard deviations obtained from three different experiments are represented. Statistical significance: * $p<0.05$, ** $p<0.01$, *** $p<0.001$.

doi:10.1371/journal.pone.0142980.g002

3. Requirement of nuclear and nucleolar localization signals for GSE24.2 and GSE4 biological activity

Dyskerin is a nucleolar protein and different cellular localization regions have been described [28]. Two of them were analyzed because their deletion or mutation altered the subcellular localization of dyskerin [28]. The first one (KRKR, named NLS1 in this article) is required for nuclear import while the second one (KKEKKKSKK, NLS2) increases the rate of nuclear and nucleolar import. Since GSE24.2 does not contain any of these regions, both were independently incorporated to the C-terminal region of the peptide to determine their possible contribution to the cellular localization and activity of the peptide. We used plasmid expression vectors with an N-terminal 6xmyc epitope (pcDNA3-myc). Cellular localization was studied by immunohystochemistry using α-myc antibodies after their expression in HeLa cells (Fig 3A). In some of these experiments nucleoli were identified using the specific SYTO RNA Select probe (Fig 3A, lower panels). The results showed that NLS1 incorporation increased the nuclear localization of GSE24.2, with low expression in nucleoli. In contrast, NLS2 incorporation resulted in an even expression in all nuclear regions. NLS1 and NLS2 incorporation to the N terminal region of GSE24.2 did not change the cellular localization (S1 Fig).

The functionality of the fusion peptides was determined by expressing them from the pcDNA3-myc vector in F9-A353V, F9 and HEK293T cells. We have previously described that expression of GSE24.2 activated TERT and c-myc promoters [18] [29]. Therefore, we studied the activity of the different constructions on the human c-myc and TERT promoters (Fig 3B). Both GSE24.2 and GSE24.2-NLS1.3 activated c-myc and TERT promoters in the three cell lines analyzed to similar levels although some of the activity increases were not statistically significant in F9 cells. However, GSE24.2-NLS2.3 only activated the TERT promoter. The effects of GSE24.2-NLS2.3 on the c-myc promoter were variable, a significant increase was observed in HEK293T cells and a significant decrease in F9 cells. None of the localization signals improved the transcriptional activity of GSE24.2. The possible activity on DNA damage was also studied using F9-A353V cells. The amount of DNA damage was estimated by evaluating the expression levels of phosphorylated γH2AX and Chk2Thr68 proteins. Quantification of DNA damage was made by Western blot using anti γH2AX and p-Chk2Thr68 antibodies (Fig 3C). In addition, the localization of DNA damage foci was observed by immunohistochemistry, evaluating the amount of γH2AX-associated foci/cell (Fig 3D). GSE24.2 expression rescued the cells from DNA damage decreasing 40 and 30% respectively of γH2AX and p-Chk2 levels (Fig 3C), as previously described [20]. NLS1.3 incorporation did not alter GSE24.2 activity while addition of NLS2.3 partially impaired this activity (Fig 3C and 3D).

The nuclear localization signal NLS1 was also added to the C-terminus of GSE4 to determine their possible influence on the activity of the peptide. GSE4 is similar to the conserved

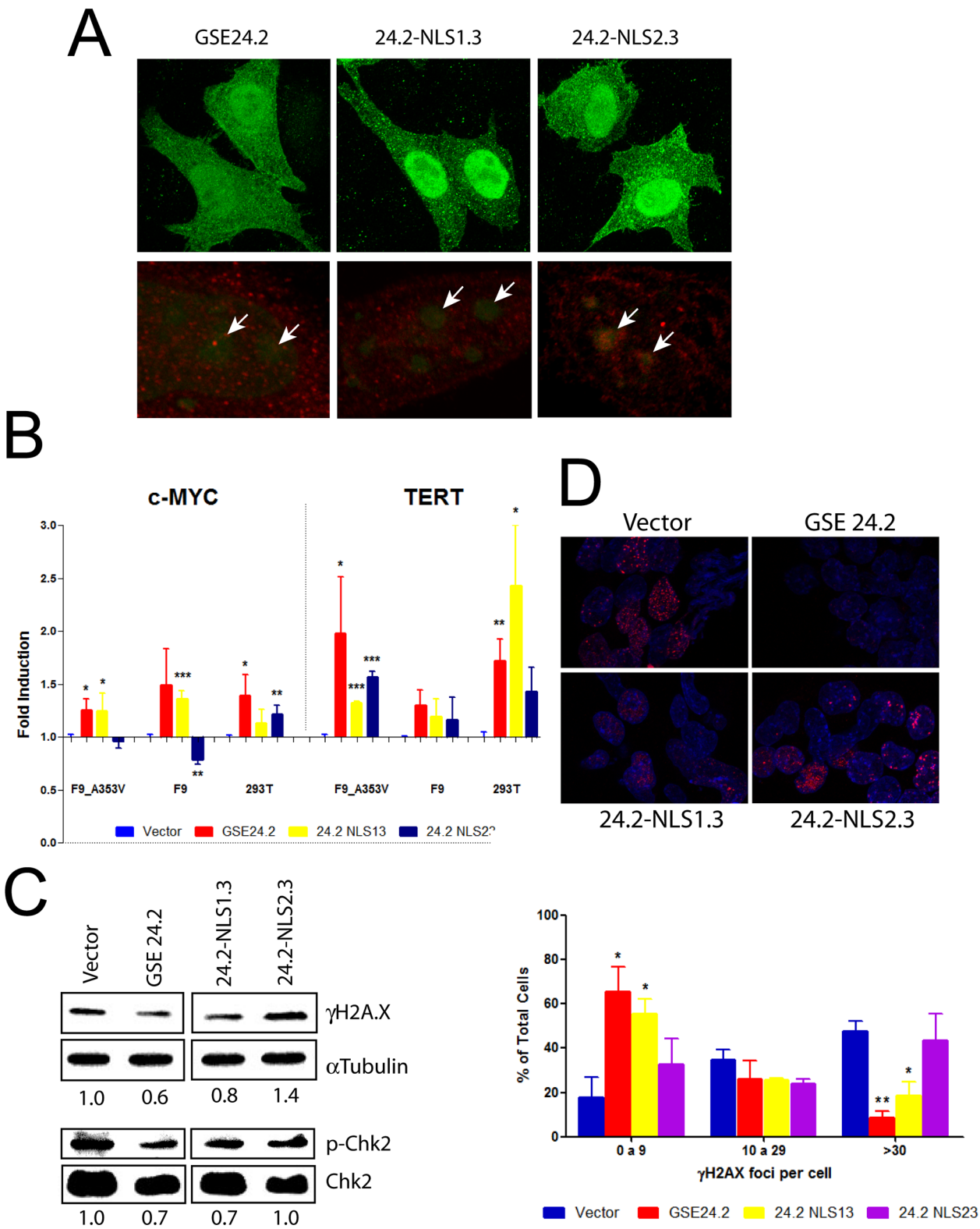

Fig 3. Functional analyses of GSE24.2-derived peptides containing nuclear localization signals. Panel A, cellular localization of the peptides. HeLa cells were transfected with pcDNA3 vectors expressing GSE24.2, GSE24.2-NLS1.3 and GSE24.2-NLS2.3 peptides fused to a N-terminal 6xmyc epitope, fixed, permeabilized and incubated with a c-myc antibody. Immunofluorescence staining of c-myc (green in top and red in the lower panels) was observed. Additionally, nucleoli were stained using 500 nM of the SYTO RNA Select Green (green in lower panels). Arrows indicate the position of nucleoli. Panel B,

effect of pcDNA3_GSE24.2, GSE24.2_NLS13 and GSE24.2_NLS23 on the activity of c-myc and TERT promoters in F9_A353V, F9 and 293T cells. These three cell lines were cotransfected with pcDNA3 empty vector (Vector), GSE24.2 and GSE24.2-derived constructions (10 μg DNA/10^6 cells) and c-myc-luc- or hTERT-luc -reporter vectors (1 μg/10^6 cells). Luciferase activity was measured following 24 hours of transfection. Data were normalized by protein concentration and referred to the empty vector. Data points represent the mean and standard deviations of 3 experiments performed in triplicate (statistical significance: * p<0.05, **p<0.01, ***p<0.001). Panels C, D, analyses of cellular DNA damage. (C) F9_A353V cells were transfected with the pRRL-CMV-IRES-EGFP empty vector (Vector), or expressing GSE24.2, GSE24.2-NLS13 and GSE24.2-NLS23 (10 μg DNA/10^6 cells). After 24 hours of transfection cells were lysed and the amount of γH2AX, α-tubulin (loading control), phosphorylated Chk2 (p-Chk2) and total Chk2 (Chk2) analyzed by western blot. The relative amounts of γH2AX/α-tubulin and p-Chk2/Chk2, normalized to the relation obtained for cells transfected with the empty vector, are indicated under each blot. (D) Upper panel. F9_A353V cells were transfected with the vectors indicated above and the presence of γH2AX analyzed by Immunofluorescence (red). Nuclear DNA was counterstained with DAPI (blue). Lower panel. Percentage of nuclei containing 0–9, 10–29 or more than 30 foci of γH2AX. More than 200 cells were analyzed for each transfection. Experiments were repeated 3 times with similar results. Asterisks indicate the statistical significance in relation to cells transfected with the empty vector (vector).

doi:10.1371/journal.pone.0142980.g003

pseudouridine synthase active centre of other enzymes, where the Aspartic acid homologous to the one present at position 6 in GSE4 is always conserved [30]. Therefore, this Aspartic acid was changed to Alanine to test its possible functional relevance. These different peptides were either chemically synthesized or expressed in the cells from plasmid or lentiviral vectors, as indicated in each specific experiment.

The cellular localization of the GSE4 and GSE4-NLS1 peptides was studied by transfecting fluorescein-labelled peptides into HeLa cells. Both peptides showed a predominant cytoplasmic localization, as shown in Fig 4A, although the incorporation of NLS1 increased the presence of the peptide in the perinuclear region. The biological activity of the peptides was determined by expressing them from the lentiviral vector pRRL-CMV-IRES-GFP in different cell lines. Transcriptional activity was determined by using the previously mentioned reporter vectors containing the human c-myc and TERT promoters. The results obtained in F9-A353V, F9 and HEK293T cells are shown in Fig 4B. GSE24.2 activity was also determined to further compare the activity of the diverse peptides. GSE4 and GSE4-NLS1 peptides showed similar capacity than GSE24.2 to activate c-myc and TERT promoters in the cell lines analyzed, including the F9-A353V mutant cells. In HEK293T cells GSE4 and GSE4-NLS1 peptides were more active than GSE24.2 but that was not the case in F9 and F9-A353V cells. The mutated GSE4-NLS1-DA peptide was also active in these assays, with the exception of the c-myc promoter in F9-A353V cells where the activity was actually decreased, indicating that this Aspartic acid residue is not required for GSE4 activity. The activity of GSE4-NLS1-DA was, however, lower than that of GSE24.2, GSE4 and GSE4-NLS1 in F9-A353V cells. The addition of the nuclear localization signal NLS1 to GSE4 resulted in increased TERT promoter activity in the three cell lines analyzed (Fig 4B).

The expression of c-myc and TERT mRNAs, and TERC (TR) RNA, in transfected F9-A353V cells was determined by Reverse Transcription and quantitative PCR (Fig 4C). The results obtained are in general agreement with the reporter expression analyses (Fig 4B). GSE24.2, GSE4 and GSE4-NLS1 induced c-myc, TERT and TERC (TR) expression while GSE4-NLS1-DA repressed the expression of these RNAs in F9-A353V cells. GSE4 was more efficient in inducing TERT and less efficient in inducing TERC (TR) than GSE24.2 and GSE4-NLS1 in these experiments.

The possible effect of the expression of GSE4 and derived peptides on DNA damage was also studied. F9-A353V cells were transfected with the expression vectors mentioned above. The amount of DNA damage in transfected cells was determined by quantification of γH2AX-associated foci/cell (Fig 5A and 5B). In addition, Western blot analyses allowed the quantification of γH2AX and p-Chk2Thr68 expression (Fig 5C). GSE4 and GSE4-NLS1 showed a protective effect on DNA damage similar to that of GSE24.2 in both assays. The mutant GSE4-NLS1-DA did not protect F9 A353V cells from DNA damage to the same extend under these experimental conditions. Altogether our results indicated that the functional activity of

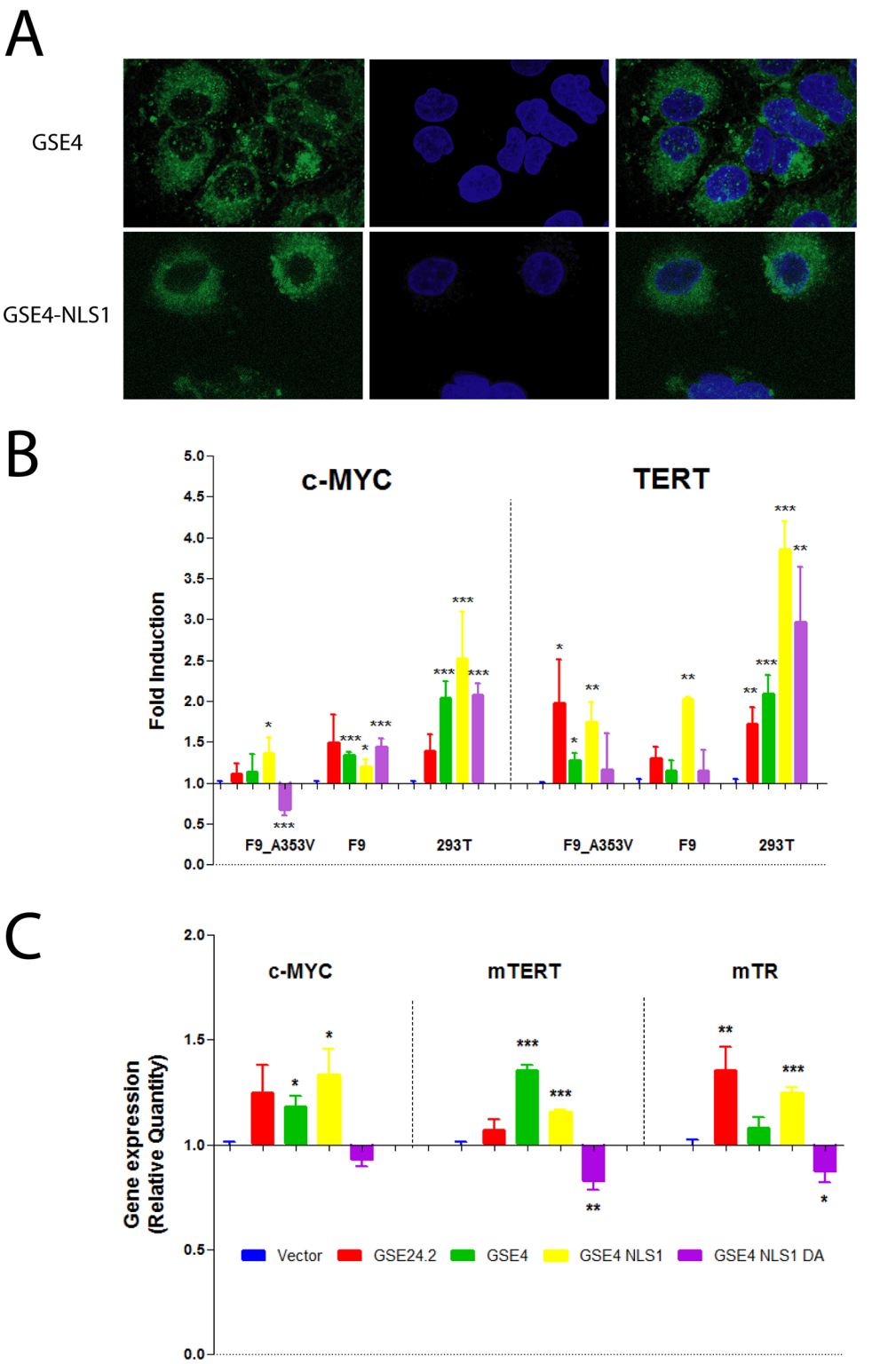

Fig 4. Cellular location and effect of GSE4 and derived peptides on promoter activity and gene expression. Panel A. HeLa cells were transfected with 15 μg of fluorescein-labelled GSE4 and GSE4_NLS1 peptides (green), fixed and visualized by confocal microscopy (left panels). DNA was counterstained with DAPI (blue, middle panels). Merged images are shown at the right panels. Panel B, promoter activity. F9-A353V, F9 and 293T cells were co-transfected with the pRRL-CMV-IRES-EGFP vector, either empty (Vector) or expressing the GSE24.2, GSE4, GSE4-NLSI or GSE4-NLS1-DA peptides (10 μg DNA/10^6 cells)

and c-myc-luc reporter or TERT-luc reporter vectors (1 μg/10^6 cells). Luciferase activity was measured 24 hours after transfection. Data were normalized by protein concentration and referred to the activity of the control vector. Data points represent the mean and standard deviations of 3 experiments performed in triplicate. Panel C, F9-A353V cells were transfected with vectors indicated on panel B. Total RNA was extracted 24 h later and the levels of c-myc, TERT and TR(TERC) expression determined by reverse transcription and quantitative PCR. Expression levels were normalized by β-actin expression and referred to the expression levels of the cells transfected with the empty vector (Vector). The data shown represent the mean and standard deviations of 3 experiments performed in triplicate. Statistical significance: * $p<0.05$, ** $p<0.01$, *** $p<0.001$.

doi:10.1371/journal.pone.0142980.g004

GSE4 peptide was similar to that GSE24.2 in all the biological assays performed in dyskeratosis congenita cells. Besides the addition of nuclear locations signals did not significantly increase the transcriptional activity of these peptides or their protection to DNA damage. In addition, the GSE4 Aspartic acid residue conserved in the pseudouridine synthase active centre of other enzymes, although not essential, is required for maximal activity of the peptide on dyskerin-mutant cells.

Discussion

Telomere biology disorders, including dyskeratosis congenita, are characterized by the progressive shortening of the telomeres and by a number of cellular responses. In particular, telomere shortening and/or low telomerase activity induces in the cells a DNA damage response [31], and oxidative stress [32]. Therefore, the p53-dependent DNA damage response pathway is activated resulting in cell cycle arrest and cellular senescence [33, 34]. These responses have an important contribution to the pathology of the diseases through the deprivation of stem cells in the more proliferative tissues. We describe in this article that a dyskerin-derived peptide of eleven amino acids (GSE4) increases telomerase activity and decreases oxidative stress and the DNA damage response in cellular models of dyskeratosis congenita. Expression of GSE4 also regulates the global response of dyskeratosis congenita cells, increasing cell proliferation and reducing cellular senescence. A fibroblastoid cell line derived from a patient carrying the Ala2-Val mutation in dkc1(patient 26 in ref [26]) was used for these studies.

The results described in the present article confirm those previously shown for the 55 amino acids long fragment of dyskerin, GSE24.2, that contains GSE4. GSE24.2 increases telomerase activity and decreases oxidative stress and the DNA damage response in dyskeratosis congenita patient cells [18, 19]. In addition, GSE4 protects F9-A353V dyskerin-mutant mouse cells from DNA damage and reduces oxidative stress, also as GSE24.2 [20]. Furthermore, we show in this article that GSE24.2 also increases cell proliferation and decreases cell senescence, which had not been reported previously. Therefore, we show that GSE4 presents the same biological activity than the longer peptide GSE24.2, which has been approved as an orphan drug for the treatment of dyskeratosis congenita. However, GSE4 presents some advantages over GSE24.2, derived from its smaller size. One of them is the lower cost of chemical synthesis. In addition, it could be easier to deliver into the cells. It would be also easier to develop variants that could have improved pharmaceutical characteristics.

The data presented also provide information about the mechanisms of action of these peptides. GSE4 increases telomerase activity in DKC1-mutated F9-A353V cells, increases expression of c-myc and the TERT and TERC telomerase components and the activity of TERT and c-myc promoters, as previously reported for GSE24.2 [19]. The activity of the TERT promoter has been shown to be higher in cancer cell lines than in transformed cells lines similar to those used in the present study [35] therefore, the possible effects of GSE4 on TERT expression in tumour cells should be tested in future studies. The structural studies indicate that GSE24.2

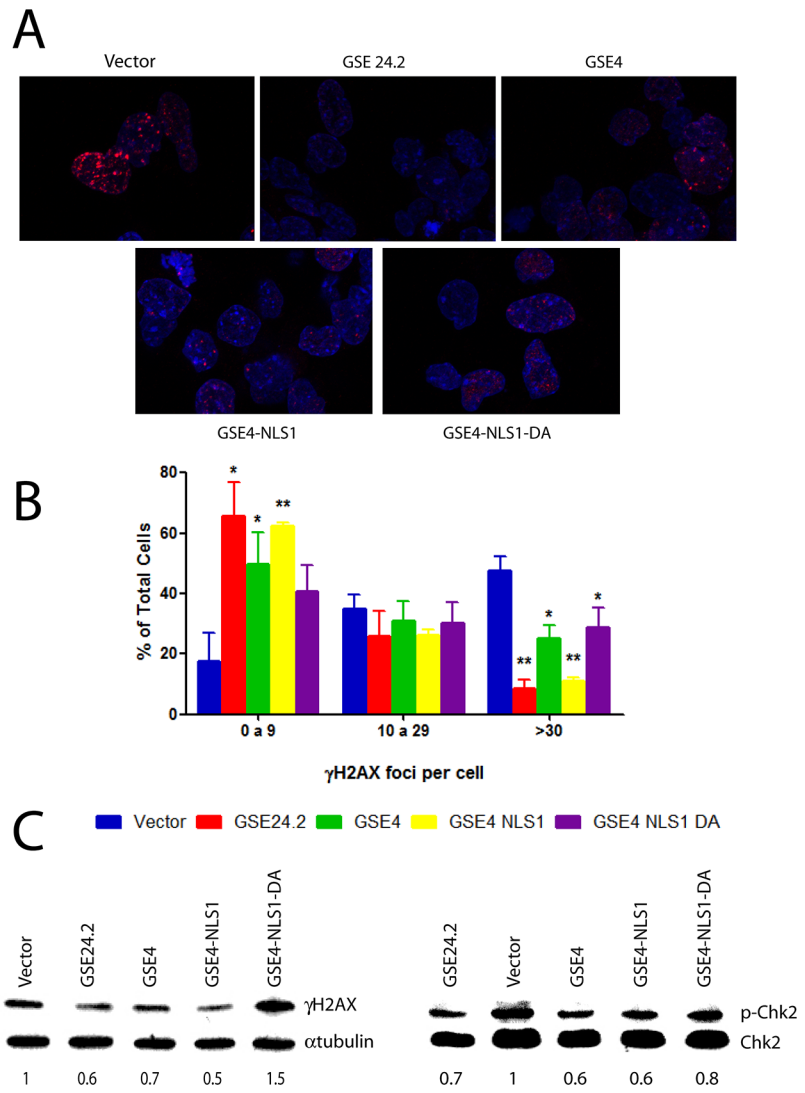

Fig 5. DNA damage protection by the expression of GSE4 and derived peptides. Panel A, F9-A353V cells were transfected with the pRRL-CMV-IRES-EGFP vector, either empty (vector), or expressing GSE24.2, GSE4, GSE4-NLS1 or GSE4_NLS1-DA (10 μg DNA/10^6 cells). After 24 hours of transfection cells were fixed and incubated with anti γH2AX and a red-labeled secondary antibody. Nuclear DNA was counterstained with DAPI (blue). Panel B, the amount of γH2AX-expressing foci shown on panel A was determined. The percentage of cells containing 0 to 9, 10 to 29 or more than 30 foci is indicated. More than 200 cells were analyzed in each cell line. Experiments were repeated 3 times with similar results. Panel C, F9_A353V cells were transfected with the plasmids indicated on panel A. Twenty four hours after transfection cells were lysed and the expression of γH2AX, α-tubulin (loading control)(left panel) phosphorylated Chk2 (p-Chk2) and total Chk2 (Chk2)(right panel) analyzed by western blot. Numbers under each blot indicate the relative γH2AX/α-tubulin and p-Chk2/Chk2 expression normalized in relation to cells transfected with the empty vector (statistical significance: * p<0.05, **p<0.01, ***p<0.001).

doi:10.1371/journal.pone.0142980.g005

and GSE4 do not require nuclear localization signals for activity. The incorporation of nuclear or nucleolar localization signals to GSE24.2 increase nuclear or nucleolar localization but the transcriptional activity of the peptide and the protective role on DNA damage are not increased. Actually, the incorporation of the nucleolar localization signal NLS2 decreases GSE24.2 activity. The GSE4 peptide containing a nuclear localization signals (GSE4-NLS1) also show a biological activity similar to that of GSE4. These observations do not discard a

nuclear function for GSE24.2 or GSE4 since the localization experiments indicate that GSE24.2 and GSE4, at a lower extend, are present both at the nucleus and the cytoplasm in the absence of nuclear localization signals, probably due to their small size.

Expression of GSE24.2 and GSE4 produces biological effects on several cell types expressing either Wild type or mutated dyskerin indicating that these peptides do not just complement dyskerin mutations. They seem to play several roles in the cell. It would be interesting to determine if there is a common mechanism for these activities or not. The data reported in this article indicate that some peptide variants differ in their activities depending on the assay and/or cell type studied. For example, GSE24.2-NLS2.3 activates TERT promoter at the same extend as GSE24.2 and GSE24.2-NLS1.3 but is less effective on c-myc promoter activation and on the protection of F9 A353V basal DNA damage. In the same sense, the GSE4-NLS1-DA variant increases transcriptional activity in F9 and HEK293T cells but is not active in the dyskerin-mutated F9-A353V cells neither in transcription activation nor in basal DNA damage protection. These data could indicate that these peptides participate in different cellular processes through different mechanisms. Some of the variant studied, like GSE4-NLS1-DA could require the presence of Wild-type dyskerin for some of their activities but other variants and the unmodified GSE24.2 and GSE4 peptides do not seem to be dependent on dyskerin for any of their biological activities.

In summary, the eleven amino acids long GSE4 peptide shows a protective effect on dyskerin mutated cells similar to the one previously shown for GSE24.2. Protection is mediated by increased telomerase activity and cell proliferation but also by decreased oxidative stress, DNA damage and cell senescence. These properties make of GSE4 a good candidate as a drug for dyskeratosis congenita treatment with some practical advantages over the already approved GSE24.2 peptide.

Supporting Information

S1 Fig. Cellular localization of the GSE24.2 peptide containing nuclear localization signals at the N-terminal region. pcDNA3 vectors were generated coding for the GSE24.2 peptide fused to the NLS1 nuclear localization signal (KRKR) or the NLS2 signal (KKEKKKSKK) fused to the N-terminal region, named 24.2-NLS1-5 and 24.2-NLS2.5 respectively. The nuclear localization signals were placed between the N-terminal 6xmyc epitope and the GSE24.2 peptide in the proteins expressed from these vectors. HeLa cells were transformed with the pcDNA3 vectors expressing GSE24.2, 24.2-NLS1.5 and 24.2-NLS2.5, fixed, permeabilized and incubated with a c-myc antibody. Immunofluorescence staining was observed after incubation of the preparations with a secondary antibody conjugated with Alexa fluor 488 using a Nikon 90i microscope. (PDF)

Acknowledgments

This work was supported by grants PI1401495 (supported by FEDER funds) and ER15PR07ACC114/757 (Fondo de Investigaciones Sanitarias, Instituto de Salud Carlos III. Spain), 201320E075 (Consejo Superior de Investigaciones Científicas) and IPT-2012-0674-090000 (Ministerio de Economía y Competitividad. Spain). CM-G is supported by the CIBER de Enfermedades Raras.

Author Contributions

Conceived and designed the experiments: LI RP LS. Performed the experiments: LI CM-G LP-B. Analyzed the data: LI JMM AM RP LS. Wrote the paper: LI RP LS.

References

1. Savage SA. Human telomeres and telomere biology disorders. Prog Mol Biol Transl Sci. 2014; 125:41–66. Epub 2014/07/06. B978-0-12-397898-1.00002–5 [pii]. doi: 10.1016/B978-0-12-397898-1.00002-5 PMID: 24993697.
2. Meyne J, Ratliff RL, Moyzis RK. Conservation of the human telomere sequence (TTAGGG)n among vertebrates. Proc Natl Acad Sci U S A. 1989; 86(18):7049–53. Epub 1989/09/01. PMID: 2780561.
3. de Lange T, Shiue L, Myers RM, Cox DR, Naylor SL, Killery AM, et al. Structure and variability of human chromosome ends. Mol Cell Biol. 1990; 10(2):518–27. Epub 1990/02/01. PMID: 2300052.
4. Greider CW, Blackburn EH. Identification of a specific telomere terminal transferase activity in Tetrahymena extracts. Cell. 1985; 43(2 Pt 1):405–13. Epub 1985/12/01. 0092-8674(85)90170-9 [pii]. PMID: 3907856.
5. Blackburn EH. Telomeres and telomerase: their mechanisms of action and the effects of altering their functions. FEBS Lett. 2005; 579(4):859–62. Epub 2005/02/01. S0014-5793(04)01426-7 [pii]. doi: 10.1016/j.febslet.2004.11.036 PMID: 15680963.
6. Cohen SB, Graham ME, Lovrecz GO, Bache N, Robinson PJ, Reddel RR. Protein composition of catalytically active human telomerase from immortal cells. Science. 2007; 315(5820):1850–3. Epub 2007/03/31. 315/5820/1850 [pii]. doi: 10.1126/science.1138596 PMID: 17395830.
7. Angrisani A, Vicidomini R, Turano M, Furia M. Human dyskerin: beyond telomeres. Biol Chem. 2014; 395(6):593–610. Epub 2014/01/29. doi: 10.1515/hsz-2013-0287 /j/bchm.just-accepted/hsz-2013-0287/hsz-2013-0287.xml [pii]. PMID: 24468621.
8. Kiss T, Fayet E, Jady BE, Richard P, Weber M. Biogenesis and intranuclear trafficking of human box C/D and H/ACA RNPs. Cold Spring Harb Symp Quant Biol. 2006; 71:407–17. Epub 2007/03/27. doi: 10.1101/sqb.2006.71.025 PMID: 17381323.
9. Wright WE, Tesmer VM, Huffman KE, Levene SD, Shay JW. Normal human chromosomes have long G-rich telomeric overhangs at one end. Genes Dev. 1997; 11(21):2801–9. Epub 1997/11/14. PMID: 9353250.
10. Palm W, de Lange T. How shelterin protects mammalian telomeres. Annu Rev Genet. 2008; 42:301–34. Epub 2008/08/06. doi: 10.1146/annurev.genet.41.110306.130350 PMID: 18680434.
11. Zou Y, Sfeir A, Gryaznov SM, Shay JW, Wright WE. Does a sentinel or a subset of short telomeres determine replicative senescence? Mol Biol Cell. 2004; 15(8):3709–18. Epub 2004/06/08. doi: 10.1091/mbc.E04-03-0207 E04-03-0207 [pii]. PMID: 15181152.
12. Glousker G, Touzot F, Revy P, Tzfati Y, Savage SA. Unraveling the pathogenesis of Hoyeraal-Hreidarsson syndrome, a complex telomere biology disorder. Br J Haematol. 2015. Epub 2015/05/06. PMID: 25940403.
13. Dokal I. Dyskeratosis congenita in all its forms. Br J Haematol. 2000; 110(4):768–79. Epub 2000/10/29. bjh2109 [pii]. PMID: 11054058.
14. Ge J, Yu YT. RNA pseudouridylation: new insights into an old modification. Trends Biochem Sci. 2013; 38(4):210–8. Epub 2013/02/09. S0968-0004(13)00003-0 [pii]. doi: 10.1016/j.tibs.2013.01.002 PMID: 23391857.
15. Schwartz S, Bernstein DA, Mumbach MR, Jovanovic M, Herbst RH, Leon-Ricardo BX, et al. Transcriptome-wide Mapping Reveals Widespread Dynamic-Regulated Pseudouridylation of ncRNA and mRNA. Cell. 2014; 159(1):148–62. Epub 2014/09/16. S0092-8674(14)01098-8 [pii]. doi: 10.1016/j.cell.2014.08.028 PMID: 25219674.
16. Carlile TM, Rojas-Duran MF, Zinshteyn B, Shin H, Bartoli KM, Gilbert WV. Pseudouridine profiling reveals regulated mRNA pseudouridylation in yeast and human cells. Nature. 2014. Epub 2014/09/06. nature13802 [pii]. doi: 10.1038/nature13802 PMID: 25192136.
17. Mason PJ, Bessler M. The genetics of dyskeratosis congenita. Cancer Genet. 2011; 204(12):635–45. Epub 2012/01/31. S2210-7762(11)00308-5 [pii]. doi: 10.1016/j.cancergen.2011.11.002 PMID: 22285015.
18. Machado-Pinilla R, Sanchez-Perez I, Murguia JR, Sastre L, Perona R. A dyskerin motif reactivates telomerase activity in X-linked dyskeratosis congenita and in telomerase-deficient human cells. Blood. 2008; 111(5):2606–14. Epub 2007/12/07. blood-2007-04-083261 [pii]. doi: 10.1182/blood-2007-04-083261 PMID: 18057229.
19. Machado-Pinilla R, Carrillo J, Manguan-Garcia C, Sastre L, Mentzer A, Gu BW, et al. Defects in mTR stability and telomerase activity produced by the Dkc1 A353V mutation in dyskeratosis congenita are rescued by a peptide from the dyskerin TruB domain. Clin Transl Oncol. 2012; 14(10):755–63. Epub 2012/08/03. doi: 10.1007/s12094-012-0865-4 PMID: 22855157.
20. Manguan-Garcia C, Pintado-Berninches L, Carrillo J, Machado-Pinilla R, Sastre L, Perez-Quilis C, et al. Expression of the Genetic Suppressor Element 24.2 (GSE24.2) Decreases DNA Damage and

Oxidative Stress in X-Linked Dyskeratosis Congenita Cells. PLoS One. 2014; 9(7):e101424. Epub 2014/07/06. doi: 10.1371/journal.pone.0101424 PONE-D-14-06623 [pii]. PMID: 24987982.

21. Mochizuki Y, He J, Kulkarni S, Bessler M, Mason PJ. Mouse dyskerin mutations affect accumulation of telomerase RNA and small nucleolar RNA, telomerase activity, and ribosomal RNA processing. Proc Natl Acad Sci U S A. 2004; 101(29):10756–61. Epub 2004/07/09. doi: 10.1073/pnas.0402560101 0402560101 [pii]. PMID: 15240872.

22. Oh S, Song YH, Kim UJ, Yim J, Kim TK. In vivo and in vitro analyses of Myc for differential promoter activities of the human telomerase (hTERT) gene in normal and tumor cells. Biochem Biophys Res Commun. 1999; 263(2):361–5. Epub 1999/09/24. doi: 10.1006/bbrc.1999.1366 S0006-291X(99) 91366-9 [pii]. PMID: 10491298.

23. Wright WE, Shay JW, Piatyszek MA. Modifications of a telomeric repeat amplification protocol (TRAP) result in increased reliability, linearity and sensitivity. Nucleic Acids Res. 1995; 23(18):3794–5. Epub 1995/09/25. l50206 [pii]. PMID: 7479015.

24. Sanchez-Perez I, Murguia JR, Perona R. Cisplatin induces a persistent activation of JNK that is related to cell death. Oncogene. 1998; 16(4):533–40. Epub 1998/03/04. doi: 10.1038/sj.onc.1201578 PMID: 9484843.

25. Giulietti A, Overbergh L, Valckx D, Decallonne B, Bouillon R, Mathieu C. An overview of real-time quantitative PCR: applications to quantify cytokine gene expression. Methods. 2001; 25(4):386–401. Epub 2002/02/16. doi: 10.1006/meth.2001.1261 S1046-2023(01)91261-7 [pii]. PMID: 11846608.

26. Carrillo J, Martinez P, Solera J, Moratilla C, Gonzalez A, Manguan-Garcia C, et al. High resolution melting analysis for the identification of novel mutations in DKC1 and TERT genes in patients with dyskeratosis congenita. Blood Cells Mol Dis. 2012; 49(3–4):140–6. Epub 2012/06/06. S1079-9796(12)00119-2 [pii]. doi: 10.1016/j.bcmd.2012.05.008 PMID: 22664374.

27. Blasco MA, Lee HW, Hande MP, Samper E, Lansdorp PM, DePinho RA, et al. Telomere shortening and tumor formation by mouse cells lacking telomerase RNA. Cell. 1997; 91(1):25–34. Epub 1997/10/23. S0092-8674(01)80006-4 [pii]. PMID: 9335332.

28. Heiss NS, Girod A, Salowsky R, Wiemann S, Pepperkok R, Poustka A. Dyskerin localizes to the nucleolus and its mislocalization is unlikely to play a role in the pathogenesis of dyskeratosis congenita. Hum Mol Genet. 1999; 8(13):2515–24. Epub 1999/11/11. ddc279 [pii]. PMID: 10556300.

29. Carrillo J, Gonzalez A, Manguan-Garcia C, Pintado-Berninches L, Perona R. p53 pathway activation by telomere attrition in X-DC primary fibroblasts occurs in the absence of ribosome biogenesis failure and as a consequence of DNA damage. Clin Transl Oncol. 2013; 16(6):529–38. Epub 2013/09/26. doi: 10.1007/s12094-013-1112-3 PMID: 24065372.

30. Hamma T, Ferre-D'Amare AR. Pseudouridine synthases. Chem Biol. 2006; 13(11):1125–35. Epub 2006/11/23. S1074-5521(06)00342-5 [pii]. doi: 10.1016/j.chembiol.2006.09.009 PMID: 17113994.

31. Gu BW, Bessler M, Mason PJ. A pathogenic dyskerin mutation impairs proliferation and activates a DNA damage response independent of telomere length in mice. Proc Natl Acad Sci U S A. 2008; 105 (29):10173–8. Epub 2008/07/16. 0803559105 [pii]. doi: 10.1073/pnas.0803559105 PMID: 18626023.

32. Gu BW, Fan JM, Bessler M, Mason PJ. Accelerated hematopoietic stem cell aging in a mouse model of dyskeratosis congenita responds to antioxidant treatment. Aging Cell. 2011; 10(2):338–48. Epub 2011/01/19. doi: 10.1111/j.1474-9726.2011.00674.x PMID: 21241452.

33. Cesare AJ, Karlseder J. A three-state model of telomere control over human proliferative boundaries. Curr Opin Cell Biol. 2012; 24(6):731–8. Epub 2012/09/06. S0955-0674(12)00132-9 [pii]. doi: 10.1016/j.ceb.2012.08.007 PMID: 22947495.

34. Alder JK, Barkauskas CE, Limjunyawong N, Stanley SE, Kembou F, Tuder RM, et al. Telomere dysfunction causes alveolar stem cell failure. Proc Natl Acad Sci U S A. 2015; 112(16):5099–104. Epub 2015/04/05. 1504780112 [pii]. doi: 10.1073/pnas.1504780112 PMID: 25840590.

35. Si SY, Song SJ, Zhang JZ, Liu JL, Liang S, Feng K, et al. Cloning of mouse telomerase reverse transcriptase gene promoter and identification of proximal core promoter sequences essential for the expression of transgenes in cancer cells. Oncol Rep. 2011; 26(2):377–82. Epub 2011/05/14. doi: 10.3892/or.2011.1303 PMID: 21567104.

OPEN ACCESS Freely available online

PLOS ONE

Expression of the Genetic Suppressor Element 24.2 (GSE24.2) Decreases DNA Damage and Oxidative Stress in X-Linked Dyskeratosis Congenita Cells

Cristina Manguan-Garcia[1,2], Laura Pintado-Berninches[1], Jaime Carrillo[1], Rosario Machado-Pinilla[1,2], Leandro Sastre[1,2], Carme Pérez-Quilis[3,4], Isabel Esmoris[3,4], Amparo Gimeno[3,4], Jose Luis García-Giménez[2,3,4], Federico V. Pallardó[2,3,4], Rosario Perona[1,2]*

1 Instituto de Investigaciones Biomédicas CSIC/UAM, Madrid, Spain, **2** CIBER de Enfermedades Raras, Valencia, Spain, **3** Biomedical Research Institute INCLIVA, Valencia, Spain, **4** Department of Physiology, Faculty of Medicine and Dentistry, University of Valencia, Valencia, Spain

Abstract

The predominant X-linked form of Dyskeratosis congenita results from mutations in *DKC1*, which encodes dyskerin, a protein required for ribosomal RNA modification that is also a component of the telomerase complex. We have previously found that expression of an internal fragment of dyskerin (GSE24.2) rescues telomerase activity in X-linked dyskeratosis congenita (X-DC) patient cells. Here we have found that an increased basal and induced DNA damage response occurred in X-DC cells in comparison with normal cells. DNA damage that is also localized in telomeres results in increased heterochromatin formation and senescence. Expression of a cDNA coding for GSE24.2 rescues both global and telomeric DNA damage. Furthermore, transfection of bacterial purified or a chemically synthesized GSE24.2 peptide is able to rescue basal DNA damage in X-DC cells. We have also observed an increase in oxidative stress in X-DC cells and expression of GSE24.2 was able to diminish it. Altogether our data indicated that supplying GSE24.2, either from a cDNA vector or as a peptide reduces the pathogenic effects of Dkc1 mutations and suggests a novel therapeutic approach.

Citation: Manguan-Garcia C, Pintado-Berninches L, Carrillo J, Machado-Pinilla R, Sastre L, et al. (2014) Expression of the Genetic Suppressor Element 24.2 (GSE24.2) Decreases DNA Damage and Oxidative Stress in X-Linked Dyskeratosis Congenita Cells. PLoS ONE 9(7): e101424. doi:10.1371/journal.pone.0101424

Editor: Gabriele Saretzki, University of Newcastle, United Kingdom

Received February 13, 2014; **Accepted** June 6, 2014; **Published** July 2, 2014

Funding: This work was supported by grants: PI11-0949 and PI12/02263 FIS, SAF2008-01338 from the Ministerio de Ciencia e Innovación. Grants, PROMETEO2010/074 from Generalitat Valenciana and Fundación Salud 2000 to FVP. CMG, JLGG and CPQ are supported by CIBER de Enfermedades Raras. The funders had no role in study design, data collection and analysis, decision to publish, or preparation of the manuscript.

Competing Interests: The authors have declared that no competing interests exist.

* Email: RPerona@iib.uam.es

Introduction

Telomeres are nucleoprotein complexes located at the ends of linear chromosomes and consist of tandem repeats of simple DNA sequences (TTAGGG in humans) and proteins that interact directly or indirectly with these sequences [1]. Sequence erosion of terminal repeats is inherent to each round of genome replication. The replenishment of the telomeric repeats is accomplished by the extension of their 3′ ends, through a reaction mediated by the telomerase complex [2]. In humans, the active telomerase complex consists of a minimum of three essential components: hTERT, hTR and dyskerin [3]. Besides forming part of the telomerase complex, dyskerin is a pseudouridine synthase component of H/ACA small nuclear RNPs [4], complexes that mediate the conversion of specific uridines (U) to pseudouridine in newly synthesized ribosomal RNAs [5] [6] [7]. Point mutations in dyskerin cause a rare disease named X-linked dyskeratosis congenita (X-DC) [8]. Individuals with X-DC display features of premature ageing, as well as nail dystrophy, mucosal leukoplakia, interstitial fibrosis of the lung and increased susceptibility to cancer [9]. The tissues affected by X-DC, such as bone marrow and skin, are characterized by the high rate of turnover of their progenitor cells.

Telomere shortening prevents the formation of the loop-like structure maintained by a nucleoprotein structure consisting of telomeric DNA and 6 proteins that are together known as shelterin [1]. This capping structure prevents the otherwise exposed ends of different chromosomes from being recognized as double strand breaks (DSBs) by the cell's DNA repair machinery which would result in telomere fusion. When telomeres become critically short or unprotected because of shelterin deficiency, they trigger a DNA damage response (DDR), leading to the activation of an ataxia telangiectasia mutated (ATM) or ataxia telangiectasia and Rad3 related (ATR)-dependent DNA damage response at chromosome ends [10] [11] [12] [13]. 53BP1 is a C-non-homologous-end-joining (C-NHEJ) component and an ATM target that accumulates at DSBs and uncapped telomeres [14] [15]. The binding of 53BP1 close to DNA breaks impacts the dynamic behavior of the local chromatin and facilitates the non-homologous-end-joining (NHEJ) repair reactions that involve distant sites [16]. ATM phosphorylates Chk2 leading to activation of cell cycle checkpoints. Chk2 acts as a signal distributor, dispersing checkpoint signal to downstream targets such as p53, Cdc25A, Cdc25C, BRCA1 and E2F1 [17].

Senescence, initially described as stable cell proliferation arrest, can be induced by telomere shortening and also by activated oncogenes, DNA damage and drug-like inhibitors of specific

enzymatic activities [18]. Senescent cells are typically characterized by a large flat morphology and the expression of a senescence-associated-β-galactosidase (SA-β-gal) activity of unknown function. In the nucleus of senescent cells chromatin undergoes dramatic remodeling through the formation of domains of heterochromatin called senescence-associated heterochromatin-foci (SAHF). SAHF contain histone modifications and proteins characteristic of silent heterochromatin such as methylated lysine 9 of histone H3 (H3K9me), heterochromatin protein 1 (HP1), and the histone H2A variant macroH2A.1 [18] [19]. Proliferation-promoting genes such as E2F-target genes (e.g. cyclin A) are recruited into SAHF, dependent on the pRB suppressor protein, thereby irreversibly silencing expression of those genes.

In cultured cells and animal models, telomere erosion promotes chromosomal instability via breakage-fusion-bridge cycles, contributing to the early stages of tumorigenesis. Telomere shortening in Dyskeratosis congenita is associated with a higher risk of some types of cancer such as head and neck squamous cell carcinoma (HNSCC) (mostly tongue), skin squamous cell carcinoma (SCC), anogenital, stomach, esophagus, and lymphomas, as well as myelodysplastic syndrome (MDS) [20] [21] [22] [23]. Altogether, these findings provide direct clinical evidence that short telomeres in hematopoietic cells are dysfunctional, mediate chromosomal instability and predispose to malignant transformation in a human disease.

We previously isolated the peptide GSE24.2, in a screen of cDNAs for those that confer survival ability on cells treated with cisplatin [24]. Intriguingly GSE24.2 turned out to be a short dyskerin fragment containing two highly conserved motifs implicated in pseudouridine synthase catalytic activity. GSE24.2 prevents telomerase inhibition mediated by different chemotherapeutic agents, including cisplatin and telomerase inhibitors. In X-DC cells and WI-38-VA13 cells, GSE24.2 induces an increase in hTERT mRNA levels and the recovery of telomerase activity [24]. Mutations in DKC1 lead to severe destabilization of telomerase RNA (TR), a reduction in telomerase activity and a significant continuous loss of telomere length during growth [25]. When a peptide encoding GSE24.2, was introduced into mutant cells, it rescued telomerase activity and prevented the decrease in TR levels induced by the Dkc1 mutation [26] GSE24.2 was recently approved as an orphan drug for the treatment of Dyskeratosis congenita (EU/3/12/1070 - EMA/OD/136/11).

To obtain more information on the biological activity of this dyskerin fragment we studied its effect on the DNA damage pathway in patient derived X-DC cells and a mouse F9 cell line carrying the A353V mutation in the *Dkc1* gene [26]. This is the mutation most frequently found in patients with X-DC (about 40% of patients) [27] [28] and is localized in the PUA RNA binding domain, the putative site for interaction with hTR. Recently, it has been described that mouse ES cells expressing a small dyskerin deletion, removing exon 15 of *Dkc1*, additionally showed decreased proliferative rate and increased sensitivity to DNA damage [29] that was independent on telomere length suggesting that decreased telomerase activity induced by the mutation in *Dkc1* resulted in induction of DNA damage probably by extratelomeric activity of *Dkc1* gene. Therefore the use of a mouse F9A353V model would allow study the effect of GSE24.2 directly on DNA damage, independently of telomeric elongation. Here we show that human X-DC cells showed both basal DNA damage foci and phosphorylation of ATM and CHK2 together with increased content of heterochromatin. Expression of the GSE24.2 was able to reduce DNA damage in X-DC patient and F9 X-DC mouse cell line models, by decreasing the formation of DNA damage foci. Finally, we also report that expression of GSE24.2 decreases oxidative stress in X-DC patient cells and that may result in reduced DNA damage. These data support the contention that expression of GSE24.2, or related products, could prolong the lifespan of dyskeratosis congenita cells.

Materials and Methods

Cell lines and constructs

Dermal fibroblasts from a control proband (X-DC-1787-C) and two X-DC patients (X-DC-1774-P and X-DC3) were obtained from Coriell Cell Repository. GSE24.2, DKC, motif I and motif II were cloned as previously described in the pLXCN vector [24]. PGATEV protein expression plasmid [30] was obtained from Dr. G. Montoya. PGATEV-GSE24.2 was obtained by subcloning the GSE24.2 fragment into the NdeI/XhoI sites of the pGATEV plasmid as previously described [24].

F9 cells and F9 cells transfected with A353V targeting vector were previously described [31] [26]. F9A353V cells were cultured in Dulbecco modified Eagle medium (DMEM) 10% fetal bovine serum, 2 mM glutamine (Gibco) and Sodium bicarbonate (1,5 gr/ml).

Cell transfection and analysis of gene expression

F9 cells were transfected with 16 μg of DNA/10^6 cells, using lipofectamine plus (Invitrogen, Carlsbad, USA), according to the manufacturer's instructions. Peptides transfection was performed by using the Transport Protein Delivery Reagent (50568; Lonza, Walkersville, USA) transfection kit. Routinely from 6 to 15 μg were used per 30 mm dish.

Antibodies. The source of antibodies was as follow: phospho-Histone H2A.X Ser139 (2577; Cell Signaling), phospho-Histone H2A.X Ser139 clone JBW301 (05-636; Millipore), macroH2A.1 (ab37264; abcam), 53BP1 (4937; Cell Signaling), anti-ATM Protein Kinase S1981P (200-301-400; Rockland), phospho-Chk2-Thr68 (2661; Cell Signaling), Monoclonal Anti-α-tubulin (T9026; Sigma-Aldrich), Anti-8-Oxoguanine Antibody, clone 483.15 (MAB3560, Merck-Millipore). Fluorescent antibodies were conjugated with Alexa fluor 488 (A11029 and A11034, Molecular Probes) and Alexa fluor 647 (A21236, Molecular Probes, Carlsbad, USA)).

Immunofluorescence and Fluorescence in situ hybridization (FISH) for telomeres

Protein localization was carried out by fluorescence microscopy. For this purpose, cells were grown on coverslips, transfected and fixed in 3.7% formaldehyde solution (47608; Fluka, Sigma, St. Louis, USA) at room temperature for 15 min. After washing with 1x PBS, cells were permeabilized with 0.2% Triton X-100 in PBS and blocked with 10% horse serum before overnight incubation with γ-H2A.X, 53BP1, p-ATM, p-CHK2 antibodies. Finally, cells were washed and incubated with secondary antibodies coupled to fluorescent dyes (alexa fluor 488 or/and alexa fluor 647).

For immuno-FISH, immunostaining of 53BP1 was performed as described above and followed by incubation in PBS 0,1% Triton X-100, fixation 5 min in 2% paraformaldehyde (PFA), dehydration with ethanol and air-dried. Cells were hybridized with the telomeric PNA-Cy3 probe (PNA Bio) using standard PNA-FISH procedures. Imaging was carried out at room temperature in Vectashield, mounting medium for fluorescence (Vector Laboratories, Burlingame, USA). Images were acquired with a Confocal Spectral Leica TCS SP5. Using a HCX PL APO Lambda blue 63×1.40 OIL UV, zoom 2.3 lens. Images were acquired using LAS-AF 1.8.1 Leica software and processed using LAS-AF 1.8.1

Leica software and Adobe Photoshop CS. Colocalization of 53BP1 foci and the PNA FISH probe was quantified in at least 200 cells.

Telomeric repeat amplification protocol (TRAP) assay

Telomerase activity was measured using the TRAPeze kit [32] (Millipore, Billerica, MA USA) according to the manufacturer's recommendations. TRAP assay activity was normalized with the internal control [24].

Real-time quantitative PCR

RNA isolation and cDNA synthesis. Total cellular RNA was extracted using Trizol (Invitrogen, Carlsbad, USA) according to the manufacturer's instructions. For reverse transcription reactions (RT), 1 μg of the purified RNA was reverse transcribed using random hexamers with the High-Capacity cDNA Archive kit (Applied Biosystems, P/N: 4322171; Foster City, CA) according to the manufacturer's instructions. RT conditions comprised an initial incubation step at 25°C for 10 min. to allow random hexamers annealing, followed by cDNA synthesis at 37°C for 120 min, and a final inactivation step for 5 min. at 95°C.

Measurement of mRNA Levels. The mRNA levels were determined by quantitative real-time PCR analysis using an ABI Prism 7900 HT Fast Real-Time PCR System (Applied Biosystems, Foster City, CA). Gene-specific primer pairs and probes for *SOD1* (*SOD Cu/Zn*), *SOD2* (*SOD Mn*), *GPX1 (Glutathione peroxidase 1)* and *CAT* (*Catalase*) (Assay-on-demand, Applied Biosystems), were used together with TaqMan Universal PCR Master Mix (Applied Biosystems, Foster City, USA) and 2 μl of reverse transcribed sample RNA in 20 μl reaction volumes. PCR conditions were 10 min. at 95°C for enzyme activation, followed by 40 two-step cycles (15 sec at 95°C; 1 min at 60°C). The levels of glyceraldehyde-3-phosphate dehydrogenase (*GAPDH*) expression were measured in all samples to normalize gene expression for sample-to-sample differences in RNA input, RNA quality and reverse transcription efficiency. Each sample was analyzed in triplicate, and the expression was calculated according to the $2^{-\Delta\Delta Ct}$ method.

GSE24.2 peptide production and purification

E. Coli DH5a cells were transformed with pGATEV GSE24.2 and lysates prepared as described [30]. The fusion protein was purified with glutathione-sepharose and purity analyzed by gel electrophoresis. GSE24.2 was obtained from the purified fusion protein by TEV protease digestion according to the manufacturer's recommendations. Typically, over 90% of the fusion protein was cleaved, as determined by SDS-PAGE. The protein was passed twice over a 5 ml Hi-Trap Ni-NTA column to remove the polyhistidine tags, un-cleaved protein, TEV protease and impurities. Synthetic GSE24.2 was obtained from Peptide 2.0 Inc (Chantilly, USA) and purified by HPLC

Western Blot

Whole-cell extracts were prepared essentially as described previously [33]. Nuclear extracts were obtained as previously reported [24]. Western blotting was performed using standard methods [33]. Protein concentration was measured by using the Bio-Rad protein assay.

Senescence analysis

Control and X-DC fibroblasts (1×10^4 cells) were plated onto 6 well plates and fixed after four days to assay the SA-β-gal (Senescence Detection Kit, BioVision, Milpitas, USA). The percentage of senescent cells was calculated in 6 images per sample taken in the bright field microscopy at 100× magnification (Nikon Eclipse TS100 Microscopy, Melville, NY, USA).

Determination of reactive oxygen species (ROS) content with dihydroethidium

Cells were cultured in 12 chamber plates for 4 days (at confluence). Afterwards cells were washed 2 times with pre-warmed PBS medium, 2 μL/mL of diluted dihydroethidium (Dihydroethidium, D7008-Sigma, St. Louis, USA) was added to the plate. Cells were incubated at 37°C for 20 min. After washing the plate with PBS, medium was replaced, and cells cultured for an additional 1 hour at 37°C. The fluorescence was measured using spectraMAX GEMINIS (Molecular Device, Sunnyvale, USA), with 530 nm of excitation wavelength and 610 nm of emission wavelength. Mean fluorescence intensity (MFI) for each cell line, was normalized by the cellular protein content.

Measurement of CuZnSOD and MnSOD activity

To determine MnSOD and CuZnSOD activity the cells were treated as described in the Cayman "Superoxide Dismutase Assay kit" (Ann Arbor, USA). After centrifugation at 10,000 g for 10 min, supernatant was used to measure CuZnSOD activity. The mitochondrial pellet was lysed using a lysis buffer compatible with the manufacturer's instructions (10 mM HEPES, pH7.9, 420 mM NaCl, 1,5 mM $MgCl_2$, 0,5 mM EDTA, 0.1% Triton X-100) for 20 min on ice. After centrifugation at 12,000 g for 5 min, the supernatant was collected for MnSOD activity assay. Measurements of CuZnSOD and MnSOD activities were performed in a 96 well plate prepared using 3–4 replicates from different cellular extracts for each sample. The final absorbance was measured at 450 nm using a spectrophotometer spectraMAXPLUS 384 (Molecular Devices, Sunnyvale, USA).

Measurement of catalase activity

The method for measuring the catalase enzymatic activity was based on the reaction of the enzyme with methanol in the presence of hydrogen peroxide to produce formaldehyde. Cells were lysed using freeze (liquid N_2, 10 s) and thaw (ice, 15 min) procedure repeated three times. After centrifugation of the cell lysate at 13,000 g, for 10 min. at 4°C, supernatants were recovered and quantified using Lowry method. A 96 well plate was prepared using at least 4 replicates for each sample, obtained from different cellular extracts.

Assay reaction consisted in mixing on a 96 well plate: 100 μL of phosphate buffer 100 mM pH 7.0; 30 μL methanol and 20 μL of the sample with the same protein concentration. Then, the reaction was started with 20 μL of 85 mM H_2O_2, maintained during 20 min at room temperature and finally stopped using 30 μL of KOH 10 M. The formaldehyde produced reacts with 35 mM purpald reagent dissolved in 0,5 M HCl during 10 min at room temperature. Finally, 10 μL of 0.5% KIO_4 in KOH 0.5 M were added and the absorbance at the wavelength of 540 nm was measured with spectrophotometer spectra MAXPLUS 384 (Molecular Devices, Sunnyvale, USA).

Measurement of glutathione peroxidase activity

Gpx activity was measured by using a glutathione peroxidase assay kit (Cayman (Ann Arbor, USA). Briefly, cells were collected and lysed using cold buffer (50 mM Tris-HCl, pH 7.5, 5 mM EDTA and 1 mM DTT) and two freeze-thaw cycles as described above. The lysates were centrifuged at 10,000 g for 15 min at 4°C and the supernatants recovered in fresh tubes. A 96 well plate was prepared using at least 3 replicates for each sample from different

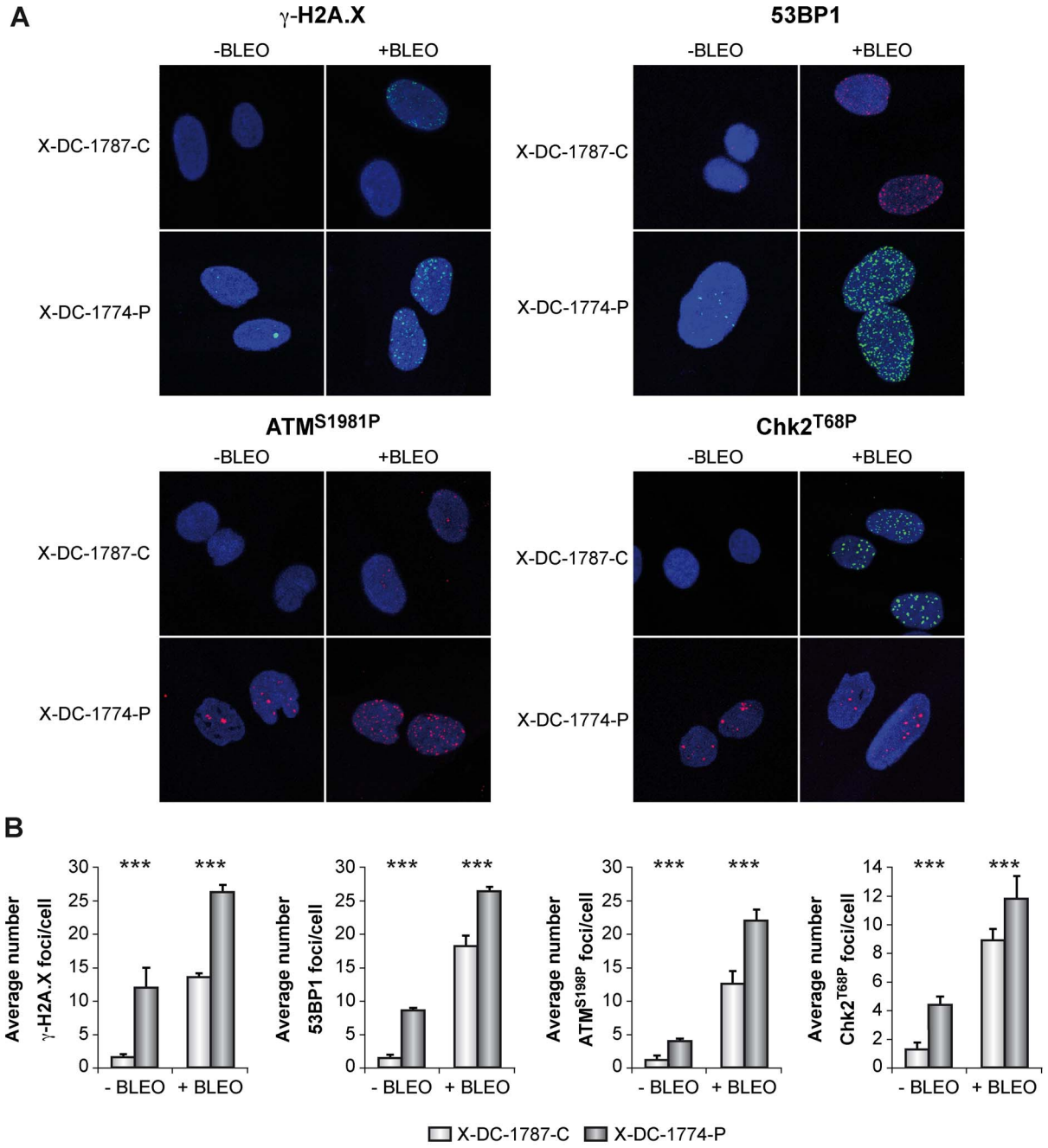

Figure 1. DNA damage signaling in X-DC patient cells. (A) Immunofluorescence staining of DNA damage proteins. Control X-DC-1787-C and patient X-DC-1774-P cells were, either not treated (-Bleo) or treated (+Bleo) with bleomycin (10 μg/ml) for 24 hours, fixed and incubated with antibodies against γ-H2AX, 53BP1, p-ATM or p-CHK1 and secondary fluorescent antibodies. Nuclear DNA was counterstained with DAPI (blue). (B). Quantification of γ-H2A.X foci, pATM, 53BP1 and pCHK2 associated foci in X-DC-1787-C and X-DC-1774-P cells. More than 200 cells were analyzed in each cell line and indicated as the average number of foci/cell. Asterisks indicate significant differences in relation to control cells lines or to untreated cells. Average values and standard deviations of two independent experiments are shown. Experiments were repeated 3 times with similar results.
doi:10.1371/journal.pone.0101424.g001

cellular extracts. After protein quantification by Lowry method, samples containing 20 μg of total proteins were added to the 96 well plate containing a solution with 1 mM GSH, 0.4 U/mL of glutathione reductase, 0.2 mM NADPH. The reaction was initiated by adding 0.22 mM of cumene hydroperoxide and the reduction of the absorbance was recorded at 340 nm each 1 min during 8 min. The Gpx activity was determined by the rate of decrease in absorbance at 340 nm (1 mU/mL Gpx). Molar coefficient extinction for NADPH was 0.00622 mM^{-1} cm^{-1}.

Statistical analysis

For the statistical analysis of the results, the mean was taken as the measurement of the main tendency, while standard deviation was taken as the dispersion measurement. T-Student was performed. The significance has been considered at *$p<0.05$, **

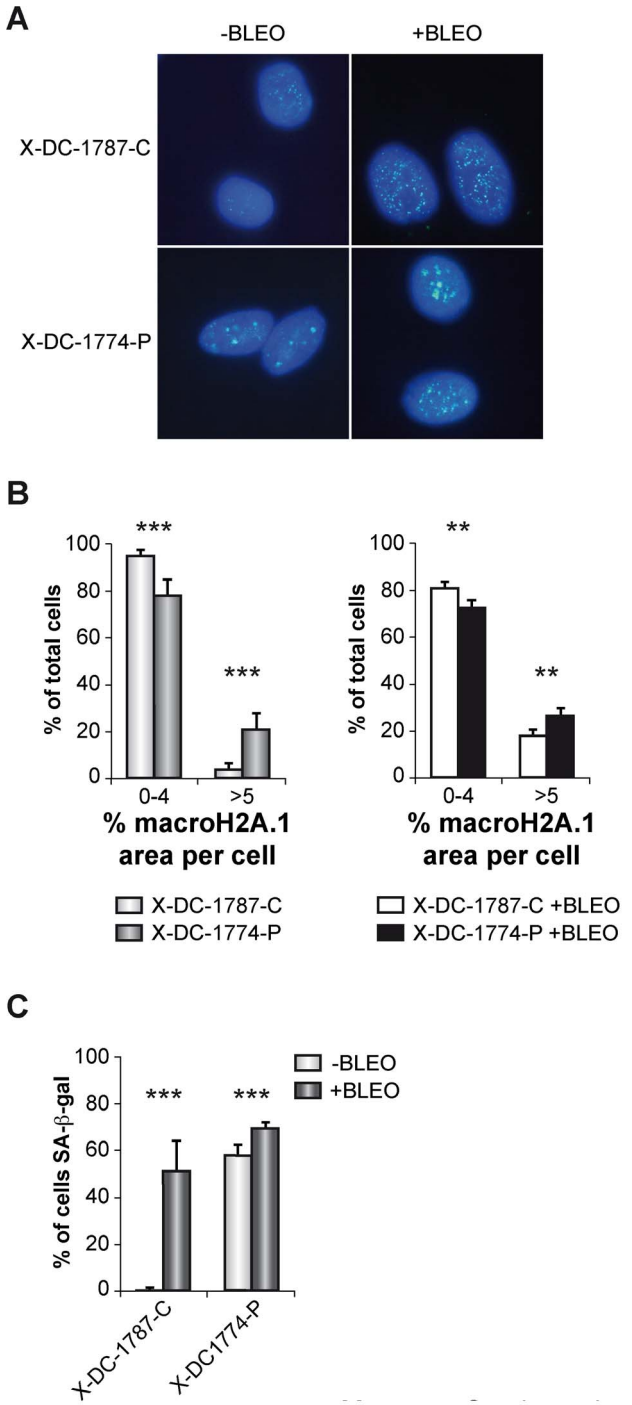

Figure 2. Determination of Histone-macroH2A.1-associated heterochromatin and senescence in X-DC cells. (A) Histone-macroH2A.1-associated heterochromatin detection in X-DC cells. X-DC-1787-C and X-DC-1774-P cells were either not treated (-Bleo) or treated (+Bleo) with bleomycin (10 mg/ml) for 24 hours, fixed and incubated with an antibody against Histone-macroH2A.1 followed by a secondary fluorescence labeled antibody. (B) Quantification of Histone-macroH2A.1-associated heterochromatin. More than 200 cells were analyzed in each cell line and grouped to the area presenting Macro H2A.1 foci per cell. Asterisks indicate significant differences between cells lines. Average values and standard deviations of two independent experiments are shown. (C) SA-β-gal activity in X-DC-1787-C and X-DC-1774-P cells either untreated (-Bleo) or treated (+Bleo) with bleomycin (10 μg/ml). Senescent cells were quantified in 6 images of random regions. Experiments were repeated 3 times with similar results. Asterisks indicate significant differences in response to bleomycin.
doi:10.1371/journal.pone.0101424.g002

for $p<0.01$ and *** for $p<0.001$. GraphPad Software v5.0 was used for statistical analysis and graphic representations.

Results

1-Basal and induced DNA damage response in X-DC cells involves 53BP1, ATM and CHK2 and results in increased heterochromatin formation and senescence

It has been previously demonstrated [29] that a pathogenic mutation in murine *Dkc1* causes growth impairment and the enhancement of DNA damage responses after treatment with the chemotherapeutic agent etoposide. In the context of telomeres of normal length, cells with the dyskerin mutation $Dkc1^{\Delta 15}$ (deletion of exon 15) showed increased number of DNA damage foci as observed by detection of p-H2A.X^{Ser139} (γ-H2A.X) foci and activation of the ATM/p53 pathway.

We have used paired human cell lines (heterozygous carrier and patient) harboring the same mutation in *DKC* gene, responsible for X-DC and studied the DNA damage response pathway. Telomere length of the control cell line (healthy carrier grandmother from X-DC-1774-P patient) was the right length for the age of this control (60 year old and 10.7 kpb). Both basal DNA damage and that produced in response to the DNA damaging agent bleomycin were studied. Our results show that the number of γ-H2A.X-associated foci/cell was dramatically higher in cells obtained from the X-DC-1774-P patient than in the carrier cell line X-DC-1787-C (Fig. 1A and B). When cells were treated with bleomycin, which induces double strand breaks, we found an increase in the number of γ-H2A.X associated foci/cell in both X-DC-1774-P and X-DC-1787-C cells. Although basal DNA damage in X-DC-1774-P was already much higher than that of control cells the increase was similar or even lower to that observed in control cells. We also investigated the presence of 53BP1 foci in these cell lines, since 53BP1 is recruited to DNA-damage associated foci. We found the average number of foci/cell was similar to that observed for γ-H2A.X, higher to that observed in control cells but even if there is an increase after bleomycin treatment, the increase in the number of foci/cell was smaller than control cells ATM protein is also recruited to DNA-damage sites at the chromatin and phosphorylated, we found that X-DC-1774-P cells showed higher number of foci/cell with phosphorylated ATM compared to carrier cells. In bleomycin treated cells both patient and carrier cells showed increased response to DNA damage although similar to what happen with the other indicators of DNA damage the increase observed in X-DC-1774-P was lower than control cells. CHK2 is a protein, substrate of ATM-kinase. We studied the number of cells with phosphorylated CHK2 at Thr68 and found a higher number of foci/cells in X-DC-1774-P in untreated cells, which increases after bleomycin treatment, but such increase is lower than control cells. Altogether these results indicate that basal DNA damage is higher in X-DC patient cells that in mutation carrier cells, in response to bleomycin this increase is not higher in X-DC cells probably due to the high basal damage observed in these cells. Furthermore we have found that the signaling pathway associated with this DNA damage, include at least 53BP1, ATM and CHK2, although we cannot exclude the participation of other proteins.

In order to verify if X-DC cells harbor an increased heterochromatin content we studied the nuclear distribution of histone-macroH2A.1-associated heterochromatin in X-DC-1774-P and X-DC-1787-C cells, both in basal conditions and after bleomycin treatment (Fig. 2A). X-DC-1774-P cells already showed an average of 20% of the nuclear area with positive expression for macroH2A.1, and after bleomycin treatment we detected an increase up to 30% (Fig. 2B). X-DC-1787-C cells showed a very

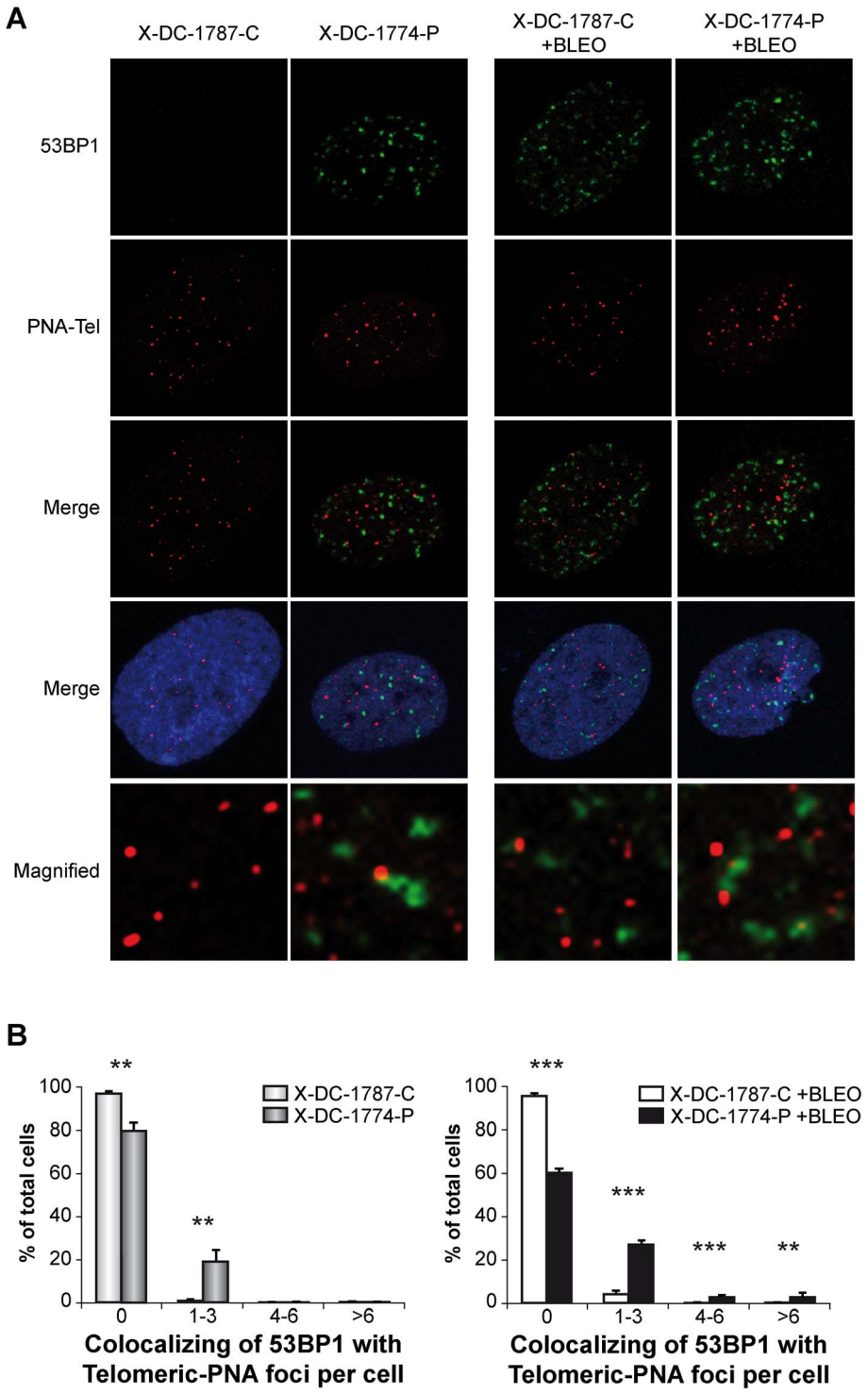

Figure 3. Localization of 53BP1 foci to telomeres in X-DC patient cells. X-DC-1787-C and X-DC-1774-P cells untreated (-Bleo) or treated (+ Bleo) with bleomycin (10 μg/ml) and incubated with γ-H2A.X and PNA-FISH probe. (A) Colocalization of 53BP1 foci (green) and telomeres as identified by hybridizing with a PNA-FISH probe (red). DNA was counterstained with DAPI (blue). Magnified views of merged images showing details of the colocalization are shown in the two lower series of panels (B) Colocalized 53BP1 foci and PNA-FISH probe at telomeres was quantified. More than 200 cells were analyzed in each cell line in an experiment performed three times with similar results. Asterisks indicate significant differences in relation to different cell lines.
doi:10.1371/journal.pone.0101424.g003

low expression in basal conditions that increases to almost 20% after bleomycin treatment (Fig. 2C). These data indicated that X-DC patient cells show extensive areas of heterochromatin that further increased in response to bleomycin. Thus, both basal and induced DNA damage may trigger a relevant silencing of gene expression in these cells. Almost 60% of X-DC-1774-P cells were

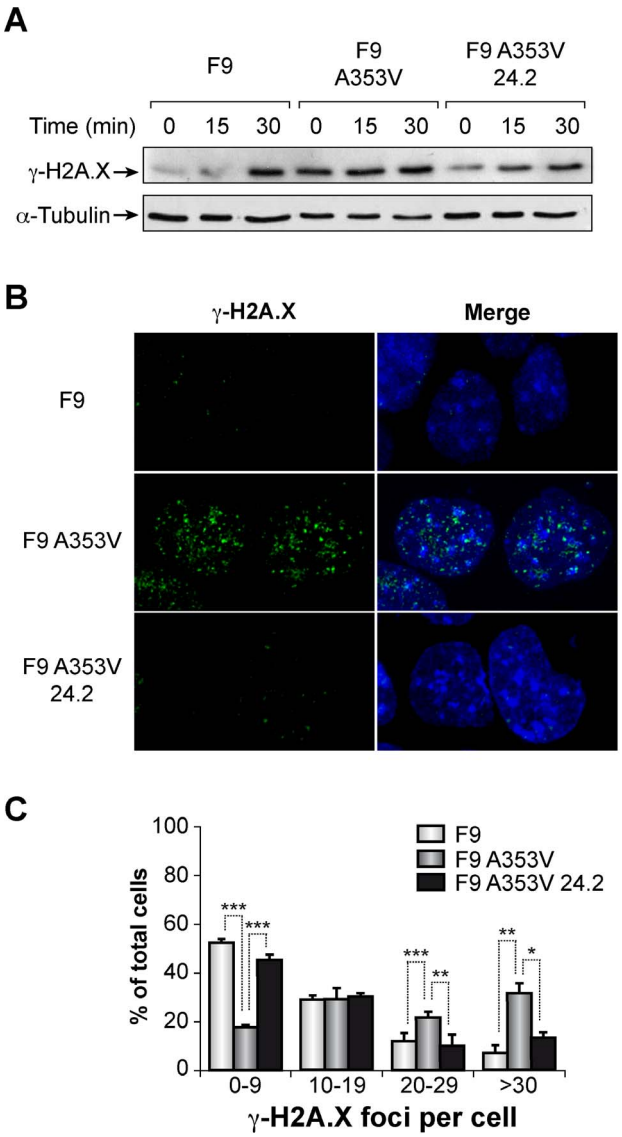

Figure 4. F9A353V cells show enhanced, basal and bleomycin induced, DNA damage response. (A) F9, F9A353V and F9A353V cells transfected with GSE24.2 (10 μg DNA per million cells). F9A353V 24.2 cells were treated with bleomycin (10 μg/ml). After 0, 15 or 30 minutes of treatment cells were lysed and the experiment analyzed by western blot with antibodies against γ-H2A.X or α-tubulin as a loading control. (B) Immunofluorescence staining of γ-H2A.X (green) in F9, F9A353V and F9A353V 24.2 cells (10 μg DNA per million cells). Nuclear DNA was counterstained with DAPI (blue). (C) Quantification of γ-H2AX foci in F9, F9A353V or F9A353V 24.2 cells. More than 200 cells were analyzed in each cell line and grouped to the number of γ-H2A.X foci observed per cell. Experiments were repeated 3 times with similar results. Asterisks indicate significant differences in relation to different cell lines.
doi:10.1371/journal.pone.0101424.g004

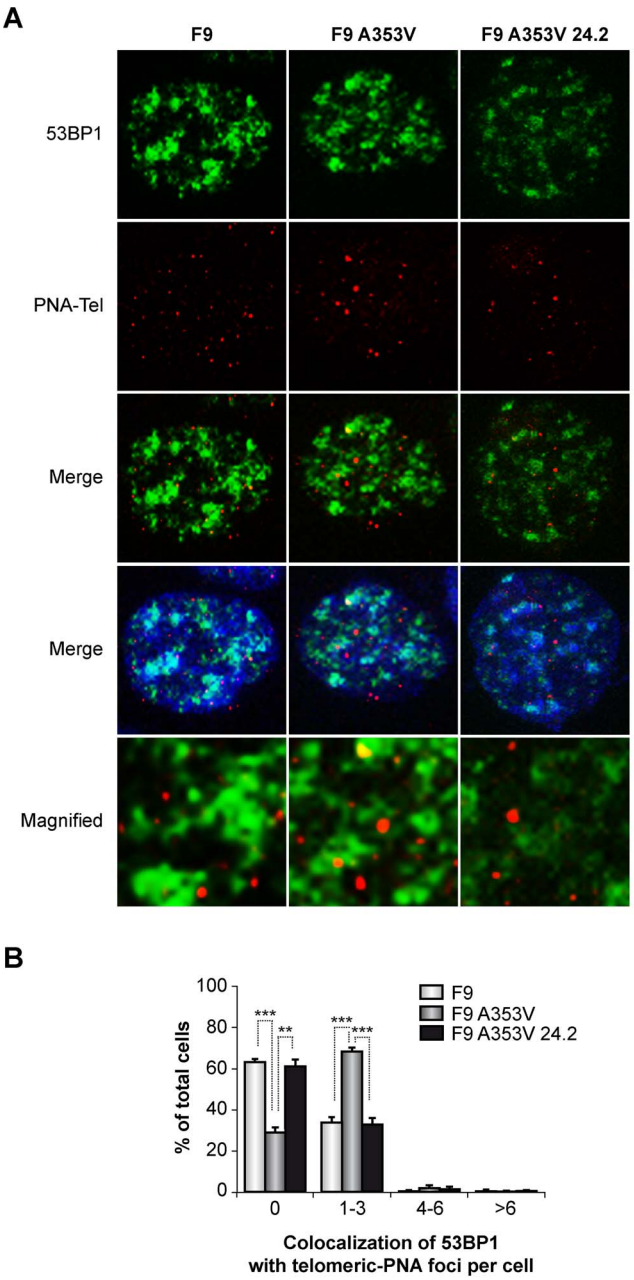

Figure 5. Localization of 53BP1 foci to telomeres in F9A353V cells. F9, F9A353V and F9A353V cells transfected with GSE24.2 (F9A353V 24.2) (F9 cells were treated with bleomycin,10 μg/ml for 24 hours) and incubated with 53BP1 antibodies and with a PNA-FISH probe. (A) Colocalization of 53BP1 foci (green) and PNA-FISH probe that identified telomeres (PNA-Tel, red). DNA was counterstained with DAPI (blue). Magnified views of merged images showing details of the colocalization are shown in the lower panels. (B) Quantification of the colocalization of 53BP1 foci and telomere signals shown in panel A. More than 200 cells were analyzed in each cell line and grouped to the number of 53BP1 foci associated to telomeres (PNA-Tel) per cell. Experiments were repeated 3 times with similar results. Asterisks indicate significant differences in relation to different cell lines.
doi:10.1371/journal.pone.0101424.g005

positive for the senescence SA-β-gal activity that increases to almost 70% after bleomycin treatment. X-DC-1787-C cells showed low expression of SA-β-gal that also increases further after bleomycin treatment.

2- DNA damage is localized in telomeres in X-DC cells

Since telomere length is greatly diminished in X-DC patient cells we investigated if DNA damage was enriched at telomeres, both in basal conditions and after DNA damage induction. In order to investigate this, we combined a PNA FISH probe as a telomere marker, and 53BP1 for DNA damage detection. The results showed that there was a high association of damaged DNA

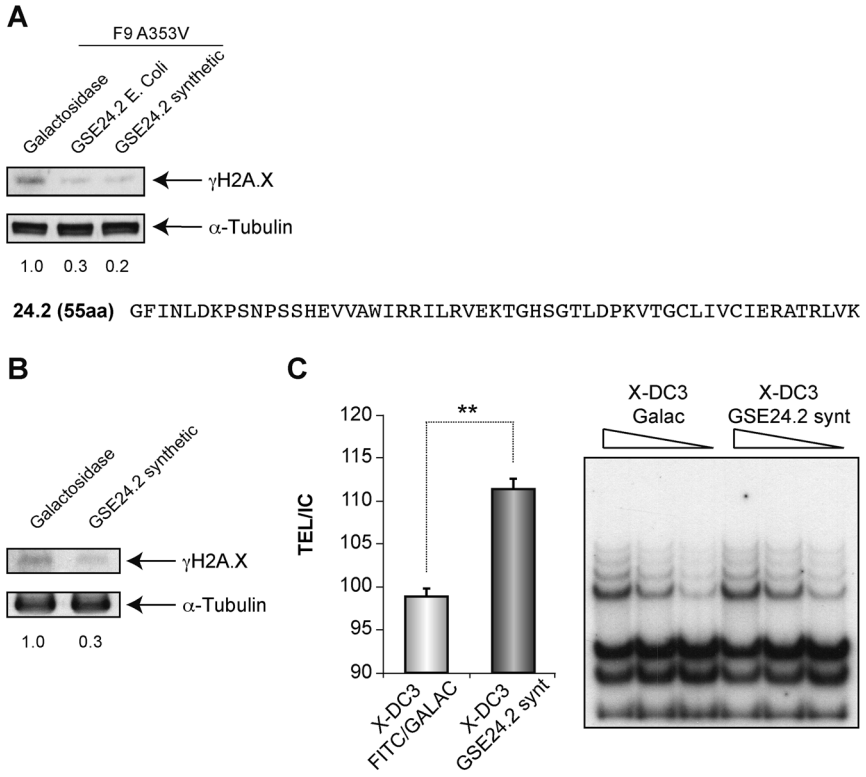

Figure 6. Activity of the GSE24.2 peptide expressed in bacteria or chemically-synthesized. (A) F9A353V cells were transfected with 15 μg of β-galactosidase as a control (galactosidase), or GSE24.2 purified from E. Coli (GSE24.2E.coli) or obtained by chemical synthesis (GSE24.2 synthetic). After 24 hours cells were lysed and the levels of γ-H2AX and α-tubulin determined by western blot. The values at the bottom were obtained after quantification of the blot and show the ration between expression levels of γ-H2AX and α-tubulin in each line and referred to those found in β-galactosidase transfected cells. (B) Same experiment described in A, performed in X-DC3 cells transfected with β-galactosidase or chemically synthesized GSE24.2. (C) Reactivation of telomerase activity by chemically synthesized GSE24.2. X-DC3cells were transfected with β-galactosidase or chemically synthesized GSE24.2 and telomerase activity determined by TRAP assay (right). Different amounts extract were used for each TRAP assay as indicated. The activity was quantified by evaluating the intensity of the bands in relation with the internal control (TEL/IC) (left panel). The values for GSE24.2 transfected cells were referred to the β-galactosidase transfected cells. The experiments were repeated at least three times with similar results. Asterisks indicate significant differences between the two different transfected peptides.
doi:10.1371/journal.pone.0101424.g006

at the telomeres in X-DC-1774-P cells that was not found in carrier X-DC-1787-C cells (Fig. 3A). Furthermore the increase in DNA damage observed after bleomycin treatment (Fig. 1B) was strongly associated with telomeres in X-DC-1774-P cells in contrast to X-DC-1787-C cells (Fig. 3) indicating the relevance of telomere shortening in the response to DNA damage in X-DC patient cells.

3-Expression of GSE24.2 impairs the induction of γ-H2A.X foci after DNA damage

Since F9 cells represent a good model system to study DNA damage responses as previously demonstrated (29), we used them in order to investigate if the expression of GSE24.2 could modify the activation of the DNA damage response. Therefore, we transfected F9A353V and control F9 cells [26] with the GSE24.2 expression plasmid and treated them either with bleomycin or etoposide, a topoisomerase inhibitor known to induce DNA double-stranded breaks. We found that, as expected, bleomycin treatment induced γ-H2A.X in both cell lines (Fig. 4A). However, the basal level of γ-H2A.X was much higher in F9A353V cells than in F9 cells expressing the WT dyskerin, indicating that the mutation renders the cells more susceptible to DNA damage. In the presence of the GSE24.2 F9A353V, γ-H2A.X decreased to values very similar to those observed in F9 cells in both, basal and bleomycin-induced levels. Similar results were obtained in etoposide-treated cells (data not shown). We next investigated the presence of γ-H2A.X containing foci in basal conditions and the results confirmed those obtained in the western blot studies (Fig. 4B and 4C). Most F9 cells showed very few foci; the number increased in F9A353V cells but was reduced at similar level to those of F9 cells when the mutant cells were transfected with GSE24.2. Altogether, the results indicated that the expression of GSE24.2 decreases the DNA damage produced by the dyskerin mutation.

Afterwards, we investigated if the increased DNA damage in F9A353V cells was enriched at the telomeres (as already found in X-DC patient cells, Fig. 3) and also whether the protection from DNA damage induced by GSE24.2 also applies to damage at the telomeres. We use combined immunological detection of 53BP1 and PNA-FISH probe. The results (Fig. 5A and 5B) indicated that F9A353V cells have a stronger association of 53BP1 to the telomeres than in F9 cells treated with bleomycin, up to 60%. However in F9A353V cells transfected with the GSE24.2 there is little association of 53BP1 foci at the telomeres (30% 1–3 53BP1 foci per cell). These results indicate that the elevated DNA damage response found in F9A353V cells is probably caused by defects at the telomeres induced by the *Dkc1* mutation, in agreement with the results obtained in $Dkc1^{\Delta 15}$ MEF cells. Interestingly, expression

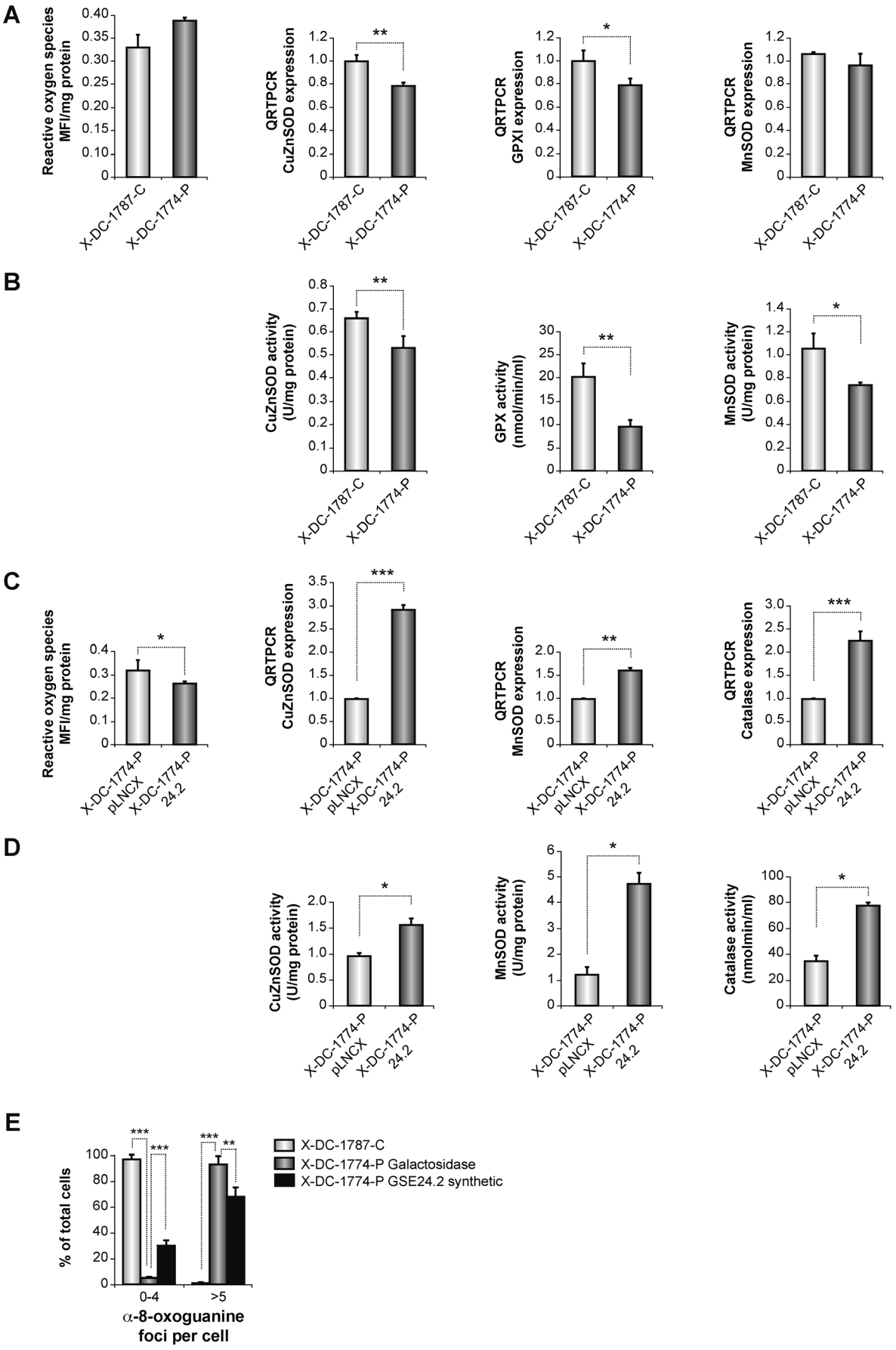
A
Reactive oxygen species MFI/mg protein
QRTPCR CuZnSOD expression
QRTPCR GPXI expression
QRTPCR MnSOD expression
X-DC-1787-C
X-DC-1774-P
B
CuZnSOD activity (U/mg protein)
GPX activity (nmol/min/ml)
MnSOD activity (U/mg protein)
C
Reactive oxygen species MFI/mg protein
QRTPCR CuZnSOD expression
QRTPCR MnSOD expression
QRTPCR Catalase expression
X-DC-1774-P pLNCX
X-DC-1774-P 24.2
D
CuZnSOD activity (U/mg protein)
MnSOD activity (U/mg protein)
Catalase activity (nmolmin/ml)
E
% of total cells
X-DC-1787-C
X-DC-1774-P Galactosidase
X-DC-1774-P GSE24.2 synthetic
0-4
>5
α-8-oxoguanine foci per cell

Figure 7. Oxidative stress analysis in X-DC fibroblasts after GSE24.2 transfection. (A) ROS levels were determined in fibroblasts from the carrier DC1787, and fibroblasts from the patient X-DC1774-P. Levels were determined using the fluorescent probe dihydroethidium in confluent cells (left panel). RNA expression was determined for CuZnSOD, MnSOD, and GPX1 by qRT-PCR (A right panels). B) Enzymatic activities of CuZnSOD,MnSOD, and Glutathione peroxidase 1 were also determined. C) ROS levels were studied in X-DC1774-P fibroblasts (expressing pLNCX vector) and X-DC-1774-P cells expressing GSE24.2 (X-DC1774-PGSE24.2, left panel). Cu/ZnSOD, MnSOD, and catalase expression levels were determined by qRT-PCR. D) Cu/ZnSOD, MnSOD, and catalase activities in confluent pLNCX and 24.2 cells are shown in left panels. E) X-DC1774-P and X-DC1774-PGSE24.2, cells were transfected with GSE24.2 synthetic peptide and levels of 8-oxoguanine studied by immunofluorescence. The 8-oxoguanine foci signal was expressed as the average number of foci/cell in 200 cells. Results are expressed as mean ± standard deviation from three independent experiments. Statistical significance is expressed as (*) $p<0.05$.
doi:10.1371/journal.pone.0101424.g007

of GSE24.2 reverted the telomere damage in F9A353V cells, indicating its biological importance in the reversion of the mutant *Dkc1* phenotype.

4-Treatment of X-DC cells with GSE24.2 peptide rescues DNA damage

We have previously reported that the GSE24.2 peptide purified from bacteria was able to increase telomerase activity in F9A353V cells [26] therefore we next tested if the activity of the GSE24.2 peptide either purified from E-coli or chemically synthesized reduced the DNA damage. We found that the levels of γ-H2A.X in F9A353V cells decreased after transfecting this peptide (Fig. 6A) either obtained from bacteria or chemically synthesized to 30 and 20%, respectively. Moreover the synthetic peptide also decreased the DNA damage in X-DC3 cells (DKC1 mutated lymphocytes) by 30% (Fig. 6B). This decrease in DNA damage correlated well with the ability of the synthetic peptide to increase telomerase activity in these cells (Fig. 6C).

5- Oxidative stress in X-DC cells is decreased by expression of GSE24.2

Oxidative stress is one of the causes of DNA damage producing both single-strand breaks (SSBs) and double-strand breaks (DSBs). SSBs are the result from the interaction of hydroxyl radicals with deoxyribose and subsequent generation of peroxyl-radicals. These reactive oxygen species (ROS) are then responsible for nicking phosphodiester bonds that form the backbone of each helical strand of DNA [34]. To clarify the presence of higher oxidation levels in X-DC cells we have studied ROS levels, and the expression of antioxidant enzymes CuZn (SOD1) and Mn (SOD2) superoxide dismutase, glutathione peroxidase 1 (GPX1) and their corresponding enzymatic activities in X-DC-1787-C and X-DC-1774-P cell lines. Levels of ROS were elevated in X-DC-1774-P cells compared with X-DC-1787-C carrier cells and also higher than in GM03348, an age-matched cell line from a healthy subject (data not shown). In agreement with this result we found a decrease in gene expression levels of the antioxidant enzymes CuZnSOD and MnSOD and GPX1 when compared the X-DC-1774-P to the carrier cell line (Fig. 7A). We also determined the activity of the three enzymes with decreased expression in the X-DC-1774-P cells that also showed decreased activity in agreement with the gene expression data (Fig. 7B).

In order to investigate if expression of GSE24.2 was able to overcome the increased oxidative stress found in X-DC-1774-P cells, we expressed in this cell line either pLNCX-GSE24.2 or the empty vector (pLNCX). The results indicated that X-DC-1774-P cells expressing GSE24.2 showed lower levels of ROS. We also studied the expression levels of CuZnSOD, MnSOD and catalase in both cell lines and found that expression levels of these antioxidant enzymes were higher in X-DC-1774-P-24.2. When the corresponding protein activities were analyzed, we observed an increase in CuZnSOD, MnSOD and catalase activities (Fig. 7C) in X-DC-1774-P-24.2 when compared with the empty vector transfected cells. Altogether, the data indicated that the observed decrease in oxidative stress in X-DC cells expressing GSE24.2 should contribute to protect these cells from DNA damage. We finally investigated if treatment with the GSE24.2 synthetic peptide was also able to induce a decrease in oxidative DNA damage. We transfected X-DC-1774-P cells with the GSE24.2 synthetic peptide and evaluated the levels of 8-oxoguanine by immunofluorescence (Fig 7E). The results showed that indeed the synthetic GSE24.4 reduced the signal obtained with 8-oxoguanine-antibody.

Discussion

We have previously reported that expression of a *dyskerin* internal peptide (GSE24.2) reactivates telomerase activity in cells that are deficient in this activity by increasing TERT and TERC levels [24] We have also reported that expression of GSE24.2 increases TR levels by stabilizing this RNA [26]. Because of this activity GSE24.2 has been recently approved as an orphan drug by EMA for the treatment of Dyskeratosis congenita. We have now studied the role of GSE24.2 in the DNA damage response of X-DC patient cells in an effort to better understand the mechanism of GSE24.2 action in X-DC. We studied several proteins involved in the DNA-damage response and found, as other authors have [35] [36], that X-DC patient cells presented higher levels of DNA damage associated foci detected by γ-H2A.X and 53BP1 and to a lesser extent p-ATM and p-CHK2. We also found increased levels of DNA damage in response to bleomycin that was more evident when we studied -H2A.X, p-ATM and p-CHK2 associated foci as previously described in mice (29) but this increase was not higher than that obtained in control cells probably because X-DC cells already have massive damage in basal conditions. Previous reports described increased levels of DNA damage in DC cells harboring mutations in *DKC1*, *TERC* or *TERT*. However in fibroblasts and lymphocytes from these patients the response to induced DNA-damage was not increased [35] in contrast to another study [29]. We have here used X-DC patient cells which exhibited short telomeres, p53 activation and senescence [37]. Indeed, a high level of DNA damage, both at basal and induced by bleomycin, was observed at telomeres suggesting that the shortening of telomeres in these cells induces further damage by preventing repair. Dysfunctional telomeres trigger a DNA damage response most likely because they are too short to adopt the normal t-loop structure needed to form the telomere with correctly ordered shelterin components. Recruitment of histone-macroH2A.1 has been associated to heterochromatin and senescent associated foci (SAHF) [18] [19]. We found that both senescence and macroH2A.1 associated-foci are increased in X-DC patient cells and also that bleomycin treatment increases these values, suggesting that the impairment in the repair of DNA lesions in X-DC cells likely contributes to the senescent phenotype.

Using the *in vitro* generated *Dkc1* mutant F9A353V cells we have found, in agreement with our previous results (and also [29]), that

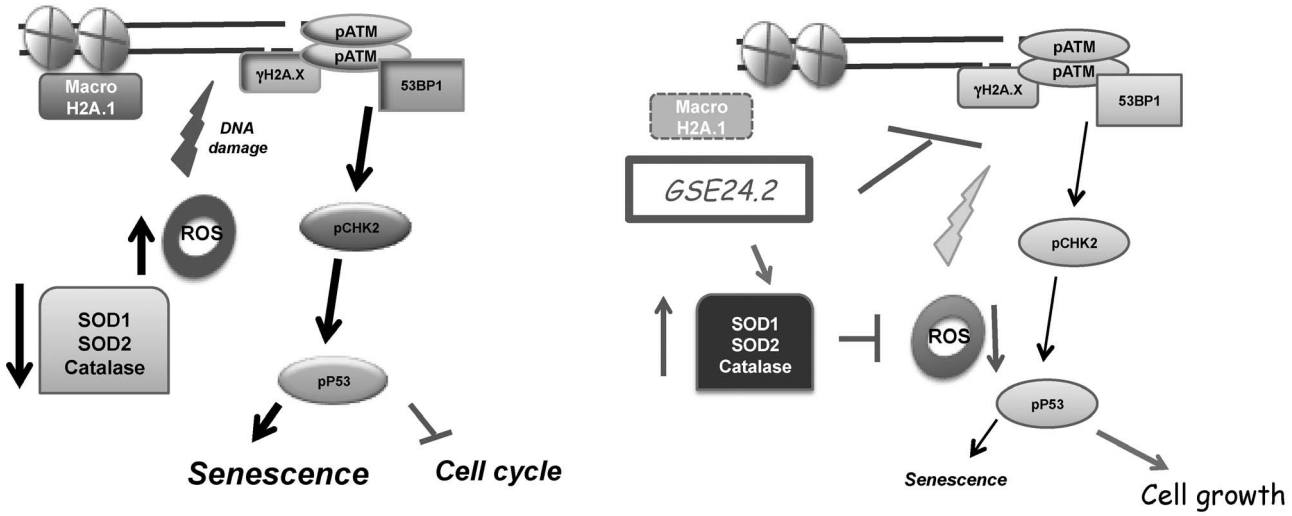

Figure 8. Proposed biological activity of GSE24.2 on DNA damage and oxidative stress. Dyskeratosis congenita cells display high basal DNA damage detected by increased γH2AX, p-ATM, p-CHK2 and 53BP1 foci. Additionally there are increased levels of ROS, and decreased expression and activity of antioxidant enzymes resulting in higher oxidative damage and senescence (left panel). GSE24.2 peptide increases expression of antioxidant enzymes and as a consequence decreased ROS levels (right panel). In parallel there is increased telomerase activity that may help to decrease global and telomeric DNA damage. Globally these two activities of GSE24.2 might result in increased viability and growth of DC cells (26).
doi:10.1371/journal.pone.0101424.g008

these cells showed increased DDR compared with F9 cells, both in the steady state and when treated with bleomycin or etoposide. Other *Dkc1* mutations such as *Dkc1*$^{\Delta 15}$ have been shown to accumulate DNA damage indicating that DC cells have cellular defects even in the context of long telomeres [29]. We previously reported that an internal fragment of Dyskerin, the peptide GSE24.2 induces an increase in telomerase activity in X-DC cells [24]. Now we are showing that expression of GSE24.2 is able to induce protection against DNA damage. Furthermore, the repair of pre-existing DNA lesions should also take place at telomeres in F9A353V cells as shown by the decrease in 53BP1 and PNA-FISH telomeric colocalization (Fig. 5B). Interestingly, the observed decrease in DNA damage mediated by GSE24.2 expression in F9A353V cells, also occurs when we used either bacterially produced or chemically synthesized peptide, reinforcing the idea that GSE24.2 reactivates telomerase activity, by acting directly at the telomeric DNA [26] and/or changing telomere folding. According with these results the transfection of the GSE24.2 synthetic peptide into X-DC3 human patient lymphocytes resulted in both increased telomerase activity and decreased DNA damage. On the other hand the consequences of A353V-X-DC mutation on DNA damage resemble to those found in cells with mutations in *Tin2* and *Pot1*, which are structural components of telomeres [38] [39].

Diseases with telomerase deficiency are linked to oxidative stress. Elevated levels of the lipoperoxide malondialdehide (MDA) [40], and MDA-DNA adducts have been reported in rare degenerative diseases [41] and in aging [42]. In addition, oxidative stress conditions caused by H_2O_2 increased the rate of telomere shortening in fibroblasts from ataxia-telangiectasia patients [43]. Furthermore, increased accumulation of ROS is involved in decreased cell growth in a *DKC*^{A15} mouse model [36], though there is very little information about oxidative stress in human X-DC cells. Interestingly, the existence of oxidative stress in lymphocytes from patients with an autosomal dominant form of DC with mutations in *TERC* has been recently reported [44]. To further increase the characterization of the oxidative stress profile in X-DC we characterize the levels of ROS and the expression and activity of the main antioxidant enzymes. We found in X-DC-1774-P an increase in ROS levels and a decrease in the expression and activity of antioxidant enzymes in patient cells when compared to carrier cells. Interestingly expression of GSE24.2 results in an increase in SOD1, SOD2 and catalase expression that might decrease ROS levels in X-DC-1774-P 24.2 cells. Different groups [45] [46] [47] [48] have reported decreased cellular ROS levels in stressed hTERT over-expressing cells, demonstrating that telomerase re-expression contributes to decrease oxidative stress [49]. The work by Westin et al. demonstrated that the reduction of the levels of superoxide in DC cells was not dependent of the localization of TERT in the mitochondria, but also p53/p21$^{WAF/CIP}$-dependent process in the context of telomere shortening in cells from DC patients. Therefore, our findings reinforce the notion that increased telomerase activity [24] and repair of DNA damage at telomeres induced by GSE24.2 is concomitant with a decrease in oxidative stress in X-DC cells. Alternatively the decreased DNA damage detected by γ-H2A.X, might corresponds to decreased oxidative damage, in agreement of our results evaluating the levels of 8-oxoguanine that decreased after transfection of the GSE24.2 synthetic peptide.

In summary our results show that, GSE24.2 attenuates the impact of the *DKC1* mutations on DNA damage and its incidence on telomeres (Fig. 8). Furthermore, oxidative stress decreases in GSE24.2 expressing cells, and this should contribute to decrease the rate of DNA damage and therefore enable restoration of cell cycle progression. Indeed, we have previously shown that expression of GSE24.2 X-DC fibroblasts restores proliferation [26].

Since GSE24.2 has been approved as an orphan drug for the treatment of DC, the results presented here indicate that expression of GSE24.2 may form the basis of a useful and safe therapeutic strategy for X-DC patients either by using it as a permanent or as a temporal telomerase activator. These results indicate that GSE24.2 expression has a broad effect on DC cells, reducing oxidative stress and DNA damage in addition to reactivating telomerase activity. All these protective effects could cooperatively contribute to increase DC cells survival and

proliferation [26] and give further support to the recent approval of GSE24.2 as an orphan drug for DC treatment.

Acknowledgments

We thank to P. Mason for the F9 cell mouse model and for the critical review of the manuscript.

References

1. Palm W, de Lange T (2008) How shelterin protects mammalian telomeres. Annu Rev Genet 42: 301–334.
2. Osterhage JL, Friedman KL (2009) Chromosome end maintenance by telomerase. J Biol Chem 284: 16061–16065.
3. Cohen SB, Graham ME, Lovrecz GO, Bache N, Robinson PJ, et al. (2007) Protein composition of catalytically active human telomerase from immortal cells. Science 315: 1850–1853.
4. Meier UT, Blobel G (1994) NAP57, a mammalian nucleolar protein with a putative homolog in yeast and bacteria. J Cell Biol 127: 1505–1514.
5. Ni J, Tien AL, Fournier MJ (1997) Small nucleolar RNAs direct site-specific synthesis of pseudouridine in ribosomal RNA. Cell 89: 565–573.
6. Yang Y, Isaac C, Wang C, Dragon F, Pogacic V, et al. (2000) Conserved composition of mammalian box H/ACA and box C/D small nucleolar ribonucleoprotein particles and their interaction with the common factor Nopp140. Mol Biol Cell 11: 567–577.
7. Decatur WA, Fournier MJ (2002) rRNA modifications and ribosome function. Trends Biochem Sci 27: 344–351.
8. Heiss NS, Knight SW, Vulliamy TJ, Klauck SM, Wiemann S, et al. (1998) X-linked dyskeratosis congenita is caused by mutations in a highly conserved gene with putative nucleolar functions. Nat Genet 19: 32–38.
9. Kirwan M, Dokal I (2008) Dyskeratosis congenita: a genetic disorder of many faces. Clin Genet 73: 103–112.
10. de Lange T (2009) How telomeres solve the end-protection problem. Science 326: 948–952.
11. Martinez P, Blasco MA (2010). Role of shelterin in cancer and aging. Aging Cell 9: 653–666.
12. Tejera AM, Stagno d'Alcontres M, Thanasoula M, Marion RM, Martinez P, et al. (2010).TPP1 is required for TERT recruitment, telomere elongation during nuclear reprogramming, and normal skin development in mice. Dev Cell 18: 775–789.
13. Martinez P, Flores JM, Blasco MA (2012) 53BP1 deficiency combined with telomere dysfunction activates ATR-dependent DNA damage response. J Cell Biol 197: 283–300.
14. Rappold I, Iwabuchi K, Date T, Chen J (2001) Tumor suppressor p53 binding protein 1 (53BP1) is involved in DNA damage-signaling pathways. J Cell Biol 153: 613–620.
15. Fernandez-Capetillo O, Chen HT, Celeste A, Ward I, Romanienko PJ, et al. (2002) DNA damage-induced G2-M checkpoint activation by histone H2AX and 53BP1. Nat Cell Biol 4: 993–997.
16. Dimitrova N, Chen YC, Spector DL, de Lange T (2008) 53BP1 promotes non-homologous end joining of telomeres by increasing chromatin mobility. Nature 456: 524–528.
17. Perona R, Moncho-Amor V, Machado-Pinilla R, Belda-Iniesta C, Sanchez Perez I (2008) Role of CHK2 in cancer development. Clin Transl Oncol 10: 538–542.
18. Zhang R, Chen W, Adams PD (2007) Molecular dissection of formation of senescence-associated heterochromatin foci. Mol Cell Biol 27: 2343–2358.
19. Xu C, Xu Y, Gursoy-Yuzugullu O, Price BD (2012).The histone variant macroH2A1.1 is recruited to DSBs through a mechanism involving PARP1. FEBS Lett 586: 3920–3925.
20. Hartwig FP, Collares T (2013). Telomere dysfunction and tumor suppression responses in dyskeratosis congenita: balancing cancer and tissue renewal impairment. Ageing Res Rev 12: 642–652.
21. Young NS (2012). Bone marrow failure and the new telomere diseases: practice and research. Hematology 17 Suppl 1: S18–21.
22. Stewart JA, Chaiken MF, Wang F, Price CM (2012). Maintaining the end: roles of telomere proteins in end-protection, telomere replication and length regulation. Mutat Res 730: 12–19.
23. Alter BP, Giri N, Savage SA, Rosenberg PS (2009) Cancer in dyskeratosis congenita. Blood 113: 6549–6557.
24. Machado-Pinilla R, Sanchez-Perez I, Murguia JR, Sastre L, Perona R (2008) A dyskerin motif reactivates telomerase activity in X-linked dyskeratosis congenita and in telomerase-deficient human cells. Blood 111: 2606–2614.
25. Zeng XL, Thumati NR, Fleisig HB, Hukezalie KR, Savage SA, et al. (2012).The accumulation and not the specific activity of telomerase ribonucleoprotein determines telomere maintenance deficiency in X-linked dyskeratosis congenita. Hum Mol Genet 21: 721–729.
26. Machado-Pinilla R, Carrillo J, Manguan-Garcia C, Sastre L, Mentzer A, et al. (2012). Defects in mTR stability and telomerase activity produced by the Dkc1 A353V mutation in dyskeratosis congenita are rescued by a peptide from the dyskerin TruB domain. Clin Transl Oncol 14: 755–763.
27. Knight SW, Heiss NS, Vulliamy TJ, Greschner S, Stavrides G, et al. (1999) X-linked dyskeratosis congenita is predominantly caused by missense mutations in the DKC1 gene. Am J Hum Genet 65: 50–58.
28. Vulliamy TJ, Marrone A, Knight SW, Walne A, Mason PJ, et al. (2006) Mutations in dyskeratosis congenita: their impact on telomere length and the diversity of clinical presentation. Blood 107: 2680–2685.
29. Gu BW, Bessler M, Mason PJ (2008) A pathogenic dyskerin mutation impairs proliferation and activates a DNA damage response independent of telomere length in mice. Proc Natl Acad Sci U S A 105: 10173–10178.
30. Kalinin A, Thoma NH, Iakovenko A, Heinemann I, Rostkova E, et al. (2001) Expression of mammalian geranylgeranyltransferase type-II in Escherichia coli and its application for in vitro prenylation of Rab proteins. Protein Expr Purif 22: 84–91.
31. Mochizuki Y, He J, Kulkarni S, Bessler M, Mason PJ (2004) Mouse dyskerin mutations affect accumulation of telomerase RNA and small nucleolar RNA, telomerase activity, and ribosomal RNA processing. Proc Natl Acad Sci U S A 101: 10756–10761.
32. Wright WE, Shay JW, Piatyszek MA (1995) Modifications of a telomeric repeat amplification protocol (TRAP) result in increased reliability, linearity and sensitivity. Nucleic Acids Res 23: 3794–3795.
33. Sanchez-Perez I, Murguia JR, Perona R (1998) Cisplatin induces a persistent activation of JNK that is related to cell death. Oncogene 16: 533–540.
34. Taghizadeh K, McFaline JL, Pang B, Sullivan M, Dong M, et al. (2008) Quantification of DNA damage products resulting from deamination, oxidation and reaction with products of lipid peroxidation by liquid chromatography isotope dilution tandem mass spectrometry. Nat Protoc 3: 1287–1298.
35. Kirwan M, Beswick R, Walne AJ, Hossain U, Casimir C, et al. (2011). Dyskeratosis congenita and the DNA damage response. Br J Haematol 153: 634–643.
36. Gu BW, Fan JM, Bessler M, Mason PJ (2011) Accelerated hematopoietic stem cell aging in a mouse model of dyskeratosis congenita responds to antioxidant treatment. Aging Cell 10: 338–348.
37. Carrillo J, Gonzalez A, Manguan-Garcia C, Pintado-Berninches L, Perona R (2013). p53 pathway activation by telomere attrition in X-DC primary fibroblasts occurs in the absence of ribosome biogenesis failure and as a consequence of DNA damage. Clin Transl Oncol. [Epub ahead of print]
38. Walne AJ, Vulliamy T, Beswick R, Kirwan M, Dokal I (2008) TINF2 mutations result in very short telomeres: analysis of a large cohort of patients with dyskeratosis congenita and related bone marrow failure syndromes. Blood 112: 3594–3600.
39. Hockemeyer D, Palm W, Wang RC, Couto SS, de Lange T (2008) Engineered telomere degradation models dyskeratosis congenita. Genes Dev 22: 1773–1785.
40. Ahamed M, Kumar A, Siddiqui MK (2006) Lipid peroxidation and antioxidant status in the blood of children with aplastic anemia. Clin Chim Acta 374: 176–177.
41. Patel KJ, Joenje H (2007) Fanconi anemia and DNA replication repair. DNA Repair (Amst) 6: 885–890.
42. Voss P, Siems W (2006) Free Radic Res. 40(12):1339–49
43. Tchirkov A, Lansdorp PM (2003) Role of oxidative stress in telomere shortening in cultured fibroblasts from normal individuals and patients with ataxia-telangiectasia. Hum Mol Genet 12: 227–232.
44. Pereboeva L, Westin E, Patel T, Flaniken I, Lamb L, et al. (2013). DNA damage responses and oxidative stress in dyskeratosis congenita. PLoS One 8: e76473.
45. Ahmed S, Passos JF, Birket MJ, Beckmann T, Brings S, et al. (2008) Telomerase does not counteract telomere shortening but protects mitochondrial function under oxidative stress. J Cell Sci 121: 1046–1053.
46. Kang HJ, Choi YS, Hong SB, Kim KW, Woo RS, et al. (2004) Ectopic expression of the catalytic subunit of telomerase protects against brain injury resulting from ischemia and NMDA-induced neurotoxicity. J Neurosci 24: 1280–1287.
47. Saretzki G (2009) Telomerase, mitochondria and oxidative stress. Exp Gerontol 44: 485–492.
48. Saretzki G, Murphy MP, von Zglinicki T (2003) MitoQ counteracts telomere shortening and elongates lifespan of fibroblasts under mild oxidative stress. Aging Cell 2: 141–143.
49. Westin ER, Aykin-Burns N, Buckingham EM, Spitz DR, Goldman FD, et al. (2011) The p53/p21(WAF/CIP) pathway mediates oxidative stress and senescence in dyskeratosis congenita cells with telomerase insufficiency. Antioxid Redox Signal;14(6):985–97.

Author Contributions

Conceived and designed the experiments: CMG LPB JC RMP LS CPQ IE AG JLGG FVP RP. Performed the experiments: CMG LPB JC RMP LS CPQ IE AG JLGG FVP RP. Analyzed the data: CMG LPB JC RMP LS CPQ IE AG JLGG FVP RP. Contributed reagents/materials/analysis tools: CMG LPB JC RMP LS CPQ IE AG JLGG FVP RP. Wrote the paper: CMG RMP LS JLGG FVP RP.

European Journal of Pharmaceutics and Biopharmaceutics 91 (2015) 91–102

Contents lists available at ScienceDirect

European Journal of Pharmaceutics and Biopharmaceutics

journal homepage: www.elsevier.com/locate/ejpb

Research paper

Development of surface modified biodegradable polymeric nanoparticles to deliver GSE24.2 peptide to cells: A promising approach for the treatment of defective telomerase disorders

Susana P. Egusquiaguirre [a,b,1], Cristina Manguán-García [c,1], Laura Pintado-Berninches [c], Laura Iarriccio [c,d], Daniel Carbajo [e,f,g], Fernando Albericio [e,f], Miriam Royo [e,g], José Luís Pedraz [a,b], Rosa M. Hernández [a,b], Rosario Perona [c,*], Manuela Igartua [a,b,*]

[a] NanoBioCel Group, Laboratory of Pharmaceutics, School of Pharmacy, University of the Basque Country (UPV/EHU), Vitoria-Gasteiz, Spain
[b] Biomedical Research Networking Center in Bioengineering, Biomaterials and Nanomedicine (CIBER-BBN), Vitoria-Gasteiz, Spain
[c] Instituto de Investigaciones Biomédicas CSIC/UAM, IDIPaz and CIBER de Enfermedades Raras CIBERER, Madrid, Spain
[d] Advanced Medical Projects, Madrid, Spain
[e] Biomedical Research Networking Center in Bioengineering, Biomaterials and Nanomedicine (CIBER-BBN), Barcelona, Spain
[f] Institut de Recerca Biomédica, Barcelona, Spain
[g] Unitat de Química Combinatòria, Parc Científic de Barcelona, Barcelona, Spain

ARTICLE INFO

Article history:
Received 7 April 2014
Accepted in revised form 28 January 2015
Available online 7 February 2015

Keywords:
Biodegradable nanoparticles
Cell-penetrating peptides
GSE24.2 peptide
Telomerase reactivation
Dyskeratosis congenita
Polycations

ABSTRACT

The aim of the present study was to develop a novel strategy to deliver intracellularly the peptide GSE24.2 for the treatment of Dyskeratosis congenita (DC) and other defective telomerase disorders. For this purpose, biodegradable polymeric nanoparticles using poly(lactic-*co*-glycolic acid) (PLGA NPs) or poly(lactic-*co*-glycolic acid)-poly ethylene glycol (PLGA-PEG NPs) attached to either polycations or cell-penetrating peptides (CPPs) were prepared in order to increase their cellular uptake. The particles exhibited an adequate size and zeta potential, with good peptide loading and a biphasic pattern obtained in the *in vitro* release assay, showing an initial burst release and a later sustained release. GSE24.2 structural integrity after encapsulation was assessed using SDS–PAGE, revealing an unaltered peptide after the NPs elaboration. According to the cytotoxicity results, cell viability was not affected by uncoated polymeric NPs, but the incorporation of surface modifiers slightly decreased the viability of cells. The intracellular uptake exhibited a remarkable improvement of the internalization, when the NPs were conjugated to the CPPs. Finally, the bioactivity, addressed by measuring DNA damage rescue and telomerase reactivation, showed that some formulations had the lowest cytotoxicity and highest biological activity. These results proved that GSE24.2-loaded NPs could be delivered to cells, and therefore, become an effective approach for the treatment of DC and other defective telomerase syndromes.

1. Introduction

Dyskeratosis congenita (DC) is an inherited bone marrow failure disease characterized for heterogeneous symptoms and multisystemic premature aging. Initially, DC was described by a triad of mucocutaneous features [1,2]. The mucocutaneous features are the first manifestations to appear, already by the age of 10 years followed by the development of bone marrow failure (BMF), present in nearly 80–90% of the diagnosed cases by the age of 30 years [3]. Notably, it has been reported that BMF is the leading cause of early mortality, followed by pulmonary fibrosis (10–15%) and different tumoral malignancies (10%) [4]. Besides, it is noteworthy the considerable variability in the age of onset of DC and the severity of the symptoms [5]. Cells derived from DC patients have short telomeres, especially in highly proliferative tissues such as bone marrow and skin. Telomeres are nucleoprotein complexes located at the ends of linear chromosomes and consist of tandem repeats of simple DNA sequences (TTAGGG in humans) and proteins that interact directly or indirectly with these sequences [6]. Sequence erosion

* Corresponding authors. Instituto de Investigaciones Biomédicas CSIC/UAM, IDIPaz and CIBER de Enfermedades Raras CIBERER, Arturo Duperier, 4, 28029 Madrid, Spain. Tel.: +34 91 585 4463; fax: +34 91 585 4401 (R. Perona). NanoBioCel Group, Laboratory of Pharmaceutics, School of Pharmacy, University of the Basque Country (UPV/EHU), Paseo de la Universidad, 7, 01006 Vitoria-Gasteiz, Spain. Tel.: +34 945 01 3875; fax: +34 945 01 3040 (M. Igartua).
E-mail addresses: rperona@iib.uam.es (R. Perona), manoli.igartua@ehu.es (M. Igartua).
[1] These two authors contributed equally to this work.

http://dx.doi.org/10.1016/j.ejpb.2015.01.028
0939-6411/

of terminal repeats is inherent to each round of genome replication [7]. Accordingly, cells with critically short telomeres enter in senescence and then undergo apoptosis; however, if the cells with short telomeres continue proliferating, it results in genomic instability, leading eventually to malignant tumors [8]. The replenishment of the telomeric repeats is accomplished by the extension of their 3′ ends, through a reaction mediated by the telomerase complex [9]. In humans, the active telomerase complex consists of a minimum of three essential components: hTERT, hTR and dyskerin [10–12]. Thereby, DC appears to be a telomere maintenance disorder characterized by a defective telomerase causing premature senescence in DC patients.

An important concern is the absence of a specific treatment, since unfortunately there are no targeted therapies for DC. Conventional treatments are intended to palliate the haematopoietic function, as BMF is the main cause of premature mortality [13,14]. Therefore, taking into account the lack of a specific strategy, many efforts are being developed in research to provide an effective cure for the disease. For this purpose, it has been previously described that the peptide GSE24.2 corresponding to an internal sequence of dyskerin is able to reactivate the telomerase, and thus, increase its activity in DC patient cells [15] in F9A353V mouse cells carrying the most frequent human mutation [16] and in the normal VA13 cells [15]. Furthermore, the expression of GSE24.2 rescues X-linked DC cells from premature senescence, suggesting that this peptide could be considered a new therapeutic approach for defective telomerase syndromes such as DC [15]. Recently GSE24.2 has been approved by EMA as an orphan drug for the treatment of DC. However, despite its promising pharmacological profile and great therapeutic value, GSE24.2, like most of the therapeutic peptides [17,18], possesses a poor stability and a high susceptibility to degradation, causing the loss of their therapeutic activity and a short circulation half-life which limits the chances to reach its target site. Additionally, it is interesting to note that the intracellular delivery of GSE24.2 peptide is one of the key requirements for its therapeutics application, so in order to overcome all these shortcomings, in this manuscript we describe the encapsulation of GSE24.2 into biodegradable polymeric nanoparticles (NPs) to construct a new drug delivery system. For this purpose, PLGA and PLGA-PEG NPs were elaborated. PLGA copolymer was chosen because of its excellent properties [19] and PLGA-PEG block copolymer because it is known to prolong the blood circulation time of polymeric NPs, avoiding the NPs from being recognized by the mononuclear phagocyte system (MPS) thanks to the shielding effect of the hydrophilic polymer chains of PEG [20]. Therefore, these two approaches were compared. Furthermore, the surface properties of nanoparticles play a crucial role in their interactions with cells and intracellular transport, fact that affects the efficacy of the encapsulated substance [21]. In such sense, different attempts have been made with the intention to modify the surface of nanoparticles, and thus, enhance their uptake into cells. On the one hand, different polycations such as polyethyleneimine (PEI) [22] or dextran (DX) [23] were chosen to modify the surface of PLGA NPs in order to obtain positively charged particles, aiming to improve their binding potential with negatively charged cell membranes and enhance their cellular uptake. On the other hand, the conjugation of nanoparticles with certain peptides that possess the ability to rapidly translocate across the cell membrane and enable the delivery of their payload to the cytoplasm or nucleus is another promising approach that seems to overcome cellular barriers for intracellular drug delivery [24]. It has been previously reported that, nonnatural γ-proline derived peptides, with amphipatic character, offer a wide range of combinations by modifying their side chain structure, with the capacity of cellular internalization via different mechanisms [25].

Taking all this together, the focus of the present study was to design biodegradable polymeric nanoparticles, elaborated with the polymer poly(lactic-*co*-glycolic) acid (PLGA) or poly(lactic-*co*-glycolic acid)-poly ethylene glycol (PLGA-PEG), either coated with polycations or with different cell penetrating peptides (CPPs), as a platform to deliver GSE24.2 peptide to cells. This promising approach may provide a new strategy for the treatment of defective telomerase syndromes such as DC.

2. Materials and methods

2.1. Materials

The polymer poly(D,L-lactide-co-glycolide) PLGA (Resomer RG® 503) 50:50 (lactic/glycolic %), with a molecular weight of 33.9 kDa and an intrinsic viscosity of 0.32–0.4 dl/g and the block copolymer poly(D,L-lactide-co-glycolide)-poly(ethylene)glycol PLGA-PEG (Resomer RGP® d50155) with a molecular weight of 50 kDa and an intrinsic viscosity of 0.51 dl/g, was purchased from Boehringer Ingelheim (Ingelheim, Germany). Dichloromethane (DCM) HPLC grade as the organic solvent, 2-propanol, poly-ethylene-glycol 400 (PEG 400) and paraformaldehyde were purchased from Panreac (Barcelona, Spain). The surfactant used in the emulsification process was poly(vinyl alcohol) (PVA, with an average MW of 30–70 kDa, 87–90% hydrolysis degree), as well as polyethyleneimine (PEI with a MW of 25 kDa, branched), diethylaminoethyl (DEAE) Dextran hydrochloride (with a MW of 500 kDa), D-trehalose (TRH with a MW of 378.33 g/mol), (1-ethyl-3-(3-dimethylaminopropyl)-carbodiimide) (EDC), N-hydroxysulfosuccinimide (Sulfo-NHS) and fluorescein were obtained from Sigma–Aldrich (Barcelona, Spain). DMEM cell culture medium and phosphate buffered saline (PBS) were obtained from Gibco, Invitrogen Life Technologies, (Germany). The reagents used in SDS–PAGE were obtained from Sigma and from Bio-Rad. All other chemicals and reagents were of analytical grade and purchased from local suppliers.

Protected amino acids were obtained from Polypeptide (Strasbourg, France) and MBHA resin (0.63 mmol/g) was supplied by Novabiochem AG. HOBt·H2O was obtained from Iris Biotech (Marktredwitz, Germany). N,N′-diisopropylcarbodiimide (DIC) and 5(6)-carboxyfluorescein (CF) were obtained from Aldrich (Milwaukee, WI). Trifluoroacetic acid was supplied by Fluorochem (Hadfield, UK). All commercial reagents and solvents were used as received. HF was obtained from Praxair Inc. (Danbury, CT), and related equipment was obtained from Peptide Institute Inc., Minoh, Osaka, Japan.

2.2. Methods

2.2.1. GSE24.2 peptide production and purification

Rosetta-2-gami cells were transformed with pGATEVGSE24.2 and lysates prepared as described [26]. The fusion protein was purified with glutathione-Sepharose and purity was analyzed by gel electrophoresis.

2.2.2. γ-Peptide synthesis

γ-Peptide synthesis was performed using a combined Fmoc/Boc/Alloc solid phase strategy on MBHA resin following a modified protocol described previously [25]. Washings between deprotection, coupling and subsequent deprotection steps were carried out with DMF (5 × 1 min) and DCM (5 × 1 min) using 10 mL solvent/g resin for each wash. Peptide backbone was elongated by the γ-amino group of (2S,4S)-4-Fmoc-amino-1-Boc-pirrolidin carboxylic acid [Fmoc-Amp(Boc)-OH, (3 eq)] or (2S,4S)-4-Fmoc-amino-1-Boc-pirrolidin carboxylic acid [Fmoc-Amp(Alloc)-OH, (3 eq)] and couplings were carried out with DIC (3 eq) and HOBt

(3 eq) in DMF for 2 h using 100 mg of MBHA resin for each peptide. The resin was washed with DMF (5 × 1 min) and DCM (5 × 1 min) after each coupling. Couplings were monitored by the Kaiser test [27].

In case of homomers, whose sequences comprised monomers that have the same side chain attached at the α-amino, Fmoc-Amp(Boc)-OH was used to build the proline backbone. Then, Boc protecting groups were removed and the side chains were introduced. On the other hand, when synthesizing heteromers, whose sequences contain monomers with diverse side chains along the sequence, both Fmoc-Amp(Boc)-OH and Fmoc-Amp(Alloc)-OH were coupled sequentially in the desired order by the γ-amino group. Once the alternate Boc/Alloc protected peptide backbone had been built, the Boc protecting groups were removed and the corresponding side chains were added simultaneously. Then, the Alloc protecting groups were removed and the second side chains were added. In all cases the side chains were introduced through acylation, reductive amination or guanidilation as described previously [25]. In the synthesis of CPP1, two pieces of Fmoc-8-amino-3,6-dioxaoctanoic acid (3 eq) were first coupled to the resin using the same coupling reagents mentioned above. Peptide synthesis then continued for CPP1 as described for the other compounds.

Once the synthesis was finished, Fmoc protecting group of the amino N-terminal was eliminated and 5(6) carboxyfluorescein incorporated using PyOAP/HOBt/DIEA (5 eq/5 eq/5 eq) coupling agent system. After 20 min treatment with 20% piperidine/DMF peptides were cleaved from the solid support by acidolysis with HF [25,28].

2.2.2.1. N^{α}-acyl side chain introduction. After removing of the corresponding N^{α}-protecting groups, acylation of the α-amino groups was carried out using RCOOH (5 eq for each amine), DIC (5 eq for each amine) and HOBt (5 eq for each amine) in DMF for 2 h at 25 °C. The resin was washed with DMF (5 × 1 min) and DCM (5 × 1 min). The acylation was monitored by the chloranil test.

2.2.3. Preparation of polymeric NPs

The PLGA and PLGA-PEG nanoparticles (NPs) loaded with GSE 24.2 were prepared by a modified water-in-oil-in-water (w_1/o/w_2) double emulsion solvent evaporation method previously reported [29]. In brief, a primary emulsion (w_1/o) was formed by emulsifying 100 μl of a 0.5% (w/w) GSE24.2 aqueous solution with 2.5% (v/v) of PEG 400, in 2 ml of a dichloromethane (DCM) solution containing 100 mg of the polymer using a probe sonicator (Branson Ultrasonic Sonifier® 250) for 30 s in an ice bath. The primary emulsion was thereafter poured into 10 ml of 5% (w/v) polyvinyl alcohol (PVA) aqueous solution and sonicated for further 60 s to form a double emulsion (w_1/o/w_2). The secondary emulsion was then diluted into 20 ml of 2% (v/v) isopropanol and stirred for 2 h to allow the organic solvent to evaporate. The NPs were then collected by ultracentrifugation at 25,000*g* for 20 min, 4 °C (Sigma 3-30K) and washed thrice to remove the excess surfactant. Prior to lyophilization (LyoBeta 15, Telstar, Tarrasa, Spain), the solid NPs were re-suspended in a cryoprotectant solution of trehalose 15% (w/w).

2.2.3.1. Cationic polymeric NPs. Cationic NPs were elaborated like the uncoated NPs and keeping the same conditions but dissolving 1.5% (w/w) of dextran (DX) in the aqueous phase or 1.3% (w/w) of polyethyleneimine (PEI) in the organic phase.

2.2.3.2. Conjugation of CPPs to polymeric NPs. For covalent attachment of the CPPs onto the NPs surface, a surface activation method by means of the EDC/sulfo-NHS chemistry was carried out [18,30]. Briefly, 100 mg of the NPs obtained above, prior to lyophilization, were suspended in 5 ml of phosphate buffered saline (PBS; 0.02 M, pH 7.4). While gentle agitation in a magnetic stir plate, 250 μl of EDC solution (1 mg/ml) and 250 μl of sulfo-NHS (1 mg/ml) in 0.02 M PBS were added drop wise to the above NPs suspension. The sample was left to stir for 4 h at room temperature on a magnetic stir plate. Then, the unreacted EDC and sulfo-NHS were removed by ultracentrifugation at 25,000*g* for 15 min at 4 °C, and the activated NPs were recovered. For the coupling of the CPPs, the activated NPs were re-suspended in 2 ml of PBS (0.02 M; pH 7.4) followed by the addition of 50 μl of the CPP solution (1 mg/ml) in PBS (0.02 M; pH 7.4) drop wise and while gentle agitation. The NPs suspension was left to stir for another 2 h at room temperature on a magnetic stir plate and then incubated overnight at 4 °C. Finally, the unconjugated CPP was removed the next day by ultracentrifugation. The pellet obtained was re-suspended in 15% (w/w) of trehalose solution and lyophilized.

2.2.4. Physicochemical characterization of polymeric NPs

The mean nanoparticle diameter (*Z*-average), polydispersity index (PDI) and zeta potential were determined using a Zeta Sizer Nano ZS apparatus (Malvern Instruments Ltd., UK). The samples were re-dispersed in distilled water at 25 °C and diluted to a suitable density. The measurements for each sample were performed in triplicate and the mean values were reported. Scanning electron microscopy (SEM; Jeol® JSM-7000F) was used for the morphological examination of the NPs.

2.2.5. GSE24.2 loading and surface adsorbed peptide

GSE24.2 loading and surface adsorbed peptide (SAP) were estimated using the Lowry assay, by the micro-BCA technique (Pierce, Thermo Scientific) [31]. Briefly, 1 mg of freeze-dried NPs was incubated in a rotary shaker at 37 ± 0.5 °C during 30 min with either 0.2 M sodium hydroxide solution (NaOH) or phosphate-buffered saline (PBS) (pH 7.4, 1 M) for the peptide loading or SAP determination, respectively. The GSE24.2 loading was estimated by extracting GSE24.2 from NPs after disintegration of the polymer with 0.2 M NaOH, whereas SAP was analyzed in the supernatant obtained after the centrifugation of the samples at 25,000*g* for 10 min. The peptide loading was represented in terms of the μg of GSE24.2 per mg of freeze-dried NPs and SAP represents the percentage of total protein loaded that is present on the NPs surface.

2.2.6. In vitro release of GSE24.2 from polymeric NPs

To determine the rate of GSE24.2 released from the NPs, an *in vitro* release study was conducted. Approximately 10 mg of freeze-dried NPs were incubated with 1 ml of phosphate-buffered saline (PBS, pH 7.4, 1 M) in a rotary shaker at 37 ± 0.5 °C. At specified time intervals, samples were centrifuged at 25,000*g* for 10 min in order to obtain free GSE24.2 in the supernatant. The clear supernatant was withdrawn and the NPs were re-suspended with fresh buffer. Assays were performed in triplicate.

2.2.7. Determination of GSE24.2 structural integrity

In order to evaluate the effects of the encapsulation process on the structural integrity of GSE24.2, sodium dodecyl sulfate–polyacrylamide gel electrophoresis (SDS–PAGE) was performed. Briefly, GSE24.2 was extracted from NPs (2 mg) by treating them with 50 μl of DMSO. Thereby, the extracted GSE24.2, the native GSE24.2 and a molecular mass standard were loaded onto a vertical slab gel (12% SDS-polyacrylamide) and subjected to electrophoresis at 120 mV for 2 h in a Tris/glycine/SDS buffer, using a Bio-Rad mini protean II dual slab cell (Bio-Rad, Hemel Hempstead, UK). The peptide band was visualized by staining the gels with Coomassie brilliant blue reagent (0.12% w/v) in water:acetic acid:methanol (75:5:20) and destained in water:acetic acid:methanol (50:10:40), which was changed periodically.

2.2.8. Cell viability and uptake studies of the polymeric NPs

2.2.8.1. Cell lines and culture conditions. Human epithelial cervix carcinoma cells (HeLa) and primary lung epithelial cells (VA13) were from ATCC. Primary murine embryonic fibroblasts (MEFs) were obtained from 12 days embryos of Balbc pregnant mice and F9A353V cells from Dr. Phil Mason [16]. Cells were cultured in Dulbecco's modified Eagle medium (DMEM) supplemented with 10% (v/v) fetal bovine serum (FBS) and nonessential amino acids 1% (v/v) L-glutamine 2 mM, 1% (v/v) fungizone, 40 μg/ml gentamicin. F9 A353V cell medium was additionally supplemented with 10% sodium bicarbonate. Cells were grown in 75 cm^2 flasks in a humidified incubator at 37 °C and 5% CO_2 atmosphere.

2.2.8.2. Cell viability assays. The cytotoxicity of the different NP formulations was evaluated on HeLa and MEF cell lines, which were seeded at a density of 2×10^4 or 1×10^4 cells per well in a 96-well culture plate, respectively, and allowed to attach overnight in a humidified incubator at 37 °C and 5% CO_2 atmosphere. Increasing concentrations of NPs (0.625; 1.25: 1.875 and 2.5 mg of NPs/ml) were added to the cells and further incubated at 37 °C and 5% CO_2 atmosphere for 48 h. Following the exposure to the NPs, the medium was removed, the cells were washed twice with 1× PBS and cell viability determined using a crystal violet staining method followed by colorimetric assay, as previously described [32].

2.2.8.3. In vitro cellular uptake of polymeric NPs. In order to visualize the internalization of NPs, these were labeled with fluorescein (λ = 515 nm) as a fluorophore and visualized in a fluorescence microscope. Fluorescein-labeled unmodified and cationic nanoparticles were prepared by the double emulsion solvent evaporation method described above, where fluorescein was incorporated into the aqueous internal phase [33]. Likewise, the CPPs used for the elaboration of the NPs were conjugated to carboxyfluorescein. The ability of NPs internalization was assessed *in vitro* in HeLa cell line. Additionally, to confirm the localization of NPs, cell nuclei were stained with DAPI. Briefly, HeLa cells were grown onto coverslips in 24-well culture plates at a density of 5×10^5 cells per well, and allowed to attach overnight in a humidified incubator at 37 °C and 5% CO_2 atmosphere. The following day, the cells were treated with 5 mg of each NP formulation per well and incubated at 37 °C and 5% CO_2 atmosphere. At different incubation time points (4 h, 8 h, 24 h, 48 h and 72 h), the medium was removed, the cells were washed twice with 1× PBS and fixed with 4% paraformaldehyde solution for 15 min at room temperature. Finally, fixed cells were washed twice with 1× PBS and mounted in Vectashield mounting medium for fluorescence (Vector Laboratories, Inc.) and DAPI to stain cell nucleus.

Confocal images were acquired using an inverted Zeiss LSM 710 laser scanning microscope. Type, numerical aperture and magnification objective lenses: plan-apochromatic 63x/1.40 Oil DIC M27. Zoom 1: Sequential scanning mode was used to avoid crosstalk between channels. Images were processed using Zen 2009 software and Adobe Photoshop CS and exported to TIFF and mounted using Adobe Photoshop CS. Maximum intensity projections are shown in the corresponding figure.

2.2.9. Western blot

Whole-cell extracts were prepared essentially as described previously [32]. Western blotting was performed using standard methods [32]. Protein concentration was measured by using the Bio-Rad protein assay (500-0006; Bio-Rad). Antibodies used were Phospho-Histone H2A.X Ser139 (2577; Cell Signaling) and Monoclonal Anti-α-tubulin (T9026; Sigma–Aldrich).

2.2.10. Telomeric repeat amplification protocol (TRAP) assay

Telomerase activity was measured using the TRAPeze kit (Intergen, Purchase, USA) according to the manufacturer's recommendations. TRAP assay activity was normalized for total protein concentration [34].

3. Results and discussion

Biodegradable nanoparticles have been widely described for their use as targeting delivery systems for decades [19]. These particulate systems are able to release their payloads over prolonged periods of time, which makes them attractive candidates for drug delivery. In recent years, many studies have been accomplished to investigate whether the surface modification of the particles could influence their cellular uptake, and therefore, increase the internalization of NPs into cells [35,36].

In the current study, our interest was to explore the uptake capacity of PLGA and PLGA-PEG NPs coated with various surface modifiers; in particular we examined the effect of polycations and cell penetrating peptides (CPPs). Coating NPs with polycations provide them a positive charge, being these cationic NPs more likely to bind to the negatively charged cell membranes, and thereby

Table 1
Physicochemical characteristics, peptide loading (μg GSE24.2/mg freeze-dried NPs) and surface adsorbed peptide (SAP) of PLGA and PLGA-PEG NPs, uncoated or coated with polycations or CPPs.

Formulation	Size (nm)	PDI	Zeta potential (mV)	Peptide loading (μg GSE24.2/mg NPs)	SAP%
PLGA NPs	231.2	0.126	−20.10	2.35	22.16
PLGA-PEG NPs	258.5	0.392	−20.70	2.65	18.48
PEI-PLGA NPs	221.9	0.144	30.40	2.08	17.03
PEI-PLGA-PEG NPs	256.4	0.248	27.80	2.71	14.00
DX-PLGA NPs	223.2	0.095	24.40	2.15	12.32
DX-PLGA-PEG NPs	260.2	0.301	22.40	2.32	13.04
CPP1-PLGA NPs	209.6	0.060	−19.60	1.11	5.89
CPP1-PLGA-PEG NPs	172.6	0.211	−20.70	1.66	6.08
CPP2-PLGA NPs	209.5	0.058	−20.60	0.95	5.54
CPP2-PLGA-PEG NPs	199.8	0.335	−21.60	1.80	5.91
CPP3-PLGA NPs	212.1	0.146	−19.00	1.78	6.77
CPP3-PLGA-PEG NPs	216.3	0.347	−23.20	1.65	6.95
CPP4-PLGA NPs	225.2	0.145	−18.90	1.41	2.89
CPP4-PLGA-PEG NPs	250.2	0.317	−22.20	1.49	7.44
CPP5-PLGA NPs	202.9	0.084	−16.40	0.80	5.66
CPP5-PLGA-PEG NPs	170.7	0.201	−19.00	1.69	8.92
CPP6-PLGA NPs	225.9	0.147	−17.00	0.99	8.32
CPP6-PLGA-PEG NPs	140.6	0.086	−16.40	1.73	6.22

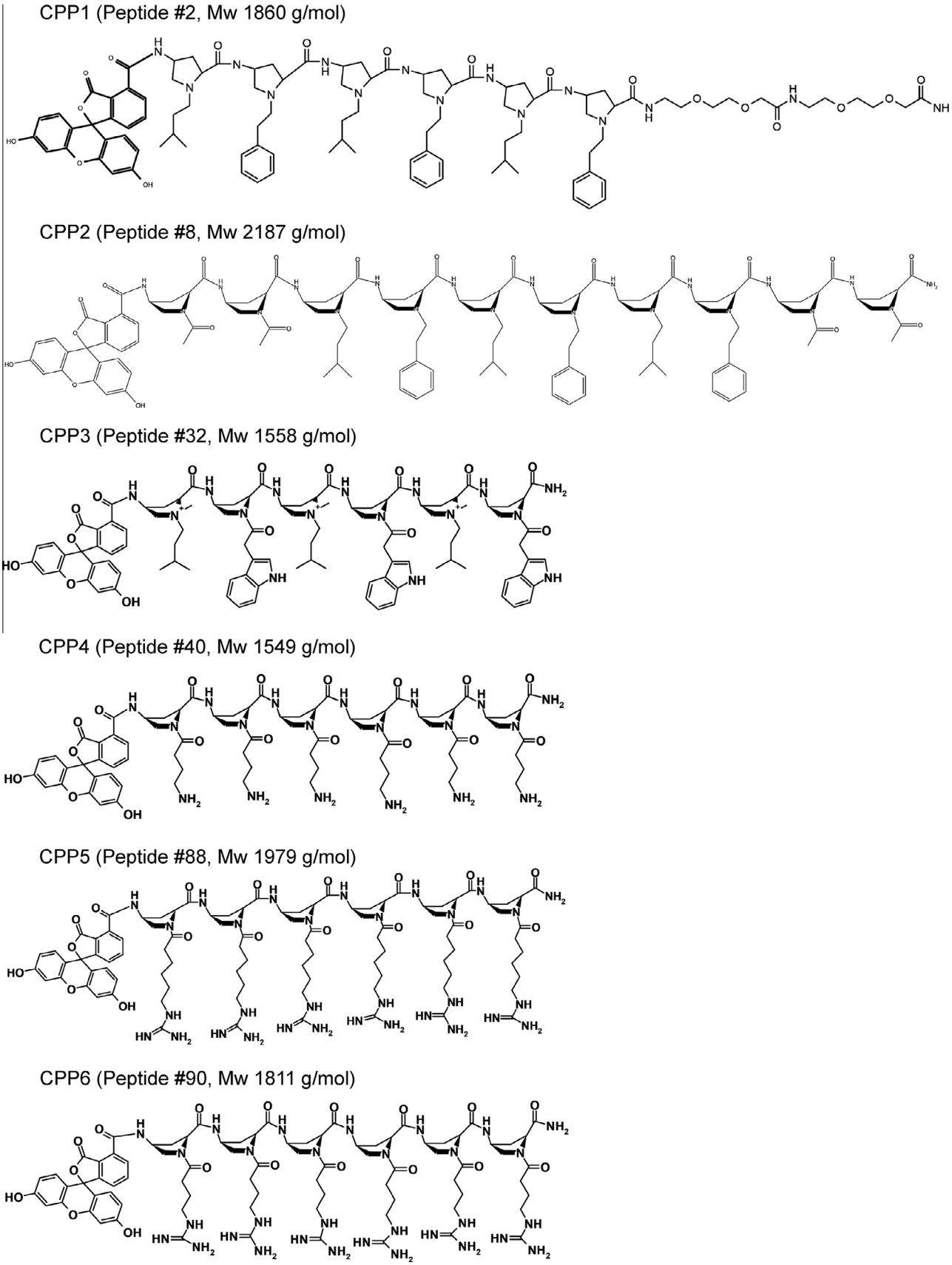

Fig. 1. Struture of γ-aminoproline monomer based γ-peptides labeled with 5(6)-carboxyfluorescein. Chemical structure and molecular weight of γ-cell penetrating peptides.

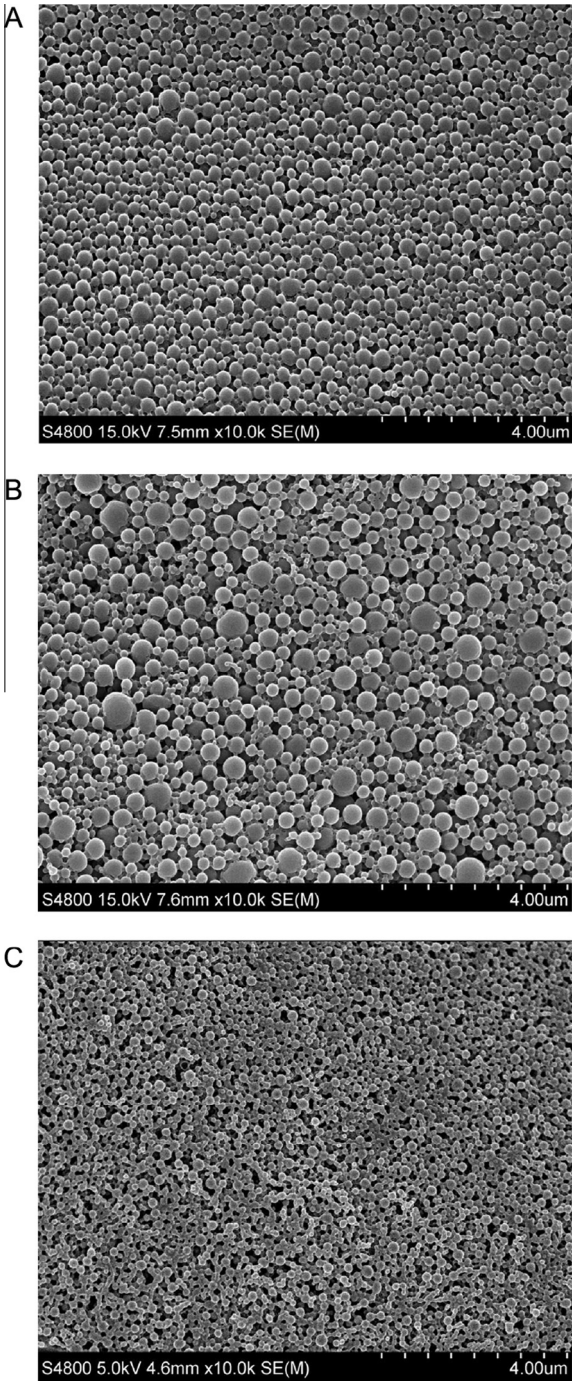

Fig. 2. Morphology of PLGA NPs loaded with GSE24.2 peptide obtained by scanning electron microscopy (SEM). (A, B and C) Show micrographs from PEI-PLGA, CPP5-PLGA and CPP6-PLGA-PEG NPs, respectively. Micrographs show small spheric particles with a smooth and uniform surface and with a nanometric size.

enhance their entry into cells. Furthermore, CPPs are formed by sequences of amphipatic amino acids enabling them to possess a translocation capacity across the cell membranes, and mediating the penetration of CPP-coated NPs intracellularly [37]. Thus, these CPPs appear to be exceptional candidates as transporters in drug delivery. Therefore, the tested NP types included uncoated PLGA and PLGA-PEG NPs and coated with the previously mentioned cationic polymers or with the different CPPs [25]. Fig. 1 shows the molecular weights and structures of the different CPPs used in this study.

3.1. Physicochemical characterization of NPs

The NPs were manufactured using the water-in-oil-in-water ($w_1/o/w_2$) double emulsion solvent evaporation method and modified with the different surface modifiers tested. Once achieving such NPs, these were characterized by particle size, zeta potential and surface morphology. The results obtained for the physicochemical characterization of the NPs are listed in Table 1.

3.1.1. Particle size

DLS (Dynamic Light Scattering) technique was used to measure the particle size of the NPs, after freeze-drying, revealing an average size around 200 nm, and exhibiting PDI values lower than 0.2. As shown in Table 1, there was not a significant change in the size of particles by adding different surface modifiers to the NPs, and according to the PDI of all samples, the formulations displayed a narrow size distribution, with a monomodal appearance.

3.1.2. Zeta potential

While all the NP formulations tested exhibited comparable size distributions, they differed significantly in their surface charge (Table 1). The surfaces of the unmodified polymeric NPs possessed a negative charge due to the ionization of the carboxyl groups in distilled water, while the addition of the polycations to the NPs dramatically changed the zeta potential to a strong positive charge, especially for PEI and DX modified NPs, indicating a successful coating of the NPs. As mentioned above, polymeric NPs carrying a cationic charge on their surface interact with negatively charged cell membranes through electrostatic interactions, and thus facilitate their cellular uptake. The mechanism suggested for the enhanced uptake could be explained by interactions through electrostatic attraction between the cationic NPs and anionic cell surfaces mediating binding and subsequent internalization [38]. Contrarily, CPP-coated polymeric NPs did not change the surface charge of the particles to positive; resulting in negative particles (Table 1).

3.1.3. NPs morphology

To further analyze the characteristics of the particles, morphology of the various NP formulations was also investigated using Scanning Electron Microscopy (SEM). As an example, a micrograph of PEI-PLGA, CPP5-PLGA and CPP6-PLGA-PEG NPs is shown in Fig. 2. The SEM images revealed a uniform spherical arrangement

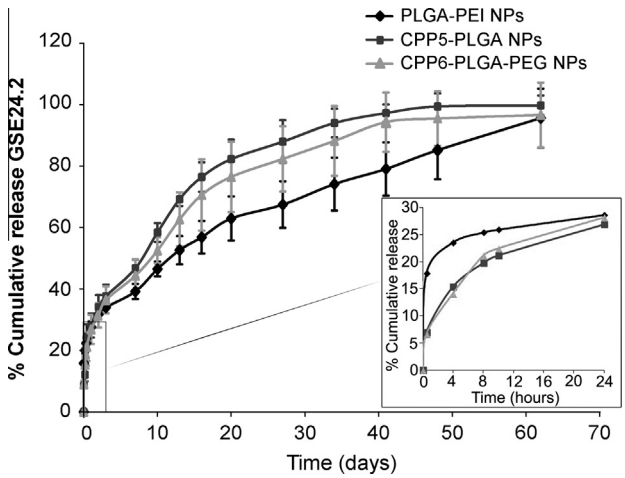

Fig. 3. *In vitro* release profile of PLGA NPs loaded with GSE24.2 peptide. The different nanoparticles loaded with GSE24.2 peptide were incubated in phosphate-buffered saline (PBS; pH 7.4, 1 M) and the amount of released peptide, represented as a percentage, was measured at specified time intervals.

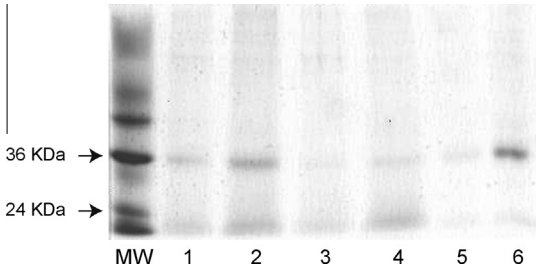

Fig. 4. Studies of structural integrity of the nanoparticles by SDS–PAGE. SDS–PAGE analysis of nanoparticles: line MW: molecular weight markers; lines 1–6: GSE24.2 peptide extracted from nanoparticles, corresponding to PEI-PLGA, CPP1-PLGA, CPP2-PLGA-PEG, CPP4-PLGA-PEG, CPP5-PLGA and CPP6-PLGA-PEG NPs (nanoparticle amount equivalent to 10 μg of GSE24.2 peptide).

with a monodispersed size distribution. Therefore, no breakage, tear or aggregation of the nanoparticles was noticed. The particle size measured from the SEM images was in good agreement with that measured by DLS, being around 200 nm.

3.2. Peptide loading and surface adsorbed GSE24.2 peptide in NPs

Table 1 shows the peptide loading in terms of μg of GSE24.2 per mg of freeze-dried NPs and the surface adsorbed peptide (SAP). Uncoated and cationic NP formulations exhibited values of drug loading around 2–2.5 μg GSE24.2/mg NPs, however, the incorporation of CPPs resulted in a lower drug loading, for NP either elaborated with PLGA or with PLGA-PEG copolymers, resulting in values around 1–1.5 μg GSE24.2/mg NPs. This low drug loading in general could be explained by the low molecular weight of GSE24.2 peptide (34 kDa) and its high hydrosolubility, which consequently makes it be easily released to the external aqueous media during the encapsulation process [39]. Additionally, this important decrease in the drug loading of the NPs conjugated to the CPPs is probably due to the long incubation period during the process of surface activation with EDC/sulpho-NHS. Furthermore, the surface adsorbed peptide (SAP) was around 20% for uncoated or cationic NPs and as expected, CPP-modified NPs resulted in lower SAP values (around 5%).

3.3. In vitro release profile of polymeric NPs

The *in vitro* cumulative release of GSE24.2 from polymeric NPs formulated with and without the surface modifiers tested was studied. For all formulations, GSE24.2 release displayed a biphasic profile, with an initial burst release in the first 30 min, that may be attributed to the fraction of peptide adsorbed on the NPs surface, which is rapidly released from the carrier material into the aqueous phase by diffusion; followed by a second slow and sustained release phase, during which the water molecules penetrate into the polymeric matrix and degrade it continuously, leading to a slow diffusion of nearly 100% of the loaded GSE24.2 in the next 60 days, amount of peptide which is localized in the core of the NPs and is released through the porous matrix to the medium. The results indicate that the NPs, either unmodified or modified with polycations or CPPs, could be useful as a controlled delivery system for the treatment of defective telomerase disorders. As an example, the *in vitro* release profile of cationic PEI-PLGA NPs as well as CPP5-PLGA NPs and CPP6-PLGA-PEG NPs is given in Fig. 3.

3.4. SDS–PAGE: structural integrity of GSE24.2 after encapsulation

During GSE24.2 encapsulation into NPs, the peptide is exposed to mechanical and chemical treatments which could contribute to a loss of structural integrity, and thus peptide denaturation and deactivation following entrapment into NPs are of great concern. Accordingly, the structural integrity of the peptide after NPs preparation was assessed. Polyacrylamide gel electrophoresis studies (Fig. 4) revealed a visible band for the GSE24.2 extracted from NPs (unmodified or incorporating the surface modifiers tested) at around 34 kDa with no additional bands indicating the presence of aggregates or fragments. This data suggest that the structural integrity of the GSE24.2 was not affected by the entrapment procedure and the peptide remained unaltered after being released.

3.5. Cellular viability study: cytotoxicity

The cytotoxicity was investigated with the aim of studying the effect of the different NPs formulations on the viability of cells, and to establish the range of NPs concentrations used for further experiments and those suitable to be used in the functional studies. Two different cell lines were chosen, since cytotoxicity is dependent on the cell type [40,41], primary mouse cells (HeLa cells) and tumoral cells (MEF cells). The toxicity was checked over 48 h to increasing concentrations of the different formulations of empty NPs, and then viability was estimated by crystal violet assay.

Once the viability was determined for each formulation in at least two different experiments performed by triplicates, we determined the IC50 for each formulation and cell line. As can be observed in Table 2, all the formulations were, in general, but not always, more toxic with MEF cells, since these are primary fibroblasts and, consequently more sensitive to foreign substances (such as NPs) than HeLa cells.

The cell viability was not affected by unmodified PLGA NPs at any concentration, showing viability values of nearly 100%. Although the PLGA-PEG NPs were not toxic for HeLa cells, they displayed an IC50 value around 1.56 mg for MEF cells. When incorporating PEI on the surface of NPs, we observed an increase in cytotoxicity, compared to untreated cells; reaching IC50 values around 1.84 and 1.53 mg for HeLa cells, and 1.38 and 1.53 mg for MEF cells, for PEI-PLGA and PEI-PLGA-PEG NPs, respectively. Thereby, PEI NPs became more cytotoxic as the concentration of the NPs was increased, showing a dose-dependent toxicity, but at our range of nanoparticle concentrations used for the experiments they were not toxic [42]. Regarding the CPPs modified NPs, all the formulations showed a similar toxicity profile with slight differences, but maintaining a moderate viability level, especially for HeLa cell

Table 2
Cytotoxicity of uncoated PLGA and PLGA-PEG NPs and coated with polycations or CPPs, and selection of adequate formulations for biological experiments.

Formulation	IC50 HeLa	IC50 MEFs	Discarded	Assay DC cells
PLGA NPs	>IC50	>IC50		YES
PLGA-PEG NPs	>IC50	1.56 mg		YES
PEI-PLGA NPs	1.84 mg	1.38 mg		YES
PEI-PLGA-PEG NPs	1.53 mg	1.53 mg		YES
DX-PLGA NPs	0.75 mg	0.42 mg	Toxic	NO
DX-PLGA-PEG NPs	2.18 mg	0.38 mg	Toxic	NO
CPP1-PLGA NPs	>IC50	1.98 mg		YES
CPP1-PLGA-PEG NPs	>IC50	1.35 mg		YES
CPP2-PLGA NPs	>IC50	1.88 mg		YES
CPP2-PLGA-PEG NPs	2.33 mg	1.25 mg		YES
CPP3-PLGA NPs	>IC50	>IC50		YES
CPP3-PLGA-PEG NPs	2.25 mg	2.02 mg		YES
CPP4-PLGA NPs	>IC50	>IC50		YES
CPP4-PLGA-PEG NPs	>IC50	2.13 mg		YES
CPP5-PLGA NPs	>IC50	1.66 mg		YES
CPP5-PLGA-PEG NPs	>IC50	1.88 mg		YES
CPP6-PLGA NPs	>IC50	>IC50		YES
CPP6-PLGA-PEG NPs	>IC50	>IC50		YES

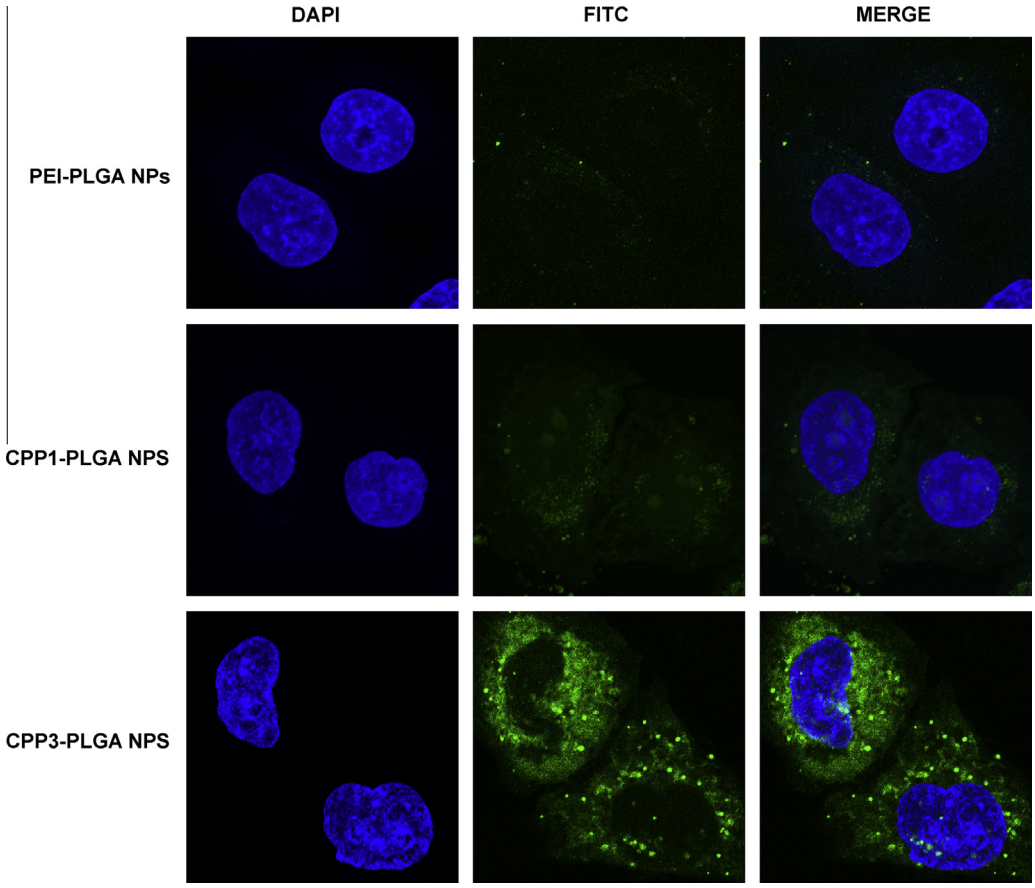

Fig. 5. Internalization of PLGA nanoparticles into HeLa cells. PEI-PLGA, CPP1-PLGA and CPP3-PLGA nanoparticles were fluorescently labeled either by conjugating them to carboxyfluorescein-attached CPPs or by encapsulating fluorescein in PEI-PLGA NPs. Subsequently, HeLa cells were treated with the NPs and at different incubation time points Confocal Laser Scanning Microscopy (CLSM) images were obtained. Showed are the images obtained with the three nanoparticle formulations 24 h after incubation. (For interpretation of the references to color in this figure legend, the reader is referred to the web version of this article.)

Table 3
Time course of internalization rate of unmodified and modified PLGA and PLGA-PEG NPs.

Formulation	4 h	8 h	24 h	48 h	72 h
PLGA NPs	+	+	+	–	–
PLGA-PEG NPs	–	+	–	–	–
PEI-PLGA NPs	+	++	++	+	+
PEI-PLGA-PEG NPs	+	+	+	+	+
CPP1-PLGA NPs	+++	+++	+++	+++	+++
CPP1-PLGA-PEG NPs	+++	+++	+++	+++	+++
CPP2-PLGA NPs	+++	+++	+++	+++	+++
CPP2-PLGA-PEG NPs	++	++	+++	+++	+++
CPP3-PLGA NPs	+++	+++	++	+	+
CPP3-PLGA-PEG NPs	+++	+++	+++	+++	+++
CPP4-PLGA NPs	+	+	+	+	–
CPP4-PLGA-PEG NPs	+	+	+	++	+
CPP5-PLGA NPs	++	++	++	+	+
CPP5-PLGA-PEG NPs	+	+	+	+	+
CPP6-PLGA NPs	++	++	++	++	+++
CPP6-PLGA-PEG NPs	++	+	+	+	++

(–) No internalization.
(+) Low internalization.
(++) Medium internalization.
(+++) High internalization.

line. As expected, there was a slight decrease of the viability as the amount of the NPs administered was increased. On the other hand, NPs incorporating DX were 10-fold more toxic than those modified with PEI, in both cell lines. PLGA and PLGA-PEG are known to be non toxic to cells [43], on the contrary, polycations are reported to induce certain cell damage due to their charge interaction with cell membranes [44]. Hence, we could summarize that surface modified polymeric NPs tested on both cell lines display a dose-dependent cytotoxicity effect and that their toxicity depends on the cell type. Based on these results, toxic formulations (DX-PLGA and DX-PLGA-PEG NPs) were dismissed, and the remaining formulations were used for the following experiments.

3.6. Intracellular uptake of polymeric NPs in HeLa cell line

In order to evaluate whether the incorporation of the surface modifiers (PEI or CPPs) into PLGA and PLGA-PEG NPs could affect their entry into HeLa cells, intracellular uptake studies were performed. For these studies, the different NP formulations were fluorescently labeled either by conjugating them to carboxyfluorescein-attached CPPs or by encapsulating fluorescein when no CPPs were used. Subsequently, HeLa cells were treated with the NPs and at different incubation time points (4 h, 8 h, 24 h, 48 h and 72 h) Confocal Laser Scanning Microscopy (CLSM) images were obtained (Fig. 5).

Table 3 represents the time course of internalization rate of the different NP formulations in terms of fluorescence, from no internalization at all (–) to a high internalization (+++). As can be seen in Table 3, unmodified PLGA and PLGA-PEG NPs were not very efficiently internalized, but the addition of PEI to the formulations, especially to PLGA NPs at 8 and 24 h slightly increased the penetration of the NPs into the cells. However, as expected, a remarkable improvement in the internalization of the NPs was observed when

A

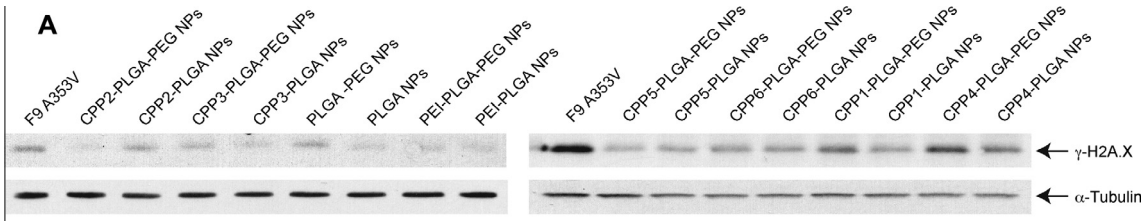

B

Formulation	Damage relative to F9 A353V	% DNA damage signal inhibition
NON	1.00	0.0
PLGA NPs	**0.80**	**20.1**
PLGA-PEG NPs	0.89	11.4
PEI-PLGA NPs	**0.62**	**38.2**
PEI-PLGA-PEG NPs	0.79	20.7
CPP1-PLGA NPs	**0.45**	**54.6**
CPP1-PLGA-PEG NPs	0.77	22.8
CPP2-PLGA NPs	0.81	18.9
CPP2-PLGA-PEG NPs	**0.50**	**50.4**
CPP3-PLGA NPs	0.71	29.0
CPP3-PLGA-PEG NPs	0.83	17.0
CPP4-PLGA NPs	0.65	34.8
CPP4-PLGA-PEG NPs	**0.39**	**60.8**
CPP5-PLGA NPs	**0.51**	**49.0**
CPP5-PLGA-PEG NPs	**0.38**	**62.0**
CPP6-PLGA NPs	1.14	-14.4
CPP6-PLGA-PEG NPs	**0.55**	**45.2**

Fig. 6. F9A353V cells show enhanced, basal and bleomycin induced, DNA damage response. (A) F9A353V cells treated with the indicated nanoparticles loaded with GSE24.2 (nanoparticle amount equivalent to 10 μg GSE24.2 peptide). After 24 h cells were lysed and the experiment analyzed by western blot with antibodies against γ-H2A.X (upper line), α-tubulin (lower line) as a loading control. Experiments were repeated 3 times with similar results. (B) Table representing the data from (A). For each nanoparticle type the damage relative to F9A353V cells was obtained after quantification of the blot and shows the ratio between expression levels of γ-H2AX and α-tubulin in each line and referred to those found in F9A353V cells. The second column represents the % of DNA damage signal inhibition from the values obtained in the parallel column.

the NPs, elaborated with either of the polymers, were conjugated to the CPPs, especially to CPP1 or CPP3, where the fluorescence intensity reached its highest levels. On the other hand, the incorporation of CPP4, CPP5 and CPP6 did not exhibit such strong fluorescence intensity, particularly for CPP4-modified formulations, and CPP5 and CPP6-PLGA-PEG NPs. This could be due to the fact that each CPP had a different structure, which would vary the internalization of the NPs into the cells.

As an example, Fig. 5 shows the Confocal Laser Scanning Microscopy (CLSM) of HeLa cells treated with some NP formulations (PEI-PLGA, CPP1-PLGA and CPP3-PLGA NPs) in terms of penetration within the first 24 h of treatment. Individual images of the nuclei (stained with DAPI), the NPs (FITC), as well as the merged images, indicate the entry of NPs into cells. Based on the data obtained from the CLSM, there was a slight increase in the uptake when the NPs were modified with PEI, though most NPs were localized mainly in the cytoplasmic area, and a considerable fraction of the cationic particles seemed to form agglomerates in culture media, which could reduce the effective concentration of the particles in the nanosize range. A similar agglomeration was previously reported by other authors with cationic chitosan-coated PLGA NPs [41].

Furthermore, as we can see in Fig. 5, the PLGA NPs conjugated to CPPs, especially CPP1 and CPP3 present a higher intracellular uptake than PEI-PLGA particles even 24 h after the administration of the particles, showing an intense fluorescence within the cytoplasmic area but mostly within the nucleus and nucleolus, representing an

important nuclear accumulation. This phenomenon not only occurred with PLGA NPs modified with the mentioned CPPs, but also with the PLGA-PEG NPs combined with these CPPs. Accordingly, these findings suggested that these CPPs modified NPs may be excellent candidates for the targeting of GSE24.2 or any other bioactive peptides or drugs into HeLa cells.

As mentioned above, the intracellular delivery of NPs is of great concern, since the cell membrane possesses a selective permeability, preventing the entrance of exogenous molecules. Therefore, both strategies proposed in this study are possible alternatives to overcome the shortcomings mentioned above and to allow a higher extent of internalization of the particles. On the one hand, the development of cationic PEI-PLGA NPs as a result of the ionic interactions established between positively charged NPs and negative cell membranes, and on the other hand, the conjugation of cell-penetrating peptides (CPPs) to the surface of the NPs, which enables their delivery to the cytoplasm and nucleus, since CPPs possess the ability to rapidly translocate across the cell membranes, capacity attributed to the presence of short amino acid sequences with amphipatic character [25].

3.7. Activity of GSE24.2 loaded NPs to recover DNA damage in A353V cells

In order to test for the biological activity of GSE24.2 loaded NPs we used F9A353V. These cells harbor the most frequent mutation found in X-linked Dyskeratosis congenita patients [16]. A353V cells exhibit basal DNA damage due to the mutation in DKC and subsequent telomere erosion [45]. This DNA damage signal can be detected and quantified by using an antibody against phosphorylated histone H2AX ser139. A353V cells were treated with the amount of all those NPs that were able to induce a relative low toxicity in HeLa or MEF cells equivalent to 15 μg of peptide (see Table 2, assay DC cells). After 24 h cells were lysed and 20 μg of protein resolved in polyacrylamide gel electrophoresis. The proteins were blotted into nylon membranes and those hybridized against and antibody that recognized pH2AXser139 histone. The membranes were then washed and hybridized against an antibody of a loading control γ-tubulin. The signals from both antibodies were quantified and the DNA damage found in A353V untreated cells considered as 1 (Fig. 6A). We repeated this assay three times for each NP and the average value was obtained. We found that PLGA and PEI-PLGA NPs were able to inhibit the DNA damage signal 20% and 38%, respectively (Fig. 6B).

Additionally, some of the NPs covered with CPPs, even if the toxicity was low and the internalization very efficient were poorly active in A353V cells. The most active NP inhibiting DNA damage was CPP5-PLGA-PEG NPs and others such as CPP5-PLGA, CPP6-PLGA-PEG, CPP1-PLGA, CPP4-PLGA-PEG and CPP2-PLGA-PEG NPs inhibited DNA damage signal to 50% in average. We additionally performed another biological assay based on the ability of GSE24.2 to upregulate telomerase activity. We treated VA13 cells, primary lung fibroblast without telomerase activity; with those NPs able to decrease DNA damage more that 30%. PLGA NPs were also used, even if the activity on rescue of DNA damage was lower than 30% as control. 24 h after treatment, cells were lysed and extracts obtained to perform the TRAP assay to measure telomerase activity. Every assay was performed by three seriated dilutions of extract. The experiment was repeated three times (Fig. 7A). The average value determined from the three dilutions was compared to that of non-treated VA13 cells and the increase obtained determined as fold activation over the VA13 value (Fig. 7B). Not all the NPs that showed high activity for recovering DNA damage were able to induce and increase telomerase

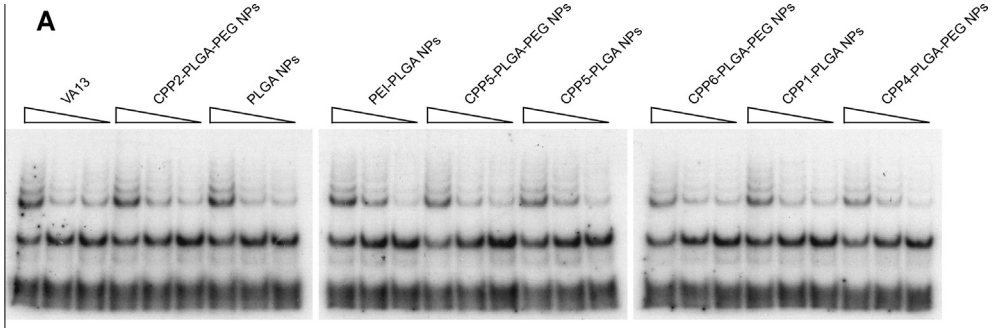

B

Formulation	% Telomerase recovery
CPP2-PLGA-PEG NPs	0.5
PLGA NPs	6
PEI-PLGA NPs	**36**
CPP5-PLGA-PEG NPs	19
CPP5-PLGA NPs	**54**
CPP6-PLGA-PEG NPs	**36.5**
CPP1-PLGA NPs	6.5
CPP4-PLGA-PEG NPs	0.25

Fig. 7. Reactivation of telomerase activity by nanoparticles loaded with GSE24.2. VA13 cells were treated with the indicated nanoparticles loaded with GSE24.2 (nanoparticle amount equivalent to 10 μg GSE24.2 peptide) for 24 h and telomerase activity determined by TRAP assay. (A) Different amounts of extract were used for each TRAP assay as indicated. (B) The telomerase activity was quantified by evaluating the intensity of the bands in relation with the internal control (TEL/IC). The values for NPs-GSE24.2 treated cells were referred to non treated VA13 cells and expressed as percentage respect to VA13 cells. The experiments were repeated at least three times with similar results.

activity, and the more active were PEI-PLGA, CPP5-PLGA, and CPP6-PLGA-PEG NPs. These results might be explained by the lisosomal pathway of the NPs. Overall, once the NPs are internalized into cells, they are uptaken by the lisosomes, and eventually, they must be adequately released from them in order to allow an efficient delivery of GSE24.2 to its target site. Therefore, since CPP1, CPP2, CPP3 and CPP4 have a more amphipatic character, they are retained within the lisosomes, and thus, although their internalization into cells was higher, the release of GSE24.2 is lower, resulting in lower telomerase activity recovery.

DNA damage is one of the landmarks of telomerase-associated disorders. Dysfunctional telomeres trigger a DNA damage response most likely because they are too short to adopt the normal t-loop structure needed to form the telomere with correctly ordered shelterin components. Recruitment of histone-macro H2A1 has been associated to heterochromatin and senescent associated foci. We have previously found (submitted manuscript) that both senescence and macro H2A.1 associated-foci are increased in X-DC patient cells, suggesting that the impairment in repair of DNA lesions in X-DC cells likely contributes to the senescent phenotype. We have also previously found that expression of GSE24.2 was able to induce protection against induced DNA damage and the repair of pre-existing DNA lesions that was also taking place at telomeres in F9A353V cells as shown by the decrease in γ-H2AX and TRF1 colocalization. The observed decrease in DNA damage induced by GSE24.2 expression in F9A353V cells, was also observed when bacterially produced peptide was used, reinforcing that idea of GSE24.2 may be acting directly at the telomere by reactivating telomerase activity and/or changing telomere folding.

4. Conclusions

In this study, cationic polymeric NPs modified with two polycations (PEI and DX) and polymeric NPs conjugated to CPPs were synthesized and characterized. The cytotoxicity assays were performed to dismiss toxic formulations (DX-PLGA and DX-PLGA-PEG NPs) and the remaining non toxic formulations were tested in the following experiments. The modification with PEI, but more remarkably the conjugation of NPs to CPPs enabled an enhanced cellular uptake in HeLa cells. In addition, according to the bioactivity assays addressed, the polymeric NPs prepared were able to rescue the DNA damage in F9 A353V cells and recovered the telomerase activity in VA13 cells, mostly PEI-PLGA NPs, CPP5-PLGA NPs and CPP6-PLGA-PEG NPs.

Therefore, based on the above presented results it can be inferred that the previously named formulations may be considered a promising approach for the intracellular delivery of GSE24.2 for the treatment of Dyskeratosis congenita and other defective telomerase disorders.

Conflict of interest

The authors declare no competing financial interest.

Acknowledgments

Susana P. Egusquiaguirre thanks the Basque Government (Gobierno Vasco, Departamento de Educación, Universidades e Investigación) for the fellowship research grant. C. Manguan-García is supported by CIBER de Enfermedades Raras. This project was partially supported by the Basque Government (Consolidated Groups, IT-407-07), MINECO from the Spanish Government (INNPACTO, IPT-2012-0674-090000). The authors gratefully acknowledge the support of University of the Basque Country UPV/EHU (UFI11/32). Besides, this work was also supported by grant PI11-00949 (supported by FEDER funds) from Instituto Carlos III.

References

[1] S.A. Savage, B.P. Alter, Dyskeratosis congenita, Hematol. Oncol. Clin. North Am. 23 (2) (2009) 215–231.
[2] M. Bessler, D.B. Wilson, P.J. Mason, Dyskeratosis congenita, FEBS Lett. 584 (17) (2010) 3831–3838.
[3] I. Dokal, Dyskeratosis congenita, in: American Society of Hematology Education Program, vol. 2011, 2011, pp. 480–486.
[4] J. de la Fuente, I. Dokal, Dyskeratosis congenita: advances in the understanding of the telomerase defect and the role of stem cell transplantation, Pediatr. Transplant. 11 (6) (2007) 584–594.
[5] A.J. Walne, I. Dokal, Advances in the understanding of dyskeratosis congenita, Br. J. Haematol. 145 (2) (2009) 164–172.
[6] W. Palm, T. de Lange, How shelterin protects mammalian telomeres, Annu. Rev. Genet. 42 (2008) 301–334.
[7] E.H. Blackburn, Structure and function of telomeres, Nature 350 (6319) (1991) 569–573.
[8] N.S. Young, Telomere biology and telomere diseases: implications for practice and research, ASH Educ. Progr. Book 1 (2010) 30–35.
[9] J.L. Osterhage, K.L. Friedman, Chromosome end maintenance by telomerase, J. Biol. Chem. 284 (24) (2009) 16061–16065.
[10] S.B. Cohen, M.E. Graham, G.O. Lovrecz, N. Bache, P.J. Robinson, R.R. Reddel, Protein composition of catalytically active human telomerase from immortal cells, Science (New York, N.Y.) 315 (5820) (2007) 1850–1853.
[11] R.J. O'Sullivan, J. Karlseder, Telomeres: protecting chromosomes against genome instability, Nat. Rev.: Mol. Cell Biol. 11 (3) (2010) 171–181.
[12] T. de Lange, How telomeres solve the end-protection problem, Science (New York, N.Y.) 326 (5955) (2009) 948–952.
[13] M. Kirwan, I. Dokal, Dyskeratosis congenita: a genetic disorder of many faces, Clin. Genet. 73 (2) (2008) 103–112.
[14] N.D. Nelson, A.A. Bertuch, Dyskeratosis congenita as a disorder of telomere maintenance, Mutat. Res./Fundam. Mol. Mech. Mutag. 730 (1–2) (2012) 43–51.
[15] R. Machado-Pinilla, I. Sanchez-Perez, J.R. Murguia, L. Sastre, R. Perona, A dyskerin motif reactivates telomerase activity in X-linked dyskeratosis congenita and in telomerase-deficient human cells, Blood 111 (5) (2008) 2606–2614.
[16] R. Machado-Pinilla, J. Carrillo, C. Manguan-Garcia, L. Sastre, A. Mentzer, B.W. Gu, P.J. Mason, R. Perona, Defects in mTR stability and telomerase activity produced by the Dkc1 A353V mutation in dyskeratosis congenita are rescued by a peptide from the dyskerin TruB domain, Clin. Transl. Oncol.: Off. Publ. Feder. Spanish Oncol. Soc. Natl. Cancer Inst. Mexico 14 (10) (2012) 755–763.
[17] C. Pinto Reis, R.J. Neufeld, A.J. Ribeiro, F. Veiga, Nanoencapsulation II. Biomedical applications and current status of peptide and protein nanoparticulate delivery systems, Nanomed. Nanotechnol. Biol. Med. 2 (2) (2006) 53–65.
[18] S.C. Yadav, A. Kumari, R. Yadav, Development of peptide and protein nanotherapeutics by nanoencapsulation and nanobioconjugation, Peptides 32 (1) (2011) 173–187.
[19] F. Danhier, E. Ansorena, J.M. Silva, R. Coco, A. Le Breton, V. Préat, PLGA-based nanoparticles: an overview of biomedical applications, J. Control. Release 161 (2) (2012) 505–522.
[20] R. Gref, M. Luck, P. Quellec, M. Marchand, E. Dellacherie, S. Harnisch, T. Blunk, R.H. Muller, 'Stealth' corona-core nanoparticles surface modified by polyethylene glycol (PEG): influences of the corona (PEG chain length and surface density) and of the core composition on phagocytic uptake and plasma protein adsorption, Colloids Surf., B: Biointerfaces 18 (3-4) (2000) 301–313.
[21] V. Labhasetwar, Nanotechnology for drug and gene therapy: the importance of understanding molecular mechanisms of delivery, Curr. Opin. Biotechnol. 16 (6) (2005) 674–680.
[22] M.Ø. Andersen, A. Lichawska, A. Arpanaei, S.M. Rask Jensen, H. Kaur, D. Oupicky, F. Besenbacher, P. Kingshott, J. Kjems, K.A. Howard, Surface functionalisation of PLGA nanoparticles for gene silencing, Biomaterials 31 (21) (2010) 5671–5677.
[23] S. Fischer, E. Uetz-von Allmen, Y. Waeckerle-Men, M. Groettrup, H.P. Merkle, B. Gander, The preservation of phenotype and functionality of dendritic cells upon phagocytosis of polyelectrolyte-coated PLGA microparticles, Biomaterials 28 (6) (2007) 994–1004.
[24] P. Jarver, U. Langel, Cell-penetrating peptides – a brief introduction, Biochim. Biophys. Acta 1758 (3) (2006) 260–263.
[25] J. Farrera-Sinfreu, E. Giralt, S. Castel, F. Albericio, M. Royo, Cell-penetrating cis-gamma-amino-L-proline-derived peptides, J. Am. Chem. Soc. 127 (26) (2005) 9459–9468.
[26] A. Kalinin, N.H. Thoma, A. Iakovenko, I. Heinemann, E. Rostkova, A.T. Constantinescu, K. Alexandrov, Expression of mammalian geranylgeranyltransferase type-II in *Escherichia coli* and its application for in vitro prenylation of Rab proteins, Protein Expr. Purif. 22 (1) (2001) 84–91.
[27] E. Kaiser, R.L. Colescott, C.D. Bossinger, P.I. Cook, Color test for detection of free terminal amino groups in the solid-phase synthesis of peptides, Anal. Biochem. 34 (2) (1970) 595–598.
[28] R. Fischer, O. Mader, G. Jung, R. Brock, Extending the applicability of carboxyfluorescein in solid-phase synthesis, Bioconjug. Chem. 14 (3) (2003) 653–660.

[29] I. Gutierro, R.M. Hernandez, M. Igartua, A.R. Gascon, J.L. Pedraz, Size dependent immune response after subcutaneous, oral and intranasal administration of BSA loaded nanospheres, Vaccine 21 (1–2) (2002) 67–77.
[30] R. Misra, S.K. Sahoo, Intracellular trafficking of nuclear localization signal conjugated nanoparticles for cancer therapy, Eur. J. Pharm. Sci. 39 (1–3) (2010) 152–163.
[31] K.J. Wiechelman, R.D. Braun, J.D. Fitzpatrick, Investigation of the bicinchoninic acid protein assay: identification of the groups responsible for color formation, Anal. Biochem. 175 (1) (1988) 231–237.
[32] I. Sanchez-Perez, J.R. Murguia, R. Perona, Cisplatin induces a persistent activation of JNK that is related to cell death, Oncogene 16 (4) (1998) 533–540.
[33] I. Youm, B.C. Youan, Uptake mechanism of Furosemide-loaded pegylated nanoparticles by cochlear cell lines, Hear. Res. 304 (2013) 7–19.
[34] W.E. Wright, J.W. Shay, M.A. Piatyszek, Modifications of a telomeric repeat amplification protocol (TRAP) result in increased reliability, linearity and sensitivity, Nucleic Acids Res. 23 (18) (1995) 3794–3795.
[35] H. Hillaireau, P. Couvreur, Nanocarriers' entry into the cell: relevance to drug delivery, Cell. Mol. Life Sci.: CMLS 66 (17) (2009) 2873–2896.
[36] M.T. Stephan, D.J. Irvine, Enhancing cell therapies from the outside in: cell surface engineering using synthetic nanomaterials, Nano Today 6 (3) (2011) 309–325.
[37] P. Lundberg, Ü. Langel, A brief introduction to cell-penetrating peptides, J. Mol. Recognit. 16 (5) (2003) 227–233.
[38] J.M. Martínez Gómez, N. Csaba, S. Fischer, A. Sichelstiel, T.M. Kündig, B. Gander, P. Johansen, Surface coating of PLGA microparticles with protamine enhances their immunological performance through facilitated phagocytosis, J. Control. Release 130 (2) (2008) 161–167.
[39] B. Patel, V. Gupta, F. Ahsan, PEG–PLGA based large porous particles for pulmonary delivery of a highly soluble drug, low molecular weight heparin, J. Control. Release 162 (2) (2012) 310–320.
[40] H. Mueller, M.U. Kassack, M. Wiese, Comparison of the usefulness of the MTT, ATP, and calcein assays to predict the potency of cytotoxic agents in various human cancer cell lines, J. Biomol. Screen. 9 (6) (2004) 506–515.
[41] N. Nafee, M. Schneider, U.F. Schaefer, C.M. Lehr, Relevance of the colloidal stability of chitosan/PLGA nanoparticles on their cytotoxicity profile, Int. J. Pharm. 381 (2) (2009) 130–139.
[42] M.D. Shau, M.F. Shih, C.C. Lin, I.C. Chuang, W.C. Hung, W.E. Hennink, J.Y. Cherng, A one-step process in preparation of cationic nanoparticles with poly(lactide-co-glycolide)-containing polyethylenimine gives efficient gene delivery, Eur. J. Pharm. Sci. 46 (5) (2012) 522–529.
[43] L. Chronopoulou, A. Cutonilli, C. Cametti, M. Dentini, C. Palocci, PLGA-based nanoparticles: effect of chitosan in the aggregate stabilization. A dielectric relaxation spectroscopy study, Colloids Surf., B: Biointerfaces 97 (2012) 117–123.
[44] D. Fischer, Y. Li, B. Ahlemeyer, J. Krieglstein, T. Kissel, In vitro cytotoxicity testing of polycations: influence of polymer structure on cell viability and hemolysis, Biomaterials 24 (7) (2003) 1121–1131.
[45] B.W. Gu, M. Bessler, P.J. Mason, A pathogenic dyskerin mutation impairs proliferation and activates a DNA damage response independent of telomere length in mice, Proc. Natl. Acad. Sci. USA 105 (29) (2008) 10173–10178.

Clin Transl Oncol (2014) 16:529–538
DOI 10.1007/s12094-013-1112-3

RESEARCH ARTICLE

p53 pathway activation by telomere attrition in X-DC primary fibroblasts occurs in the absence of ribosome biogenesis failure and as a consequence of DNA damage

J. Carrillo · A. González · C. Manguán-García · L. Pintado-Berninches · R. Perona

Received: 30 July 2013 / Accepted: 10 September 2013 / Published online: 25 September 2013

Abstract
Background Dyskeratosis congenita (DC) is a rare inherited bone marrow failure syndrome with high clinical heterogeneity. Various mutations have been reported in DC patients, affecting genes that code for components of H/ACA ribonucleoproteins, proteins of the telomerase complex and components of the shelterin complex.
Objectives We aim to clarify the role of ribosome biogenesis failure in senescence induction in X-DC since some studies in animal models have reported a decrease in ribosome biogenesis as a major role in the disease.
Methods Dyskerin was depleted in normal human fibroblasts by expressing two *DKC1* shRNAs. Common changes in gene expression profile between these dyskerin-depleted cells and X-DC fibroblasts were analyzed.
Results Dyskerin depletion induced early activation of the p53 pathway probably secondary to ribosome biogenesis failure. However, the p53 pathway in the fibroblasts from X-DC patients was activated only after an equivalent number of passes to AD-DC fibroblasts, in which telomere attrition in each division rendered shorter telomeres than control fibroblasts. Indeed, no induction of DNA damage was observed in dyskerin-depleted fibroblasts in contrast to X-DC or AD-DC fibroblasts suggesting that DNA damage induced by telomere attrition is responsible for p53 activation in X-DC and AD-DC fibroblasts. Moreover, p53 depletion in senescent DC fibroblasts rescued their proliferative capacity and reverted the morphological changes produced after prolonged culture.
Conclusions Our data indicate that ribosome biogenesis do not seem to play an important role in dyskeratosis congenita, conversely increasing DNA damage and activation of p53 pathway triggered by telomere shortening is the main activator of cell senescence.

Keywords Dyskeratosis congenita · Dyskerin · TERT · TERC · p53 · Senescence

J. Carrillo · A. González · C. Manguán-García · L. Pintado-Berninches · R. Perona (✉)
Instituto de Investigaciones Biomédicas de Madrid CSIC/UAM, IDIPaz (Biomarkers and Experimental Therapeutics Group), C/Arturo Duperier, 4, 28029 Madrid, Spain
e-mail: rperona@iib.uam.es

J. Carrillo · A. González · C. Manguán-García · L. Pintado-Berninches · R. Perona
CIBER de Enfermedades Raras, Valencia, Spain

Introduction

Dyskeratosis congenita (DC) is a rare inherited disease characterized by bone marrow failure in the first or second decade of life, which is the principal cause of mortality [1]. DC patients are also at high risk of developing other malignancies. Cells isolated from DC patients have short telomeres, especially in highly proliferative tissues such as bone marrow and skin. These patients harbor mutations in genes involved in telomere biology such as those coding for components of telomerase complex (*TERT*, *TERC*, *DKC1*, *NHP2* and *NOP10*), or proteins involved in telomerase trafficking (*TCAB1*), and telomere protection or replication (*TINF2* and *CTC1*). *DKC1* mutations are the most frequent [2, 3], appearing in 30 % of DC patients, in some of them are associated with the most severe variant of DC. *DKC1* gene encodes the nucleolar protein dyskerin, which is ubiquitously expressed. *TERC* forms part of the active telomerase complex and *TERT* is the reverse transcriptase catalytic moiety of telomerase whose expression is inhibited in many adult tissues, with the exception of stem

and progenitor cells and pathological situations such as cancer. Mutations in *TERC* [4] and *TERT* [5] impair telomere elongation. Recently decreased *DKC1* expression has been associated with DC in a small number of patients who did not show mutations in any of the above described genes [6]. Dyskerin harbors a highly conserved RNA-binding motif (PUA domain) and the catalytic domain with pseudouridine synthase activity (TRUB domain). Dyskerin ablation in mouse liver inhibits rRNA processing with the consequent accumulation of large precursors [7]. As part of the RNP-complex dyskerin binds to *TERC* maintaining its stability. Accordingly, *DKC1* mutations reduce *TERC* levels affecting the telomerase activity and elongation of telomeres. Alteration of both dyskerin functions, is believed to be important for the development of DC. Hypomorphic *dkc*1 mice show significant rRNA defects in the first generation, however telomere shortening does not appear until the fourth generation [8], suggesting that changes in the ribosome processing machinery also play an important role in the pathogenicity of DC. Other reports of DC animal model systems, based on inhibition of *Nop10* [9] or *Dkc1* [10] expression in zebrafish, have described deficient ribosomal RNA modification as one of the mechanism driving bone marrow failure.

To ascertain in human cells if a decrease in dyskerin levels modified both ribosome biogenesis and telomere length, we depleted control skin fibroblasts from dyskerin. We detected a slight downregulation in 18S and 28S rRNAs that could induce a ribosome biogenesis failure, and consequently an early activation of the p53 pathway, cell cycle arrest and a slight increase in apoptotic cells [11]. However, fibroblasts of one AD-DC and 3 X-DC patients showed DNA damage and overexpression of p53 targets only after the number of cell divisions in culture. This indicates that DNA damage activated by telomere attrition is necessary in patient's fibroblasts to induce p53 activation.

Materials and methods

DC patient's fibroblasts

F49IIB and F64IIB fibroblasts were established in our laboratory from skin biopsies of control probands. Dermal fibroblasts from a control proband (X-DC1787-C) and two X-DC patients (X-DC1774-P and X-DC4646-P) were obtained from Coriell Cell Repository [12–14]. F26IIB and F66IIB fibroblasts belonging to an X-DC and an AD-DC patient respectively, were established in our laboratory from a skin biopsy [12]. All primary fibroblasts were maintained in MEM (Minimum Essential Medium, Gibco) supplemented with 15 % FBS, gentamicin and L-glutamine.

Cell cycle analysis

Control and X-DC fibroblasts were plated onto 10 cm dishes and stained with propidium iodide in PBS containing DNase-free RNase A. Then cells were analyzed with FACScan flow cytometer (Becton–Dickinson) and WinMDI v2.8 software.

Western blot

Whole cell extracts were resolved on SDS-polyacrylamide and electroblotted to Immobilon-P membranes (Millipore). Antibodies used were anti-Dyskerin (Sta. Cruz Biotechnology) and anti-α-tubulin (Sigma, St. Louis, MO, USA). Western blot analysis was conducted using ECL reagent (Santa Cruz Biotechnology).

Senescence and DNA damage analysis

Cells (1×10^4 cells) were plated onto 6-well plates and fixed after four days to assay acid-β-galactosidase (SA-β-gal) (Senescence Detection Kit, BioVision, USA). The percentage of senescent cells was calculated in 6 images/sample taken in the bright field microscopy (Nikon Eclipse TS100 Microscopy, USA). DNA damage was analyzed by fluorescence microscopy using γ-H2AX-ser139 Ab (Cell Signaling) followed by secondary antibody coupled to Alexa fluor 488 (A11029, Molecular Probes). Image acquisition was carried out with a Confocal Espectral Leica TCS SP5, microscope using a HCX PL APO Lambda blue 63X1.40 OIL UV, zoom 2.3-lens, and processed with ImageJ software.

Inhibition of DKC1 and p53 expression by small hairpin RNAs

Lentivirus expressing a *DKC1* or *p53* shRNA (Open Biosystems, USA) were obtained by transfection of 15 μg of the specific lentiviral vector (pLKO-shDKC1-3, pLKO-shDKC1-4 or pGIPZ-shp53.3) in 293T cells and used for infection of X-DC1787-C fibroblasts. DC-senescent fibroblasts were infected with non-silence or shp53-3 lentivirus and maintained to analyze PLDs.

Real-time quantitative PCR

Total RNA was extracted from control and DC fibroblasts with TriReagent (Sigma), and 1 μg of RNA transcribed into cDNA. *DKC1* expression levels were analyzed by qPCR with 80 ng of cDNA using 0.3 μM of each primer in a sybr green master mix (Applied Biosystems, USA). Each sample was normalized by *GAPDH* expression. The primers used were: GAPDH F 5′-GAGAGACCCTCACTGCTG-3′;

GAPDH-R-5′-GATGGTACATGACAAGGTGC-3′; DKC1-F5′ GGGAATTCGGTTTCATTAATCTTGACAA-3′; DKC1-R5′-CCCTCGAGCTTCACCAAGCGAGTGGCTC-3′; TERC-F5′-TCTAACCCTAACTGAGAAGGGCGTAG-3′; TERC-R5′-GTTTGCTCTAGAATGAACGGTGGA AG-3′.

The expression levels of the other genes were determined with 50 ng of cDNA using 1× Taqman probes (Applied Biosystems, USA) in Taqman master mix (Applied Biosystems, USA), and normalized with *GAPDH* expression.

Microarrays

RNA extracted from two independent experiments of X-DC1787-C fibroblasts, 4 days later after infection with sh-non-silence or shDKC1-3 lentivirus, were hybridized in microarrays 4 × 44 K (Whole Human Genome 4 × 44 K, Agilent Technologies, USA). Genes upregulated or downregulated at least twofold and with a p value lower than 0.02 were selected and analyzed with the software Gene Ontology TreeMachine to identify biological functions with gene enrichment.

Results

Different *DKC1* and *TERT* mutations harbored in X-DC and AD-DC primary fibroblasts induce early senescence by G2/M arrest

A decrease of 94 % in *TERC* RNA levels was observed in X-DC versus control fibroblasts [15], in accordance with the role of dyskerin in *TERC* RNA stabilization, while F66IIB primary fibroblasts derived from an AD-DC patient showed *TERC* levels similar to control fibroblasts (Fig. 1a). At PDL8, 64–98 % of X-DC and 23 % of AD-DC fibroblasts showed expression of SA-β-gal versus 2–4 % of control fibroblasts (Fig. 1b). Moreover, these cells showed typical alterations of senescent cells (Fig. 1c). X-DC and AD-DC fibroblasts also showed an increase in the number of G2/M arrested cells, 12–30 % versus 4 % in control fibroblasts (Fig. 1d). However, when X-DC and AD-DC fibroblasts were analyzed at lower than 5-PLDs (F26IIB and F66IIB), they grew with kinetics similar to control fibroblasts (Fig. 1e), indicating no increase in the number of senescent or G2/M arrested cells.

Dyskerin depletion in human primary fibroblasts induces early activation of p53 pathway independent of DNA damage response

In order to generate a cellular model of X-DC, we inhibited *DKC1* expression in X-DC1787-C control fibroblasts using a *DKC1*-small-hairpin (shDKC1-3) lentiviral vector and compared it with non-silence shRNA. *DKC1* mRNA levels decreased by 90 % after 2 days, and dyskerin levels by 80 % by day 4 (Fig. 2a, b) and *TERC* mRNA levels to 90 %. Although, X-DC1787-C control fibroblasts showed a slight increase of 7 % in G2/M arrested and 3 % in apoptotic cells after 8 days of *DKC1* interference (data not shown), a decrease of 60–70 % in cell number was observed after 28 days of *DKC1* interference, indicating that dyskerin depletion induces early senescence within 4–8 days by G2/M arrest which increases apoptosis (Fig. 2c).

Analysis of gene expression profile in dyskerin-depleted fibroblasts showed deregulation of a significant number of genes related with p53 and ribosome biogenesis pathways and others such as focal adhesion, actin cytoskeleton, metabolism and cancer also showed a significant number of deregulated genes (Fig. 2d). Some genes belonging to p53 (Fig. 2e) or ribosome biogenesis (Fig. 2f) pathways were chosen to be validated by qPCR in dyskerin-depleted fibroblasts using two different *DKC1* shRNAs, which showed similar levels of *DKC1*-downregulation (data not shown).

Activation of p53 pathway was addressed by evaluating *CDKN1A* expression, and found that expression levels were increased over threefold after *DKC1*-interference with shDKC1-3 or 1–4 at 4 days and maintained at day 8 (Fig. 3a). Another target of p53, *CDKN2B*(p15), was overexpressed by twofold with both shDKCs at 4 days and slightly increased at 8 days. *CCND1*(cyclin D1) was not deregulated by shDKC1-3, but was downregulated 3 to 11-fold by shDKC1-4 (8 days). Overexpression of *CDKN1A* and *CDKN2B* was observed at 4–8 days of dyskerin depletion, while *CCND1,* involved in cell cycle progression, was not overexpressed. Moreover, 25–42 % of cells were SA-β-gal positive after 8 days (Fig. 3b). On the other hand, the overexpression of genes that induce apoptosis via p53 activation (*CASP9*, *BBC3*, *BAX* and *PTEN)* was also detected in the arrays, explaining the increased levels of apoptotic cells (Fig. 2e).

p53 targets, *DDB2* (DNA damage-binding protein 2) and *RRM2B* (ribonucleotide reductase M2-B), were downregulated twofold by both shDKC1-4/1-3 (Fig. 3a). Analysis of DNA damage showed very few γ-H2AX foci/cell in dyskerin-depleted fibroblasts similar to non-silence fibroblasts even after 8 days (Fig 3c), suggesting that activation of p53 pathway in these cells was not triggered by DNA damage.

Gene expression profile of dyskerin-depleted fibroblasts showed deregulation of ribosomal protein mRNAs, which bind to rRNAs and as dyskerin is a pseudouridine synthase involved in rRNA processing [7, 9], ribosome biogenesis could be altered and trigger p53 activation. Expression levels of *RPL37A* and *RPL7A* ribosomal mRNAs were similar in dyskerin-depleted and non-silence fibroblasts with both shDKCs (data not shown). However, a modest decrease in 18S and 28S rRNA levels was observed for

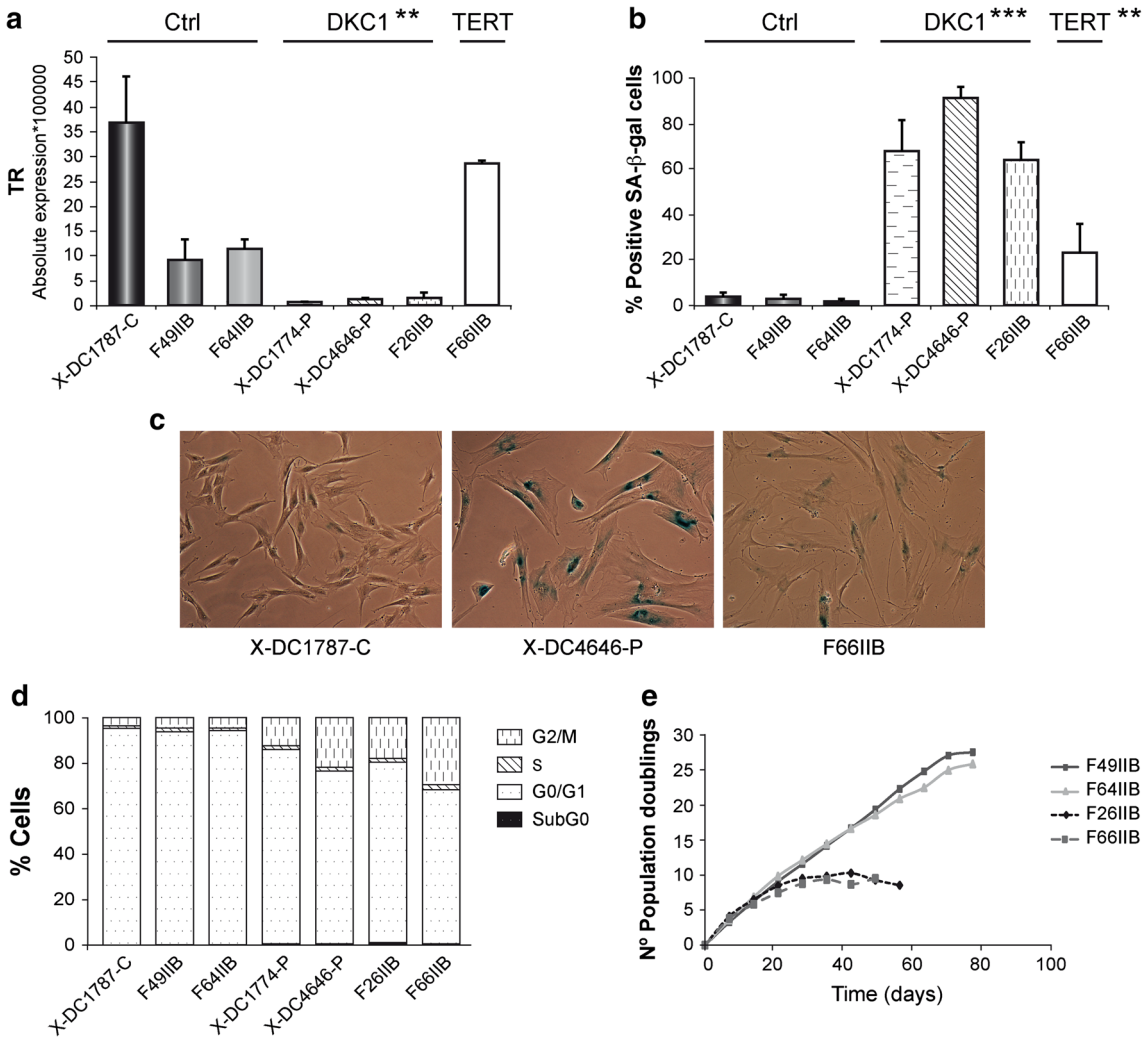

Fig. 1 X-DC fibroblasts show lower *TERC* mRNA levels, higher SA-β-gal activity and a stronger G2/M arrest than control fibroblasts. **a** Absolute expression of *TERC* in control fibroblasts (X-DC1787-C, F49IIB and F64IIB), X-DC (X-DC1774-P, X-DC4646-P and F26IIB) and AD-DC (F66IIB) patient's fibroblasts normalized by *GAPDH* expression, at PDL8. Media of 2 experiments is provided. **b** Quantification of positive SA-β-gal cells in control and patient's fibroblasts, 4 days after seeded. Six images of random regions were taken in each case. Experiments were repeated three times with similar results. **c** Representative images of control and patient's fibroblasts staining with SA-β-gal at PDL8. **d** Cell cycle analysis of control and patient's fibroblasts with IPr (propidium Iodide). Experiments were repeated three times with similar results. **e** Number of PDLs versus time in control fibroblasts (F49IIB and F64IIB), X-DC (F26IIB) and AD-DC (F66IIB) patient's fibroblasts. $^{**}p < 0.01$ and $^{***}p < 0.001$ in X-DC or AD-DC vs. control fibroblasts

shDKC1-3 (Fig. 3d). These modest changes could indicate that activation of p53 pathway in dyskerin-depleted fibroblasts could be triggered by ribosome biogenesis failure, although it is possible that a complete *DKC1*-depletion should be necessary to detect more evident changes in rRNAs levels or ribosomal protein mRNAs.

Activation of the p53 pathway in X-DC and AD-DC primary fibroblasts occurs by activation of DNA damage response

Expression levels of p53 target genes deregulated in dyskerin-depleted fibroblasts, were analyzed in X-DC and AD-DC patient's fibroblasts, and compared with control fibroblasts at 8PLDs. *CDKN1A*, *CDKN2B* and *CCND1* mRNAs levels were upregulated 2.5 to 5-fold in X-DC and AD-DC fibroblasts (Fig. 4a). *RRM2B and DDB2* mRNAs levels were upregulated by threefold in X-DC fibroblasts and 1.6-fold in AD-DC fibroblasts (8-PLD), but not in X-DC or AD-DC fibroblasts when were analyzed at low PLDs (<PDL4, data not shown). This analysis could be done only with control or DC fibroblasts established from patient skin biopsies in our laboratory because commercially available control or DC fibroblasts were obtained at higher PDLs (PDL5-8).

DNA damage in X-DC and AD-DC fibroblasts at PDL8 was analyzed by detection of γ-H2AX/foci number/per

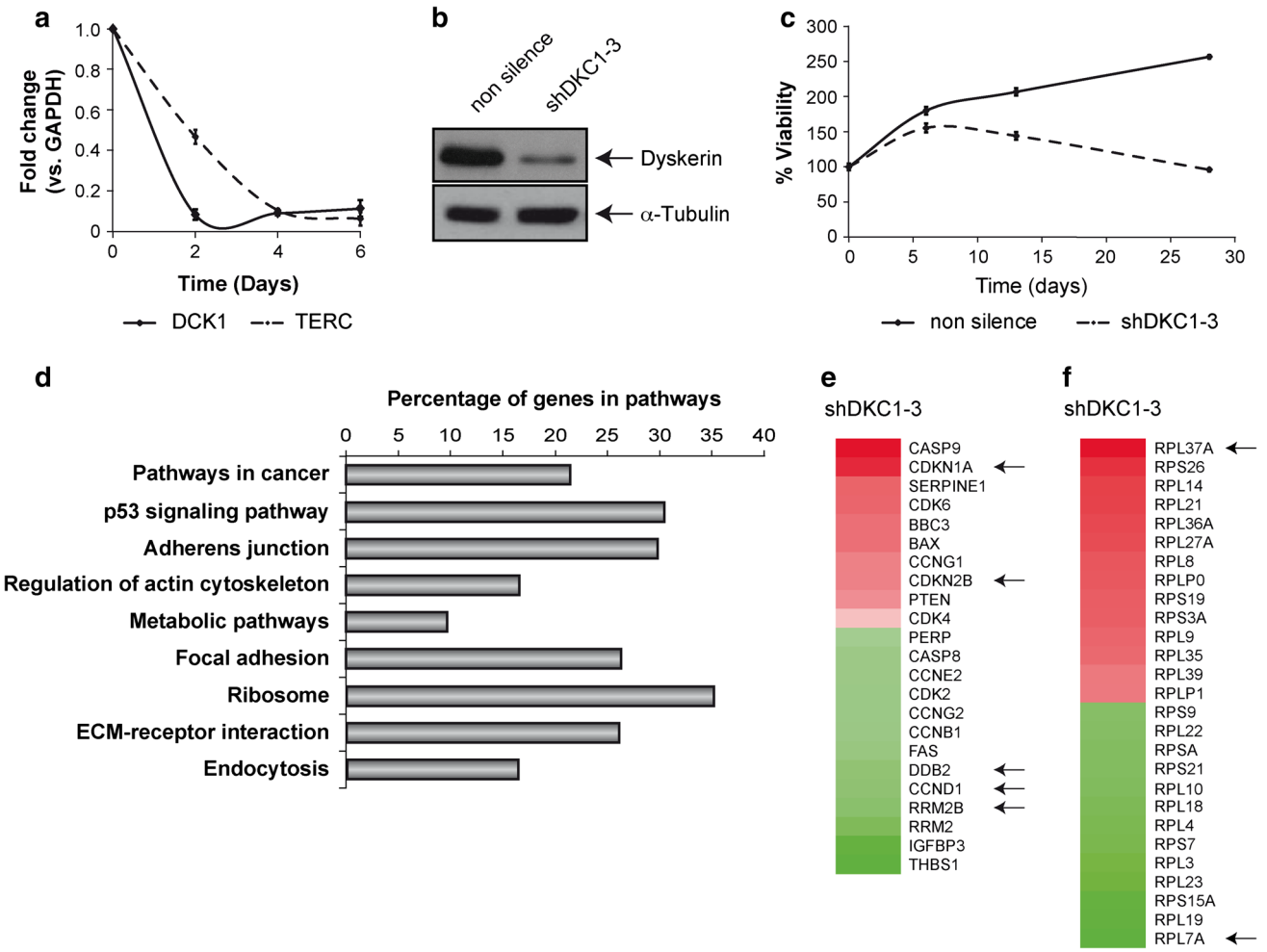

Fig. 2 Dyskerin depletion in control fibroblasts induced a reduction of proliferative capacity and alteration of gene expression profile. **a** *DKC1* and *TERC* relative expression in X-DC1787-C control fibroblasts versus non-silence shRNA, after 2, 4 and 6 days of *DKC1* interference with a lentiviral vector expressing a small hairpin *DKC1* RNA (shDKC1-3) and normalized with *GAPDH* expression. Media of 2 independent experiments is showed. **b** Dyskerin levels of X-DC1787-C fibroblast after 4 days of *DKC1* interference determined with specific antibodies to dyskerin by western blot and normalized with α-tubulin. **c** Viability of *DKC1* interfered X-DC1787-C fibroblasts versus non-silence fibroblasts along 1 month in cell culture, considering the initial cell number seeded as 100 %. **d** Percentage of deregulated genes with at least twofold change and a *p* value lower than 0.02, grouped by biological function using the software Gene Ontology TreeMachine. **e** Deregulated genes related to p53 pathway or **f** ribosomal protein mRNAs after 4 days of *DKC1* interference and versus non-silence fibroblasts, determined by microarrays with at least twofold change and a *p* value lower than 0.02. *Red* upregulated genes. *Green* downregulated genes. Genes validated by qPCR are marked with an *arrow*

cell. The percentage of cells with more of five γ-H2AX/ foci was increased to 60–80 % in X-DC and AD-DC fibroblasts versus 20 % observed in control fibroblasts (Fig. 5a). However, γ-H2AX foci/number was not increased in X-DC or AD-DC versus control fibroblasts when they were analyzed at low PLDs (<PDL4, data not shown). The increase in DNA damage observed in DC fibroblasts could be induced by critically short telomeres, because they are recognized as double-strand brakes [16–18]. DC fibroblasts or PBMCs of these patients showed shorter telomeres than control population versus age (Fig. 5b), explaining why they could only divide few times before entering into senescence. On the other hand, 18S and 28S rRNAs levels were not deregulated in X-DC and AD-DC (Fig. 5c), indicating that p53 pathway was not activated by ribosome biogenesis failure.

Recovery of the proliferative capacity of senescent DC fibroblasts, after p53 depletion

In order to demonstrate the role of p53 in senescence induction of DC fibroblasts, p53 expression was inhibited in senescent X-DC and AD-DC fibroblasts at PDL8 using a lentiviral vector expressing a p53 shRNA. X-DC and AD-DC fibroblasts showed a 90 % decrease of p53 mRNA after

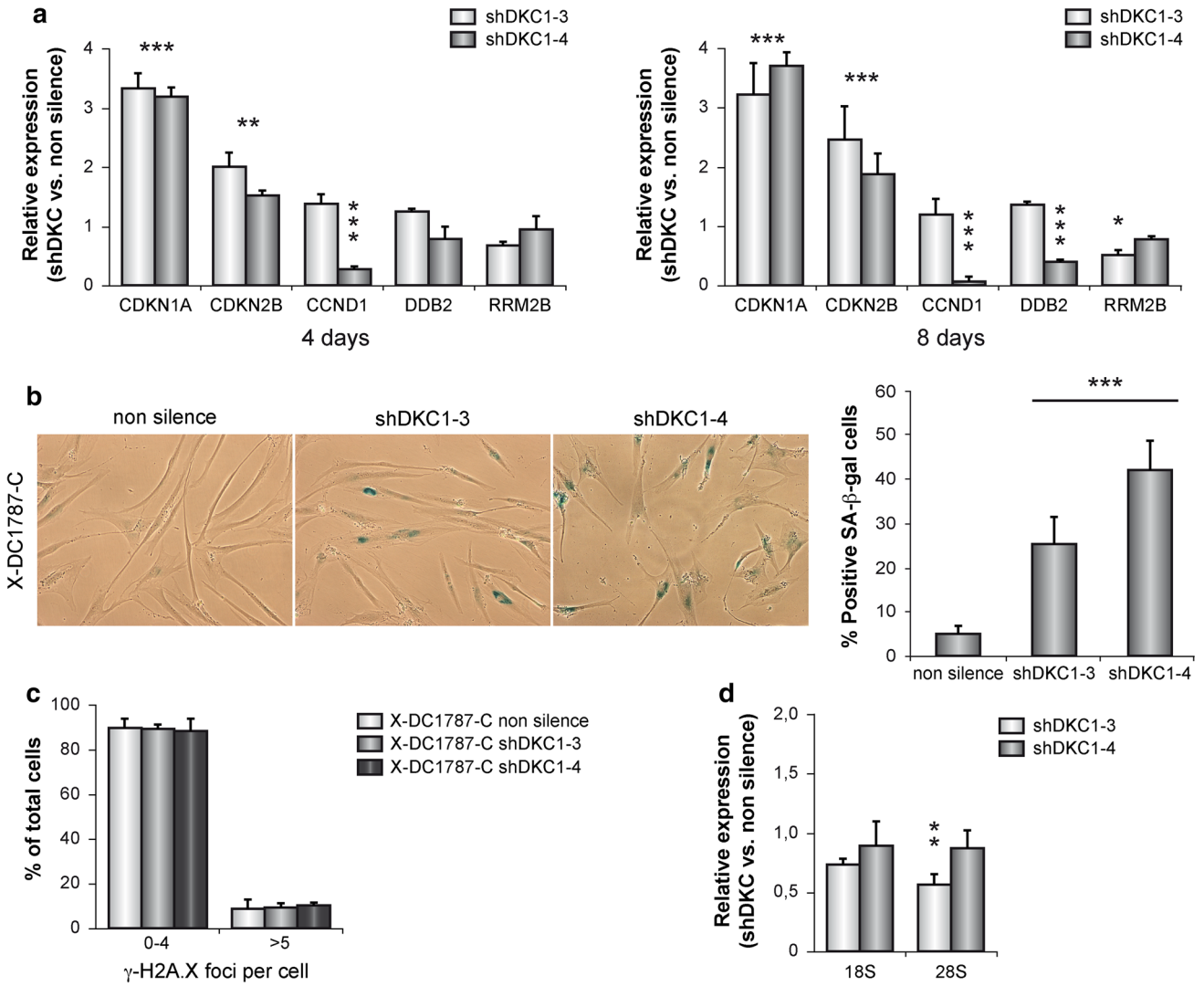

Fig. 3 Dyskerin depletion in control fibroblasts induced activation of p53 pathway, independent of DNA damage response. **a** Relative expression of *CDKN1A*, *CDKN2B*, *CCND1*, *DDB2* and *RRM2B* genes in X-DC1787-C control fibroblasts after 4 or 8 days of dyskerin depletion with shDKC1-3 or shDKC1-4 versus non-silence fibroblasts determined by qPCR and normalized by *GAPDH* expression. Mean of 2 independent experiments performed by duplicate is showed for every determination. **b** Quantification of positive SA-β-gal cells in X-DC1787-C control fibroblasts after 8 days of dyskerin depletion with shDKC1-3 or shDKC1-4, and versus non-silence fibroblasts. Representative images are showed. Senescent cells quantification was performed in six images of random regions. Experiments were repeated three times with similar results. **c** Quantification of γ-H2AX foci in X-DC1787-C fibroblasts after 8 days of dyskerin depletion with shDKC1-3 or shDKC1-4, and versus non-silence fibroblasts, determined by immunofluorescence in 200 cells for each case. **d** Relative expression of *18S* and *28S* genes in X-DC1787-C control fibroblasts after 8 days of dyskerin depletion with shDKC1-3 or shDKC1-4 versus non-silence fibroblasts determined by qPCR and normalized by *GAPDH* expression. Mean of 2 independent experiments performed by duplicate is showed for every determination. $*p < 0.05$, $**p < 0.01$ and $***p < 0.001$ in shDKCs X-DC1787-C fibroblasts versus non-silence fibroblasts

4 days of p53 shRNA expression versus non-silenced fibroblasts (data not shown). A number of weeks later, both, p53-depleted X-DC and AD-DC fibroblasts recovered their proliferative capacity. In contrast, non-silence fibroblasts continued arrested and a decrease in the number of PDLs was observed (Fig. 6a). Moreover, senescent X-DC and AD-DC fibroblasts showed morphological changes after p53 depletion, suggesting that activation of p53 signaling pathway was primarily involved in the induction of senescence in DC fibroblasts (Fig. 6b) in response to DNA damage elicited by shortening of telomeres.

Discussion

The main purpose of this work was to ascertain if mutations in *DKC1* found in DC patients are affecting ribosome biogenesis and bone marrow failure, since some reports in

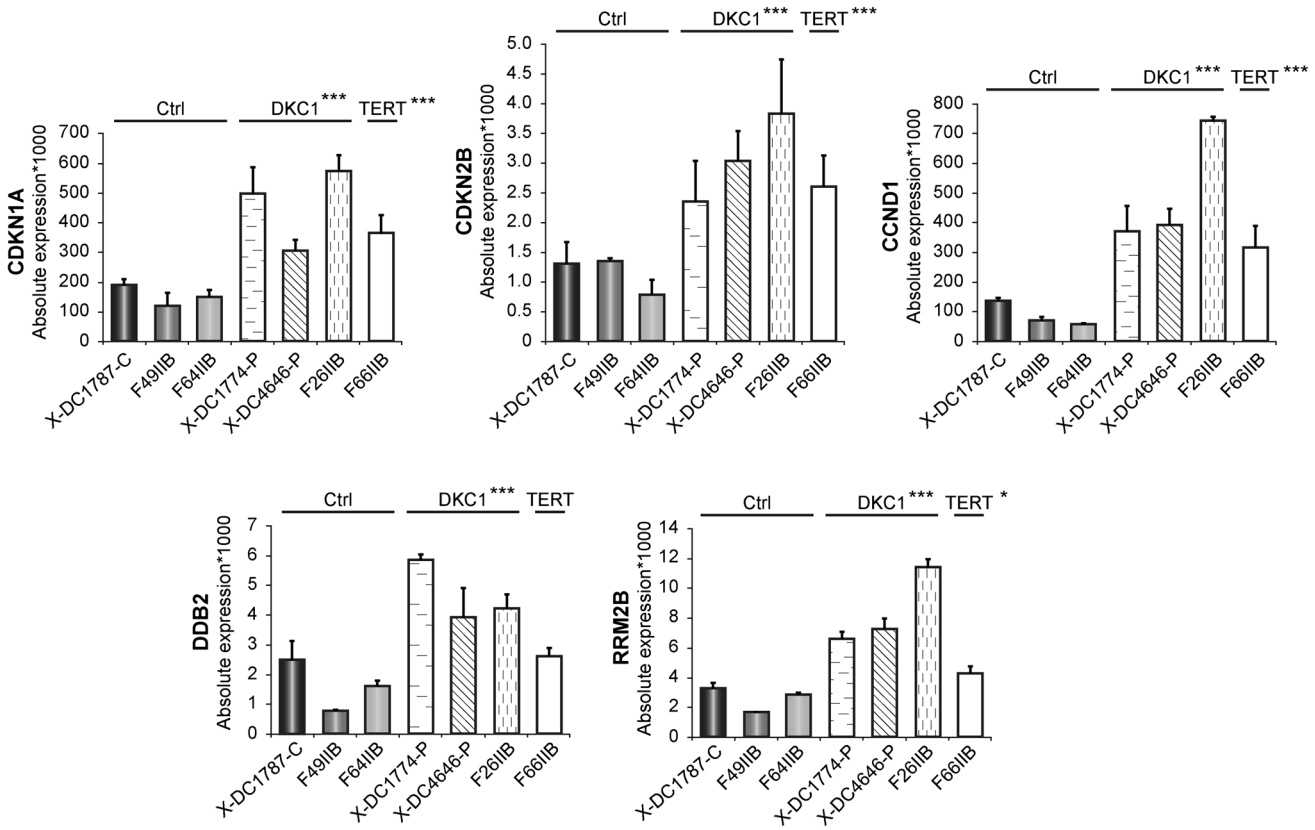

Fig. 4 Early activation of p53 pathway in X-DC and AD-DC patient's fibroblasts. Absolute expression of *CDKN1A*, *CDKN2B*, *CCND1*, *DDB2* and *RRM2B* genes in control fibroblasts (X-DC1787-C, F49IIB and F64IIB), X-DC (X-DC1774-P, X-DC4646-P and F26IIB) and AD-DC (F66IIB) patient's fibroblasts at PDL8, determined by qPCR and normalized with *GAPDH*. Mean of 2 independent experiments is showed. $*p < 0.05$ and $***p < 0.001$ in X-DC or AD-DC vs. control fibroblasts

the literature point to an important role of this pathway in the development of the disease. Mostly, these reports are based on the inhibition of *Nop10* [4] or *Dkc1* [5] expression in zebrafish, or mouse expressing an hypomorphic *Dkc1* mutant [19]. We compared gene expression profiles in normal fibroblasts depleted of *DKC1* and those derived from X-DC patients. We also analyzed molecular changes associated with the senescent phenotype in both X-linked (*DKC1*mut) and AD-DC (*TERT*mut) fibroblasts. We found a decrease in *TERC* mRNA levels in fibroblasts derived from 3 X-DC patients with different *DKC1* mutations VS control fibroblasts, in agreement with reports in DC patients with *DKC1*, *TERC* and *NOP10* mutations [15, 20]. We have also found that a big proportion of X-DC and AD-DC fibroblasts expressed SA-β-gal and that a high number of cells remained in G2/M phase, indicating that cells entered early into senescence.

After silencing *DKC1* expression we observed a decrease in *TERC* levels and activation of p53 pathway since different p53 target genes (*CDKN1A* and *CDKN2B)* were overexpressed and *CCND1* inhibited after 4 days of dyskerin depletion. However, other p53 targets, important for DNA repair or synthesis, were downregulated indicating the lack of DNA damage. Accordingly, dyskerin-depleted fibroblasts showed no increase in number of γ-H2AX foci per cell, most probably because at this time, telomeres had not undergone shortening. Due to p53 pathway activation, dyskerin-depleted fibroblasts ceased to grow after 6 days, showing an increase in SA-β-gal expressing cells and a slight increase of G2/M arrested and apoptotic cells (data not shown). These observations already indicated that the induction of senescence occur in dyskerin-depleted cells by a mechanism that is independent of telomere length. However, X-DC patient fibroblasts showed activation of the p53 pathway (*CDKN1A* and *CDKN2B* overexpression) after 1 month (≈PDL8) of cell culture, as observed in two DC-patient's fibroblasts established from skin biopsies. Indeed, expression of *CCND1*, *DDB2* and *RRM2B* was upregulated in X-DC and AD-DC fibroblasts since telomere shortening and γ-H2AX foci are found in DC fibroblasts. These cells also showed an increase in G2/M cells since eroded telomeres in senescent human fibroblasts recruit DNA damage response factors in G2 by a p53-dependent delay in G2 [21]. The differences observed between control fibroblasts infected with *DKC1*-shRNA lentiviral vectors and DC patient's fibroblasts can

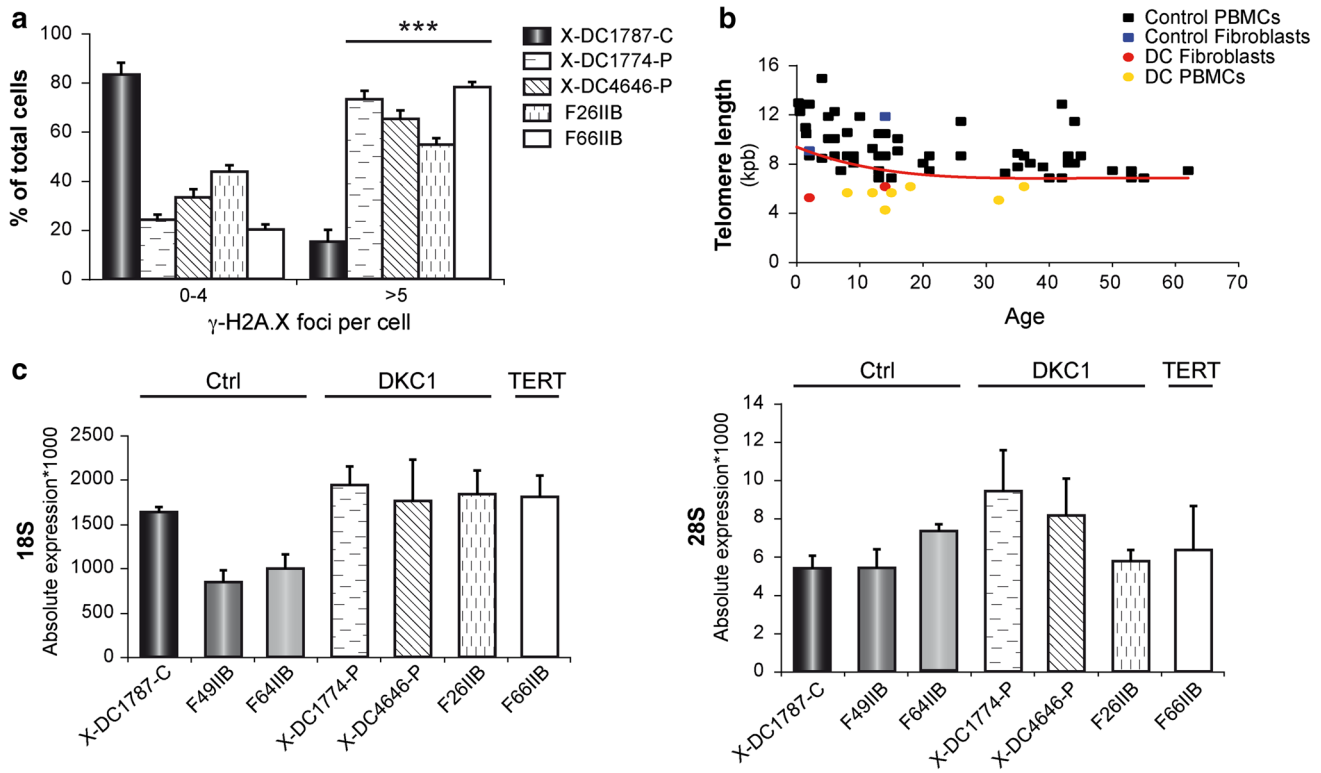

Fig. 5 Increased γ-H2AX foci per cell in X-DC and AD-DC patient's fibroblasts by telomere attrition and no ribosome biogenesis changes. **a** Quantification of γ-H2AX foci in control fibroblasts (X-DC1787-C), X-DC (X-DC1774-P, X-DC4646-P and F26IIB) and AD-DC (F66IIB) patient's fibroblasts at PDL8, determined by immunofluorescence in 200 cells for each case. **b** Mean telomere length of patient's fibroblasts (*red circles*) or patient's PBMCs (*orange circles*) harboring *DKC1* or *TERT* mutations measured by southern blot, plotted against age, and compared with control population (*black squares* for PBMCs and *blue squares* for fibroblasts). *Red line* indicates the first centile of control population against age. **c** Absolute expression of 18S and 28S rRNAs in control fibroblasts, X-DC and AD-DC patient's fibroblasts at PDL8, determined by qPCR and normalized with *GAPDH*. For all determinations mean of 2 independent experiments is showed. ***$p < 0.001$ in DC fibroblasts versus X-DC1787-C control fibroblasts

be explained if p53 activation or stabilization occurs through different pathways such as those induced by ribosome biogenesis failure or telomere attrition. Our results showed that dyskerin depletion induced early (4-days) activation of p53 pathway very likely by ribosome biogenesis failure as observed by alteration of 18S and 28S rRNAs expression. A reduction in rRNA levels especially 28S may be inducing the downregulation of ribosomal protein expression, to avoid the increase of free ribosomal proteins.

In X-DC and AD-DC fibroblasts we did not observe activation of the p53 pathway until 7-8PDLs (≈1 month), although the fibroblasts harbored *DKC1* or *TERT* mutations. We did not detect noticeable changes either in 18S or 28S rRNA levels, neither in expression level of ribosomal protein genes. Then these cells do not have major changes in ribosome biogenesis. Since we have detected shorter telomeres in X-DC and AD-DC fibroblasts and in PBMCs, the activation of the p53 pathway is very likely induced by telomere attrition.

Although we have X-DC fibroblasts with 3 different mutations, more than 50 different mutations have been described in *DKC1* associated with X-DC disease. However, very few cases of mutations in the TRUB domain of *DKC1* have been described which may indicate that the mutation might be lethal due to their important role in ribosomal biogenesis and early activation of the p53 pathway.

In X-DC animal models, based on inhibition of *Nop10* [9] or *Dkc1* [10] expression or expression of an hypomorphic *Dkc1* mutant [8], authors have described deficient ribosomal RNA modification as the mechanism driving bone marrow failure. This effect on RNA processing may be equivalent to our findings in the DKC1-depleted cell model. When expression of *DKC1* or *Nop10* is acutely interrupted, the more dynamic processes controlled by dyskerin such as ribosome biogenesis, are those affected first and this impairment in protein synthesis induces the activation of the p53 signaling pathway. In fibroblasts isolated from DC patients, changes in ribosome biogenesis

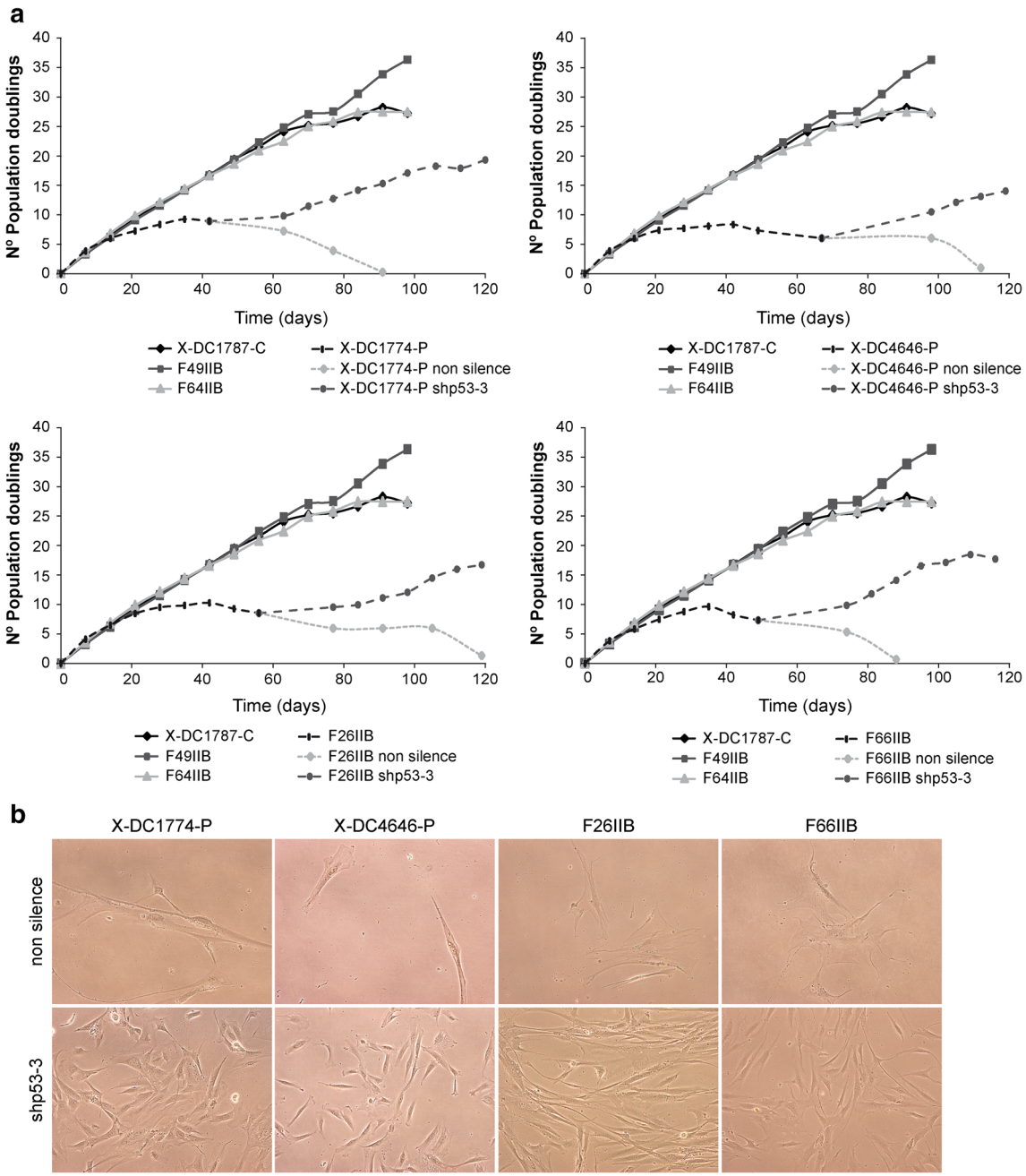

Fig. 6 Proliferative capacity rescue of DC fibroblasts by p53 depletion. **a** Number of PDLs versus time in senescent X-DC1774-P, X-DC4646-P, F26IIB and F66IIB DC fibroblasts after p53 depletion or non-silence interference (control), and compared with control fibroblasts (X-DC1787-C, F49IIB and F64IIB). Growth of shp53 cell lines is only indicated after the infection which was performed between 40 and 60 days of cell growth and when the parental cells stop dividing. **b** Images of DC fibroblasts some weeks after p53 depletion or non-silence interference

may occur, but cells should develop compensatory mechanisms to maintain protein synthesis activity to levels compatible with cell growth. Once telomeres shorten after a defined number of cell duplications, by decreased telomerase activity, there is not a compensatory mechanism to overcome the shortening. In agreement with this, we did not detected induction of DNA damage in dyskerin-depleted cells, but on the contrary X-DC fibroblast showed an intense induction of the DNA damage.

Lastly, p53 depletion in patient's fibroblasts harboring *DKC1* or *TERT* mutations resulted in the recovery of the proliferative capacity of these fibroblasts, over time and increased lifespan and maintenance of proliferative capacity.

In summary, our study demonstrated that p53 signaling pathway is activated in DC-patient fibroblasts only after telomere attrition when cells entered into senescence. These results are in contrast to those describing deficiencies in ribosomal metabolism in animal models for DC. Based on our results efforts to recover the proliferative capacity in X-DC cells should be focused on re-establishing *TERC* stability and hence telomerase activity in these cells. This has been obtained by expression of both a small internal fragment of dyskerin (GSE24.2) [22] and *TERC* [23]. GSE24.2 has been recently approved as an orphan drug for the treatment of DC (EU/3/12/1070–EMA/OD/136/11).

Acknowledgments This work was supported by grants: 11/00949 from FIS and Fundación Ramón Areces. C. Manguán-García and J. Carrillo were supported by CIBER de Enfermedades Raras. We gratefully acknowledge to Leandro Sastre for helpful discussions and critical reading of the manuscript.

References

1. Bessler M, Wilson DB, Mason PJ. Dyskeratosis congenita. FEBS Lett. 2010;584(17):3831–8.
2. Savage SA, Blanche P. Alter dyskeratosis congenita. Hematol Oncol Clin North Am. 2009;23(2):215–31. doi:10.1016/j.hoc.2009.01.003.
3. Dokal I, Vulliamy T, Mason P, Bessler M. Clinical utility gene card for: dyskeratosis congenita. Eur J Hum Genet. 2011;19:231–5. doi:10.1038/ejhg.2011.90.
4. Vulliamy T, Marrone A, Szydlo R, Walne A, Mason PJ, Dokal I. Disease anticipation is associated with progressive telomere shortening in families with dyskeratosis congenita due to mutations in TERC. Nat Genet. 2004;36(5):447–9.
5. Yamaguchi H, Calado RT, Ly H, Kajigaya S, Baerlocher GM, Chanock SJ, et al. Mutations in TERT, the gene for telomerase reverse transcriptase, in aplastic anemia. N Engl J Med. 2005;352(14):1413–24.
6. Parry EM, Alder JK, Lee SS, Phillips JA, Loyd JE, Duggal P, et al. Decreased dyskerin levels as a mechanism of telomere shortening in X-linked dyskeratosis congenita. J Med Genet. 2011;48(5):327–33.
7. Ge J, Rudnick DA, He J, Crimmins DL, Ladenson JH, Bessler M, et al. Dyskerin ablation in mouse liver inhibits rRNA processing and cell division. Mol Cell Biol. 2010;30(2):413–22.
8. Ruggero D, Grisendi S, Piazza F, Rego E, Mari F, Rao PH, et al. Dyskeratosis congenita and cancer in mice deficient in ribosomal RNA modification. Science. 2003;299(5604):259–62.
9. Pereboom TC, van Weele LJ, Bondt A, MacInnes AW. A zebrafish model of dyskeratosis congenita reveals hematopoietic stem cell formation failure resulting from ribosomal protein-mediated p53 stabilization. Blood. 2011;118(20):5458–65.
10. Zhang Y, Morimoto K, Danilova N, Zhang B, Lin S. Zebrafish models for dyskeratosis congenita reveal critical roles of p53 activation contributing to hematopoietic defects through RNA processing. PLoS One. 2012;7(1):e30188.
11. Panic L, Montagne J, Cokaric M, Volarevic S. S6-Haploinsufficiency activates the p53 tumor suppressor. Cell Cycle. 2007;6(1):20–4.
12. Carrillo J, Martínez P, Solera J, Moratilla C, González A, Manguán-García C, et al. High resolution melting analysis for the identification of novel mutations in DKC1 and TERT genes in patients with dyskeratosis congenita. Blood Cells Mol Dis. 2012;49(3–4):140–6.
13. Nagasawa H, Little JB. Suppression of cytotoxic effect of mitomycin-C by superoxide dismutase in Fanconi's anemia and dyskeratosis congenita fibroblasts. Carcinogenesis. 1983;4:795–9.
14. Heiss NS, Knight SW, Vulliamy TJ, Klauck SM, Wiemann S, Mason PJ, et al. X-linked dyskeratosis congenita is caused by mutations in a highly conserved gene with putative nucleolar functions. Nat Genet. 1998;19(1):32–8.
15. Wong JMY, Kyasa MJ, Hutchins L, Collins K. Telomerase RNA deficiency in peripheral blood mononuclear cells in X-linked dyskeratosis congenita. Hum Genet. 2004;115:448–55.
16. d'Adda di Fagagna F, Reaper PM, Clay-Farrace L, Fiegler H, Carr P, Von Zglinicki T, et al. A DNA damage checkpoint response in telomere-initiated senescence. Nature. 2003;426:194–8.
17. Chan SS, Chang S. Defending the end zone: studying the players involved in protecting chromosome ends. FEBS Lett. 2010;584(17):3773–8.
18. d'Adda di Fagagna F, Teo SH, Jackson SP. Functional links between telomeres and proteins of the DNA-damage response. Genes Dev. 2004;18:1781–99.
19. Vulliamy T, Beswick R, Kirwan M, Marrone A, Digweed M, Walne A, et al. Mutations in the telomerase component NHP2 cause the premature ageing syndrome dyskeratosis congenita. Proc Natl Acad Sci. 2008;105(23):8073–8.
20. Walne AJ, Vulliamy T, Marrone A, Beswick R, Kirwan M, Masunari Y, et al. Genetic heterogeneity in autosomal recessive dyskeratosis congenita with one subtype due to mutations in the telomerase-associated protein NOP10. Hum Mol Genet. 2007;16(13):1619–29.
21. Jullien L, Mestre M, Roux P, Gire V. Eroded human telomeres are more prone to remain uncapped and to trigger a G2 checkpoint response. Nucleic Acids Res. 2013;41(2):900–11. doi:10.1093/nar/gks1121 (Epub 2012 Nov 27).
22. Machado-Pinilla R, Sanchez-Perez I, Ramon Murguia J, Sastre L, Perona R. A dyskerin motif reactivates telomerase activity in X-linked dyskeratosis congenita and in telomerase-deficient human cells. Blood. 2008;111(5):2606–14.
23. Westin ER, Aykin-Burns N, Buckingham EM, Spitz DR, Goldman FD, Klingelhutz AJ. The p53/p21$^{WAF/CIP}$ pathway mediates oxidative stress and senescence in dyskeratosis congenita cells with telomerase insufficiency. Antioxid Redox Signal. 2011;14(6):985–97.